

1,4-DIOXANE REMEDIATION USING A CONSTRUCTED WETLAND

by

William Jackson Ward

Copyright © William Jackson Ward 2008

A Dissertation Submitted to the Faculty of the

GRADUATE INTERDISCIPLINARY PROGRAM IN ARID LANDS
RESOURCE SCIENCES

In Partial Fulfillment of the Requirements

For the Degree of

DOCTOR OF PHILOSOPHY

In the Graduate College

THE UNIVERSITY OF ARIZONA

2008

THE UNIVERSITY OF ARIZONA
GRADUATE COLLEGE

As members of the Dissertation Committee, we certify that we have read the dissertation prepared by William Ward entitled 1,4-Dioxane Remediation using a Constructed Wetland and recommend that it be accepted as fulfilling the dissertation requirement for the Degree of Doctor of Philosophy

Date: 3/25/2008
David Quanrud

Date: 3/25/2008
Martin Karpiscak

Date: 3/25/2008
Stuart Marsh

Date: 3/25/2008
Charles Hutchinson

Final approval and acceptance of this dissertation is contingent upon the candidate's submission of the final copies of the dissertation to the Graduate College.

I hereby certify that I have read this dissertation prepared under my direction and recommend that it be accepted as fulfilling the dissertation requirement.

Date: 5/05/2008
Dissertation Director: David Quanrud

STATEMENT BY AUTHOR

This dissertation has been submitted in partial fulfillment of requirements for an advanced degree at the University of Arizona and is deposited in the University Library to be made available to borrowers under rules of the Library.

Brief quotations from this dissertation are allowable without special permission, provided that accurate acknowledgment of source is made. Requests for permission for extended quotation from or reproduction of this manuscript in whole or in part may be granted by the copyright holder.

SIGNED: William Jackson Ward

ACKNOWLEDGEMENTS

I am very grateful to Dr. David Quanrud, my advisor, for his kind guidance and helpful reviews of this research. Many thanks are due Drs. Martin Karpiscak, Stuart Marsh, and Charles Hutchinson for participating on my dissertation committee.

An expression of gratitude is extended to Glenn France, Sandy Teske, Joy Rogers, Brian Barbaris, Anita Finnell, and Kelley Riley for providing field site, laboratory, and administrative help. Their support helped overcome various hurdles.

Guidance, equipment, and facilities support was provided by Drs. Robert Arnold, Mike Yao, Ken Foster, and Wendell Ela. Their support made the research effort possible. The Pima County Department of Wastewater Management provided financial support for the CERF wetlands, the field site of this research.

My willingness to push forward every day was supported by encouraging words from family and friends. A special thank you goes to Drs. Gene Cafarelli, Jerry Alderman, and Phil Wolf. Further thanks to Joan McMahon, Glynis Coulter, and my sons Bill and Kevin.

DEDICATION

This dissertation is dedicated to my grandfather Enoch Jacob Ward. His desire and support of higher education for his children has inspired three generations and now resides with Austin and Caitlin, my grandchildren.

TABLE OF CONTENTS

ABSTRACT	22
1.0 INTRODUCTION	24
1.1 Objectives.....	27
1.2 Organization of Dissertation	29
2.0 LITERATURE REVIEW	31
2.1 1,4-Dioxane Background	31
2.1.1 1,4-Dioxane Properties	31
2.1.1.1 1,4-Dioxane Water Contamination.....	32
2.1.1.2 1,4-Dioxane Air Contamination	33
2.1.2 1,4-Dioxane Contamination in the Environment.....	34
2.1.2.1 Primary Contaminant Sources	34
2.1.2.2 Secondary Contaminant Sources	35
2.1.2.3 Contaminant Recalcitrance	35
2.1.2.4 World Wide Use and Contamination.....	36
2.1.2.5 United States 1,4-Dioxane Contamination	37
2.1.2.6 State of Arizona 1,4-Dioxane Contamination.....	37
2.1.2.7 Potential Contaminated Areas in Arizona	38
2.1.2.8 1,4-Dioxane Environmental Risk Assessment	39
2.1.3 1,4-Dioxane Toxicology.....	40
2.1.3.1 Chronic Effects to 1,4-Dioxane Exposure	40
2.1.3.2 Contaminant Acute Exposure Toxicity	41
2.1.3.3 1,4-Dioxane Target Organ Toxicology.....	42
2.1.3.4 Contaminant Genotoxic Effects.....	42
2.1.4 Pre-Concentration Techniques	43
2.1.4.1 Solid Phase Extraction.....	44
2.1.4.2 Single Contact Liquid-Liquid Extraction	45
2.1.4.3 Purge and Trap Techniques	45
2.1.4.4 Continuous Liquid-Liquid Extraction (LLE).....	46
2.1.4.5 U.S. EPA Vacuum Distillation Method.....	47
2.1.5 1,4-Dioxane Gas Chromatography / Detection	47
2.1.5.1 Gas Chromatography Principles.....	47
2.1.5.2 Gas Chromatography Key Factors.....	48
2.1.5.3 Gas Chromatography Detectors.....	49
2.1.5.3.1 Flame Ionization Detectors	49
2.1.5.3.2 Mass Spectrometry Detectors	50
2.1.5.4 Experimental Determination of 1,4-Dioxane	51
2.2 Remediation	51

TABLE OF CONTENTS - *Continued*

2.2.1	Advanced Oxidation Processes	52
2.2.1.1	Photoinduced Oxidation Using UV Light and Hydrogen Peroxide	52
2.2.1.2	Fenton's Reagent and Ozone with Hydrogen Peroxide	53
2.2.1.3	Chlorine Degradation of 1,4-Dioxane	54
2.2.1.4	UV Light and Titanium Dioxide	54
2.2.1.5	Ultrasound Sonication	55
2.2.1.6	Disadvantages of Advanced Oxidation Treatments	56
2.2.2	Biodegradation Treatments	56
2.2.2.1	Actinomyces Biodegradation	57
2.2.2.2	Monooxygenase Expressing Bacteria Biodegradation	58
2.2.2.3	Bioreactors	59
2.2.2.4	In-Situ Bioremediation	59
2.2.2.5	Bioremediation Field Studies	60
2.2.3	Phytoremediation	60
2.2.3.1	Phytoremediation Design Elements	61
2.2.3.2	1,4-Dioxane Phytoremediation Potential	62
2.2.4	1,4-Dioxane Contamination Case Histories	63
2.2.4.1	Menlo Park, California	63
2.2.4.2	Ann Arbor, Michigan	64
2.2.4.3	Seymour, Indiana	65
2.2.4.4	San Jose, California	65
2.3	Treatment Wetlands	66
2.3.1	Natural Wetlands	66
2.3.2.1	Wetland Attributes Enhance Contaminant Remediation	66
2.3.2.2	Wetland Plants	67
2.3.2	Constructed Wetlands	68
2.3.2.1	Type and Use of Constructed Wetlands	68
2.3.2.2	Constructed Wetland Advantages	69
2.3.2.3	Constructed Wetlands Reduce Harmful Microorganisms	69
2.3.2.4	Constructed Wetlands Suitable for Most Climates	70
2.3.2.5	Constructed Wetlands Offset Loss of Natural Wetlands	71
2.3.2.6	Constructed Wetlands Field Studies Database	72
2.3.3	Pilot-Scale Wetlands	72
2.3.3.1	Cottonwood Trees (<i>Populus fremontii</i> S. Wats.)	73
2.3.3.1.1	Laboratory Studies to Determine Cottonwood Suitability	75
2.3.3.2	Cottonwood Tree Uptake and Transpiration of 1,4-Dioxane	76
2.3.3.3	1,4-Dioxane Fate and Partitioning in Cottonwood Trees	77
2.3.3.4	Pilot-Scale Project Design	78
2.3.3.4.1	Goal of Pilot-Scale Project	79
2.3.3.4.2	Wetland Project Examples Supporting Pilot-Scale Projects	79
3.0	METHODS	82

TABLE OF CONTENTS - *Continued*

3.1 Experimental Site: Constructed Ecosystems Research Facility (CERF)	82
3.1.1 Location of CERF Facility	82
3.1.2 Site Layout.....	84
3.1.3 Experimental and Control Wetland Tanks	86
3.1.4 Feed and Discharge Collection Tanks.....	87
3.1.5 Evaporation Ponds and Retaining Wall.....	87
3.1.6 Tank Orientation and Shading.....	89
3.2 Inflow & Discharge Operations	90
3.2.1 Infrastructure Modifications.....	90
3.2.1.1 Secondary Effluent Piping.....	90
3.2.1.2 Refurbishment and Planting of Wetland Tanks.....	91
3.2.1.3 Refurbishment of Feed and Discharge Collection Tanks	92
3.2.1.4 Construction of Evaporation Ponds	92
3.2.1.5 Emergency Back-up Tank and Pond	93
3.2.1.6 Valves and Piping Installation.....	94
3.2.1.7 Storage Capacity Balance and Safety Margins.....	95
3.2.1.8 Adherence to Flow and Sampling Schedule.....	96
3.2.2 Tanks/Piping for Inflow/Discharge of Tap Water.....	96
3.2.2.1 Spiked Tap-Water Feed Preparation.....	96
3.2.2.2 Influent Flow Rate	98
3.2.2.3 Spiked Tap-Water Delivery to Experimental Wetland Tanks	98
3.2.2.4 Spiked Tap-Water Feed Changeover.....	99
3.2.2.5 Wetland Tanks Discharge Collection and Transfer to Ponds	100
3.2.2.6 Reconfiguration of Post Spiked Discharge to CERF.....	101
3.2.3 Tanks/Piping for Inflow/Discharge of Secondary Effluent.....	102
3.2.3.1 Un-spiked Secondary Effluent Discharge to Sewer System.....	102
3.2.3.2 Spiked Secondary Effluent Feed Preparation	102
3.2.3.3 Spiked Secondary Effluent Delivery to Experimental Wetland Tanks	103
3.2.3.4 Spiked Secondary Effluent Feed Changeover	103
3.2.3.5 Secondary Effluent Discharge Collection and Transfer to Ponds .	104
3.2.3.6 Maintenance of Tanks and Ponds at Conclusion of All Experimental Runs	104
3.3 Flow Measurements	105
3.3.1 Potable Water	105
3.3.2 Secondary Effluent	105
3.3.3 Hydraulic Mass Balances	106
3.3.3.1 Discharge Tanks Mass Balance	106
3.3.3.2 Ponds Mass Balance	107
3.3.4 Pond Volume	107
3.3.4.1 Tank Discharge Adjusted Volume Measurement.....	107

TABLE OF CONTENTS - *Continued*

3.3.4.2	Pond Volume Direct Measurement	109
3.3.4.3	Pond Measurement Method Summary	109
3.4	Wetland Tank Hydraulics	110
3.4.1	Hydraulic Loading Rate	110
3.4.2	Hydraulic Gradient	111
3.4.3	Hydraulic Conductivity	111
3.4.4	Flow Dwell Time.....	112
3.4.5	Bromide Tracer Study	112
3.4.5.1	Bromide Tracer Study Sampling Locations	113
3.4.5.2	Immediate Tracer Sample Processing	115
3.4.5.3	Tracer Study Results Validate Estimated Dwell Time	116
3.5	Tree Planting in Wetland Tank	117
3.5.1	Pre-preparation and Placement.....	118
3.5.1.1	Cottonwood Cuttings.....	118
3.5.1.2	Cottonwood Cutting Placement.....	118
3.5.2	Tree Growth & Irrigation	119
3.5.2.1	Early Growth and Watering Schedule	119
3.5.2.2	First Year Dominant Cutting Growth	120
3.5.2.3	Initial Secondary Effluent Introduction	121
3.5.2.4	Tree Trimming and Tree Loss	122
3.6	Wetland Tank Temperature & Soil Moisture.....	123
3.6.1	Temperature Measurement.....	123
3.6.1.1	Weekly Thermometer Temperature Readings.....	123
3.6.1.2	Automated Thermocouple Measurement and Data Collection	123
3.6.1.3	Thermocouple Installation in Tanks and Ponds.....	124
3.6.1.4	Thermocouple Calibration	125
3.6.2	Tensiometer Soil Moisture Measurement	125
3.6.2.1	Tensiometer Locations.....	125
3.6.2.2	Tensiometer Measurements	126
3.6.3	Time Domain Reflectometry	126
3.6.3.1	TDR Measurement Unit	127
3.6.3.2	TDR Probe Characteristics	127
3.6.3.3	TDR Probe Installation	128
3.6.3.4	TDR Waveform Post Processing.....	128
3.6.3.5	TDR Waveform Equation for Conversion to Soil Moisture.....	129
3.7	UV/Solar Light and Volatilization.....	130
3.7.1	Full Day UV and Solar Measurement	130
3.7.1.1	UV and Solar Measurement Equipment	130
3.7.1.2	UV and Solar Measurements	131
3.7.1.3	UV and Solar Measurement Results.....	132

TABLE OF CONTENTS - *Continued*

3.7.2 UV and Solar Contaminant Degradation Side Experiment.....	133
3.7.2.1 Side Experiment Set-Up	133
3.7.2.2 Sampling and Contaminant Measurement.....	134
3.7.3 Follow-up UV and Solar Side Experiment.....	134
3.7.3.1 Side Experiment Set-up.....	135
3.7.3.2 Sampling and Contaminant Measurement.....	135
3.7.4 UV-B and Solar Sun Side Experiment	136
3.7.4.1 UV-B Side Experiment Set-up	136
3.7.4.2 Solar Sun Side Experimental Set-up.....	137
3.7.4.3 Experimental Flow Rate and Run Time	138
3.7.4.4 UV-B and Solar Sun Experimental Results.....	139
3.7.5 Volatilization Process.....	139
3.8 Laboratory Methodology	141
3.8.1 Sample Collection and Storage	142
3.8.2 Sample Filtering	143
3.8.2.1 Apparatus.....	143
3.8.2.2 Initial Filtering with Glass Fiber Filters	144
3.8.2.3 Final Filtering with PVDF Filters.....	145
3.8.2.4 Filtering Sample Identification Procedure.....	145
3.8.3 Sample Extraction Methods	146
3.8.3.1 Liquid-Liquid Extraction	147
3.8.4 Liquid-Liquid Extraction Equipment Set-up.....	147
3.8.4.1 Jacketed K-D Concentrator.....	147
3.8.4.2 Extractor Allihn Condenser	148
3.8.4.3 Corning Extractor 1.0 L Vessel	148
3.8.4.4 Extractor Operation and Contaminant Sample Collection	149
3.8.4.5 Extractor Efficiency and Variation.....	150
3.8.5 1,4-Dioxane Measurements: Gas Chromatography / Flame Ionization Detection Methods.....	151
3.8.5.1 Gas Chromatography Analysis Procedures	151
3.8.5.2 Gas Chromatography Operation	153
3.8.5.3 1,4-Dioxane Calibration Standard Curves.....	155
3.8.5.3.1 Dilution Calibration Standard Curves.....	155
3.8.5.3.2 Extracted Calibration Standard Curves.....	155
3.8.5.3.3 1,4-Dioxane Concentrations Established by Extracted Standard Curves	156
3.8.5.4 GC Equipment Constraints	157
3.8.5.4.1 Equipment Gas Flow Failure	157
3.8.5.4.2 Column Degradation Problems.....	157
3.8.5.4.3 Elution Timing Equipment Problems	158
3.8.5.5 Surrogate Operating Constraints.....	158

TABLE OF CONTENTS - *Continued*

3.8.5.6	Internal Standard Elution Problems.....	160
3.8.5.7	Impact of Bromide on 1,4-Dioxane Samples	160
3.8.5.8	Laboratory Contaminant Lower Detection Limit	161
3.8.5.9	Methods to Improve Lower Detection Limit.....	161
3.8.6	Bromide Tracer, Turbidity, pH, Conductivity Methods.....	162
3.8.6.1	Sample Collection and Storage.....	162
3.8.6.2	Bromide Measurement.....	162
3.8.6.3	pH Measurement.....	164
3.8.6.4	Specific Conductivity Measurement.....	165
3.8.6.5	Turbidity Measurement	165
4.0	EXPERIMENTAL RESULTS – WETLAND TANK HYDRAULIC CHARACTERIZATION	167
4.1	Introduction.....	167
4.2	Characterization of Wetland Hydraulics.....	167
4.2.1	Pre-Experiment Bromide Tracer Study.....	168
4.2.1.1	Tracer Study Results.....	168
4.2.1.2	Quantitative Evaluation of Tracer Study Breakthrough Curve	170
4.2.1.3	Key Operating Parameters Established by Tracer Study.....	176
4.2.1.4	Tracer Study Results From Upper Side Ports.....	177
4.2.1.5	Tracer Study Results From Lower Side and Discharge Ports	178
4.2.2	Experimental Run Bromide Tracer Results.....	179
4.2.2.1	Lapse Time Peak of Bromide Tracer and Contaminant	179
4.2.2.2	Total Mass Bromide Tracer Breakthrough	184
4.2.2.3	Bromide and Contaminant Lapse Time Variation.....	184
4.2.2.4	Experimental Run Bromide Tracer Initial Breakthrough	185
4.2.3	Experimental Run Bromide Tracer Longitudinal Dispersion	186
4.2.4	Experimental Run Bromide Tracer Loss.....	187
4.2.4.1	Bromide Tracer Measurement	187
4.2.4.2	Plant Uptake of Bromide	188
4.2.4.3	Bromide Recovery Results	189
4.2.4.4	Post Experimental Run Bromide Sampling.....	191
4.2.4.5	Correlation of Bromide Mass Variation	192
4.2.4.5.1	Surface Saturation Correlation to Bromide Variation.....	192
4.2.4.5.2	Rainfall Correlation to Bromide Variation	193
4.3	Soil Moisture.....	194
4.3.1	Soil Moisture Balance	194
4.3.1.1	Wetland Tank Inflow Rate.....	194
4.3.1.2	Wetland Tank Discharge	196
4.3.2	Root Zone Soil Moisture	198
4.3.2.1	Soil Moisture and Contaminant Uptake	198

TABLE OF CONTENTS - *Continued*

4.3.2.2	Time Domain Reflectometry Results	199
4.3.2.3	TDR Measurement Problems	202
4.3.2.4	Significant Drying Events.....	203
4.4	Tree Growth	203
4.4.1	Tree Height.....	203
4.4.2	Tree Diameter at Breast Height.....	203
4.4.3	Tree Leaf Size and Color.....	205
4.5	Discussion	206
4.5.1	CERF & AF Plant 4 Study Site Comparison.....	206
4.5.1.1	CERF Tree Height Measurements.....	206
4.5.1.2	Correlation of CERF and Experimental Cottonwood Trees.....	206
4.5.2	Air Force Plant 4 Study - Cottonwood Growth.....	207
4.5.2.1	A.F. Plant 4 Study Background	207
4.5.2.2	Correlation of A.F. and Experimental Project Tree Height and Diameter	208
4.5.3	Transpiration Measurements	210
4.5.3.1	Transpiration.....	210
4.5.3.2	A.F. Plant 4 Study Tree Transpiration.....	210
4.5.3.3	Tree Transpiration Rate Correlated with Temperature.....	211
4.5.4	Temperature Measurements	212
4.5.4.1	Air Temperature Differences.....	212
4.5.4.2	Sub-Surface Temperature Differences.....	214
4.5.4.3	Impacts of Shading by Trees	214
4.5.5	Seasonal Factors	215
4.5.5.1	Deciduous / Temperature.....	216
4.5.5.2	Experimental Run Rainfall Events	218
4.5.5.3	Humidity/ Solar Radiation.....	219
4.5.6	Edge Effects.....	221
4.5.7	Hydrologic Effects.....	222
4.5.7.1	Experimental Wetland Tank Cottonwood Initial Growth Patterns	222
4.5.7.2	Increased Flow Correlated to Increased Height of Higher Growth Trees	223
4.5.7.3	Lower Soil Moisture and Growth of Midstream Plants.....	225
4.5.8	Sunlight/Shadow Effects	225
4.5.9	Longitudinal Dispersion Effects.....	227
4.6	Conclusions	228
4.6.1	Pilot-Scale to Full-Scale Wetland Considerations	228
4.6.2	Simulate Full-Scale Operating Factors for Pilot-Scale Wetlands	229
4.6.3	Full-Scale Example Without a Pilot-Scale Project.....	229
4.6.4	Experimental Pilot-Scale Project Benefits to Full-Scale Implementation	230

TABLE OF CONTENTS - *Continued*

4.6.5 Recommendations to Improve Experimental Wetlands Study.....	231
5.0 EXPERIMENTAL RESULTS – SUBSURFACE WETLAND TREATMENT	233
5.1 Introduction	233
5.1.1 Contaminant Contact Time.....	233
5.1.2 Evapotranspiration.....	234
5.1.3 Cottonwood Tree Growth.....	235
5.1.4 Discharge Measurements.....	236
5.2 Wetland Tank Key Parameter Results	237
5.2.1 Specific Conductivity	237
5.2.2 pH	241
5.2.2.1 Discharge pH Measurements.....	241
5.2.2.2 Discharge Tanks pH Peaks	242
5.2.2.3 Time Correlation of pH Peak and Spiked Feed.....	243
5.2.2.4 True Cause of pH Peak in Discharge Collection Tanks	243
5.2.3 Turbidity.....	244
5.2.4 Dissolved Organic Carbon	246
5.3 1,4-Dioxane Results	247
5.3.1 Wetland Tank Influent.....	247
5.3.2 Wetland Tank Effluent	249
5.3.2.1 Planted and Control Wetland Tank Results.....	249
5.3.3 Discharge Collection Tanks	250
5.4 Experimental Run 1,4-Dioxane Mass Breakthrough	251
5.4.1 Mass Balance Overview	252
5.4.2 Mass Balance Approach.....	253
5.4.2.1 Comparison of Wetland Tank Mass Discharge Results	253
5.4.3 Wetland 1,4-Dioxane Mass Removal.....	256
5.4.3.1 1,4-Dioxane Mass Removal in the Planted Wetland.....	256
5.4.3.2 1,4-Dioxane Mass Removal in the Unplanted Wetland	257
5.5 Correlation of 1,4-Dioxane Uptake to Environmental Factors	258
5.5.1 Transpiration Correlation to 1,4-Dioxane Uptake.....	259
5.5.2 Planted Tank 1,4-Dioxane Uptake Correlation to Maximum Air Temperature.....	260
5.6 Determination of 1,4-Dioxane Uptake Efficiency	262
5.7 Discussion	263
5.7.1 Comparison of Experimental Wetlands to Laboratory Studies.....	265
5.7.2 Experimental Run Uptake Rate Compared to Previous Laboratory Study	268

TABLE OF CONTENTS - *Continued*

5.7.3 Experimental Run 1,4-Dioxane Discharge Variations in Wetlands Tanks	272
5.7.4 Control Tank 1,4-Dioxane Removal Rate Due to Evaporation.....	275
5.7.5 Comparing Tap Water and Secondary Effluent Experimental Runs.....	277
5.7.5.1 Experimental Run 3 (Tap-Water) and Run 4 (Secondary Effluent)	277
5.7.5.2 Experimental Run # 4 Operational Factors	278
5.7.6 Pilot-Scale and Full-Scale Wetland Contaminant Removal.....	279
5.7.7 Fate of Contaminant	281
5.7.7.1 No Biodegradation of 1,4-Dioxane.....	281
5.7.7.2 Fate of 1,4-Dioxane After Tree Uptake	282
5.7.8 Sampling Frequency.....	282
5.7.9 Discharge Tank Sampling Concerns	283
5.8 Conclusions	284
5.9 Future Research.....	285
5.9.1 Treatment and Disposal of Trace Level Contaminated Discharge.....	285
5.9.2 Atmosphere Degradation Pathways for 1,4-Dioxane	285
6.0 EXPERIMENTAL RESULTS – OPEN POND TREATMENT	286
6.1 Pond Volume Measurement: Method Comparison.....	286
6.2 Temperature Measurement.....	287
6.2.1 Average Pond Temperature.....	287
6.2.2 Pond Diurnal Temperature Variations.....	288
6.3 1,4-Dioxane Reduction in Ponds.....	289
6.3.1 1,4-Dioxane Discharged to Ponds	289
6.3.1.1 Pond Sampling Schedule	291
6.3.1.2 1,4-Dioxane Initial Pond Sample Compared to Discharge Starting Mass	292
6.3.1.3 Comparison of Contaminant Mass Reduction and Pond Volume Evaporation.....	293
6.3.2 Calculating 1,4-Dioxane Removal Rate	294
6.3.3 1,4-Dioxane Removal Rate Kinetics	295
6.3.4 Determination of First Order Loss Rate Constants and Half Lives.....	296
6.4 Determination of 1,4-Dioxane Removal Mechanism: Side Experiment Results	299
6.4.1 Grey Tub Side Experiment Results	299
6.4.2 Pool Side Experiment Results	300
6.4.3 Remaining Contaminant in Grey Tub and Pool Side Experiments.....	301
6.4.4 Grey Tub and Pool Elimination Rate Constant Comparison.....	302

TABLE OF CONTENTS - *Continued*

6.5	Pond and Pool Side Experiments 1,4- Dioxane Mass Flux	303
6.5.1	Key Differences of Experimental Ponds and Side Experiments	304
6.5.2	Aqueous Solubility Influence on Contaminant Air Water Partition Coefficient	306
6.6	Algae Growth and Effect on Pond pH	306
6.6.1	Algae Blooms	307
6.6.1.1	Qualification of Algae Volume	307
6.6.1.2	Algae Identification	308
6.6.1.3	Impact of Algae on 1,4-Dioxane Fate.....	308
6.6.2	Pond Carbonate System Change on Contaminant Concentration	309
6.7	1,4-Dioxane Laboratory Photo-oxidation Experiment.....	309
6.7.1	UV-B / Solar Sun Light Side Experiment Exposure	310
6.7.2	UV-B / Visible Light 1,4-Dioxane Reduction.....	310
6.8	Discussion	311
6.8.1	Experimental Pond, Grey Tub, and Pool Contaminant Elimination	311
6.8.1.1	Determination of First Order Reaction Process.....	311
6.8.2	Volatilization as Pond Contaminant Elimination Process.....	313
6.8.2.1	1,4-Dioxane in Ponds Volatilization Factors.....	313
6.8.2.2	Contaminant Chemical Properties Indicative of Volatilization.....	313
6.8.2.3	Henry's Law Level of Contaminant Volatilization in Contrast to Fugacity Models	314
6.8.3	Temperature Dependency of Elimination Rate Constant.....	315
6.8.3.1	Diffusion Coefficient Key to Volatilization Process	315
6.8.3.2	Pond Experimental Results Correlated to Volatilization Process..	316
6.8.3.3	Experimental Reduction Results Infer Multiple Elimination Processes.....	318
6.8.4	Experimental Side Studies.....	319
6.8.4.1	Significant Contaminant Reduction Without Sunlight Exposure..	319
6.8.4.2	1,4-Dioxane Mass Flux Water to Air Transfer	319
6.8.4.3	Environmental Factors Influencing Contaminant Air Water Partition Coefficient	320
6.8.4.4	UV / Solar Sun Side Experiments Demonstrate Contaminant Removal Potential.....	322
6.9	Conclusions	322
6.9.1	1,4-Dioxane Degradation Potential	323
6.9.2	Experimental Results Verify First Order Process	323
6.9.3	Experimental Results Suggest Diffusion Temperature Dependency	324
6.9.4	Various Operational Conditions Impact Diffusion Processes	324
6.9.5	Diffusion Plus Other Contaminant Elimination Processes.....	325

TABLE OF CONTENTS - *Continued*

6.9.5.1 UV / Solar Grey Tub and Pool Experimental Site Side Experiments	325
6.9.6 Open Pond Treatment for Full-Scale Wetland Operation	326
6.9.6.1 Constraints of Contaminant Remediation Using Open Ponds.....	326
6.10 Future Research.....	327
7.0 SUMMARY	328
7.1 Future Study Recommendations	333
7.1.1 General	333
7.1.2 Specific.....	334
APPENDIX A. SCHEDULE AND RECORDED MEASUREMENTS	
EXPERIMENTAL RUNS 1-6.....	336
APPENDIX B. CALIBRATION AND DATA VALIDATION	362
B.1 Equipment Calibration.....	362
B.1.1 Calibration Solutions	362
B.1.2 Bromide Tracer Calibration.....	363
B.1.3 pH Calibration.....	365
B.1.4 Conductivity Calibration.....	366
B.1.5 Turbidity Calibration	367
B.1.6 TDR Probe Calibration	369
B.1.7 Dissolved Organic Carbon Calibration.....	369
B.1.8 1,4-Dioxane Calibration.....	370
B.1.9 Calibration Results.....	373
REFERENCES	385

LIST OF ILLUSTRATIONS

Figure 2.1. Molecular Structure of 1,4-Dioxane.....	31
Figure 3.1. Schematic layout of wetlands at the Constructed Ecosystems Research Facility in Tucson, AZ. The wetlands received and treated secondary effluent from the Roger Road Wastewater Treatment Plant.....	83
Figure 3.2. Aerial Photo of steel tank wetland demonstration system located adjacent to the CERF wetlands in Tucson, AZ.	85
Figure 3.3. Discharge Collection Tanks C & D.....	88
Figure 3.4. Solar Experimental Ponds.	88
Figure 3.5. Retaining Wall Between Tanks C & D and Ponds 1 & 2.....	89
Figure 3.6. Discharge Collection Tanks C & D.....	90
Figure 3.7. Bulk Density of Replaced Sand in Experimental Tanks 1 & 2.	91
Figure 3.8. Experimental Site Valve and Piping Layout.	95
Figure 3.9. Remediation Site Layout Pictorial.....	101
Figure 3.10. Experimental Runs 1 – 6 Total Pond Volume (Discharge plus Rain minus Pan Evaporation).....	108
Figure 3.11. Experimental Run 4,5, & 6 Total Pond Volume (L) based on water depth measurements.....	110
Figure 3.12. Bromide Tracer Study Sample Locations.....	114
Figure 3.13. Cumulative recovery (in percent) of the bromide tracer from Tanks 1 and 2.	117
Figure 3.14. UV Cs-Te Photodiode Typical Detector Response (Ryer, 1998).....	131
Figure 3.15. UV-B One Day Solar Radiation.....	132
Figure 3.16. UV-B One Day Response with NS254 Filter.....	133
Figure 3.17. UV Lamp with Flow-Through Cell.....	137
Figure 3.18. Solar Light Connection to Spiked Flow.	138
Figure 3.19. Solar Experiment Set-Up.....	139
Figure 3.20. Filter Flasks and Vacuum Manifold.....	144
Figure 3.21. Typical GC Chromatogram Showing 1,4-Dioxane Peak Position at 2.083 minutes.....	152
Figure 3.22. Typical Area Percent report showing Detector Response Integrated Area Summary. The 1,4-Dioxane Peak is at 2.083 Minutes.	152
Figure 4.1. Bromide Tank Discharge Tracer Results.	169
Figure 4.2. Tank 1 Pre-Experiment Bromide Tracer Study Results.....	170
Figure 4.3. Tank 1 Bromide Tracer Study QTRACER2 Program Output.....	175
Figure 4.4. Bromide Tracer Breakthrough Curve Exp. Runs 1 – 6, Tank 1.....	183
Figure 4.5. Bromide Tracer Breakthrough Curve Exp. Runs 1 – 6, Tank 2.....	183
Figure 4.6. Experimental Run # 6 Tracer & 1,4-Dioxane.	185
Figure 4.7. Rainfall Events During Experimental Runs 1 – 6.	187
Figure 4.8. Exp. 3-6 Tank 1 Pan Evaporation to Percent Bromide Tracer Mass Loss..	190
Figure 4.9. Experimental Runs 1-3 Surge Tank Flow.	196
Figure 4.10. Wetland Tank Total Volume Discharge (L) for each Experiment.	197

LIST OF ILLUSTRATIONS - *Continued*

Figure 4.11. TDR Soil Moisture Tank 1 Midstream.....	200
Figure 4.12. TDR Soil Moisture Tank 1 Downstream.....	200
Figure 4.13. TDR Soil Moisture Tank 2 Midstream.....	201
Figure 4.14. Cottonwood Tree Height (cm).....	204
Figure 4.15. Correlation Cottonwood Tree Height and Chest Height Tree Diameter... ..	205
Figure 4.16. CERF Cottonwood Tree Height History.	207
Figure 4.17. AF Plant 4 Whip and Caliper Tree Height.	209
Figure 4.18. AF Plant 4 Whip and Caliper Tree Trunk Diameter.	209
Figure 4.19. Experimental Run Transpiration Rate Vs. PM Air Temperature.	212
Figure 4.20. Water Temperature Readings from Covered and Uncovered Pools.	215
Figure 4.21. Monsoon and Winter Rainfall Measured at CERF from 1997 to 2006.....	219
Figure 4.22. CERF Average Monthly Humidity (2005).....	220
Figure 4.23. Tree Growth Height Pattern and Relative Position.	222
Figure 4.24. Average Tree Height by Category (H, M, L) and Influent Flow Rate.	224
Figure 4.25. Experimental Site UV Solar Radiation Measurements Conducted in 2004 at the Field Site.	226
Figure 5.1. Influent & Discharge Conductivity during Exp. 3 (Tap Water) & Exp. 5 (Secondary Effluent).....	238
Figure 5.2. Correlation Tank 2 Discharge Conductivity to Pan Evaporation Rate.....	240
Figure 5.3. Correlation of Tank 1 Discharge Conductivity to Total Transpiration Volume.....	241
Figure 5.4. Tank C & D pH for Experimental Runs 1-6.....	242
Figure 5.5. 1,4-Dioxane Experimental Run Sample Timeline.....	244
Figure 5.6. Experimental Run 1 – 6 Turbidity Results Tank 1 Discharge.....	245
Figure 5.7. Experimental Run 1 – 6 Turbidity Results Tank 2 Discharge.....	246
Figure 5.8. DOC Concentration in Discharge From Tank 1 and 2 (Experiment # 5) - Influent DOC averaged 15 mg/L.	247
Figure 5.9. 1,4-Dioxane Mass Removal from Tank 1 / Tank C Discharge Mass Balance Calculations.....	257
Figure 5.10. 1,4-Dioxane Mass Removal from Tank C and Tank D Discharge Mass Balance Calculations.....	259
Figure 5.11. Experimental Runs 3, 5, and 6 Planted Tank 1,4-Dioxane Uptake to ETo (in/day).....	260
Figure 5.12. Experimental Runs 3, 5, and 6 Planted Tank 1,4-Dioxane Uptake to Maximum Daily Temperature (°C).....	261
Figure 5.13. 1,4-Dioxane Cumulative Mass Recovery Percentage During Experimental Runs 3 - 6 From Tanks C and D.	273
Figure 5.14. Bromide Cumulative Recovery Percentage During Experimental Runs 3-6 From Tanks C and D.....	274
Figure 5.15. Tank D 1,4-Dioxane Mass Loss (%) Vs Pan Evaporation (mm/day) for Experimental Runs 3, 4, 6.....	276
Figure 5.16. Experimental Wetland Cottonwood Tree Growth (1 yr).....	281

LIST OF ILLUSTRATIONS - *Continued*

Figure 6.1. Water Temperature in Ponds 1 and 2 during Experimental Run # 4 (typical diurnal temperature variation).....	289
Figure 6.2. 1,4-Dioxane Remaining in Ponds (mg).	294
Figure 6.3. 1,4-Dioxane concentration correlated to contaminant reduction rate.	296
Figure 6.4. Characteristic Kinetic Plot of Exp 3 Pond 2 1,4-Dioxane Elimination.	298
Figure 6.5. First Solar/UV and Evaporation Side Experiment (one tub was covered)..	300
Figure 6.6. Second Trial of Solar/UV Side Experiment (one tank covered).	301
Figure 6.7. Remaining 1,4-Dioxane in Grey Tub and Pool Side Experiments (mg).....	302
Figure 6.8. Experimental Run # 6 Pond pH.....	307
Figure 6.9. Correlation Test for Arrhenius Relationship on Experimental Run 2 - 6 Pond 1 1,4-Dioxane Reduction Rate and Avg. Pond Temperature (°K).....	317
Figure 6.10. Correlation Test for Arrhenius Relationship on Experimental Run 2 - 6 Pond 2 1,4-Dioxane Reduction Rate and Average Pond Temperature (°K).	317
Figure B.1. Bromide Tracer Calibration Curve.	363
Figure B.2. DOC Calibration Curve.	370
Figure B.3. Initial GC 1,4-Dioxane Standard Curve.	372

LIST OF TABLES

Table 3.1. Bromide Tracer Sample Designations.....	115
Table 4.1. Tank 1 Discharge Bromide Concentrations (mg L ⁻¹) for Experimental Run 1-6 Lapse Time (Hr.).....	180
Table 4.2. Tank 2 Discharge Bromide Concentrations (mg L ⁻¹) for Experimental Run 1-6 Lapse Time (Hr.).....	181
Table 4.3. Experimental Run 3 – 6 Péclet Number.....	182
Table 4.4. Bromide Breakthrough Lapse Times (Hrs).....	184
Table 4.5. Tank 1 and 2 Bromide Mass Recovery to Input For Experimental Runs 2-6.....	190
Table 4.6. Experimental Run 1-6 Key Dates.....	193
Table 4.7. Influent Rate (L Hr ⁻¹) Tanks 1 and 2 Experimental Runs 4, 5, and 6.....	195
Table 4.8. Discharge Rate (L Hr ⁻¹) Tanks 1 and 2 Experimental Runs 4, 5, and 6.....	198
Table 4.9. TDR Average Soil Moisture Results.....	201
Table 4.10. Exp. Runs 1 – 6 Air and Subsurface Average A.M. & P.M. Temperatures (°C) in Tanks 1 & 2.....	213
Table 5.1. Specific Conductivity and Total Volume (Influent/Discharge) for Exp. 3-6 Tank 1 & 2 for Experimental Lapse Time Hours 71-251.....	239
Table 5.2. Measured 1,4-Dioxane Influent Concentrations (mg L ⁻¹) During Experimental Runs 3-6.....	248
Table 5.3. 1,4-Dioxane Wetland Tank Discharge Concentrations (mg L ⁻¹) During Experimental Runs 3-6.....	249
Table 5.4. 1,4-Dioxane Discharge Collection Tank Concentrations (mg L ⁻¹) During Experimental Runs 4 – 6.....	250
Table 5.5. 1,4-Dioxane Breakthrough Lapse Times (Hrs.).....	251
Table 5.6. Cumulative 1,4-Dioxane Mass (mg) in Discharge from Tanks 1 & 2 and Tanks C & D during Experiment 3.....	254
Table 5.7. Cumulative 1,4-Dioxane Mass (mg) in Discharge from Tanks 1 & 2 and Tanks C & D during Experiment 4.....	255
Table 5.8. Cumulative 1,4-Dioxane Mass (mg) in Discharge from Tanks 1 & 2 and Tanks C & D during Experiment 5.....	255
Table 5.9. Cumulative 1,4-Dioxane Mass (mg) in Discharge from Tanks 1 & 2 and Tanks C & D during Experiment 6.....	256
Table 5.10. Experimental Runs 3-6 1,4-Dioxane Uptake Rates.....	262
Table 5.11. Planted Tank Exp. Runs 3-6 Lapse Hr. 1,4-Dioxane Uptake Rates (mg L ⁻¹).....	263
Table 5.12. Comparison of Experimental Factors Related to Variable 1,4-Dioxane Uptake.....	270
Table 5.13. Experimental Runs 3 and 4 Environmental Factor Comparison.....	277
Table 6.1. Average Pond & Air Temperatures (°C).....	288
Table 6.2. Total Mass of 1,4-Dioxane Delivered to Pond 1 & 2 During Experimental Runs 4-6.....	290

LIST OF TABLES - *Continued*

Table 6.3. Mass of 1,4-Dioxane in Pond 1 & 2 in Experimental Run 4 – 6 at 191 hour lapse time.	292
Table 6.4. Experimental Runs 2-6 Ponds 1 and 2 First Order Rate Constants.	297
Table 6.5. Experimental Runs 2-6 Ponds 1 and 2 Contaminant Half-Life.	299
Table 6.6. First Order Rate Constants Derived from the Grey Tub and Kiddie Pool Side Experiments (18 days).	303
Table 6.7. Comparison of pond / pool / grey tub mass flux of 1,4-Dioxane.	304
Table 6.8. UV/Solar Light Side Experiment 1,4-Dioxane Percentage Reduction.	311
Table A.1. Schedule and Recorded Measurements – Experimental Run # 1.	336
Table A.2. Schedule and Recorded Measurements – Experimental Run # 2.	337
Table A.3. Schedule and Recorded Measurements – Experimental Run # 3.	339
Table A.4. Recorded 1,4-Dioxane GC Measurements – Experimental Run # 3.	342
Table A.5. Schedule and Recorded Measurements – Experimental Run # 4.	343
Table A.6. Recorded 1,4-Dioxane GC Measurements – Experimental Run # 4.	348
Table A.7. Schedule and Recorded Measurements – Experimental Run # 5.	349
Table A.8. Recorded 1,4-Dioxane GC Measurements – Experimental Run # 5.	354
Table A.9. Schedule and Recorded Measurements – Experimental Run # 6.	355
Table A.10. Recorded 1,4-Dioxane GC Measurements – Experimental Run # 6.	361
Table B.1. 1,4-Dioxane Standard and Extracted Calibration Curve Slopes and r^2 Values.	373
Table B.2. 1,4-Dioxane Standard Curve Ratio to Extracted Calibration Curves for 100, 1000, and 5000 mg L ⁻¹ (0.1, 1.0, and 5.0 extracted).	376
Table B.3. Experiment Run 3 Calibration Standard Results.	377
Table B.4. Experiment Run 4 Calibration Standard Results.	379
Table B.5. Experiment Run 5 Calibration Standard Results.	381
Table B.6. Experiment Run 6 Calibration Standard Results.	383

ABSTRACT

This research addressed the question whether a constructed wetland system with phytoremediation could successfully uptake 1,4-Dioxane in groundwater and secondary effluent. It further addressed whether open pond storage could successfully treat wetland discharge. The project was located at the University of Arizona's Constructed Ecosystems Research Facility (CERF) in Tucson, Arizona. This two-year field study was motivated by previous laboratory studies which demonstrated the capability of plants to remediate the recalcitrant contaminant 1,4-Dioxane.

The study was conducted in two open steel tanks configured to simulate constructed wetlands. The efficacy of 1,4-Dioxane uptake by cottonwood trees was tested in a side-by-side comparison utilizing planted and unplanted tanks. The sub-surface hydraulic conditions were fully characterized by bromide tracer studies. Six experiments were conducted, in which tapwater or secondary effluent was spiked with 5.2 mg L^{-1} 1,4-Dioxane and fed to the planted and unplanted (control) tank. The tank discharges were retained in separate open ponds to test if open pond storage would reduce 1,4-Dioxane content. Additional side experiments were conducted to examine the role of volatilization and UV degradation.

Comparison of 1,4-Dioxane mass discharge from the planted and the control tank demonstrated an 18-48 percent uptake by the cottonwood trees. Mass balance assessments showed 1,4-Dioxane uptake efficiency was positively correlated to

cottonwood transpiration rates in the planted tank. The open pond 1,4-Dioxane measurements demonstrated a 64-85 percent reduction in 1,4-Dioxane concentration due to volatilization during the initial 120 hours pond lapse time. Elimination of 1,4-Dioxane from the ponds followed first order kinetics. Field and laboratory side experiments demonstrated the potential for UV photo degradation of 1-4-Dioxane.

1.0 INTRODUCTION

1,4-Dioxane is an organic contaminant of emerging concern and a probable human carcinogen. Due to current usage and historic disposal practices, 1,4-Dioxane is a contaminant in municipal wastewaters and ground waters in the state of Arizona and elsewhere in the United States and world. Most 1,4-Dioxane contamination originates as a solvent additive or process by-product that is not removed from the consumer end item. The scarcity of potable water in the State of Arizona, and elsewhere in the United States, drives efforts to protect known water resources and expand water reclamation practices. Often future growth and development depend on demonstration and implementation of methods for removing trace organic contaminants, including 1,4-Dioxane, from water resources. As an emerging contaminant, limited scientific assessments, with widely varying conclusions, are available. A level of controversy historically accompanies most emerging contaminants until adequate scientific investigation resolves unknown elements. Some of the most recognized hazardous materials today (mercury, asbestos, beryllium, lead) had similar controversial histories.

The compound 1,4-Dioxane is used in numerous industrial processes and is contained in a variety of consumer and commercial products. It is widely used as a solvent in paper manufacturing and in paints and inks. Soaps and cosmetics containing ethoxylated surfactants may also contain 1,4-Dioxane (Mohr, 2001). World wide production was 8,000 – 10,000 tons in 1994 (Full Public Report, 1998). The state of California has

established an action level of 3.0 parts per billion (ppb) while Washington State has an action level of 7.0 ppb. The USEPA has established a drinking water health advisory for 1,4-Dioxane at 0.3 mg/L (U.S. EPA, 2002).

1,4-Dioxane is a possible human carcinogen classified Group 2B by the International Agency for Research on Cancer (IARC) in 1999. The liver is the critical organ for adverse effects from 1,4-Dioxane in chronic animal studies, where effects include hepatocyte degeneration, hyperplasia, adenoma, carcinoma and cholangioma (Ashby, 1994). Presently, there are only limited scientific assessments available for the fate, transport, toxicity, and remediation of 1,4-Dioxane and in some instances with widely varying conclusions. Recent studies have shown 1,4-Dioxane induced micronuclei of liver and bone marrow from chromosomal breakage and significant genotoxic effects on young CD-1 mice (Roy *et al.*, 2005).

As a contaminant in ground water, 1,4-Dioxane is particularly problematic due to its physical properties and resistance to biodegradation. It is very mobile in ground water due to its high solubility ($4.31 \times 10^5 \text{ mg L}^{-1}$), nonvolatile vapor pressure (37 mm Hg at 25 °C), and low log octanol-water partition coefficient ($\log K_{ow} = -0.27$). The compound is not retarded in aquifers and can cause widespread contamination in both surface and ground water (Beckett and Hua, 2003). Researchers at chlorinated solvent contamination sites (world wide) have discovered four times larger plumes containing 1,4-Dioxane. The 1,4-Dioxane plumes, previously undetected and fully miscible in water, are forcing

regulatory and remediation managers to seek new treatments to clean-up this recalcitrant solvent additive. The compound 1,4-Dioxane was primarily used as a solvent stabilizer in Trichloroethane (TCA) which was phased out of production by 1996. However, the groundwater TCA contamination that remains is making 1,4-Dioxane an emerging environmental contaminant of concern. As awareness increases of the potential exposure and health concerns, this is driving new toxicological research and regulatory guidance for its control and treatment.

Options for remediation/removal of 1,4-Dioxane in contaminated surface water or ground water are very limited. Alternatives include advanced oxidation processes (AOPs), specialized sorbents, and bioremediation. Currently available advanced treatment methods for 1,4-Dioxane removal are not cost effective and are ineffective for waters containing suspended solids. One emerging low cost treatment technology that has potential is phytoremediation. In a phytoremediation laboratory study, over 50 percent of 1,4-Dioxane was removed by transpiration (Aitchison *et al.*, 2000). Phytoremediation is a broad set of decontamination processes that utilize plants for *in situ* and *ex situ* treatment of contaminated soil, sludges, sediments, wastewater, and groundwater. The phytoremediation processes are phytoaccumulation, phytodegradation, phytostabilization, phytovolatilization, rhizodegradation, and rhizofiltration that result in contaminant degradation, removal, or stabilization (Mueller and Goswami, 2003). Phytoremediation has been utilized to remediate pesticides, metals, solvents, explosives, petroleum hydrocarbons, polycyclic aromatic hydrocarbons that have contaminated soils and a

variety of wastewaters including storm runoff, primary and secondary effluent, and industrial discharge (Green and Hoffnagle, 2004).

1.1 Objectives

This research evaluated phytoremediation and open pond storage as methods to remediate contaminant plumes and reduce the contaminant level in water sources, respectively. The primary research objective was to critically examine the uptake efficiency of 1,4-Dioxane contaminated water in a wetland/phytoremediation system. Field-based experiments were performed using tap-water (Phase 1) and secondary effluent (Phase 2) that were spiked with 1,4-Dioxane. A secondary objective was to examine the role of specific processes (volatilization, UV-photo degradation) on 1,4-Dioxane removal during open pond storage.

The primary research objective responds to the research question whether a wetland/phytoremediation system can remediate 1,4-Dioxane contaminated water. The research hypothesis proposed that cottonwood trees in a wetland system would uptake 1,4-Dioxane contaminated tap-water and secondary effluent. This hypothesis was supported by recent 1,4-Dioxane phytovolatilization laboratory experiments that achieved 50 percent uptake (Kelley *et al.*, 2001). An existing dual-chambered steel tank at the Constructed Ecosystems Research Facility (CERF) was utilized to replicate on-ground conditions of a sub-surface flow wetland. One steel tank was planted with Cottonwood

trees while the other steel tank remained unplanted (negative control). The steel tanks allowed a demonstration-scale field experiment without concern for possible soil and/or groundwater contamination. Comparison of the discharge contaminant mass from the two tanks established whether the Cottonwood wetland treatment system provided an enhanced remediation benefit.

The secondary research objective responds to the research question whether the specific processes of volatilization or UV-photo degradation would reduce the contaminant concentration in water. The research hypothesis proposed that both processes would remove 1,4-Dioxane from water. This hypothesis was supported in part by laboratory studies in which light-assisted 1,4-Dioxane oxidative degradation occurred under heterogeneous photocatalytic conditions in the presence of titanium dioxide and in homogeneous solution with inorganic peroxides (Maurino *et al.*, 1997). The discharge from the planted and unplanted tanks was pumped to open-air shallow ponds where UV/solar light exposure and volatilization could occur. The ponds were double lined allowing a demonstration-scale field experiment without the concern for possible soil and/or groundwater contamination. Contaminant concentration from each pond was measured over a period of several weeks to establish the removal effect of evaporation and UV-photo degradation.

1.2 Organization of Dissertation

A general literature review of the properties, toxicology, and treatment alternatives including advanced oxidation treatments, bioremediation options, and phytoremediation for 1,4-Dioxane is provided as Chapter 2.

Chapter 3 describes the field site preparation of the dual-chambered steel tank wetland system and the evaporation ponds. Methods are described for measurements of solar radiation and wetland tank hydraulics along with procedures for data collection, sample processing, and analytical methods for measurement of 1,4-Dioxane.

Results and discussion of wetland tank hydraulic characterization, subsurface wetland treatment, and open pond treatment are covered in Chapters 4, 5, and 6, respectively. Each chapter (4, 5, & 6) presents findings and conclusions that support the research objectives and form the basis for future independent publications.

Chapter 4 presents experimental tank hydraulics and operating parameters reflecting on impact to wetland plant growth. A quantitative evaluation of the pre-experimental run subsurface hydraulics in the planted and control tanks is given.

In Chapter 5, the 1,4-Dioxane uptake by cottonwoods was determined by mass balance. The efficiency of 1,4-Dioxane uptake was established by determining the transpiration stream concentration factor for the planted tank system.

In Chapter 6, the effect of volatilization and visible/UV light on 1,4-Dioxane removal is evaluated and the kinetics of removal is determined.

Chapter 7 summarizes the research findings and provides recommendations for future work. The findings are instructive for remediation method selection of 1,4-Dioxane contaminated waters subject to cleanup and water utilization goals.

2.0 LITERATURE REVIEW

2.1 1,4-Dioxane Background

2.1.1 1,4-Dioxane Properties

The compound 1,4-Dioxane ($C_4H_8O_2$), Figure 2.1, is a cyclic ether and is currently used as a solvent in numerous industrial organic products (paints, varnishes, inks, dyes, part of the surfactant mixture in fire fighting foams), and is found as a byproduct in many consumer products (cleaners, cosmetics, shampoos, laundry detergents) (Stickney *et al.*, 2003).

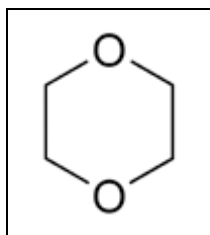


Figure 2.1. Molecular Structure of 1,4-Dioxane.

It is also a natural component in certain foods such as tomatoes, shrimp, and coffee (Stickney *et al.*, 2003). There are 19 synonyms for 1,4-Dioxane (e.g. Diethylene dioxide, Glycol ethylene ether, Tetrahydro-*para*-dioxin, 1,4-dioxacyclohexane, Dioxane) (Full Public Report, 1998). The molecular weight is $88.12 \text{ g mole}^{-1}$ and the boiling point is $101.5 \text{ }^\circ\text{C}$. 1,4-Dioxane is a Lewis base due to the two oxygen atoms having electrons to

share (Mohr, 2001). The two oxygen atoms (Figure 2.1) make 1,4-Dioxane hydrophilic and infinitely soluble in water. The ether functional groups are not capable of hydrogen bonding to each other, but the electronegative oxygen atoms have a partial negative charge capable of interacting with the O-H dipoles of water molecules (Vallombroso, 2001). Ethers such as 1,4-Dioxane are very stable requiring approximately 360 kJ mol^{-1} of energy for cleavage (Zenker *et al.*, 2004). This stability, under a wide variety of conditions, makes 1,4-Dioxane very suitable for use as an organic solvent.

2.1.1.1 1,4-Dioxane Water Contamination

The photooxidation half-life of 1,4-Dioxane in water, by reaction with aqueous hydroxyl radicals, is one year (Mohr, 2001) to 9 years (Full Public Report, 1998). Its hydrophilic nature and low octanol/water partition coefficient (-0.27), prevents significant bioconcentration in aquatic organisms (Mohr, 2001). In Japan, 1,4-Dioxane was decreased by 50-60 percent in acclimatized activated sludge from a chemical plant. The 1,4-Dioxane was readily desorbed from the sludge with water (Abe, 1999).

The compound is very resistant to biodegradation. Laboratory studies have shown that indigenous microorganisms in soil and waste water are not effective in degrading 1,4-Dioxane (Zenker *et al.*, 2004). One year-long tests of the compound in wastewater treatment plant effluent showed no degradation at concentrations from 100 to 900 parts per million (Klecka and Gonsior, 1986). If present in sewage sludge applied on

farmland, it would be mobilized by rainwater. Fugacity modeling by the U.S. EPA predicts partitioning of 1,4-Dioxane as 91 percent to water and 9 percent to air (Full Public Report, 1998).

2.1.1.2 1,4-Dioxane Air Contamination

In the air, 1,4-Dioxane can degrade through reaction with OH radicals to produce alkyl radicals. This reaction starts with the H atom abstraction followed by the addition of O₂ to form a cyclic alkylperoxy radical (Maurer *et al.*, 1999). In the presence of NO_x a reaction opens the chain producing an alkoxy radical. A reaction with O₂ produces peroxy radicals that react again with oxygen to produce the primary product ethylene glycol diformate (EDF) (Geiger *et al.*, 1999). The rate coefficient for this reaction is $1.24 \times 10^{-11} \text{ cm}^3 \text{ molecule}^{-1} \text{ s}^{-1}$ as reported by Maurer *et al.* (1999). The EDF reacts with •OH radicals and Cl atoms with a rate coefficient of $4.27 \times 10^{-13} \text{ cm}^3 \text{ molecule}^{-1} \text{ s}^{-1}$ and $3.52 \times 10^{-12} \text{ cm}^3 \text{ molecule}^{-1} \text{ s}^{-1}$, respectively. The compounds 1,4-Dioxane and EDF have a maximum lifetime in the troposphere of 22.4 hours and 24 days, respectively. The primary atmosphere loss process of the alkyl diformates is by gas phase reaction with •OH radicals and wet precipitation. Both processes will result in acid formation (formic) which could lead to additional atmosphere acid burden (Maurer *et al.*, 1999). A similar 1,4-Dioxane oxidization study by Platz *et al.* (1977) show the residence time of 1-2 days in the atmosphere.

2.1.2 1,4-Dioxane Contamination in the Environment

The contamination in the environment caused by 1,4-Dioxane can be due to both point and nonpoint sources. Point sources include spills and previous land disposal practices. Nonpoint sources include wastewater effluent discharged to waterways.

2.1.2.1 Primary Contaminant Sources

The compound 1,4-Dioxane (C₄H₈O₂, CAS No., 123-91-1) is a colorless, flammable liquid with a faint, pleasant odor. It has a moderate boiling point (101 °C) and its vapors are heavier than air (U.S. EPA, 1996). It is made by heating and distilling diethylene glycol with a dehydrated catalyst such as sulfuric acid (Ahn-Ercan *et al.*, 2006).

Historically, the bulk of 1,4-Dioxane contamination in groundwater resulted from its use as an industrial solvent stabilizer. The 1,4-Dioxane acted as an acid scavenger in TCA chlorinated solvents and would concentrate in degreaser stills and sumps at approximately 8 percent by volume. Where TCA groundwater contamination existed, there is a high correlation ($r^2 = 0.87$) of finding 1,4-Dioxane contamination. The decrease in use of TCA has concurrently diminished 1,4-Dioxane contamination occurrence but the existing contamination plumes persist in the environment (Mohr, 2001).

2.1.2.2 Secondary Contaminant Sources

1,4-Dioxane is used as a solvent/reagent in the manufacture of pharmaceutical products and is a compound remaining from the manufacturing of surfactants used in cosmetics and detergents. It is a component in paint and varnish, and is a wetting and dispersion agent used in the textile industry. Adhesive products used in celluloid film processing, contain 1,4-Dioxane and it is a residue in the manufacture of organophosphorus fire retardant and fire fighting foams, and an impurity formed during the manufacture of alkyl ether sulphates and other ethoxylated substances. It is found in commercially available shampoos, cosmetics, liquid soaps, and lotions in concentrations from 3.4-108 mg kg⁻¹ unless the manufacturing process utilizes vacuum removal (Italia and Nunes, 1991). Measurements of 1,4-Dioxane reported by Black *et al.* (2001) in cosmetics were up to 279 mg L⁻¹ and over 85 mg L⁻¹ in children's shampoos. In consumer products, such as shampoos, 1,4-Dioxane is created through the dimerization of ethylene oxide during the forming of polyethoxylated alcohols.

2.1.2.3 Contaminant Recalcitrance

As a result of its presence in a wide variety of consumer products, it is all but certain that 1,4-Dioxane is present in municipal wastewater. As a contaminant in ground water, 1,4-Dioxane is particularly problematic, because of its physical properties and resistance to biodegradation. The vapor pressure of 1,4-Dioxane at 25 °C (37 mm Hg) suggests

volatilization is possible but the low Henry's constant (3×10^{-6} atm-m³/mol) indicates transfer of this contaminant from water to air is negligible (Mohr, 2001). It is very mobile in ground water with a high solubility (4.31×10^5 mg L⁻¹) and low log octanol-water partition coefficient ($K_{ow} = -0.27$). With a low organic carbon partition coefficient (K_{oc} 1.23), 1,4-Dioxane will not sorb to suspended sediments or soil. Many 1,4-Dioxane-contaminated aquifers in the United States are the result of land disposal of 1,1,1-trichloroethane (TCA). In most TCA-contaminated aquifers, 1,4-Dioxane has migrated significantly beyond the chlorinated solvent plume and contaminates a volume 8-10 times greater than the TCA (Walsom and Tunnicliffe, 2002).

2.1.2.4 World Wide Use and Contamination

Its continuing use and persistence in the environment is demonstrated by world wide contamination of 1,4-Dioxane. With the advent of improved extraction techniques from environmental samples and advances in detection methods using gas chromatography - mass spectroscopy (GC-MS), reports of 1,4-Dioxane contamination in the environment are increasing worldwide. For example, in the Niigata Prefecture, Japan, 1,4-Dioxane was found in river water impacted by industrial discharge, residential sewage discharge, and hazardous waste disposal sites at concentrations of 0.4-4,020 µg L⁻¹, 1.0-97 µg L⁻¹, and 1.1-109 µg L⁻¹, respectively (Kawata *et al.*, 2003). A later study of 91 surface and groundwater treatment plants in Japan found low levels of 1,4-Dioxane in 42 percent of the water samples (Simazaki *et al.*, 2006). At the Gloucester Landfill in Ontario, Canada,

1,4-Dioxane was detected in ground water located 100 meters away from the landfill site at concentrations ranging from 100-500 $\mu\text{g L}^{-1}$ (Woodbury *et al.*, 1998). In Sydney, Australia, the use of solvents contributed to a 1,4-Dioxane concentration of 61 $\mu\text{g L}^{-1}$ in raw sewage (Full Public Report, 1998).

2.1.2.5 United States 1,4-Dioxane Contamination

In the United States, 1,4-Dioxane contamination in ground water ranged from 0.1 to 2.5 mg L^{-1} in 37 percent of samples taken near a landfill site in Delaware in 1977 (Full Public Report, 1998). The U.S. occurrence of 1,4-Dioxane has been documented at various public water supply systems such as the Norwalk system serving Southern California, with a concentration range of 2-21 $\mu\text{g L}^{-1}$ in the 2004 public water quality report. In Bally, Pennsylvania, low levels of 1,4-Dioxane were detected at an EPA groundwater remediation site. As of 2007, a feasibility study is currently underway to determine the best method to treat this newly-discovered contaminant (Cron, 2005).

2.1.2.6 State of Arizona 1,4-Dioxane Contamination

In the state of Arizona, 1,4-Dioxane is a known groundwater or landfill contaminant at several sites. Contaminated groundwater sites include Potrero (Nogales), Motorola (Phoenix), and the Tucson Airport TIAA CERCLA site (Karura, 2002). At the Tucson airport site, concentrations of 1,4-Dioxane in ground water range from 5-25 $\mu\text{g L}^{-1}$ in a

plume significantly larger than the current trichloroethylene (TCE) remediation area (Modeer, 2002). Previous remediation efforts for TCA utilizing pump and treat air stripping technologies have shown to be ineffective in removing 1,4-Dioxane from the ground water (Walsom and Tunnicliffe, 2002).

2.1.2.7 Potential Contaminated Areas in Arizona

Other sites, including landfills, contaminated with 1,1,1-TCA include United Musical Instruments, Nogales; Indian Bend Wash, Tempe; Allstate Sub-site, Tempe; and the Bennett Family Landfill, Phoenix. These sites are likely also contaminated with 1,4-Dioxane since it was an approximate 8 percent constituent of TCA until 1996.

Throughout Arizona, several National Priorities List sites were contaminated with TCA and TCE. These sites may have groundwater plumes of 1,4-Dioxane. Further, biosolids containing 1,4-Dioxane have been applied to fields where runoff may have carried 1,4-Dioxane into ground water. Other sites, such as the Superfund site for United Musical Instruments, Nogales, Arizona, may contain significant levels of 1,4-Dioxane in perched water tables. The potential exists for the movement of 1,4-Dioxane through the saturated clay soil of the perched contamination zone. As one example of the emerging nationwide concern regarding 1,4-Dioxane, ground water in Orange County, California has become contaminated with 1,4-Dioxane as a result of direct injection of finished product water from Water Factory 21, an advanced wastewater remediation plant. The presence of 1-4-

Dioxane in Water Factory 21 product water was highly surprising and caused considerable local concern. The finished water is injected to the local aquifer to prevent seawater intrusion. Water Factory 21 treats secondary effluent to near distilled water quality using a combination of treatment steps including microfiltration, reverse osmosis, and UV disinfection. In 2000, routine groundwater monitoring detected 1,4-Dioxane at a concentration of $17 \mu\text{g L}^{-1}$ (Mohr, 2001). As a result, Orange County completed a second feasibility study to consider other treatment technologies such as advanced oxidation techniques for remediation of 1,4-Dioxane in contaminated surface water or ground water. Currently available advanced treatment methods for 1,4-Dioxane are not cost effective and are ineffective for waters containing suspended solids. The California Department of Health Services has established an action level of $3 \mu\text{g L}^{-1}$ for 1,4-Dioxane (Walsom and Tunnicliffe, 2002).

2.1.2.8 1,4-Dioxane Environmental Risk Assessment

Australia's environmental risk assessment results indicate most 1,4-Dioxane winds up in sewage and thus is received by wastewater treatment plants. Fifty to sixty percent of 1,4-Dioxane partitioned to an acclimatized activated sludge, but was easily desorbed with water from the sludge (Abe, 1999). Land applied sludge containing 1,4-Dioxane will likely leach to ground water, based on the estimated log soil adsorption coefficient (K_{oc}) of 1.07. Rapid degradation (half life of < 7 hours) of 1,4-Dioxane is expected in the atmosphere, but photo oxidation half life in water, based upon measured rates for reaction

with hydroxyl radicals in water, is up to 9 years (Full Public Report, 1998). The recalcitrant properties of 1,4-Dioxane allow it to exist in the natural environment for extensive periods of time (Beckett and Hua, 2003).

2.1.3 1,4-Dioxane Toxicology

The emerging environmental contaminant, 1,4-Dioxane, is listed as a Group 2B probable human carcinogen by the U.S. EPA. Limited scientific assessments available for 1,4-Dioxane have widely varying conclusions resulting in controversy regarding human health effects. Health effect controversy historically accompanies most emerging contaminants until adequate scientific investigation resolves unknown elements.

2.1.3.1 Chronic Effects to 1,4-Dioxane Exposure

Effects from long-term exposure to 1,4-Dioxane in humans are not well characterized. Epidemiological studies of workers potentially exposed to 1,4-Dioxane show significant increases in the incidence rate of liver cancer (OEHHA, 2003). Other animal studies have shown that chronic exposure to 1,4-Dioxane induces adverse effects in the liver (Ashby, 1994).

Chronic effects observed in animals include lesions (neoplastic and non-neoplastic) in kidney, liver, nose, testes, lung and spleen. The chronic no observed adverse effect levels

(NOAELs) in rats for oral exposure to 1,4-Dioxane is 10-40 mg kg⁻¹day⁻¹. The International Agency for Research on Cancer (IARC) classifies 1,4-Dioxane in Group 2B as possibly carcinogenic to humans (Simazaki *et al.*, 2006). The carcinogen slope factor (CSF) for 1,4-Dioxane is 0.011 mg kg⁻¹day⁻¹ and the health based limit (HBL) at 10⁻⁶ risk level is 0.003 mg L⁻¹. A reference dose (RfD) and a maximum contaminant level (MCL) have not been established for 1,4-Dioxane (U.S. EPA, 1996) but various exposure limits have been established. The limit for OSHA PEL is 100 mg L⁻¹ (360 mg m⁻³) with an assigned "skin notation" indicating the potential for dermal absorption. The ACGIH TLV for dermal exposure is 25 mg L⁻¹ and 90 mg m⁻¹ for inhalation. The NIOSH IDLH is 500 mg L⁻¹ (U.S. EPA, 1996).

2.3.1.2 Contaminant Acute Exposure Toxicity

Toxicity data indicate that acute exposure to 1,4-Dioxane can cause respiratory irritation, headache, nausea, vomiting, drowsiness, dizziness, and central nervous system depression. Chronic exposure can cause liver and kidney damage in animals. The established LD50 for acute exposure in rats via the oral route is 5,200 mg kg⁻¹. The LC50 for rats via the inhalation route is 46 gm m⁻³ (U.S. EPA, 1996).

2.3.1.3 1,4-Dioxane Target Organ Toxicology

A critical organ for adverse effects from 1,4-Dioxane in chronic animal studies is the liver, where effects include hepatocyte degeneration, hyperplasia, adenoma, carcinoma and cholangioma. It is considered a weak genotoxin due to its unexpected activity as a rat nasal carcinogen (Ashby, 1994). Previous testing for rat DNA damage is insufficient to clearly establish either a linear or non-linear low dose relationship (Kitchin and Brown, 1994); (McFee *et al.*, 1994). As a result, newer pharmacokinetic models (PBPK) suggest the EPA CSF overestimates the potential cancer risk from 1,4-Dioxane (Stickney *et al.*, 2003). The controversy will likely be resolved with a formal reevaluation of the carcinogenic potency. In the interim, a wide array of action levels will exist such as The Transport Canada "action level" of $66.5 \mu\text{g L}^{-1}$ while the guideline in California is $3 \mu\text{g L}^{-1}$ and $7 \mu\text{g L}^{-1}$ in Washington State (Walsom and Tunnicliffe, 2002).

2.3.1.4 Contaminant Genotoxic Effects

A recent study to determine 1,4-Dioxane genotoxic effects on bone marrow erythrocytes and liver hepatocytes has been conducted on male and female mice. The results show dose related increases in micronuclei for both the liver and bone marrow. Further analysis determined the induced micronuclei of both tissues originated from chromosomal breakage. Decreases in hepatocyte proliferation as well as the ratio of bone marrow PCE:NCE were observed. At doses between $2,500\text{-}3,500 \text{ mg kg}^{-1}$, 1,4-Dioxane

exerts significant genotoxic effects on young CD-1 mice (Roy *et al.*, 2005). These results are in stark contrast to the negative results in other standard genotoxicity assays.

2.1.4 Pre-Concentration Techniques

A number of analytical techniques can be used to determine the concentration of 1,4-Dioxane in water samples. Technique options include sample preparation processes (filtration, concentration, extraction) and the choice of analytical instrument for quantification. Common analytical techniques/instruments include direct aqueous injection (DAI) gas chromatography, purge and trap gas chromatography and mass spectrometry (GC-MS), and gas chromatography with flame ionization detection (GC-FID). Factors for selecting appropriate process and equipment relate to contaminant concentration, matrix effects, accuracy requirements, and equipment capabilities.

Most aqueous samples need pre-concentration prior to analysis in a gas chromatograph (GC). The common techniques include liquid-liquid extraction (LLE), solid phase extraction (activated carbon, resin adsorption, solid phase micro-extraction), and liquid-gas extraction (static head-space, dynamic head-space). No concentration is required for DAI. However with DAI, the water can damage the column, disrupt the chromatograph, and result in errors due to low concentrations. An experiment determining 1,4-Dioxane in glycols by Pundlik *et al.* (2001) detected the contaminant in water using DAI with a packed column (OV-351). Their concern for deterioration of column performance

required switching to a capillary column (BP20) (Pundlik *et al.*, 2001). Success detecting 200 mg L⁻¹ concentrations of 1,4-Dioxane with DAI was demonstrated using a 105 meter megabore (0.53 mm id) capillary column with a packed column inlet. The injection volume was limited to 1 µL because larger volumes would extinguish the FID flame (Draper *et al.*, 2000).

2.1.4.1 Solid Phase Extraction

Solid phase extraction has been used successfully for recovering 1,4-Dioxane from water samples. A study involving activated carbon disks utilized 80 ml groundwater samples and 1.2 ml acetone to achieve 98% recovery of 1,4-Dioxane. The procedure required 30 minutes of repeated in-vial ejections of solvent to elute the 1,4-Dioxane from the carbon disks (Isaacson *et al.*, 2006). Another experiment utilized a styrene divinyl benzene cartridge in series with an activated carbon cartridge (AC-2) eluted with acetone and measured on a GC-MS (Park *et al.*, 2005). Both SPE experiments above indicated problems with higher concentrations of 1,4-Dioxane resulting from breakthroughs. Utilizing a modified SPE method for detecting 1,4-Dioxane in cosmetics demonstrated success with µg L⁻¹ detection limits. The process utilized cosmetics in an aqueous sample extracted by single contact liquid-liquid extraction followed by SPE and eluted with acetonitrile (Song and Zhang, 1997).

2.1.4.2 Single Contact Liquid-Liquid Extraction

Single contact liquid-liquid extraction (LLE) can elute 1,4-Dioxane from water samples. Research results report varying levels of success. Draper *et al.* (2000), concluded the partition coefficients for 1,4-Dioxane lead to low recoveries in single contact LLE. Further, large solvent to water ratios are needed for successful elution (Draper *et al.*, 2000). Another study concludes that single contact LLE is a convenient and reliable method to detect low ($\mu\text{g L}^{-1}$) levels of 1,4-Dioxane in water with recoveries ranging from 86-102 percent (Park *et al.*, 2005).

2.1.4.3 Purge and Trap Techniques

A consensus among researchers was found regarding the purge-and-trap technique to separate 1,4-Dioxane from water samples. While the U. S. Environmental Protection Agency approves Method 1624, the technique has problems with interferences and poor purge efficiency (Song and Zhang, 1997). The results from one study show 1,4-Dioxane detection limits at 100 times higher than similar volatile organic compounds due to the poor purge efficiency (Draper *et al.*, 2000). Another study showed memory effect of the trap portion and gave higher detection method limits (Park *et al.*, 2005).

2.1.4.4 Continuous Liquid-Liquid Extraction (LLE)

The continuous LLE method has been utilized successfully in numerous labs to extract low $\mu\text{g L}^{-1}$ concentrations of 1,4-Dioxane from groundwater. The method employs extraction vessels operated for a minimum of six hours and containing one liter samples with 100 ml solvent (Isaacson *et al.*, 2006). The U. S. Environmental Protection Agency Method 8270C outlines the procedure for continuous LLE with isotope dilution and GC-MS analysis for determining semi-volatiles (1,4-Dioxane). The EPA laboratory analytical methods for continuous LLE are outlined in the EPA Analytical Methods for AROCLORS (U.S. EPA, 2005). Determination of 1,4-Dioxane at trace levels requires efficient extraction, enrichment, and sensitive quantification. Continuous LLE extractors utilizing methylene chloride have extraction efficiencies of 70-75 percent after a 6 hour extraction period (Draper *et al.*, 2000). The one liter sample with a final 1 ml extraction volume yields a 1000-fold concentration factor that greatly improves the overall detection sensitivity. The useful level of quantitation lower limit for continuous LLE extraction is $0.2 \mu\text{g/L}$ (Draper *et al.*, 2000). A Corning (NY, USA) Model 3915 continuous LLE extraction apparatus, having a hydrophobic membrane, was utilized in Draper *et al.* (2000) experiments. The apparatus was operated in accordance with the manufacturers instructions with the condenser cooled to $6\text{ }^{\circ}\text{C}$ and the solvent heated to $85\text{ }^{\circ}\text{C}$. The sample was concentrated to approximately 2 ml and then nitrogen evaporated to 1 ml (Draper *et al.*, 2000).

2.1.4.5 U.S. EPA Vacuum Distillation Method

The U.S. Environmental Protection Agency has established Method 8261A for extracting volatile organic compounds by vacuum distillation in combination with GC-MS (VD-GC-MS) (U.S. EPA, 2006). The vacuum distillation process effectively concentrates the sample by 10-fold. This method was marginal in determining trace levels of 1,4-Dioxane in Triton-100 raw materials with GC-MS (Poss *et al.*, 2003). A new extraction process for the separation of 1,4-Dioxane from water is in development. This technique utilizes a recently developed electroosmotic membrane separation process. Early development has demonstrated increased separation of 1,4-Dioxane as the concentration or the electrical potential increases. The process is limited to components with similar boiling temperatures which also have a large difference in dielectric constant (Jain and Srivastava, 1996).

2.1.5 1,4-Dioxane Gas Chromatography / Detection

2.1.5.1 Gas Chromatography Principles

Gas chromatography (GC) methods separate target analytes from each other and from matrix components and the solvent. This is accomplished by partitioning the compounds between a stationary phase (the column packing or coating) and a moving phase (a gas). Compounds with minimal partitioning into the stationary phase elute first. Compounds which absorb to the column have slower elution times (retarded). Henry's law ($q=Bc$)

governs the partitioning of the concentration of analyte in the stationary phase (q) and the concentration of analyte in the gas phase (c). The measure of adsorption of the analyte in the adsorbent is a constant (B) (Littlewood, 1970). The partition constant (coefficient) is a function of the vapor being eluted and operating variables of the column. The column variables include dead volume, pressure drop across the column, and weight/composition of stationary phase. Thermodynamic variables of the eluted vapor include its chemical nature and the temperature of the column (Littlewood, 1970). Since elution is based on physical properties, retention time is an attribute of a molecule and can be used to determine identity when analyzed on similar columns and conditions.

2.1.5.2 Gas Chromatography Key Factors

Stationary phase composition and thickness are key factors in selecting a column to elute a specific compound such as 1,4-Dioxane. 1,4-Dioxane contains electronegative oxygen molecules that possess a partial negative charge. This negative charge is capable of interacting with the O-H dipoles of water molecules. The extracting solvent (methylene chloride) is non-polar requiring the column stationary phase to also be non-polar. Non-polar solvents typically separate compounds in the order of their boiling points. For surface coated open tubular (SCOT) small diameter (0.252 mm) capillary columns, the stationary phase thickness should have a beta value of 16-100 based on the molecular weight of 1,4-Dioxane ($88.12 \text{ g mole}^{-1}$) (Guy, 2003). The beta value is calculated from the internal diameter of the column divided by the thickness of the stationary phase times

four. The use of capillary columns can limit the injected sample size or require the injected sample to be split at the injection point. The type and thickness of the stationary phase also determines the injected sample size based on the efficiency of the capillary column. The column efficiency places demands on the instrument data collection capability to ensure an accurate representation of the eluted peak is obtained (Guy, 2003).

2.1.5.3 Gas Chromatography Detectors

The eluted peak (based on plug flow of the injected sample) is quantified by a sensitive detector response to either the concentration or mass flow of the vapor entering the detector. Detectors typically utilized for determination of 1,4-Dioxane are mass spectrometry (MS) or flame ionization detection (FID).

2.1.5.3.1 Flame Ionization Detectors

In FID detectors, the response is proportional to the mass flow of the vapor. The area count under the peak provides a measurement of the compound of interest. The FID detector responds to the ionized gas of the compound being eluted but is insensitive to the carrier gas (Helium) and common inorganic chemicals (Littlewood, 1970). FID detection is linear over a range of six decades and is independent of gas flow rate. In FID, the gas sample is introduced to a hydrogen/oxygen flame that ionizes the organic compounds. The ionized particles migrate to a charged detector plate that produces an electric current

in proportion to the mass flow of the particles (U.S. Army Corps of Engineers, 1997).

The sensitivity of FID for 1,4-Dioxane is in the low parts per million.

2.1.5.3.2 Mass Spectrometry Detectors

The other common detection method for 1,4-Dioxane is mass spectrometry (MS). The MS instrument interfaces with the column discharge from a GC unit. The detector converts a small sample of the gas into electrically charged ions (U.S. Army Corps of Engineers, 1997). The MS mass filter separates the ions by charge on the ion and by mass. This separation is accomplished by a quadrupole mass filter. Only at a specific predetermined frequency can the ion of interest impact the electron multiplier detectors causing electrons to be ejected. The number of electrons is directly proportional to the number of ions reaching the detector (Knight, 1996). Mass spectrometry identifies the chemical composition of the sample by measuring the molecular weights and fragments of its molecules (U.S. Army Corps of Engineers, 1997). Each element has its own mass spectrum (or signature) that can be identified and quantified. The disadvantage of MS is the complexity and cost of the instrumentation. It can detect 1,4-Dioxane at parts per billion concentrations.

2.1.5.4 Experimental Determination of 1,4-Dioxane

The experimental determination of 1,4-Dioxane in glycols by Pundlik *et al.* (2001) demonstrated GC-FID detection capability of 2 mg L^{-1} using both packed and capillary columns. The experimental study by Song *et al.* (1997) demonstrated GC-MS detection limits of $0.05 \text{ } \mu\text{g ml}^{-1}$ using a 1 ml sample. In a laboratory methods study utilizing both FID and MS in detecting 1,4-Dioxane, direct aqueous injection into a FID had a detection limit of $2 \text{ } \mu\text{g ml}^{-1}$. Samples prepared by LLE were analyzed both by GC-FID and GC-MS. The GC-FID utilized a 105 meter megabore column operated isothermally at $90 \text{ } ^\circ\text{C}$ with $2 \text{ } \mu\text{l}$ injection volumes. The lower FID detection limit was $0.1 \text{ } \mu\text{g ml}^{-1}$ with external standards due to the 1,4-Dioxane and internal standard not being completely resolved (Draper *et al.*, 2000). The GC-MS method utilized $1 \text{ } \mu\text{l}$ or $5 \text{ } \mu\text{l}$ injection volumes and a 30 meter X 0.25 mm i.d. DB-5 capillary column. The MS was specifically tuned to improve sensitivity to 1,4-Dioxane with a reduced scan range. The MS detection limit was $1.1 \text{ } \mu\text{g L}^{-1}$ for groundwater samples (Draper *et al.*, 2000).

2.2 Remediation

A number of alternative remediation technologies are potential candidates for clean-up of 1,4-Dioxane contaminated sites. The technologies range from simple in-situ enhancement of natural microorganisms to costly advanced oxidation processes. Some remediation technologies do not have consensus on their potential for success (carbon

adsorption, air stripping) while other technologies have a more universal acceptance but have not had wide field testing (phytoremediation, biodegradation).

Proven options for remediation of 1,4-Dioxane at contaminated sites are limited. The more common methods (advanced oxidation processes (AOPs), specialized sorbents, and bioremediation) have operational and financial limitations. The conventional treatment technologies for TCE and TCA removal (i.e. air stripping and carbon adsorption) are ineffective in removing 1,4-Dioxane.

2.2.1 Advanced Oxidation Processes

A series of AOPs have been developed that utilize the generation of hydroxyl radicals ($\bullet\text{OH}$) as the oxidant. These processes include ozone and hydrogen peroxide, UV light and hydrogen peroxide, UV light and ozone, high energy electron beam, Fenton's reagent (hydrogen peroxide & ferrous iron- Fe II), and ultrasonic acoustic cavitation (Oppelt, 1998). Other AOPs which have potential include various combinations of these processes.

2.2.1.1 Photoinduced Oxidation Using UV Light and Hydrogen Peroxide

The photoinduced oxidation method using UV light and hydrogen peroxide has proven to be very efficient in removal of 1,4-Dioxane from ground and river waters. An

experimental analysis of the process showed the degradation rate of 1,4-Dioxane correlated well with the fraction of UV absorbed by the hydrogen peroxide. The homogeneous light driven process occurs in dilute aqueous solutions (1 mM 1,4-Dioxane, 15 mM H₂O₂) where the bulk of UV light absorbed by the hydrogen peroxide (58.8 percent) create hydroxyl radicals by direct photolysis (Stefan and Bolton, 1998).

The 1,4-Dioxane absorbs only 0.15 percent of the UV light producing minimal direct photolysis. The •OH radicals react with 1,4-Dioxane producing several intermediates as aldehydes (formaldehyde, acetaldehyde, glyoxal) organic acids (formic, methoxyacetic, acetic, glycolic, oxalic) and diformate esters of 1,2-ethanediol. Most of the 1,4-Dioxane is depleted within the first 5 minutes of irradiation. The intermediate byproducts undergo further oxidative degradation initiated by •OH radicals forming glycolic and acetic acids (Stefan and Bolton, 1998).

2.2.1.2 Fenton's Reagent and Ozone with Hydrogen Peroxide

Processes involving Fenton's reagent and ozone with hydrogen peroxide generate •OH radicals in dark reactions. The Fenton's process with ozone initiates the formation of hydroxyl radical chain reaction producing a high rate of oxidation (Payne *et al.*, 2003). This process is useful for in-situ remediation using unique means of ozone well injection. A similar process using a continuous reactor with ozone and hydrogen peroxide feeds has proved successful in both pilot and full implementation installations. The process utilizes

higher concentration of ozone which improves the 1,4-Dioxane reaction rate. In a pilot test running 50 gallons per minute, 1,4-Dioxane reduction was from $300 \mu\text{g L}^{-1}$ to $25 \mu\text{g L}^{-1}$. The 1,4-Dioxane destruction is a function of applied ozone. An 84 percent reduction is obtained at 8.67 mg L^{-1} applied ozone. At 17.34 mg L^{-1} applied the reduction increased to 99 percent (Odah, 2003). Another study on hydrogen peroxide and ozone optimization revealed that ratios greater than 0.4 mole per mole $\text{H}_2\text{O}_2 : \text{O}_3$ resulted in reduce 1,4-Dioxane removal (Suh and Mohseni, 2004).

2.2.1.3 Chlorine Degradation of 1,4-Dioxane

Chlorine causes rapid degradation of 1,4-Dioxane. Utilizing a 12-fold molar excess molecular chlorine or hypochlorous acid (pH 2 – 6), 80 percent 1,4-Dioxane was degraded in 8 hours at 6.0 pH (Klecka and Gonsior, 1986). The experiment by Klecka and Gonsior (1986) did not observe secondary byproducts of the reaction. Chlorination byproducts are 12 to 1,000 times more toxic than 1,4-Dioxane. This raises questions as to whether chlorination of 1,4-Dioxane-contaminated drinking water may lead to creation of highly toxic byproducts (Mohr, 2001).

2.2.1.4 UV Light and Titanium Dioxide

Other processes utilize UV or sunlight and titanium dioxide (TiO_2). The UV light reacts with the metal semiconductor to produce conduction band electrons and valance band

holes. Oxygen and water molecules in contact with the titanium dioxide particle undergo a redox reaction thereby forming hydroxyl radicals capable of degrading 1,4-Dioxane (Oppelt, 1998). A significant problem with semiconductor photoconductivity is the electron hole reversal process. This reversal can significantly reduce the photocatalytic activity. One method to increase the activity is to add irreversible electron acceptors (IEA) or oxidants to the matrix. Hydrogen Peroxide is an IEA. Following reaction with O_2 or accepting an electron from the conduction band, the IEA dissociates and provides routes for $\bullet OH$ generation (Oppelt, 1998). Some halides (chloride and bromide) can be oxidized by the valance band holes and impact the contaminant reduction rate. The halides simply reduce the number of available reaction sites (Calza and Pelizzetti, 2001).

Light induced processes have fast reactions but can be significantly hindered by other contaminants or radical scavengers present in the system (Kosaka *et al.*, 2000).

Experimental work is being conducted on new UV lamp reactor designs providing a 10-20 fold increase in surface area per unit volume than immersion type reactors (Ray, 1998).

2.2.1.5 Ultrasound Sonication

Another AOP useful in the treatment of 1,4-Dioxane is ultrasound sonication. The acoustic bubbles produced by sonication form $\bullet OH$ radicals. These radicals are formed by the large pressure gradients and temperatures within the cavitation bubble due to

homolytic cleavage of water molecules (Beckett and Hua, 2003). The resulting $\bullet\text{OH}$ radicals are able to interact and degrade the contaminant. Both ultrasonic power and frequency are key determinants in degradation of specific contaminants. For 1,4-Dioxane, the most effective frequencies in order of sonolysis efficiency are 358, 618, 1017 and 205 kHz (Beckett and Hua, 2003). Another study (focused on field implementation potential) addresses 20 kHz sonication plus the addition of an oxidant. The results show similar 20 percent improvement in 1,4-Dioxane degradation with the addition of either Fe^{2+} or peroxydisulfate (Son *et al.*, 2006).

2.2.1.6 Disadvantages of Advanced Oxidation Treatments

Disadvantages of AOPs include requirements of significant energy input, sophisticated equipment, and high capital/operating costs. Additionally, AOPs are seldom feasible for waters containing significant turbidity (e.g. wastewater effluent). Advanced oxidation processes can break down 1,4-Dioxane, but are not considered cost effective treatment methods.

2.2.2 Biodegradation Treatments

In-situ bioremediation has historically been avoided because 1,4-Dioxane exhibits a negligible biological oxygen demand and is considered to be relatively non-biodegradable (Mohr, 2001). Recently, however, there is increasing awareness that

bioremediation may be a cost effective treatment strategy for 1,4-Dioxane (Zenker *et al.*, 2003). Recent studies have demonstrated that specific species of plants (phytoremediation) and microorganisms (bioaugmentation) can successfully treat 1,4-Dioxane.

2.2.2.1 Actinomycetes Biodegradation

Biodegradation research has been successful in identifying some strains of actinomycetes that have the capability of utilizing (degrading) 1,4-Dioxane.

The actinomycete, *Amycolata* sp. CB1190, has degraded 1,4-Dioxane at the rate of 0.33 mg/minute per mg protein (Parales *et al.*, 1994). The actinomycete was isolated from 1,4-Dioxane-contaminated industrial sludge found in Darlington, South Carolina. Cultures grown in basal salts medium (BSM) mineralized 59.5 percent of the 1,4-Dioxane in 18 hours (Parales *et al.*, 1994). A study by Kelley *et al.* (2001) utilized unplanted bioreactors and found that augmenting the soil with CB1190 (10^7 cells/g-soil) increased mineralization of 1,4-Dioxane from 8.0 percent (no treatment) to 25 percent (Kelley *et al.*, 2001).

Using a trickling filter, Zenker *et al.* (2004) was able to maintain for one year a 1,4-Dioxane degrading capability (93%-98%) utilizing tetrahydrofuran (THF) as the growth substrate (Zenker *et al.*, 2004). Zenker *et al.* (2004) was using a consortium of bacteria

from a 1,4-Dioxane contaminated aquifer. Previous work showed THF somehow stimulated 1,4-Dioxane biodegradation (Zenker *et al.*, 2002).

2.2.2.2 Monooxygenase Expressing Bacteria Biodegradation

Other research has focused on monooxygenase expressing bacteria that have enzymes (similar to mammalian cytochrome P-450) that have the ability to degrade 1,4-Dioxane in reaction analogous to their cytochrome P-450 counterpart (Mahendra and Alvarez-Cohen, 2006).

These research findings have shown *Pseudonocardia* strains growing on 1,4-Dioxane and recombinant *E. coli* strains expressing toluene monooxygenase were capable of degrading 1,4-Dioxane. The mammalian cytochrome P-450 monooxygenase enzyme is a 1,4-Dioxane degrader. The experiment identified four (4) distinct monooxygenase expressing pure cultures – 1) *Methylosinus*, 2) *Mycobacterium*, 3) *Pseudomonas*, and 4) *Ralstonia*. Of the four, the *Pseudonocardia* produced a 1,4-Dioxane degrading enzyme (Sharp *et al.*, 2005).

Typically monooxygenases insert one atom of the oxygen molecule into the substrate and the other atom becomes reduced to water. This reaction consumes energy and has a requirement for a reducing equivalent in the form of NADPH (Lee, 2006). For 1,4-

Dioxane, ring-hydroxylating monooxygenases can attack oxygen substituted aromatic compounds and break the ether bond (Lee, 2006).

2.2.2.3 Bioreactors

Three continuous flow slip stream bioreactors have been operating since 2002 to clean up the 1,4-Dioxane contaminated Lowry Landfill leachate near Denver, Colorado. The microbial community requires THF to degrade 12,000 $\mu\text{g L}^{-1}$ 1,4-Dioxane contamination down to effluent levels of under 200 $\mu\text{g L}^{-1}$ (Shangraw *et al.*, 2003). The biological process was selected upon unsuccessful trials of many AOP processes.

2.2.2.4 In-Situ Bioremediation

In-situ bioremediation using butane as a growth substrate has been utilized to successfully clean up petroleum contaminated sites. A laboratory experiment demonstrated the potential for degrading 1,4-Dioxane (Perriello *et al.*, 2003). This success is contrasted by numerous studies showing indigenous soil bacteria do not possess the metabolic ability to degrade 1,4-Dioxane (Mohr, 2001).

2.2.2.5 Bioremediation Field Studies

At present, there are no published field studies using biodegradation strategies for remediation of 1,4-Dioxane contaminated sites. Research to date indicates that indigenous soil bacteria do not possess the metabolic ability to biodegrade ethers, including 1,4-Dioxane (Mohr, 2001). However, phytoremediation and bio-augmentation were shown to degrade 1,4-Dioxane in bench-scale laboratory studies and at small experimental field sites (Kelley *et al.*, 2001). Specifically, bio-augmentation with the actinomycete microorganism *Amicolata* sp. CB1190 (a bacterium) and phytoremediation utilizing root exudates from Poplar trees (*Populus* sp.) were shown to be effective in removing 1,4-Dioxane from water (Ouyang, 2002). Poplar tree root exudates have been shown to enhance 1,4-Dioxane degradation in the presence of CB 1190, suggesting that the rhizosphere may be favorable for 1,4-Dioxane biodegradation and that a wetland may provide a suitable environment for the biodegradation of 1,4-Dioxane (Kelley *et al.*, 2001).

2.2.3 Phytoremediation

Phytoremediation is a broad set of decontamination processes that utilize plants for *in situ* and *ex situ* treatment of contaminated soil, sludges, sediments, wastewater, and groundwater. The phytoremediation processes are phytoaccumulation, phytodegradation,

phytostabilization, phytovolatilization, rhizodegradation, and rhizofiltration that result in contaminant degradation, removal, or stabilization (Li *et al.*, 2005).

Phytoremediation has been utilized to remediate pesticides, metals, solvents, explosives, petroleum hydrocarbons, and polycyclic aromatic hydrocarbons that have contaminated soils and a variety of wastewaters including storm runoff, primary and secondary effluent, and industrial discharge.

2.2.3.1 Phytoremediation Design Elements

Phytoremediation occurs in natural system such as wetlands. Natural wetlands possess most of the physical, plant, and hydrological characteristics needed for successful remediation of contamination. Adapting the positive characteristics of a natural wetland to a constructed wetland permits better flow and contact control while ensuring the contaminant is contained within the treatment system.

Phytoremediation applications must consider key design elements including contaminant chemistry, contaminant fate, remediation media, soil-plant-atmosphere interactions, site characteristics, secondary remediation products, and regulatory requirements. The contaminant will influence many key design parameters of a phytoremediation system. The subject contaminant may require chemical, biological, or physical alterations of the surrounding media to permit successful phytoremediation.

Secondary design considerations cover a large array of requirements including site hydrology, operating parameters, seasonal considerations, fallow/regeneration processes, and contaminant removal and disposal. Typical phytoremediation requires the contaminant to be mobile and available to the plant roots for plant uptake or rhizosphere degradation.

2.2.3.2 1,4-Dioxane Phytoremediation Potential

A laboratory study using hybrid poplar cuttings in soil showed that 80 percent of the 1,4-Dioxane taken up by the tree was transpired from leaf surfaces into the atmosphere. This finding was further validated in a mathematical one-dimensional coupled transport model that also showed the leaves as transpiring the 1,4-Dioxane. The model predicted a 30 percent reduction in soil contaminant concentration in 7 days based on the phytovolatilization of the contaminant (Ouyang, 2002).

In utilizing phytovolatilization as a viable phytoremediation alternative, consideration must be given to the fate of the contaminant in the air. Previous lab studies have shown 1,4-Dioxane transpired through plant leaves is degraded by photo-oxidation through reactions with hydroxyl free radicals or ozone. The half life for 1,4-Dioxane is 12 hours in the atmosphere and ethylene glycol diformate (EDF), the primary byproduct of OH

oxidization of 1,4-Dioxane, can exist for 24 days if rainfall does not remove it from the air (Maurer *et al.*, 1999).

2.2.4 1,4-Dioxane Contamination Case Histories

Treating surface, ground, or waste waters contaminated with 1,4-Dioxane presents an array of locale, site, hydrological, concentration, cost, regulatory, and community issues and concerns. Primary considerations include available treatment options and the fate of the contaminant and resulting byproducts after remediation. Numerous communities are finding 1,4-Dioxane contamination in well water and river streams. Often the source of the contamination is from an industrial complex or waste site, a landfill, or associated with a previous trichloroethylene (TCE) contaminated area. However, one study in Japan discovered 1,4-Dioxane in river flows which are upstream of any industrial installations. This upstream contamination is believed to be the result of 1,4-Dioxane in consumer products such as soaps, cosmetics, and paints at concentrations of $0.15 - 0.25 \mu\text{g L}^{-1}$ (Abe, 1999) that are introduced into municipal wastewater.

2.2.4.1 Menlo Park, California

A contaminated site at the Stanford Linear Accelerator Center, Menlo Park, California, showed three areas of 1,4-Dioxane contamination. One area was a local plating shop where past practices introduced solvent to the local groundwater. The other areas were

the former underground solvent waste storage tank, and the former hazardous waste storage area (Odah, 2003). The concentrations at the various areas range from $3 \mu\text{g L}^{-1}$ to $7,300 \mu\text{g L}^{-1}$. Currently a granular activated carbon filter system is being used to treat concentrations of $1,500 \mu\text{g L}^{-1}$. A contaminant correlation between 1,4-Dioxane and 1,1-Dichloroethene (a daughter product of TCA) was found. The TCA contaminant was not found in 2003 sampling.

2.2.4.2 Ann Arbor, Michigan

One of the largest releases of 1,4-Dioxane occurred at the Pall-Gelman Sciences site near the city of Ann Arbor, Michigan. In the manufacture of micro-porous filters, 1,4-Dioxane was utilized as a solvent for the cellulose acetate and was subsequently released into the ground through state-permitted unlined treatment ponds. These ponds were utilized from early 1960 to mid-1980. The contaminant plumes have migrated over the past 17 years 9,000 feet easterly and 3,000 feet westerly from the probable source areas in a complex glacial sediment. The concentrations in ground water near the source were $300,000 \mu\text{g L}^{-1}$ (Fatouhi and Brode, 2003). In addition to purging groundwater at multiple sites, groundwater treatment using UV light and hydrogen peroxide was implemented. The influent concentrations were $3,000\text{-}4,000 \mu\text{g L}^{-1}$ and the treatment operating cost \$ 4.00 - \$ 5.00 per 1000 gallons. During the time period 1997 – 2003 the remediation of 2 trillion gallons (purged, treated and discharged) removed 55,000 pounds

of 1,4-Dioxane at \$ 5.5 million dollars operating costs per year (Fatouhi and Brode, 2003).

2.2.4.3 Seymour, Indiana

The Seymour, Indiana superfund site, a previous solvent recovery and recycling plant, found 1,4-Dioxane had migrated significant distances in varying concentrations over the span of six years. Their analysis utilized a combination of the USGS MODFLOW and SWIFT modeling transport code to predict transport distances of various contaminants. Travel distance for 1,4-Dioxane was 2.5 times farther than tetrahydrofuran, even though the two compounds have identical retardation factors and solubilities. The difference is likely due to tetrahydrofuran being slightly biodegradable while 1,4-Dioxane is not typically amenable to biodegradation (Mohr, 2001).

2.2.4.4 San Jose, California

The Clean Harbors Site (formally Safety-Kleen and Solvent Services) near San Jose, California, had a groundwater contamination concentration of $250,000 \mu\text{g L}^{-1}$. Remediation attempts with carbon adsorption and air stripping did not work. In 2003, a solvent extraction trench was installed down gradient of the contamination source. Other treatment options are being investigated (Christian, 2003).

2.3 Treatment Wetlands

2.3.1 Natural Wetlands

Natural wetlands ecosystems, which occur at the interface between land and water, have for many years been utilized for cleaning up polluted waters. As the benefit of natural wetlands remediation potential became known, engineers and scientists began directing more waste and sewage effluents to these areas.

2.3.2.1 Wetland Attributes Enhance Contaminant Remediation

The physiological and chemical properties of wetlands provide many positive attributes for remediating contaminants. The unsaturated areas provide a wide array of aerobic, anaerobic and facultative microorganisms that utilize and degrade a wide array of organic and inorganic molecules. The saturated areas create redox conditions in most wetland soil/sediment zones that offer unique pathways for chemical and biological processes requiring reducing conditions.

The rhizosphere of wetland shrub and tree species provides a unique microbial zone rich in degradation components (Williams, 2002). The root rhizosphere has a continuous throughput of plant derived substances (exudates). This rhizodeposition, which includes soluble plant products as well as root material, accounts for 7-27 percent of the total plant

mass annually (Kamath *et al.*, 2004). The root system and rhizosphere play a critical role in successful remediation of many organic contaminants in conversion and uptake (Green and Hoffnagle, 2004).

2.3.2.2 Wetland Plants

Wetland plants themselves are very unique in terms of their ability to survive both submerged and drought conditions. Wetland plants for phytoremediation have unique attributes allowing uptake and storage or degradation of targeted contaminants. The uptake of chemicals into plants through roots depends on the plant's uptake efficiency, the source concentration, and the transpiration rate.

The uptake efficiency factor, defined as the transpiration stream concentration factor (TSCF) by Dietz, is the ratio of contaminant concentration in the transpiration stream to that in the soil water. The chemical uptake rate (mg day^{-1}) is calculated from the product of the uptake efficiency (TSCF - dimensionless) times the transpiration rate (L day^{-1}) times the soil water concentration of the chemical (mg day^{-1}) (Dietz and Schnoor, 2001). The TSCF depends on physico-chemical properties, chemical speciation, and specific plant properties (Dietz and Schnoor, 2001)

Transpiration rate is a key variable in the selection of plants for phytoremediation applications. Transpiration rate is dependent on plant type, leaf area, nutrients, soil

moisture, temperature, wind condition and relative humidity. Plants with high transpiration rate (rapid uptake) such as fast growing phreatophytes (hybrid poplars, willows) with large leaf area are often selected (Dietz and Schnoor, 2001).

2.3.2 Constructed Wetlands

Only in the last few years has the importance of wetland systems been elevated for their potential to effectively treat a variety of waste waters. This elevation has led numerous communities world wide to either restore previous wetland areas or create constructed wetlands.

2.3.2.1 Type and Use of Constructed Wetlands

Research and implementation of constructed wetlands for remediation of polluted waters has occurred within the past 25 years (Dahab and Surampalli, 2001). Constructed wetlands systems include surface flow and sub-surface flow through gravel or soil media and aquatic systems with a variety of ground or floating aquatic plants (Karpiscak *et al.*, 1999). Most of the constructed wetlands today are treating primary or secondary effluent from municipalities or from livestock facilities. Constructed wetlands are also being used to treat industrial, food processing, agricultural, landfill leachates, pulp and paper, and refinery wastes (Karpiscak *et al.*, 1999).

2.3.2.2 Constructed Wetland Advantages

Two primary advantages of constructed wetlands are first, the ability to control the many variables (hydrological, biological, chemical) which could otherwise disrupt successful operation and second, the lower installation and operating cost (Dahab and Surampalli, 2001). Numerous studies have shown artificial wetlands to be very effective in treating wastewater. Ponds, surface flow (SF), and sub-surface flow (SSF) wetlands have been shown to remove 95–98 percent of indicator bacteria, coliphage, and enteric pathogens (Gerba *et al.*, 1999).

Other unique advantages of constructed wetlands include a higher degree of process control and greater contact of contaminated water with the root system. A limited number of contaminants have been evaluated for successful constructed wetlands treatment. Data from pilot studies is needed to support further implementation.

2.3.2.3 Constructed Wetlands Reduce Harmful Microorganisms

Constructed wetlands have demonstrated success in removing harmful microorganisms from wastewater. Early studies demonstrated success at removing bacterial indicators while studies in the last 20 years have shown effective removal of viral pollution (Gersberg *et al.*, 1987).

A study at the Constructed Ecosystems Research Facility (CERF) in Tucson, Arizona demonstrated smaller microorganisms were removed more efficiently in SSF than SF wetlands. This study also found SSF wetlands achieved greater removal of coliphage, total, and fecal coliforms at 95, 99, and 98 percent, respectively (Gerba *et al.*, 1999). A later study at the CERF facility found multi-species SSF wetlands with a retention time of four days would reduce coliphage by 95.2 percent and *Giardia* cysts and *Cryptosporidium* oocysts by 87.8 and 64.2 percent, respectively (Thurston *et al.*, 2001). This same study reviewed microorganisms in a potable water supplied wetland and found higher temperature and increased animal activity added to the microbial discharge of this wetland system (Thurston *et al.*, 2001).

2.3.2.4 Constructed Wetlands Suitable for Most Climates

Constructed wetlands have proven to be effective in a wide range of climate conditions. They have been successful in the northern United States and Canada as well as the southwest deserts of Arizona (Gearheart, 2006).

In 1990, Arizona had four (4) constructed wetlands treating municipal wastewater. By 1997 that number had grown to 26 with 24 more planned in the near future (Gelt, 1997b). The town of Jerome, Arizona selected a constructed wetland over the conventional waste treatment facility because of the lower monthly operating costs. The city of Sierra Vista,

Arizona, as of 2004, recharges 2000 acre-feet of treated wastewater annually using 50 acres of constructed wetlands (Eden *et al.*, 2007).

2.3.2.5 Constructed Wetlands Offset Loss of Natural Wetlands

Population growth, supported by groundwater pumping, has continued unabated in the southwest deserts. The resulting aquifer depletion has negatively impacted numerous riparian habitats along seasonal and perennial water channels. The loss of natural habitats can be partially offset through the creation of constructed wetlands.

This concept is being tested in the full-scale Tres Rios constructed wetlands in Phoenix, Arizona. A mixture of open water and emergent marsh areas in a 50 percent ratio was found to optimize management and water quality benefits (Wass, 2006). The Tres Rios wetlands treat secondary advanced level effluent which has fewer nutrients and is of higher quality than secondary treated wastewater (Gelt, 1997a).

Constructed wetlands have the ability to treat both primary effluent as well as highly contaminated industrial wastewater. The Apache Nitrogen Products Wetland near St. David, Arizona treats ground water containing 200 mg L^{-1} of nitrate. The various anaerobic and aerobic ponds discharge effluent containing less than 10 mg L^{-1} nitrate-N to the San Pedro River (Roudebush, 2006).

2.3.2.6 Constructed Wetlands Field Studies Database

A phytoremediation field studies database, funded by the U.S. Environmental Protection Agency, included guidelines for establishing a phytoremediation system. In addition to site characteristics, the field study publication recommend completing 1) feasibility studies, 2) phytotoxicity studies, and 3) plant selection studies as part of the initial design development (Green and Hoffnagle, 2004). This data base highlighted 44 sites using phytoremediation for metals removal (lead, arsenic, mercury) at a cost of \$ 5,000 - \$ 4 million per acre. Metal hyperaccumulator plants and poplar trees were most often the selected plant (Green and Hoffnagle, 2004). The data base contained 47 sites removing chlorinated solvents. The common contaminant was trichloroethylene or perchloroethene that was being removed by hybrid poplar and phragmites (Green and Hoffnagle, 2004). The database showed hybrid poplars as the most commonly used plant for the treatment of pesticides at 19 sites. The cost is \$ 6,000 - \$ 5.4 million per acre. The higher cost reflects pilot or demonstration sites (Green and Hoffnagle, 2004).

2.3.3 Pilot-Scale Wetlands

Two key elements are critical in determining the potential success of a constructed wetland remediation project. Given the contaminant is known, the first key element is to identify plants which will successfully remove and possibly degrade the contaminant for

a selected site. The second key element is to conduct a field pilot-scale project to verify and validate planned operating parameters in a full-scale constructed wetland.

2.3.3.1 Cottonwood Trees (*Populus fremontii* S. Wats.)

Trees from the genus *Populus* are frequently selected for use in phytoremediation projects. These trees are capable of using water from the water table or its capillary fringe. They grow robustly and consume large amounts of ground water (Hauser *et al.*, 1999). They have adequate rooting depth and in the Western United States can reach water table depths of 6-12 feet (Hauser *et al.*, 1999). Where the phytoremediation goal is plume capture, it is possible to grout bore holes to ensure roots of phreatophytic trees grow 3-5 m deep and reach the surficial aquifer (Schnoor, 2002). Phreatophytes such as cottonwoods can tolerate occasional submergence of part or all the root mass below the water for up to 20 days (Braatne, 1999). However, they are not very shade tolerant (National Plant Data Center, 2002).

The hybrid poplar tree (*Populus deltoids nigra*) is the most successfully used phytoremediating tree species (Williams, 2002). The poplar tree can be submerged for extended periods without harm. These trees also have the ability to establish adventitious roots under waterlog conditions. Cottonwood trees and other plants have the ability to transfer oxygen from the roots to the rhizosphere. Oxygen release rates, measured for

laboratory hydroponic cultures, showed *Typha latifolia* (cat tail) released 1.41 mg hr^{-1} between a redox range of -250 to -150 mV (Williams, 2002).

Poplars also has rapid stomata closing ability in response to atmosphere and soil water conditions (Braatne, 1999). A recent study of cottonwoods in riparian areas in southern Arizona has demonstrated considerable difference in transpiration, leaf area index, and root depth depending on whether the associated stream is perennial or seasonal (Gazal *et al.*, 2006).

Cottonwood transpiration rates vary with temperature, humidity, solar radiation, soil water availability, rainfall, and plant age and growth. In Ohio, two 15 m tall cottonwood trees were monitored for an entire season with transpiration rates ranging from 189 to 1,323 liters per day (Ouyang, 2002). For mature trees with roots in groundwater the transpiration rate is 600-900 gallons per tree per year. Plantings around 2 years in age will transpire 200 gallons per year (Schnoor, 1997).

A study in Fort Worth, Texas demonstrated July transpiration rates for second season growth starting with whips at 1.705 gallons per day, starting with 5 gallon plants at 3.3 gallons per day, and a mature tree at 365 gallons per day (Harvey, 2003).

2.3.3.1.1 Laboratory Studies to Determine Cottonwood Suitability

Wetland phytoremediation studies typically involve laboratory bench analysis from microcosm and mesocosm perspectives utilizing plant extracts, root components, and plant cuttings (Williams, 2002). The laboratory findings provide solid rationale for further study of the potential of a wetland system to uptake contaminants in water or soil.

A laboratory experiment involving hybrid poplar cuttings in both planted and unplanted flasks has demonstrated success in reducing the spiked levels of 1,4-Dioxane in solution.

The planted flasks contained 200 ml half-strength Hoagland's solution spiked with 4.5 mg 1,4-Dioxane representing a total 22.7 mg L⁻¹ concentration. At the end of 9 days, an average of 54 percent of the 1,4-Dioxane (30-78 percent) was removed. A positive correlation ($r^2 = 0.97$) existed between the 1,4-Dioxane removed and total transpiration (Aitchison *et al.*, 2000). Using the planted experimental set-up, a transpiration stream concentration factor was established at 0.72 TSCF (Aitchison *et al.*, 2000).

The soil laboratory experiment utilized wastewater treatment lagoon soil near Salisbury, North Carolina. The soil, augmented with de-ionized water to 80 percent field capacity, had numerous organic pollutants including 21 mg kg⁻¹ 1,4-Dioxane. The hybrid poplar cuttings transpired 55 percent of the 1,4-Dioxane (Aitchison *et al.*, 2000). This

experimental study provides a good insight into the potential for phytoremediation to remediate 1,4-Dioxane contaminated waters.

2.3.3.2 Cottonwood Tree Uptake and Transpiration of 1,4-Dioxane

For chemicals taken into plant roots to reach the phloem, the endodermis forces all materials through at least one cell membrane. It is this combination of contaminant solubility in water and solubility within the cell membrane that determines passage and availability of contaminant for transport and transpiration (Collins *et al.*, 2006).

Cottonwood trees have high transpiration rates and due to the hydrophilic nature of 1,4-Dioxane, the contaminant can hydrogen bond with the transpiration water and be taken up and translocated to stem and leaf tissue (Dietz and Schnoor, 2001). Contaminant translocation efficiency is expressed as a TSCF factor, defined previously in Section 2.3.3.1.1.

Experimental studies by Briggs *et al.* (1982) established a relationship of the TSCF to $\log K_{ow}$ (octanol/water partition) using non-ionized chemicals into barley plants. This study established an optima (high uptake potential) at 1.8 $\log K_{ow}$ with a range of 1.0-3.0 $\log K_{ow}$ (Collins *et al.*, 2006) leading to the conclusion that contaminants with low $\log K_{ow}$ (e.g. 1,4-Dioxane, -0.27) would not have a high TSCF.

In contrast to Briggs *et al.* (1982), an experimental study of hybrid poplar cuttings showed they had a high propensity to uptake 1,4-Dioxane from aqueous solution, with a TSCF factor of 0.72 (Aitchison *et al.*, 2000).

2.3.3.3 1,4-Dioxane Fate and Partitioning in Cottonwood Trees

A computer simulation of 1,4-Dioxane translocation in the xylem and phloem systems of poplar cuttings suggested that the transpiration stream concentration factor is relatively high (0.72) even though its Log K_{ow} is extremely low (-0.27) (Dietz and Schnoor, 2001). The simulation model suggests that 1,4-Dioxane would readily translocate to the leaves with a lower concentration in the roots. The simulation determined that 30 percent of 1,4-Dioxane in saturated sediments would be removed in seven days, mainly by root uptake. The 1,4-Dioxane translocated to the leaves would transpire to the atmosphere and be readily dispersed and photodegraded (Ouyang, 2002).

There was good correlation between the model predictions and the experimental results that showed accumulations of 1,4-Dioxane mass in roots (12%), leaves (28%) and stem (60%) after 168 hours. Accounting for root, stem, and leaf volume differences, the concentration of 1,4-Dioxane found in the leaves ($2,600 \mu\text{g cm}^{-3}$), stem ($1,000 \mu\text{g cm}^{-3}$), and roots ($350 \mu\text{g cm}^{-3}$) supports the findings of Aitchinson *et al.* (2000). (Ouyang, 2002). The simulation model predicted similar concentrations in both stem xylem and phloem systems.

Experimental data showed a low and constant 1,4-Dioxane concentration in the xylem while the phloem stem concentration increased exponentially over the 168 hour period (Ouyang, 2002). As hypothesized by Ouyang (2002), the 1,4-Dioxane is not incorporated into the xylem tissue since it is not a nutrient needed for the poplar tree but small amounts are carried from leaves to stem along with other photosynthesis products.

2.3.3.4 Pilot-Scale Project Design

After a thorough understanding of the fate and transport of contaminants in the phytoremediation system, a pilot study should be conducted to validate the laboratory findings, ensure processes and mechanism are scalable, and to understand and optimize the operating conditions.

This progression from laboratory to pilot testing is standard operating procedure in most highly controlled industrial processes and is even more important in field projects where environmental variables have wide ranges, matrix effects are common place, and unanticipated impacts of nature and science occur on an all too frequent basis.

2.3.3.4.1 Goal of Pilot-Scale Project

A field pilot test can document phytoremediation results under real site conditions and, if successful, may generate design and cost data toward a full-scale implementation. Pilot testing may consist of planting the appropriate plant species, installing instrumentation, and developing a monitoring plan for the fate and transport of the contaminant (Tossell *et al.*, 1997). The main goal of the pilot test is to assess the remediation capacity of the system and plant under on-site conditions.

2.3.3.4.2 Wetland Project Examples Supporting Pilot-Scale Projects

Most constructed wetlands projects incorporate a pilot-scale demonstration project or pilot-scale start up to understand implementation and operational challenges.

The Tres Rios wetlands in Phoenix, Arizona started as a pilot project that was both a operating facility and a testing laboratory (Gelt, 1997a). The pilot project successfully established the water quality effects (COD, TDS, and Nitrogen) and the anticipated levels of residual chlorine. The pilot also established the optimum mixture of open water and emergent marsh areas.

Initially the pilot system was planted with the same vegetation in fringe and deep water areas. A valuable vegetation lesson learned was the stress on plants in deep water which

required re-planning the full-scale system to include hummocks (submerged mounds).

The current pilot system treats 2 million gallons per day where the full-scale facility will have a peak flow of 450 million gallons per day (Wass, 2006).

The Sweetwater Wetlands in Tucson, Arizona, initially utilized the University of Arizona CERF facility as the pilot-scale wetlands. Sweetwater developed their wetlands, in addition to inputs from the CERF research facility, with a wide array of federal, state, and local agencies and numerous non-governmental organizations assisting the committee, city staff, and consultant team in project planning and facility layout (Gelt, 1997a).

Without a viable pilot-scale study, a constructed wetlands project can experience large setbacks as happened with the Apache Nitrogen Wetland near St. David, Arizona. Their planned project proceeded in three phases: establishment, start-up, and full-scale operations. During the establishment period, cattail growth and senescence resulted in sufficient biomass for denitrification. However, recurrent caterpillar infestations consumed large quantities of the cattails creating a delay in project start-up (Roudebush, 2006).

A phytoremediation demonstration site using cottonwoods (*Populus deltoides*) was implemented in April 1996 at Carswell Golf Club on the Naval Air Station Fort Worth, Texas which is adjacent to Air Force Plant # 4. This demonstration site planted a total of 662 cottonwood trees above a TCE contaminated shallow aquifer. The upgradient

planting consisted of 7 rows 438 whips at 1.25 m on center. The downgradient planting was seven rows 224 caliper trees at 2.5 m on center (Harvey, 2003).

The eastern cottonwood tree was selected for this demonstration based on the cottonwoods fast growth, high transpiration rate, and phreatophytic properties. These characteristics allow cottonwoods to rapidly transpire water from a saturated zone and establish an extensive below grade root system.

3.0 METHODS

3.1 Experimental Site: Constructed Ecosystems Research Facility (CERF)

3.1.1 Location of CERF Facility

The experimental site for this research effort was on the grounds of the Constructed Ecosystems Research Facility (CERF) in Tucson, Arizona. At the time of this study, CERF was jointly operated by Pima County Wastewater Management and the University of Arizona. The site adjoins the Pima County Roger Road Waste Water Treatment facility to the West and the City of Tucson Sweetwater Wetlands to the South.

Subsequent to the completion of this study, the CERF facility was closed in December 2006.

The CERF facility received unchlorinated secondary effluent from Pima County's Roger Road Wastewater Treatment Plant. The CERF facility feed first flows through a duckweed pond prior to being supplied to the CERF wetlands. The CERF site began operation in 1989 and consisted of five raceways (61 m long by 8.2 m wide by 1.4 m deep) and one additional, larger raceway (64.6 m by 11 m by 2.6 m) (Figure 3.1). All raceways were underlain by 30-mil 3-ply Hyperlon (heavy plastic sheeting) to prevent seepage losses. Raceways # 2-5 were subsurface horizontal-flow wetland cells containing 0.61-0.91 m of gravel and various herbaceous shrub and tree species.

Raceway # 6 was an aquatic pond maintained at a fluid depth of 0.91 m and covered with

duckweed (*Lemna* spp.). Raceways received either unchlorinated secondary effluent from the Roger Road Wastewater Treatment Plant or potable water (ground water) as influent. Raceway # 6 provided pretreatment (suspended solids removal) for effluent that was sourcewater for raceways # 3 and # 5. The experimental wastewater effluent source was taken from Raceway # 6 inlet feed. Potable water was supplied by a hose bib connected to the city municipal supply located near raceway # 5.

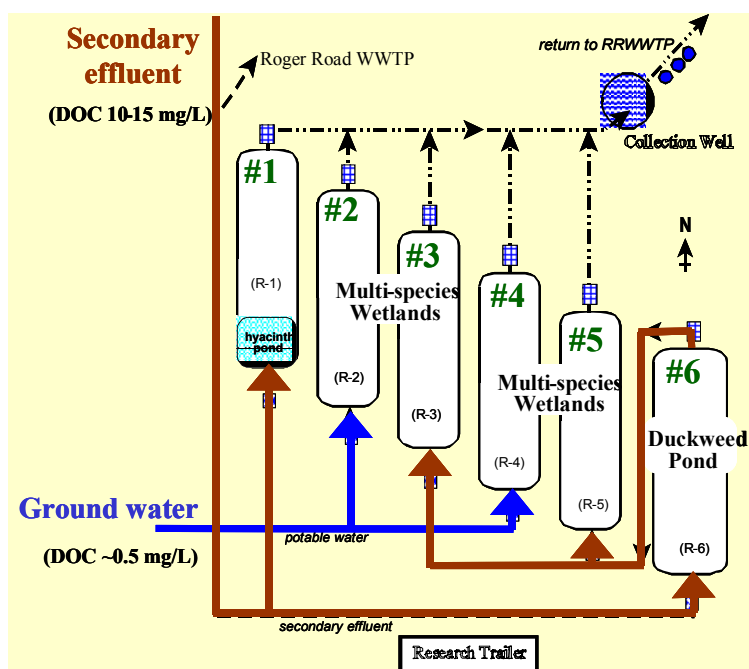


Figure 3.1. Schematic layout of wetlands at the Constructed Ecosystems Research Facility in Tucson, AZ. The wetlands received and treated secondary effluent from the Roger Road Wastewater Treatment Plant.

3.1.2 Site Layout

The experimental site was 243.8 m to the East of the CERF duckweed pond (Raceway #6). The bulk of the site area was a constructed drainage retention basin with higher ground (4.3 m elevation) to the East. The elevated area contained two open round stock Tanks A & B (193cm & 173cm diameter respectively) and the experimental dual-chambered wetland tank, (Figure 3.2). In addition, three open evaporation ponds were located downstream of the dual-chambered tank. The site had electrical (110 VAC) power within 2 m of the upstream portion of Tank 2. Utilizing heavy duty extension cords routed through steel conduit provide adequate power to operate all pumps and other electronic devices.

The aerial photo of the experimental site (Figure 3.2) designates tanks, ponds, and side experiment locations. General flow of water was from East to West with feed stock of 1,4-Dioxane and bromide in Tank A being pumped to Tanks 1 and 2 along with un-spiked influent from Tank B. Manifolds in Tank 1 and 2 mixed the applied spiked and un-spiked influent (52 L hr^{-1}) through drip channels in the upstream (East) end of Tanks 1 and 2. Sub-surface flow through the planted (Tank 1) and control (Tank 2) was discharged into Tank C and D, respectively. Tank C and D discharge, during the experimental run (lapse time hours 191-250), was pumped to Pond 1 and 2 respectively.

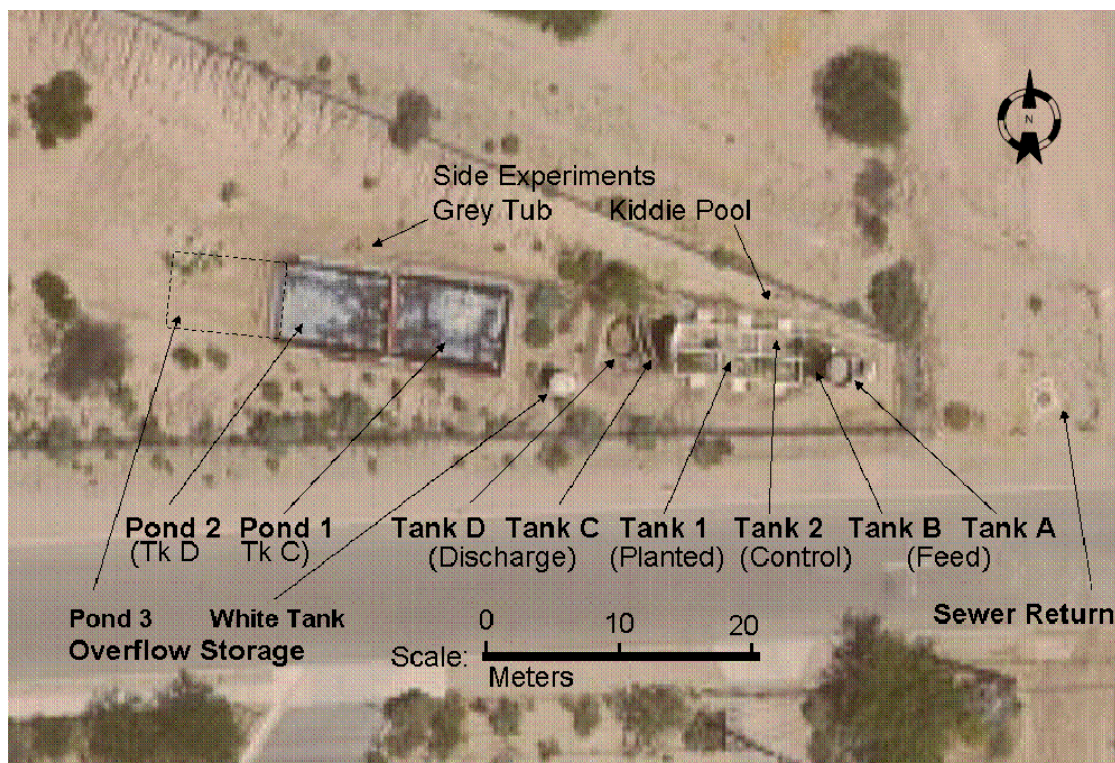


Figure 3.2. Aerial Photo of steel tank wetland demonstration system located adjacent to the CERF wetlands in Tucson, AZ.

At all other times, un-spiked Tank 1 and 2 discharge was pumped to CERF discharge or the sewer manhole located East of Tank A. During rainstorm events when the capacity of Pond 1 and 2 would be exceeded, pond water was temporarily stored in the 1892.7 L white tank and Pond 3, respectively. Before the next experimental run, Pond 1 and 2 were cleaned (residue removal) after all water and 1,4-Dioxane evaporated.

The grey tub and kiddie pool side experiments (Section 6.4) were located as shown in Figure 3.2. Tap water and secondary effluent was supplied from the CERF facility through underground piping to the East of Tank A.

3.1.3 Experimental and Control Wetland Tanks

The dual-chambered wetland tank was constructed from 0.32 cm steel measuring 9.1m long, 3.1 m wide, and 2.1 m high by Nogales Highway Iron and Steel (Ellman, 1997). The tank had a divided wall creating two side-by-side cells (Tanks 1 and 2) 152 cm wide. The cells originally were coated with a high build epoxy paint to prevent rusting. Both chambers contained sieved (>0.02 mm) mortar sand to a depth of 152 cm that was on top of 15 cm layer of 3.8-7.6 cm river rock covered with a highly permeable geo-textile cloth (Ellman, 1997). The tanks were situated on a bed of sand (sloped 1 percent) that had been underlain by an impermeable liner and PVC pipe collection trench (Ellman, 1997). This tank system was originally used during the mid 1990s to study the performance of constructed wetlands for treatment of raw sewage (Ellman, 1997).

At the beginning of the current experiment, the original dual-chamber tank system was in good condition and only needed minor refurbishment for use on the current project. Instrumentation (tensiometers) was left in place during the sand excavation and replacement (described in Section 3.2.1.2). The tensiometers (3 sets of 5 per tank) were utilized to measure soil moisture during the first year of tree growth. The main modifications to the tanks involved replacing the influent piping and creating additional tank discharge ports at 30.5 cm below grade.

3.1.4 Feed and Discharge Collection Tanks

The lower discharge round collection (stock) Tanks C and D (218 cm, 231 cm diameter, respectively) rested 76 cm below the bottom of the experimental Tanks 1 & 2. Tank C was adjacent to Tanks 1 & 2 with Tank D 230 cm farther away (Figure 3.3). Tanks A, B, C, and D required extensive cleaning and recoating prior to use in this research. A special non-toxic Farbertite coating was used (Protection Engineering, Pittsburg, California). The Farbertite coating is a coal tar compound containing inert mineral fillers. The coating is recommended for sealing potable water supply systems.

3.1.5 Evaporation Ponds and Retaining Wall

Ponds 1, 2, and 3 were located 4.1 m West of Tank D in the bottom of the drainage basin (Figure 3.4). The ponds lowest elevation was 25 cm above the bottom elevation of Tanks C & D. Additional care was required to ensure a vacuum break was present in the piping between Tank C & D and the discharge ponds. A timber retaining wall with an earthen berm was constructed between Tank D and Pond 1 (Figure 3.5). The berm prevented rain runoff from eroding the surrounding soil and filling the low area occupied by Tanks C and D. The ponds were located in the center of the sloping drainage basin and drainage channels were created along the lateral edges to prevent damage from erosion to the pond earthen sidewalls. The low point of the drainage basin was 10 meters farther west of



Figure 3.3. Discharge Collection Tanks C & D.



Figure 3.4. Solar Experimental Ponds.

Pond # 3 and 15 cm below the pond elevation. Rain events during the experimental runs would collect in the basin but did not encroach upon the ponds.



Figure 3.5. Retaining Wall Between Tanks C & D and Ponds 1 & 2.

3.1.6 Tank Orientation and Shading

Experimental Tanks 1 & 2 were oriented in an East/West direction. This orientation shadowed plants in the midstream of the tank from solar exposure in the morning and afternoon. Tank C and D were in shade during the morning hours. Tank C was significantly shadowed being adjacent to the significantly higher Tanks 1 and 2 (Figure 3.6). The ponds had full exposure to sunlight throughout the day.



Figure 3.6. Discharge Collection Tanks C & D.

3.2 Inflow & Discharge Operations

3.2.1 Infrastructure Modifications

3.2.1.1 Secondary Effluent Piping

Site infrastructure modifications during the first year (March-August, 2004) included trenching and installing approximately 243.8 linear m of piping for transferring effluent to and from the experimental site.

3.2.1.2 Refurbishment and Planting of Wetland Tanks

From the previous experiment at the site, both Tank 1 & 2 chambers were filled with 152 cm of sand. The top 30 cm of sand was removed from both chambers and replaced with new mortar sand. The sand was added in 15 cm lifts with the volume adjusted for moisture content, and compacted to a target bulk density (1.68 g cm^{-3}). Measurements of in-situ dry bulk density were based on ring sample measurements as shown in Figure 3.7. The ring sample (two from each 15 cm lift) was dried in a microwave oven and weighed. Final dry weight of each sample was recorded when subsequent 15 minute heating (high microwave setting) resulted in no additional sample weight loss. Sample final dry weight divided by ring volume equaled bulk density. Existing soil moisture sensors (tensiometers) in the tanks were repaired and readings began in September 2004.

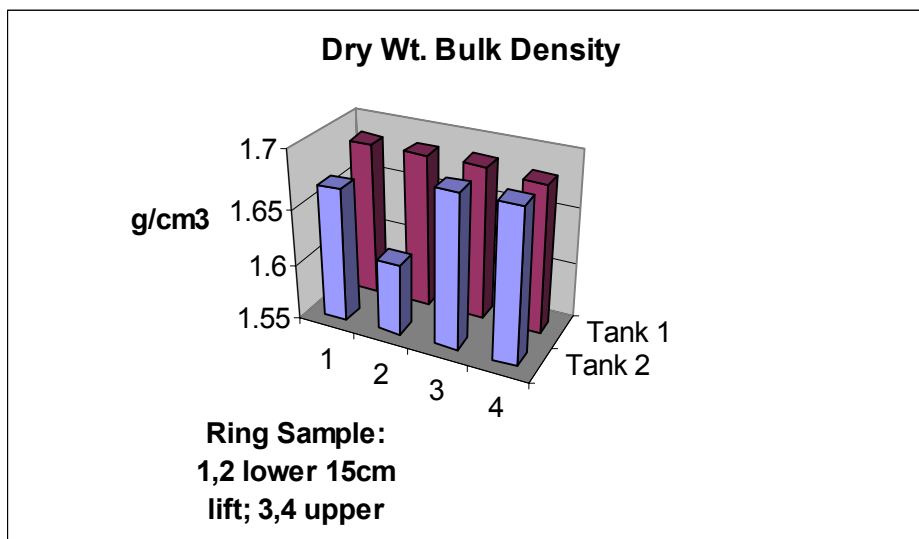


Figure 3.7. Bulk Density of Replaced Sand in Experimental Tanks 1 & 2.

Cuttings from Cottonwood trees at the CERF raceways were planted in the experimental steel Tank #1 (15 locations) and in five plastic pots on the last day of July 2004. Drip irrigation of potable water was supplied to each plant and the control steel Tank # 2. Measurements of soil temperature (15cm & 61cm depths), plant height, and soil moisture levels were taken weekly after planting.

3.2.1.3 Refurbishment of Feed and Discharge Collection Tanks

Four existing 1,324-1,893 L open stock tanks were cleaned and recoated. Two tanks (A & B) provided contaminant and effluent input mixing & settling with the remaining two tanks (C & D) providing discharge collection from the planted and control steel tanks. A 100-cm high platform, constructed from cinder building block, elevated the contaminant input tank such that gravity could feed the solution into the settling tank.

3.2.1.4 Construction of Evaporation Ponds

The UV degradation experiment was conducted in two evaporation ponds each 5.18 m wide by 8.23 m in length (Figure 3.4). Each pond was constructed with a secondary containment 6 mil thick polypropylene black plastic layer. Above the secondary containment was one layer of geo-textile cloth. The next layer, the primary containment layer, was an 8 mil thick polypropylene sheet of added strength due to a woven

interlayer. The ponds were designed to hold 1,893 L of discharge from the respective steel Tanks 1 & 2. The planned 1,893 L volume would equate to a 9 cm pond fluid depth with approximately 30 cm of freeboard. This amount of freeboard was fortunate due to rainstorm events requiring storage of 7,570 L per pond. Based on summer evaporation rates, estimated to be 0.86 cm day^{-1} from 2004 CERF pan evaporation rate data, it was anticipated that a full pond (1,893 L) would evaporate in 11 days. Due to rainfall during experiments 1, 3, 5, and 6, the actual time for full pond evaporation required several weeks. The service life of the evaporation pond plastic (in a desert environment) was expected to be 18 months.

3.2.1.5 Emergency Back-up Tank and Pond

A 1,893 L plastic tank, located near the evaporation ponds, provided emergency back up should any tank or pond experience temporary failure or overload due to rain or other unforeseen problems (Figure 3.2).

Rainfall was a significant uncontrolled variable affecting wetland discharge volumes and cottonwood evapotranspiration rates during experimental runs 1, 3, 5 and 6. Rainfall was recorded daily at the CERF facility. Dilution of tank discharge and reduction of tree transpiration rate due to the higher humidity both impacted the 1,4-Dioxane results.

Due to excessive rainfall during experiment number 1, storage and pumping problems were identified. To alleviate future surge problems, a third 5.18 m wide by 8.23 m in length dual-lined evaporation pond was constructed. This pond provided adequate surge capacity and received any overflow from Ponds 1 & 2 cleanout at the end of each experimental run. The time frame for starting a new experimental run, after the end of a previous run, was shortened due to the availability of the third pond. Additionally, the third pond was utilized as the primary overflow for pond number 2, leaving the 1,893 L emergency back up tank as the primary overflow for Pond 1. This system worked very well during experiment number 6 when one 66-mm rainstorm required all tanks to be utilized to their maximum capacity to prevent spillage.

3.2.1.6 Valves and Piping Installation

Installation of valves and piping allowed easy flow control of 1,4-Dioxane-spiked effluent and tank discharge as needed to maintain experiment operating parameters as shown in Figure 3.8. Perforated drain pipe (10-cm diameter) was installed vertically at the downstream outside corners of each Tank 1 and 2 to determine water depth. Additional outflow ports at 30.5 cm below grade were added to each tank.

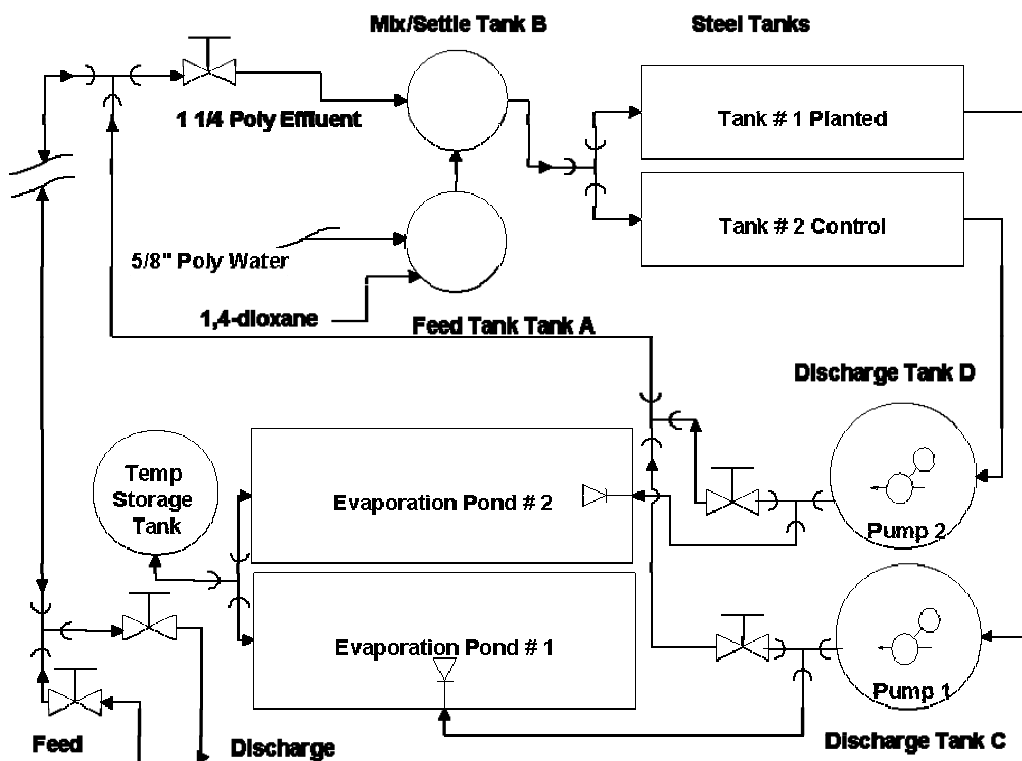


Figure 3.8. Experimental Site Valve and Piping Layout.

3.2.1.7 Storage Capacity Balance and Safety Margins

The tank and pond storage capacity was designed to hold the 1,4-Dioxane-contaminated discharge for the experiment lapse time interval of 35 hours to 251 hours. This lapse time provided adequate safety margins so that no contaminated discharge would be pumped back to the CERF facility or to the Pima County Roger Road waste treatment facility. This time period and the operating parameters for each experimental run were derived from the bromide tracer study conducted prior to the experimental runs. The operating parameters, and the upper spiked feed storage capacity, dictated the maximum

duration 1,4-Dioxane spiked feed could be sent to the experimental tanks. The spiked feed would start and stop at 0.0 and 71 hours lapse time, respectively.

3.2.1.8 Adherence to Flow and Sampling Schedule

Each experimental run had its own schedule and sampling plan detailing lapse time, date, time, flow change, and sample number to ensure strict adherence to the experimental operating plan. The schedule was reviewed daily so no event was overlooked and contaminated influent or discharge had proper disposition.

3.2.2 Tanks/Piping for Inflow/Discharge of Tap Water

3.2.2.1 Spiked Tap-Water Feed Preparation

For experimental runs 1, 2 and 3, the upper feed Tank A was filled with tap water from a CERF facility hose bib and was supplied on site through 243.8 linear m 1.6 cm diameter black poly tubing. Feed Tank A was filled with 1,412 L of tap water and stock solutions of sodium bromide and 1,4-Dioxane were added and immediately stirred with a PTFE paddle for 5-10 minutes. The stock solutions were 37.5 ml 1,4-Dioxane for all but experiment number 1 which had 7.5 ml. Additionally, 480 g of sodium bromide was added to the tap water. The tank was stirred again after a 2-hour dwell time to ensure the bromide and 1,4-Dioxane were evenly distributed throughout the feed tank solution. Total flow into each tank was 52 L hr^{-1} through a down pipe and mixing drip assembly.

The combined flow consisted of 9 L hr⁻¹ from Tank (A) and 43 L hr⁻¹ of un-spiked influent. The sodium bromide addition (480 grams) resulted in a 50 mg L⁻¹ bromide target concentration into Tanks 1 and 2 during the 72-hour spike addition.

Experimental run number 1 had a target 1,4-Dioxane influent concentration of 1.0 mg L⁻¹. In all subsequent experiments, the 1,4-Dioxane influent target concentration was increased to 5.2 mg L⁻¹. The 5.2 mg L⁻¹ concentration was achieved using a mixture of 9.0 liters per hour per tank of a spiked feed that contained 1,4-Dioxane stock concentration of 29.6 mg L⁻¹ with the un-spiked influent at 43 L hr⁻¹. The 50 mg L⁻¹ bromide concentration was achieved using the same volume of spiked influent with a bromide tracer stock concentration 230 mg L⁻¹. Influent samples were collected each day during an experiment to verify the applied 1,4-Dioxane and bromide concentration.

The duration of 1,4-Dioxane-spiked influent flow to the wetland tanks during an experiment was 72 hours, at which point flow was switched back to unspiked influent. This spike duration was dictated by the collection capacity of the solar treatment ponds and the detention time of the wetland tanks. Under a full-scale implementation, the influent concentration would be consistent unless the wetland system was designed for surge flow. The experimental pilot-scale system treatment capacity was adequate to determine contaminant uptake rates.

3.2.2.2 Influent Flow Rate

For experimental runs 1-3, the feed Tank (A) was metered into the experimental Tanks (1 & 2) by a single peristaltic pump feeding two arrays of drip emitters. The un-spiked tap water addition, in order to achieve $52 \text{ L hr}^{-1} \text{ tank}^{-1}$, was also metered by two arrays of drip emitters. For experimental runs 4 – 6 the feed Tank (A) was metered into experimental Tanks (1 & 2) by a dual-head peristaltic pump. Another dual-head peristaltic pump was metering the un-spiked secondary effluent. The mixing of the higher concentration feed with the un-spiked influent was accomplished by an inverted slotted drain channel inset with a pre-drilled sliding channel. The sliding channel was adjusted to provide a continuous drip feed (50 holes) across the width of the tank. The drain channel length was a few centimeters shorter than the width of the experimental Tanks 1 and 2.

There was a 2-6 hour delay after mixing the spiked tap water before the solution was pumped into the experimental tanks. To prevent degradation of 1,4-Dioxane from sunlight, a cover over Tank A was constructed on July 18, 2005.

3.2.2.3 Spiked Tap-Water Delivery to Experimental Wetland Tanks

The 1,4-Dioxane spiked solution was pumped from Tank A to a manifold system feeding both Tank 1 and Tank 2. The manifold system consisted of four drip emitters per tank

feeding directly into influent piping. The drip emitters, under constant pressure from the peristaltic pump (Cole Palmer 7553-10), provided an equal consistent volume to both the planted and control tanks. To maintain a 52 L hr^{-1} inflow, additional drip emitters were also feeding directly into influent piping. These emitters were fed from the CERF tap water source providing the make-up volume needed to maintain 52 L per hour per tank inflow. This mixing of raw and spiked influent was required because Tank A lacked sufficient capacity to maintain 52 L per hour per tank spiked feed for 71 hours. The influent piping inside each experimental tank was configured to enhance mixing and even distribution across the entire width of the tank by utilizing a slotted double sliding gate feed mechanism that contained 20 or more outlet holes per tank.

3.2.2.4 Spiked Tap-Water Feed Changeover

The 1,4-Dioxane feed stock would be replaced with the same volume tap water feed at 71 hours lapse time. The $52 \text{ L hour}^{-1} \text{ tank}^{-1}$ inflow would continue until the end of the experiment. Between experimental runs 1, 2 and 3, the tap water feed to the tanks would be reduced. This surge type operating condition provided a means to assess impacts to wetlands where varying influent or surge flow was common.

3.2.2.5 Wetland Tanks Discharge Collection and Transfer to Ponds

For each experimental run, prior to 1,4-Dioxane being discharged from Tank 1 and 2, both discharge lines were directed to Tank C that was automatically (float value) pumped back to the end of the CERF raceways. This return to CERF continued during 0 – 35 hours lapse time for experimental runs 1, 2 and 3. At 35 hours lapse time, Tank C would be pumped down and the automatic return of discharge to CERF would be stopped. Piping would be added to capture discharge from Tank 1 and Tank 2 into Tank C and D, respectively. From 35 to 251 hours lapse time, Tanks C and D would be pumped every 35 hours to Ponds 1 and 2, respectively. A pictorial of the treatment flow is shown in Figure 3.9. At the inflow rate of $52 \text{ L hour}^{-1} \text{ tank}^{-1}$, Tanks C and D could collect 35 hours of discharge and still have adequate safety margin to prevent overflow. The pumping occurrences, being manually controlled, were critical events for each experimental run master schedule. At no time during the experimental runs was a pumping event skipped allowing contaminated discharge to overflow the collection tanks.

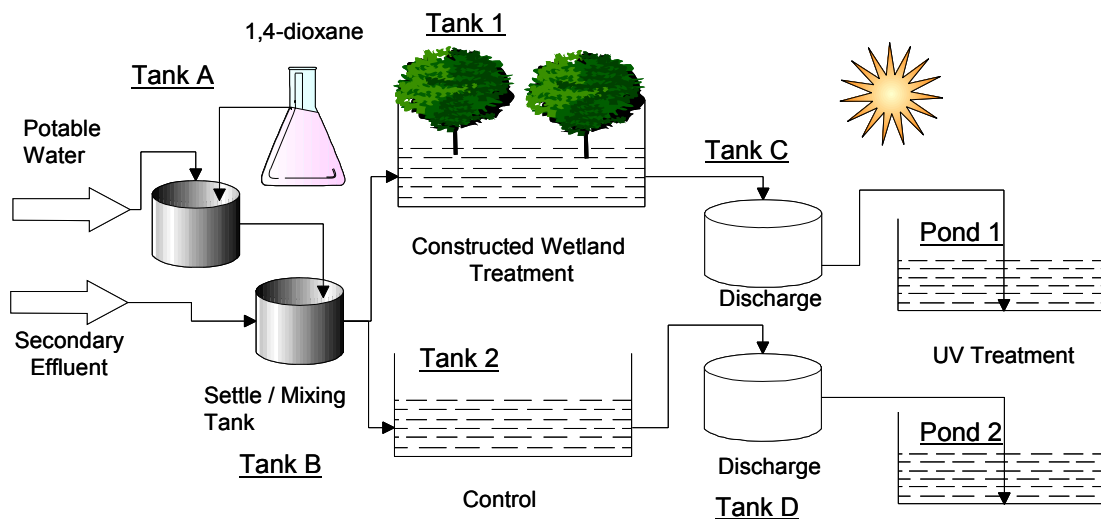


Figure 3.9. Remediation Site Layout Pictorial.

3.2.2.6 Reconfiguration of Post Spiked Discharge to CERF

At 251 hours lapse time for each experimental run, the discharge collected in Tanks C and D would be pumped to the respective ponds and the discharge from Tank 1 would again be recombined with the discharge going to Tank C. The automatic (float valve) pump would be re-connected and directional valves switched to allow Experimental run 1, 2, and 3 discharge to be returned to the CERF facility. The return line to the CERF facility was 243.8 linear meters of 3.175 cm black poly tubing originally installed to deliver secondary effluent to the experimental site.

3.2.3 Tanks/Piping for Inflow/Discharge of Secondary Effluent

3.2.3.1 Un-spiked Secondary Effluent Discharge to Sewer System

At the beginning of experimental runs 4, 5 and 6, both a discharge line (existing) and a secondary effluent feed line (to be added) was required. Utilizing the single line to CERF for both feed and discharge would require extensive switching every few hours. This constraint was resolved prior the start of the experimental runs with Roger Road Waste Treatment Facility personnel installing a threaded fitting on the manhole cover located just East of the experimental site. This added manhole cover access to the sewage system resolved the secondary effluent switching problem by allowing uncontaminated discharge to be pumped back to the sewage system. The secondary effluent feed was piped to the project site via the buried 3.175 cm black poly tubing from the CERF facility.

The discharge system for the secondary effluent experimental runs 4, 5 and 6 was timed and configured the same as the earlier experimental runs except that uncontaminated discharge was directed back to the sewer system through the manhole cover rather than being directed to the CERF facility.

3.2.3.2 Spiked Secondary Effluent Feed Preparation

Secondary effluent feed required changing the flow control mechanics for experimental runs 4, 5 and 6. Similar to the tap water experiments, Tank A was utilized as the spiked

feed source. The tank was filled with secondary effluent piped from the beginning of the CERF facility raceway number 5. The 1,4-Dioxane spike and bromide tracer, 37.5 ml and 480 grams respectively, was added and mixed with the secondary effluent. To provide consistent and controllable feed volume, two peristaltic pump heads were added to the pump motor feeding Tank 1 and 2, respectively. Additional tank covers were installed to prevent algae from growing in the secondary effluent feed tanks.

3.2.3.3 Spiked Secondary Effluent Delivery to Experimental Wetland Tanks

The secondary effluent feed make up volume was supplied differently than the previous tap water drip emitters in order to maintain total influent flow of $52 \text{ L hour}^{-1} \text{ tank}^{-1}$.

The make up volume of secondary effluent feed was pumped from un-spiked secondary effluent supplied to Tank B. Tank B had a continuous flowing supply of secondary effluent from the CERF facility. Tank 1 and 2 feed make up volume was pumped from Tank B using a second set of higher volume peristaltic pump heads. The combined spiked and make up secondary effluent volume was $52 \text{ L hour}^{-1} \text{ tank}^{-1}$.

3.2.3.4 Spiked Secondary Effluent Feed Changeover

The 1,4-Dioxane feed stock was added to Tanks 1 and 2 for 71 hours. Tank A and B feed, utilizing the peristaltic pumps, would be stopped at that time and immediately the piping would be reconfigured to provide un-spiked secondary effluent input at 52 L

hour⁻¹ tank⁻¹. Tank A would start receiving a continuous flow of secondary effluent similar to Tank B. Tank A discharge piping utilized a valve that could maintain an outflow of 102 L per hour which would be gravity fed into Tank B. Tank B piping would be configured to allow overflow discharge to be gravity fed to Tanks 1 and 2 at 52 L hour⁻¹ tank⁻¹.

3.2.3.5 Secondary Effluent Discharge Collection and Transfer to Ponds

The discharge collection and transfer of discharge to the respective pond was the same for both the tap-water and secondary effluent experimental runs. Tank 1 & 2 post spiked secondary effluent discharge, at 251 lapse time hours, would be re-directed to only Tank C. The automatic pumping would send the discharge to the sewer system in lieu of sending the discharge back to CERF as was done during the tap-water experimental runs.

3.2.3.6 Maintenance of Tanks and Ponds at Conclusion of All Experimental Runs

At the conclusion of each experimental run, Tanks A, C, & D plus Ponds 1 and 2 would be completely cleaned and dried prior to the start of the next experimental run.

3.3 Flow Measurements

Accurate inflow and discharge measurements from the experimental runs provide the basis to calculate mass flow from point-in-time concentration sampling. The discharge measurements were utilized to calculate mean discharge parameters and to conduct mass balance assessments of tracer and contaminant.

3.3.1 Potable Water

Flow measurements for experimental runs 1, 2 and 3 were primarily derived from the discharge volume in Tanks C and D. Prior to pumping Tanks C and D to the ponds, at experimental lapse times 71, 107, 143, 179, 215, and 251, the discharge fluid depth of each tank would be measured and recorded. The depth measurement converted to volume provided total flow over a 36 hour period. The input and discharge flow volumes would be checked on a regular basis to ensure the drip emitters were supplying a consistent input source.

3.3.2 Secondary Effluent

For experimental runs 4, 5 and 6, flow measures were taken prior to pumping Tanks C and D to the ponds. Inflow and discharge flow rates from Tanks 1 and 2 would be measured every 12 hours between experimental lapse times of 0 and 251 hours. Pond

depth measurements were taken every 24 hours between experimental lapse times of 265-623 hours from a reference point in each pond. Pond depth measurements were utilized to calculate remaining and evaporation volume. The conversion from depth measurement to pond volume utilized a pond depth/volume conversion table created prior to the experimental runs.

3.3.3 Hydraulic Mass Balances

3.3.3.1 Discharge Tanks Mass Balance

The cumulative mass of 1,4-Dioxane discharged from Tank 1 and 2 during an experiment was a summation of the mass discharged in between each sampling event. For a given sampling, the discharge concentration (mg L^{-1}) was multiplied by the volume of discharge (L) since the previous sampling. The experimental run discharge volume was measured at regular intervals based on Tanks C and D depth measurements. The depth measurements were converted to volumes given the known diameter of the round discharge tanks. Tanks 1 and 2 discharge volume measurements were taken every 1.5 days at 71, 107, 143, 179, 215, and 250 hour lapse times for each experimental run. These volumes were multiplied by the respective sample contaminant concentrations to derive the total 1,4-Dioxane mass discharged during the experiment from each tank.

3.3.3.2 Ponds Mass Balance

Pond sampling was conducted after a 12-hour equalization period after each tank discharge addition. The ponds were initially sampled at 191 hours lapse time. The Tank C and D additions occurred at 71, 107, 143, 179, 215, and 257 hour lapse times. Pond sample concentrations were multiplied by the respective pond volume derived from adjusting the Tank C & D discharge volumes or through direct measurement as detailed in Sections 3.3.4.1 and 3.3.4.2, respectively to derive 1,4-Dioxane mass.

3.3.4 Pond Volume

An accurate measurement of pond influent volume was required in order to track contaminant mass over time. Pond influent volume was measured by two different techniques. The direct measurement method used pond fluid depth (cm) and converted to volume (L) by a pre-established depth to volume conversion factor. The adjusted measurement method relied upon summation of Tank C & D discharge volumes with adjustments for rainfall (added) and pan evaporation (subtracted) measurements.

3.3.4.1 Tank Discharge Adjusted Volume Measurement

The tank discharge method of measuring influent volume utilized the summation of measured volumes from Tanks C & D discharge prior to pumping the tanks to the ponds.

The volume was adjusted for specific rainfall events. The rainfall-adjusted volume was then corrected for evaporation loss utilizing pan evaporation rate data recorded every 1-3 days at the CERF facility. The adjusted tank discharge volume measurement in each pond ranged from 2,000-8,000 L in experimental runs 4, 5 & 6 (Figure 3.10). Pond 1 received the discharge from Tank 1 (planted). In experimental run 4 and 5, Pond 1 volume was 3,000 and 2,000 L, respectively.

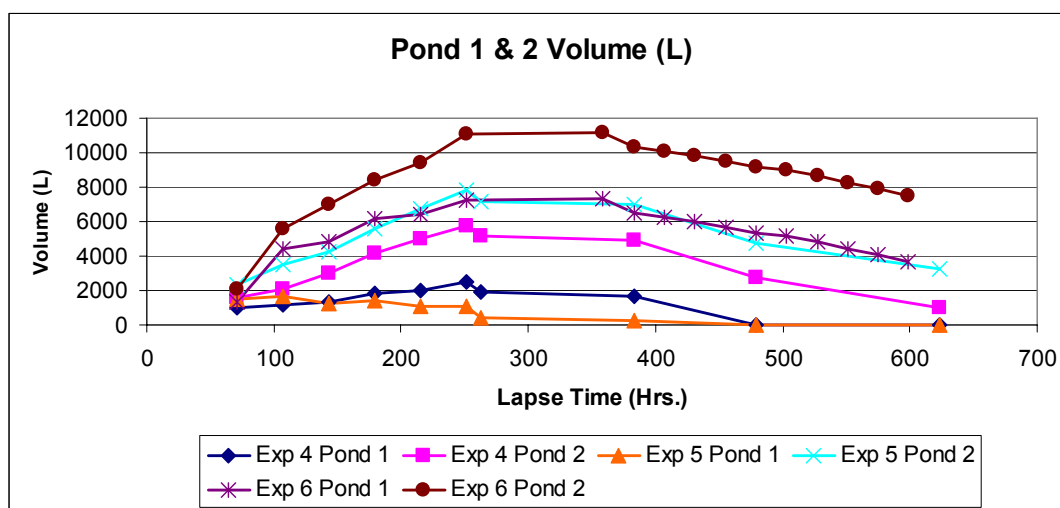


Figure 3.10. Experimental Runs 1 – 6 Total Pond Volume (Discharge plus Rain minus Pan Evaporation).

Pond 2 received the discharge from Tank 2 (unplanted). Experimental runs 4, 5 and 6 Tank 2 volume was 8,804, 10,947, and 11,428 L, respectively. This range is reflective of the lower discharge from Tank 1 due to tree transpiration.

3.3.4.2 Pond Volume Direct Measurement

The direct measurement method utilized a ruler to measure the depth of fluid at a fixed point in each pond at intervals in experimental run lapse time. This measurement was converted to volume (L) through a pre-established conversion table. The conversion table was developed by taking depth measurements in 50-gallon-addition increments.

The direct volume measurement accounted for additions (rainfall & tank discharge) and subtractions (evaporation) to the tank volume as shown for experimental runs 4, 5, & 6 in Figure 3.11. Experimental run 6 Pond 1 and 2 had significantly higher volumes due to rainstorms that added 99.6 mm (4,233 L equivalent pond volume). Experimental runs 1, 2 and 3 did not have direct measurements conducted.

3.3.4.3 Pond Measurement Method Summary

The adjusted measurement method was intended to be the primary means to establish total pond volume. This method was employed for experimental runs 1, 2 and 3. The direct measurement method was added for experimental runs 4, 5 and 6. The adjusted method inaccuracy was attributed to applying pan evaporation data with a 3-4 day sampling frequency.

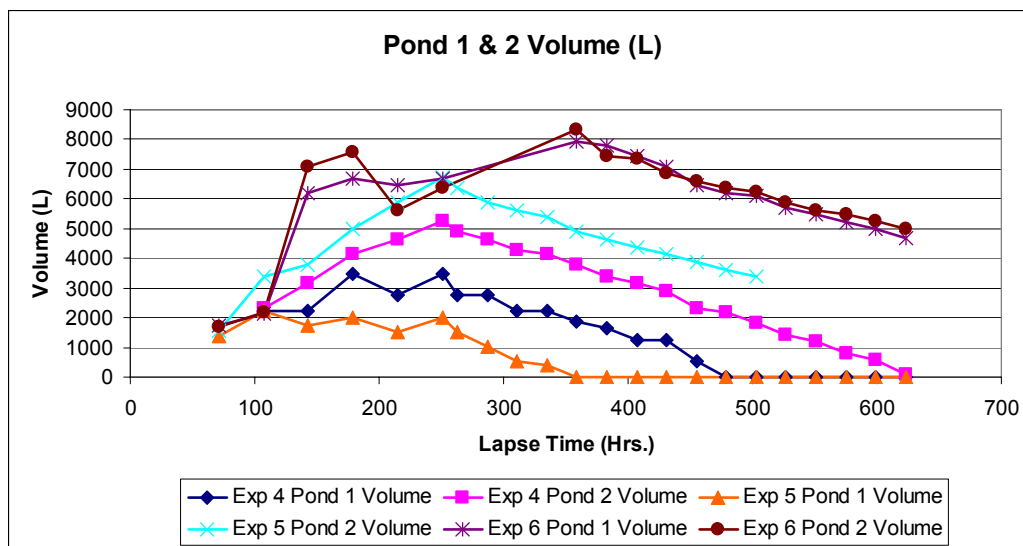


Figure 3.11. Experimental Run 4,5, & 6 Total Pond Volume (L) based on water depth measurements.

3.4 Wetland Tank Hydraulics

3.4.1 Hydraulic Loading Rate

The flow rate during experimental runs was $52.0 \text{ L hour}^{-1} \text{ tank}^{-1}$. Dividing the equivalent volume (1.248 m^3) by the area of each cell (13.94 m^2) equals the hydraulic loading rate of 8.955 cm per day which kept both tanks near 100 percent saturation level at the influent quadrant. The saturation level in the downstream quadrant of Tank 1 would vary during daylight hours due to tree uptake.

3.4.2 Hydraulic Gradient

The tank was situated on a sloped surface equivalent to 1 percent grade (Quinonez-Diaz *et al.*, 2001). This slope over the run length of the tank equated to 9.1 cm in height added to the outflow port at 30.5 cm below grade. The total elevation head was 0.396 meters. The hydraulic gradient is derived from the elevation head divided by the length of the tank (9.144 meters) and equals $0.043307 \text{ cm cm}^{-1}$. Since the presence of standing water was minimal, pressure head was negligible.

3.4.3 Hydraulic Conductivity

The hydraulic conductivity is the velocity at which water moves through soil in response to pressure gradients. Hydraulic conductivity is related to the physical properties of the material as well as properties of the fluid flowing through the material (Yeh, 1999). While some of the material and fluid properties can be estimated or established, the intrinsic permeability factor relating to the shape of passages and the tortuosity of flow paths is not readily obtained without experiments to measure hydraulic conductivity (Yeh, 1999). Numerous single ring infiltrometer (SRI) measurements from a previous study, utilizing the same tanks and mortar sand, were used to establish hydraulic conductivity. The most repeatable test was the falling head technique using iron rings measuring 25.4 cm and 30.5 cm in diameter. The measured hydraulic conductivity at the beginning of the experiment was $1.8 \times 10^{-4} \text{ m sec}^{-1}$ (Ellman, 1997).

3.4.4 Flow Dwell Time

Utilizing the hydraulic conductivity as derived from falling head SRI tests, the breakthrough or dwell time of the experimental tanks can be calculated from Darcy's Law (Yeh, 1999).

Darcy's Law is an empirical equation where discharge (Q) equals the hydraulic conductivity (K) times the hydraulic gradient (i) times the cross sectional area (A) expressed as ($Q = Ki A$). The cross sectional area (A) constitutes both solid and void spaces. This equation can be rewritten where (q) is the Darcian velocity or specific discharge. Darcian velocity must be divided by the porosity (n) of mortar sand (0.348) in order to derive the seepage velocity ($q = Ki/n$) (Yeh, 1999).

Taking into account the above factors, including a cross sectional area of 2.32 m^2 and assuming an average porosity of mortar sand to be 34.8 percent, the overall seepage velocity equals $0.0000224 \text{ m sec}^{-1}$ resulting in breakthrough at 4.74 days or 113.4 hours.

3.4.5 Bromide Tracer Study

To confirm the estimated breakthrough time and establish a baseline to compare tracer timelines in later experiments, a bromide tracer study was conducted prior to the beginning of the experimental runs with 1,4-Dioxane.

The source compound was Sodium Bromide from Sigma Chemical Company (S-9756). A bromide concentration of 230 mg L^{-1} was pumped to the inlet of each tank at 52 L hour^{-1} for a total lapse time of 72 hours. From 72 hours until the end of the tracer study, unspiked tap water was fed to the tanks at the same flow rate. The total feed was a mixture of $15.45 \text{ L hour}^{-1}$ of a bromide stock solution mixed with $36.55 \text{ L hour}^{-1}$ tap water. Tap water (only) followed the bromide mixture for days 3 through 12.5 at 52 L hour^{-1} . The bromide tracer study sample locations are shown in Figure 3.12. The background bromide concentration was 0.55 mg L^{-1} .

3.4.5.1 Bromide Tracer Study Sampling Locations

The bromide tracer study commenced May 21, 2005 and concluded June 2, 2005. Samples were taken every 2 hours the first day, and every 4 hours the remaining days. Sample locations (Figure 3.12) included input and discharge ports for both tanks as well as sample tubes located on the vertical centerline axis of the upstream, midstream and downstream third of each tank. The tanks also had three sets of 4 stainless steel porous cup suction ports per tank. The porous cup suction ports, located vertically at 15.2 cm, 30.5 cm, 61.0 cm, and 91.4 cm below the soil surface, were accessible for vacuum hookup from the outside of each tank. The porous cups sampled along the vertical axis centerline of each tank with extension tubes connecting the porous cup to the outside wall

of the tanks. The viability of these existing stainless steel solution sample porous cups (24) was tested prior to the start of the bromide tracer study. Sixteen of the 24 cups

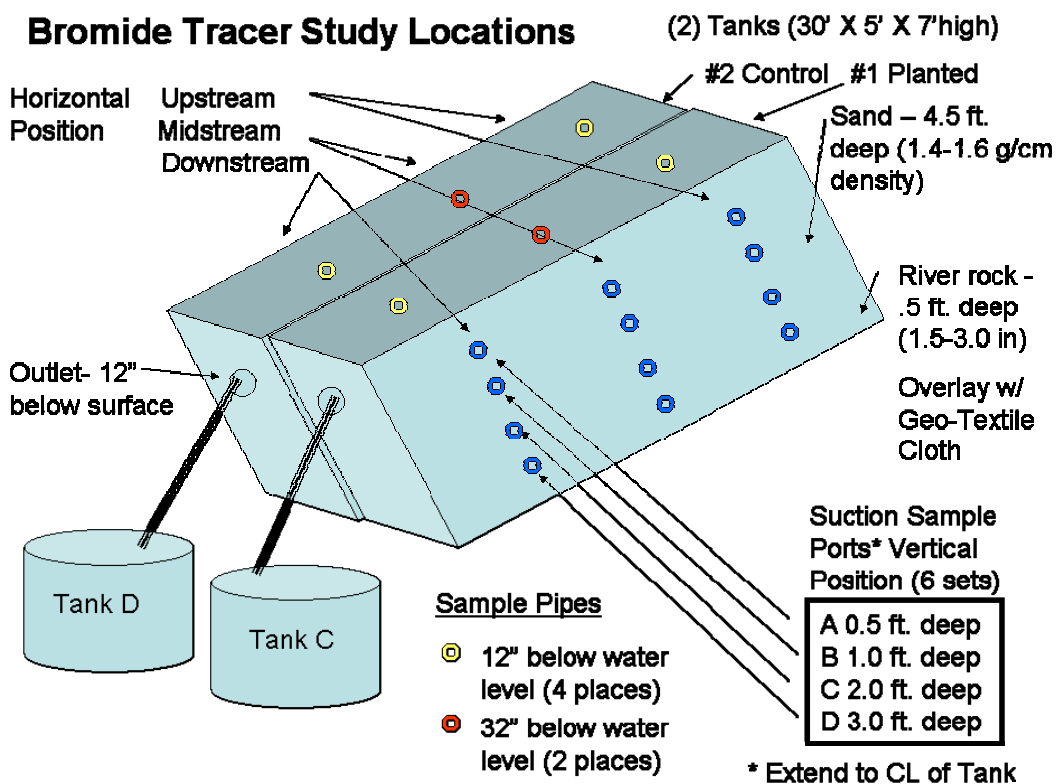


Figure 3.12. Bromide Tracer Study Sample Locations.

remained functional and provided adequate capability for collecting liquid samples along the flow paths in each tank chamber. Bromide sample designations are shown in Table 3.1.

Table 3.1. Bromide Tracer Sample Designations.

Bromide Tracer Study Sample Location Descriptions			
Sample Designator	Location	Suction Sample Ports	
	Tank #	Horizontal	Vertical Position
1	1	Lower	B
2	1	Lower	C
3	1	Middle	C
4	1	Middle	D
5	1	Upper	C
6	1	Upper	D
7	2	Lower	C
8	2	Middle	C
9	2	Upper	C
10	2	Upper	D
11	1	Full Tank C prior to pumping to pond	
12	2	Full Tank D prior to pumping to pond	
13	1	Planted Discharge	
14	2	Un-Planted Discharge	
15	1	Lower Drain (No Samples Taken)	
16	2	Lower Drain (No Samples Taken)	
17	1	Upper	Centerline Pipe @ 12" below water level
18	2	Upper	Centerline Pipe @ 12" below water level
19	1	Middle	Centerline Pipe @ 32" below water level
20	2	Middle	Centerline Pipe @ 32" below water level
21	1	Lower	Centerline Pipe @ 12" below water level
22	2	Lower	Centerline Pipe @ 12" below water level

3.4.5.2 Immediate Tracer Sample Processing

The samples were analyzed immediately after collection. The laboratory set up and procedure for the bromide tracer study was identical to the set up and process utilized on

all experimental sample runs. A calibration curve was established and method blanks were ran to confirm the measurement process.

3.4.5.3 Tracer Study Results Validate Estimated Dwell Time

The bromide tracer study provided adequate subsurface flow detail of the tracer slug. Sample locations 13 and 14 were the discharge pipes from Tank 1 and 2, respectively and showed maximum bromide concentrations at 109 hours. This peak breakthrough time was very close to the predicted breakthrough at 113.4 hours or 4.74 days shown above. The tailing of the bromide tracer concentration did not reach background after 300 hours at which time the tracer study was stopped.

Bromide tracer samples from the upstream suction sample ports (sample location 5 & 9 for Tanks 1 & 2 respectively) showed a very fast response to the bromide tracer front starting at 28 hours lapse time. Sample locations 21 and 22 from the downstream centerline pipe at 30.5 cm below grade showed a delayed response to the bromide tracer front. The effect was more pronounced in the planted tank with maximum bromide concentration at 212 and 189 hours for Tanks 1 and 2, respectively. This effect was likely due to the lack of saturation of the downstream upper surface area.

A 91 and 95 percent recovery of the bromide tracer for Tanks 1 and 2, respectively, was achieved over the 300 hours of sampling. Averaged Tank 1 and 2 recovery of the tracer

study is shown in Figure 3.13. The tracer study did show some bromide loss in Tank 1 which is further discussed in Section 4.2.3.

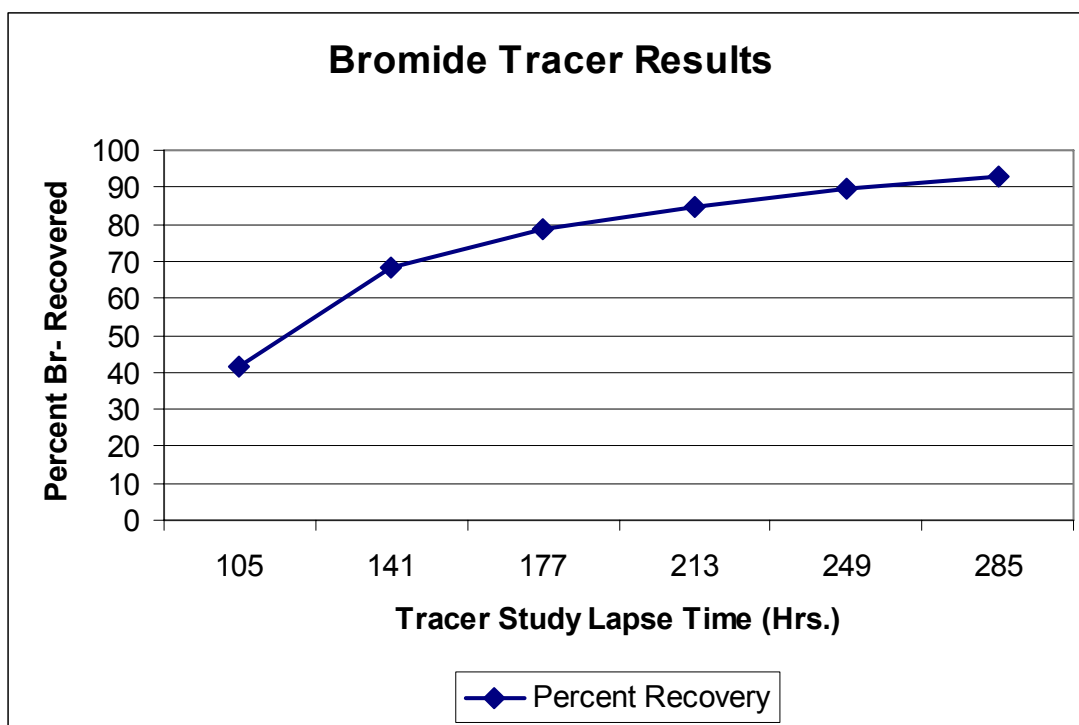


Figure 3.13. Cumulative recovery (in percent) of the bromide tracer from Tanks 1 and 2.

3.5 Tree Planting in Wetland Tank

The cottonwood tree (*Populus fremontii* S. Wats.) was selected for the constructed wetlands experimental study based upon the successful 1,4-Dioxane uptake and transpiration laboratory results reported in previous published studies. Cottonwood was also selected due to the fast growth, ability to withstand periods of flooding, and

tolerance of 1,4-Dioxane. Cuttings were taken from the cottonwood trees growing at the CERF facility.

3.5.1 Pre-preparation and Placement

3.5.1.1 Cottonwood Cuttings

After completing the preparation of the planted and control tanks as indicated in the previous section, cuttings were obtained from the cottonwood trees at the CERF facility. The process for obtaining the cuttings was outlined by Dr. Karpiscak in a paper document titled “Planting Procedure for Cottonwood Branches”, undated. Branch pieces (122 cm long and 1.9 cm diameter) were removed from various cottonwood trees with the cut end immediately placed in a 18.9 L bucket filled with water. The leaves were removed while maintaining the cut end under water.

3.5.1.2 Cottonwood Cutting Placement

Placement for the cuttings in Tank 1 was determined by the overall tank length and width, allowing $0.9 \text{ cm}^2 \text{ tree}^{-1}$. A staggered two-row placement of the cuttings allowed for 15 trees. The left row (South side of Tank 1) cuttings, from upstream to downstream, were numerically identified 1-7. The right row (North side of Tank 1) cuttings, from upstream to downstream, were numerically identified 8-14. Cutting 15 was centered between the two rows in the furthest downstream location. To aid in planting the

approximate 122-cm long cuttings, 61 cm long sections of 15.24 cm diameter plastic pipe were installed vertically in the wet sand. After making a fresh cut on the lower end of each cutting, two or three cuttings per location were inserted into the plastic pipe open end and backfilled with wet sand. Drip irrigation was immediately started after each planting with continuous flow of $1.89 \text{ L hour}^{-1} \text{ plant}^{-1}$ location. The top of each cutting was trimmed to 10.1 cm above the sand and a spray pruning sealant applied to the cut end. Six cuttings were planted in plastic buckets to be utilized as spares which were located just outside the tanks and watered the same as those planted in the experimental tank. All cuttings were placed on July 31, 2004.

The plastic pipe sleeves remained in place for two weeks to ensure adequate moisture was maintained around each group of cuttings.

3.5.2 Tree Growth & Irrigation

3.5.2.1 Early Growth and Watering Schedule

Signs of growth were evident on each cutting by August 21, 2004 with the highest growth at plant location 8, 9, 10, 11, and lowest growth at plant location 2, 3, 7, 13, and 15. By September 18, 2004 new growth height ranged from 7.62-99 cm with a varying number of smaller shoots.

On October 3, 2004, the height of the dominant cutting at all plant locations ranged from 74-152 cm. Cuttings at plant location # 3 remained at 2.54 cm and appeared dead. Location # 3 cuttings were replaced by one of the spare plants on October 23, 2004. Watering duration of drip emitters was reduced to 30 minutes every 8 hours (1.89 L hr^{-1} emitters) due to lower daytime temperatures.

The rate of drip irrigation was reduced to 15 minutes every 24 hours on November 13, 2004 and Christmas tree lights were installed in each tank at the end of November to prevent tree damage due to freezing weather. Dominant tree height continued to be measured each week. New growth appeared on all the plants January 22, 2005 following a rainstorm the night before.

3.5.2.2 First Year Dominant Cutting Growth

All tree locations were trimmed to a single dominant cutting with the single cutting lower branches removed on February 13, 2005. Tree height ranged from 61-200 cm and the 1.89 L hr^{-1} emitter duration was increased to 15 minutes every 8 hours on March 3, 2005. Irrigation was increased to 30 minutes every 6 hours on March 26, 2005. On April 17, 2005 tree # 3 was accidentally broken off and was replaced by another of the spare trees. Irrigation was increased to 1 hour every 6 hours.

A pattern of lower tree height for the midstream trees (3, 4, 5, 10, 11 and 12) was identified in May 2005. The difference in tree height was initially attributed to potential higher moisture content on the outflow of the tanks where slight upwelling would occur. Higher soil moisture content at the inflow of the tank would also exist due to infusion rate when drip irrigation was stopped and inflow from the feed tanks was utilized during the bromide pre-experiment tracer studies and subsequent experimental runs.

For most of 2005, increased irrigation flow occurred for the duration for each experimental run. In 2005 potable water at a flow rate of 52 L hour⁻¹ tank⁻¹ was utilized for the pre-experiment bromide tracer run (5/21/2005-6/1/2005), experimental run # 1 (7/18/2005-7/30/2005), experimental run # 2 (9/12/2005-10/2/2005), and experimental run # 3 (10/10/2005-10/22/2005). At the end of 2005, tree height ranged from 279 cm to 551 cm (excluding tree # 3).

3.5.2.3 Initial Secondary Effluent Introduction

By January 15, 2006 the trees started to bud. On January 28, 2006, after new growth developed, the potable feed water was augmented with 10 percent secondary effluent supplied from the CERF inflow. The secondary effluent was taken from the feed source at the CERF wetlands.

The secondary effluent percentage was increased to 20 percent on February 6, 50 percent on February 11, 60 percent on February 21, and finally 100 percent on February 26. The slowly increasing level of secondary effluent allowed adequate time for the trees to acclimate to the changing irrigation source. After the addition of secondary effluent, the upstream trees developed significantly larger dark green leaves than downstream trees. In order to stabilize the flow rate prior to starting an experimental run, the secondary effluent flow rate was increased to 50 liters per hour on April 20, 2006 and was maintained at that level for the duration of all remaining experimental runs. The secondary effluent experimental runs for Tanks 1 and 2 occurred May 1, 2006 – May 12, 2006 (experimental run # 4), June 5, 2006 – June 16, 2006 (experimental run # 5), and July 24, 2006 – August 4, 2006 (experimental run # 6).

3.5.2.4 Tree Trimming and Tree Loss

During experimental run # 4, surface ponding was observed in the upstream area of the tanks. This may have been the result of reduced infiltration rate due to higher solids content of the secondary influent. During a significant wind storm (June 17, 2006) tree # 1 started to lean. By July 2, 2006, tree # 1 had fallen over and was cut down. Increasing temperature and increasing transpiration of the trees was decreasing discharge from Tank 1 which would have negatively impacted the overall experimental run # 6 results. Lower branches were removed on June 24, 2006 and immediately resulted in increased outflow from Tank 1.

3.6 Wetland Tank Temperature & Soil Moisture

3.6.1 Temperature Measurement

3.6.1.1 Weekly Thermometer Temperature Readings

Soil temperature readings were taken one time per week between September 4, 2004 and April 12, 2005. Temperature measurements at 15.2 cm and 61 cm below grade were taken in the upstream, midstream and downstream sections of each tank. The weekly temperature history using thermometers inserted in tank media did not provide adequate resolution for the experimental runs.

3.6.1.2 Automated Thermocouple Measurement and Data Collection

In early April 2005, thermocouples were installed 15.2 cm and 61 cm below grade in the upstream, midstream and downstream sections of each tank as well as ambient air reference thermistor probes. Additional thermocouples were installed in each of the discharge tanks and ponds. Once a week, temperature data from a total of 16 thermocouples was downloaded to a laptop computer. The thermocouples, installed in the steel tanks, discharge tanks, and evaporation ponds, were linked to a Campbell Scientific AM416 multiplexer and CR10X data logger. A recently charged battery was exchanged to power the data logger every other week to ensure no data loss. A relatively complete record of hourly temperature readings (averaged from 15 minute readings) for

the various tanks and ponds was established for the period April 12, 2005 to December 22, 2006.

3.6.1.3 Thermocouple Installation in Tanks and Ponds

A temperature sensor was located in each discharge tank and pond that recorded temperature every 15 minutes and averaged the readings every hour. Averaged temperature readings for the tanks and ponds, during experimental runs 1 – 6, were recorded every hour, between 0-624 hours lapse time.

The thermocouples in the tanks at 61 cm depth below grade and in the discharge tanks and ponds were Campbell Scientific 229-L heat dissipation sensors (HDS). The heat dissipation sensors consisted of a resistive heat element and thermocouple combination inside a hypodermic needle size tube surrounded by a porous ceramic plug.

When used as a heat dissipation sensor, line current is supplied to the heat element for approximately 20 seconds and the thermocouple takes temperature measurements at one second and 20 seconds. Once calibrated, the resulting temperature increase can be correlated to soil water content. The use of HDS to function as simply a thermocouple probe was due to availability. The heating element was never connected in the experimental set up. The 15.2 cm below grade thermocouples were Campbell Scientific 105T-L thermocouples.

3.6.1.4 Thermocouple Calibration

The thermocouples were calibrated prior to installation at 0.0, 20.0, 30.0, and 40.0 degrees centigrade. The calibration process showed slight variations among the heat dissipation sensors at the lower temperature. All sensors (except TC # 1) were closely correlated at 30-40 degrees centigrade. A trial of the thermocouple data logger set-up was conducted on April 12 2005. The trial took readings every minute and averaged every 5 minutes over a 24-hour period.

3.6.2 Tensiometer Soil Moisture Measurement

3.6.2.1 Tensiometer Locations

An attempt to measure soil moisture began in September 2004 utilizing three sets of five existing soil moisture sensors (tensiometers) in the planted and control tanks (Soil Measurements Systems, Tucson, Arizona). The tensiometer sets, installed at 30, 40, 70, 100, and 130 centimeters below grade, were located in the upstream one-third, midstream, and downstream one-third of each tank. These tensiometers were left in place from a previous experiment. The tensiometer devices consisted of a ceramic porous cup connected to a PVC tube filled with water and sealed with a rubber septum stopper.

3.6.2.2 Tensiometer Measurements

The tensiometers were fitted with new rubber septums and water tension measurements were taken each week with a Soil Measurement System battery operated pressure transducer identified as a tensimeter (US Patent No: 4520657). The tensimeter consisted of a pressure transducer with digital readout (Soil Measurements Systems, Tucson, Arizona) utilizing a hypodermic needle to pierce the rubber septum stopper atop each tensiometer and read the resulting pressure. Minimal variation of the readings was due to saturated conditions within the tanks at all tensiometer depths and locations. The saturated conditions, at or below 30 centimeters below grade, did not provide meaningful results for soil moisture in the unsaturated root zone and soil tensiometer readings were stopped May 1, 2005.

3.6.3 Time Domain Reflectometry

Time domain reflectometry (TDR) has become increasingly popular for determining soil water content. The advantages of TDR include superior accuracy ($\pm 1-2$ percent) in measuring volumetric water content. The system has minimal calibration requirements and does not use radioactive or other hazardous materials. The TDR system has excellent spatial and temporal resolution (Or *et al.*, 2004). TDR principles and processes are readily documented in literature which provided an adequate background to attempt TDR probe construction and measurement for the experimental project.

3.6.3.1 TDR Measurement Unit

TDR measurement of soil moisture was started in December 2005. A TDR unit (Textronic 1502) was purchased and configured to interface with a portable computer. The computer interface was a 16 bit analog to digital converter and RS232 interface that included a separate voltage operational amplifier circuit.

3.6.3.2 TDR Probe Characteristics

In order to measure soil moisture with the TDR unit, twelve trifilar probes were constructed. Probe characteristics were established from previous conductivity measurements of the experimental tanks and the anticipated soil moisture conditions.

The probe prongs were stainless steel welding rods (CLSS316L) 0.3173-cm diameter cut to length (Source: Pima Welding Supply, Tucson, Arizona). The coax cable was RG-58AU (M4210) with CBRS ug-88 c/u connectors (Source: Electronic City, Tucson, Arizona). The epoxy resin for the probe handle was GE Potting Epoxy 19-823A & B (Source: Elliott Electronics, Tucson, Arizona).

3.6.3.3 TDR Probe Installation

The constructed probes were installed horizontally in Tanks 1 and 2 on March 4, 2006 at 6, 16, 26, and 36 centimeters below grade. The four probes, at the depths indicated, constituted a probe set. Probes sets 1 & 2 were installed in the center of Tanks 1 & 2, respectively. Probe set number 3 was installed in the downstream 1/3 of the planted tank.

3.6.3.4 TDR Waveform Post Processing

Time domain reflectometry (TDR) was initially developed to determine breaks or discontinuities in cables (Jones *et al.*, 2002). At high frequencies (1.77 GHz), the reflected signal highlights propagation velocity changes as the signal travels down the cable. The velocity changes are a function of dielectric impedance (dielectric constant) changes due to line breaks or frayed insulation. The TDR-reflected signal actually measures time which is converted into distance internally by the TDR equipment based on propagation velocity (Evet, 2000).

The TDR wave form was captured on a PC and post analyzed to determine soil moisture content utilizing G. C. Topp's polynomial equation. This equation is based on the linear relationship of soil moisture content in sand causing an impedance time delay of the reflected TDR signal. This time delay can be interpreted from the captured wave form.

3.6.3.5 TDR Waveform Equation for Conversion to Soil Moisture

The same principles in wire break detection are applied when using TDR to measure soil bulk dielectric constant (ϵ_b). The soil bulk dielectric constant (soil relative permittivity) is governed by the dielectric constant of water (81) (Or *et al.*, 2004). The dielectric constant (ϵ_b) of a medium is the ratio squared of the propagation velocity in a vacuum to that in the medium. The dielectric constant is insensitive to soil composition, texture, and temperature (Heathman *et al.*, 2003). The relationship between soil bulk dielectric constant (ϵ_b) and volumetric water content (θ_v) was an empirical model derived by Topp *et al.* (1980). They fitted a third-order polynomial to observed relationships of (ϵ_b) and (θ_v) for multiple soils (Or *et al.*, 2004). The polynomial from Topp *et al.* (1980) is

$$\text{percent H}_2\text{O} = [-5.3 \times 10e-2] + [(2.92 \times 10e-2) (\epsilon_b)] - [(5.5 \times 10e-4) (\epsilon_b^2)] + [(4.3 \times 10e-6) (\epsilon_b^3)]$$

where: ϵ_b = dielectric constant and e = exponent (Kelleners *et al.*, 2005). This soil moisture equation is applicable when utilized with soil relative permittivity. The soil relative permittivity is the difference between the true length of the probe and the length experienced by the voltage pulse (Kelleners *et al.*, 2005). The new length, utilized to determine (ϵ_b), is established by instrument and probe measurements in air or de-ionized water (Kelleners *et al.*, 2005). The measured electrical impedance travel time is utilized to determine (ϵ_b) (Heathman *et al.*, 2003).

3.7 UV/Solar Light and Volatilization

3.7.1 Full Day UV and Solar Measurement

To assess the ultra violet (UV) light and solar (photo oxidation) potential at the project site, one full day of UV and Solar sampling was conducted on June 18, 2005. The readings were taken on a cloudless day with no haze in the sky. The location of each reading was the influent point of experimental Tank # 2.

3.7.1.1 UV and Solar Measurement Equipment

A solar-blind vacuum photodiode detector (IL 9ED240) was used with a research radiometer (IL 1700). The photodiode detector cathode material (determines spectral sensitivity) was Cs-Te providing only UV light sensitivity (Ryer, 1998). The typical Cs-Te photodiode detector cathode detector wavelength response is shown in Figure 3.14. The unit had been re-calibrated on December 30, 2004.

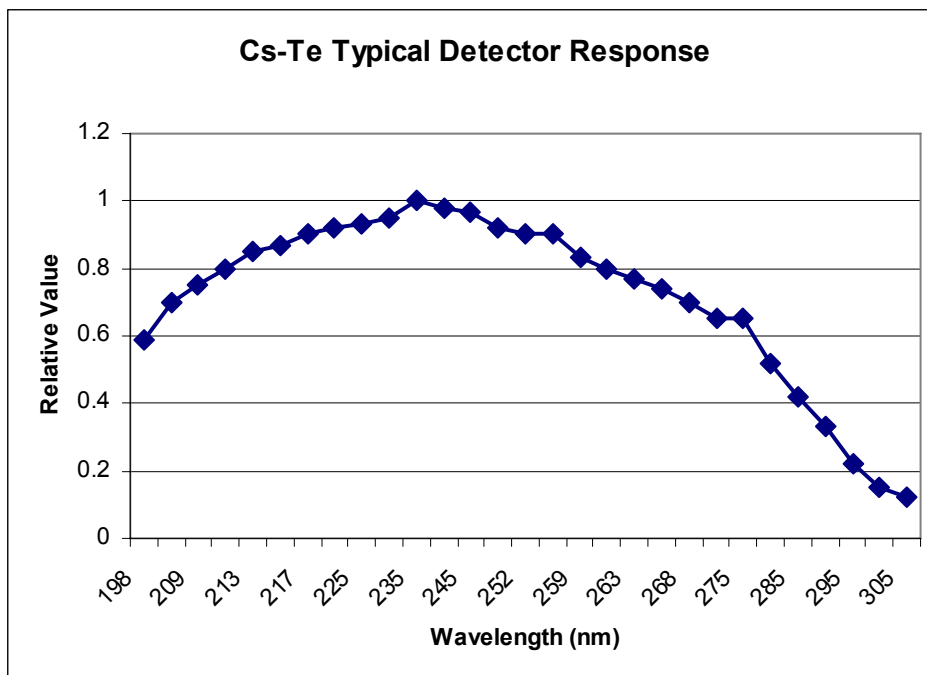


Figure 3.14. UV Cs-Te Photodiode Typical Detector Response (Ryer, 1998).

3.7.1.2 UV and Solar Measurements

Four sets of 30 light intensity readings were taken every 30 minutes (5:00 A.M. - 7:30 P.M.). Each set consisted of detector readings without filters, only a narrow UV filter (NS254), only a cosine (W9266) filter, and the UV and Cosine filter combined. The UV filter has a narrow response (peak at 252 nanometers) which limits the UV detection range to 240 – 270 nm (Ryer, 1998).

3.7.1.3 UV and Solar Measurement Results

The resulting maximum UV response occurred at 12:00 P.M. (0.003 watts cm^{-2}). The detector unit may have been out of calibration since the daily cumulative UV exposure from the readings would be orders of magnitude higher than other experimental studies (see Figure 3.15 and 3.16). A hand held UV lamp output was also measured with readings of 0.00402 watts cm^{-2} .

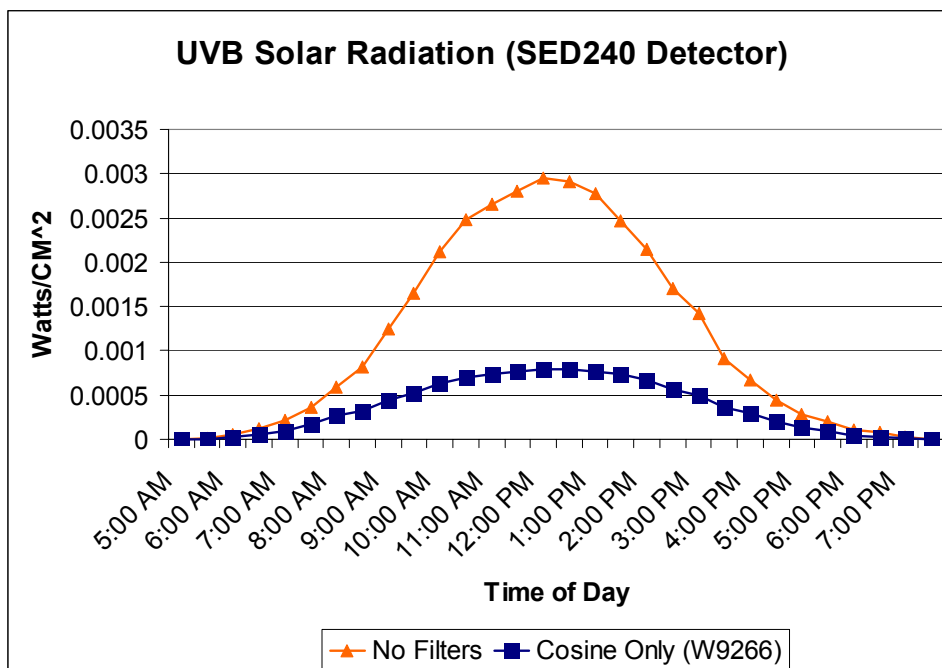


Figure 3.15. UV-B One Day Solar Radiation.

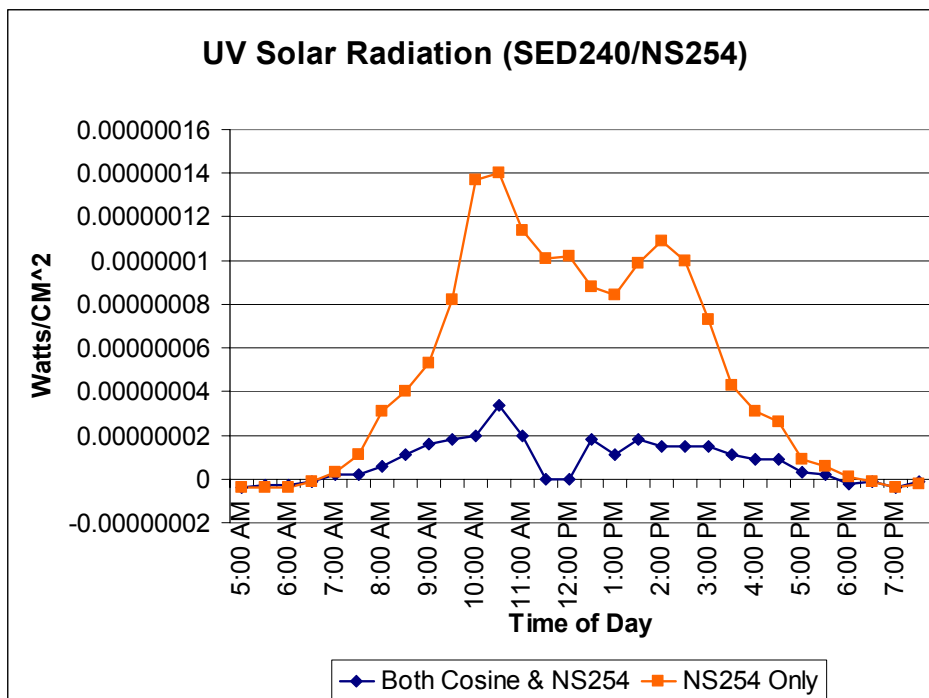


Figure 3.16. UV-B One Day Response with NS254 Filter.

3.7.2 UV and Solar Contaminant Degradation Side Experiment

In order to determine the extent of UV degradation and surface evaporation of the 1,4-Dioxane, a side experiment was conducted October 21, 2005.

3.7.2.1 Side Experiment Set-Up

At the end of the sixth and final pumping from Tanks C & D for experimental run # 3, a separate side experiment was conducted. This side experiment utilized two 378 L tubs that were 68.6 centimeters deep. The tubs were filled with tap water and 1,4-Dioxane

was added to each tub to achieve a 10 mg L^{-1} concentration. To isolate evaporation without the solar component, a cover was placed over one of the tubs, leaving a 7.62 centimeter air gap between the top of the tub and the bottom of the tub cover. The other tub remained uncovered and exposed to sunlight. 1,4-Dioxane concentrations in the tubs were measured at 9 and 18 days lapse time. The tubs were located near Ponds 1 & 2.

3.7.2.2 Sampling and Contaminant Measurement

One liter samples were taken from each of the grey tubs at the same time pond samples were obtained. Additionally, the fluid level drop (inches) was measured to establish evaporation volume. The tub samples were extracted and measured on the HP 5790 GC using the same process as experimental run # 3 samples. The results from each tub showed only a minimal difference in 1,4-Dioxane concentration indicating the overarching reduction mechanism was likely surface evaporation and not UV or solar degradation.

3.7.3 Follow-up UV and Solar Side Experiment

To validate the first side experiment, a second side experiment study was conducted in conjunction with experimental run # 4 starting May 12, 2006. This second experiment was performed to see if the results from the first experiment could be replicated. Data

logger thermocouples were placed in the pools and readings were obtained every 15 minutes and averaged every hour.

The second experiment utilized a 1,4-Dioxane concentration of 5.3 mg/L. The side experiment was conducted concurrently with experimental run # 4 pond experiments. The cover was installed with the same air gap (7.62 centimeter) between the top of the pool and cover bottom as the initial side experiment.

3.7.3.1 Side Experiment Set-up

The grey tubs from the first side experiment were replaced with shallow wading pools for the second side experiment. Each of the wading pools in the second side experiment study received 110 liters secondary effluent spiked with 0.57 ml 1,4-Dioxane. The first side experiment (grey tubs) solution was 91.44 cm deep while the second side experiment wading pool depth was 17.0 cm. The wading pool depth closely matched the nominal pond depth of 15 cm.

3.7.3.2 Sampling and Contaminant Measurement

Samples and depth measurements were taken at the same frequency as the ponds and processed the same as the experimental run # 4 samples. The covered and uncovered wading pool results were very similar to the first side experiment which utilized tap-

water. A slightly lower contaminant concentration of the uncovered pool indicated a potential UV and solar degradation component. The majority of contaminant loss was attributed to surface evaporation.

3.7.4 UV-B and Solar Sun Side Experiment

In an attempt to quantify the 1,4-Dioxane reduction attributed to UV or solar radiation, a third side experiment was established that utilized individual UV-B and sun solar intensity lamps. Experiments were conducted using UV-B (253.7 nm wavelength), visible light without the UV-B component (330 nm wavelength cutoff), and no light (negative control) for time periods of 1, 2.5, and 5 days. At the end of each experiment the liquid was removed for laboratory extraction and GC measurement of 1,4-Dioxane.

3.7.4.1 UV-B Side Experiment Set-up

The UV-B lamp source was a hand held lamp with a short wave filter (Ultraviolet Products SL2537) with 90 percent output at 253.7 nanometer wavelength having a measured UV-B radiation output of 0.00402 watts per cm^2 (3.1 mm distance between lamp and detector). The cumulative UV-B output of the lamp for a 24-hour time frame was 217.08 watts per cm^2 or approximately 200 times greater than the equivalent day of sunlight UV-B exposure. The UV-B lamp was configured with a flow thru well of 10

cm² area (see Figure 3.17). This flow thru well allowed the 1,4-Dioxane spiked solution to directly contact the lamp filter glass.



Figure 3.17. UV Lamp with Flow-Through Cell.

3.7.4.2 Solar Sun Side Experimental Set-up

The other light source was a Cermax Xenon lamp (LX300-F). The F lamp reflector was coated with a silver alloy that attenuates the UV-B spectral output at 330 nanometers wavelength (Cermax, 1998). This lamp was installed in an Optoelectronic Research Centre (ORC) illuminator (6000) with a (4) channel fiber optic cable. The fiber optic cable was configured to plastic piping tees such that the light output was in direct contact with the flowing 1,4-Dioxane-spiked solution as shown in Figure 3.18.

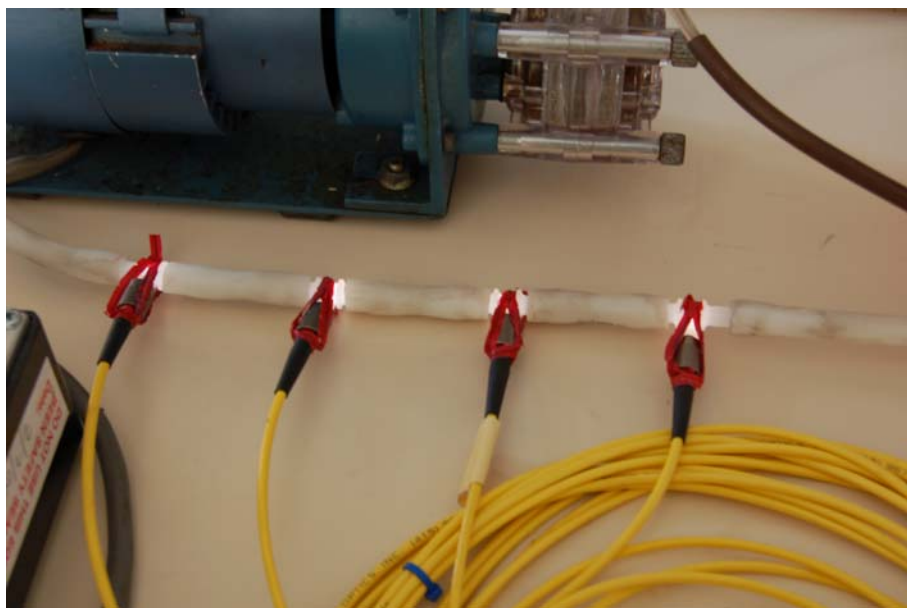


Figure 3.18. Solar Light Connection to Spiked Flow.

3.7.4.3 Experimental Flow Rate and Run Time

The experimental setup consisted of a three head peristaltic pump configured to a pump motor flowing at 5 ml per second. The three 1- liter containers were configured with sealed tops allowing re-circulation of the two spiked solutions (UV & Solar) and the control (see Figure 3.19). The system was operated at room temperature (27 °C) continuously for a total of 5 days for the first set of samples and 2.5 days, and 1.0 day for the remaining set of samples. Since only a fraction of the 1-liter solution was exposed to UV light at any given moment, the cumulative UV-B equivalent exposure during the experiment was 50 percent less than would have occurred under continuous exposure to natural sunlight. This accounted for the 24-hour per day lamp exposure and the partial 24-hour period solar exposure.

3.7.4.4 UV-B and Solar Sun Experimental Results

The water samples collected during the UV and Solar experiments were extracted and processed the same as the Experimental run # 6 samples. The experimental set up was successful for the 5 day exposure. The other UV samples (2.5 and 1.0 days) were not viable due to seal leakage between the UV lamp and the exposure well thereby allowing air to purge the 1,4-Dioxane.



Figure 3.19. Solar Experiment Set-Up.

3.7.5 Volatilization Process

The volatilization elimination process is first order with the process rate constants reflecting half-life reductions of the contaminant. The half-life of the rate constant is

independent of the starting concentration for any process that is first order. When one half of the original amount of the contaminant has been eliminated, $M = \frac{1}{2}M_0$. The half-life derivation utilized to calculate the half-life values from the rate constant is shown below (Schwarzenbach *et al.*, 1993). Time (t) is hours.

$$\frac{1}{2}M_0 = M_0e^{-Ket} \quad (3.1)$$

$$\frac{1}{2} = e^{-Ket/2} \quad (3.2)$$

$$\ln(\frac{1}{2}) = -Ket^{1/2} \quad (3.3)$$

$$t_{1/2} = \ln 2/ke = 0.693/Ke \quad (3.4)$$

Diffusion is a thermally activated process whose rate is defined by a diffusion coefficient. Contaminant flux is a change in contaminant concentration per unit area and time. This process is similar to the elimination rate process that reflects a change in contaminant concentration with respect to time. The Arrhenius equation defines the logarithmic relationship between the rate constant and temperature (Schwarzenbach *et al.*, 1993). The Arrhenius equation for contaminant elimination is as follows:

$$K_e = Ae^{-E_a/RT} \quad (3.5)$$

Where (K_e) is the elimination rate constant,

A is the frequency (collision) factor,

E_a is the activation energy,

R is the Gas Constant, and

T is temperature ($^{\circ}\text{K}$).

If a measured elimination process follows the exponential Arrhenius equation, then a plot of the natural log of the rate constant (K_e) to the reciprocal of the absolute temperature ($1/T$) will produce a straight line with a slope of E_a/R and the y-intercept of the natural log a (A) (Schwarzenbach *et al.*, 1993).

3.8 Laboratory Methodology

The analytical methods to extract and measure 1,4-Dioxane in the water samples were based on EPA Method 8270C. A Corning One-Step liquid-liquid extraction system was used to separate and concentrate the 1,4-Dioxane from 1-liter samples. A gas chromatograph with flame ionization detection (FID) was used for compound detection. The extractions and measurements were performed in an Environmental Engineering department laboratory.

3.8.1 Sample Collection and Storage

The 1-liter samples were collected in muffled (4 hours at 550 °C) 1.3 liter amber glass jars. After collecting a sample, the jar was immediately sealed utilizing a Teflon jar lid liner. The samples were stored at 4°C prior to extraction. Extraction would typically take place within 3-5 days of collection.

The handling and storage parameters followed guidance from Aerotech Environmental Laboratories Standard Operating Procedure (SOP) titled EPA 8270C Modified 1,4-Dioxane By Isotope Dilution, Extraction and GC-MS Analysis, July 2004. The guidelines directed: 1) Water samples should be taken in clean, 1-liter amber glass jars with Teflon-lined lids and should be stored at $4 \pm 2^\circ\text{C}$ following sampling until extraction; 2) Water samples should be extracted within 7 days of sampling and analysis must be completed within 40 days of extraction; and 3) Sample extracts should be stored at $-10 \pm 2^\circ\text{C}$, protected from light, in sealed vials equipped with un-pierced PTFE-lined septa.

The preservation and storage stability of 1,4-Dioxane in water was previously investigated by the Sanitation and Radiation Laboratory Branch, California Department of Health Services. The research was a limited study of 1,4-Dioxane (2.0 mg L^{-1}) added to Northern California lake surface water and chlorinated ($1.9 \text{ mg Cl}_2 \text{ L}^{-1}$) tap water. Sample treatments included pH adjustment and de-chlorination by the addition of HCL

and sodium sulfite, respectively. The results showed no statistically significant change in the concentration of 1,4-Dioxane with or without treatments (Draper *et al.*, 2000). The results indicate that 1,4-Dioxane is stable under typical preservation conditions used in drinking water compliance monitoring. Further, 1,4-Dioxane did not appear to degrade in the presence of chlorine (or chloramine) at the dosages found in drinking water disinfection (Draper *et al.*, 2000). Thus, no additional sample preservation procedures were employed in this project.

3.8.2 Sample Filtering

3.8.2.1 Apparatus

The filtering apparatus consisted of a Van Waters & Rogers (26316-708) glass filter holder with fritted glass support, silicone stopper on the support glass stem, filter cup, and attachment clamp to secure the filter cup to the fritted glass support. Prior to initial use, the filter glassware was washed in 0.1 N HCL followed by rinses in milli-Q water.

All filter glassware and hardware was washed in laboratory detergent and tap water, followed by triple rinse with tap water, and a final rinse in milli-Q water. Glassware was dried thoroughly prior to use. Due to the large mouth of the sample jars, a glass funnel was utilized to decant, without spillage, the first 200 ml from each sample. The glass funnel was washed and dried as indicated above prior to re-use on the next sample. The filter assembly stopper was positioned above a 1000-ml vacuum flask which would catch

the filtrate. The final filtrate was poured into the extraction vessel within minutes following final filtration. Vacuum for the filtration process was supplied by an oil-less compressor connected through a three port PVC manifold system (Figure 3.20).



Figure 3.20. Filter Flasks and Vacuum Manifold.

3.8.2.2 Initial Filtering with Glass Fiber Filters

Samples with high concentrations of organic matter (algae) were pre-filtered with 3.0 μm muffled glass fiber filters. Samples from the ponds would often require 6-7 3.0 μm filters to complete the 1.0 L sample.

All samples were vacuum filtered through 0.7 μm muffled glass fiber filters. The samples with higher organic matter would require 2-3 0.7 μm filters to complete the 1.0 L sample.

3.8.2.3 Final Filtering with PVDF Filters

After the glass fiber filtration step(s), all samples were then vacuum filtered through 0.455 μm polyvinylidene fluoride (PVDF) Vericel filters (PALL FP450). The PVDF Vericel filter was selected based on recommendations from the filter manufacturer. Personal E-mail correspondence with the manufacturer technical representative established the suitability of the PVDF Vericel filter for use with aqueous samples containing 1,4-Dioxane.

3.8.2.4 Filtering Sample Identification Procedure

To maintain sample identification, all filter flasks were labeled with the sample number prior to the filter process. The sample number was removed from the filter flask and transferred to the extraction apparatus immediately after the final filtrate was added to the extraction vessel. Approximately 50 ml from the sample jar was decanted to a smaller sample plastic container for other measurements. The original label from the sample container was transferred to the small sample plastic container. For experimental runs 5

and 6, an additional 40 ml from the final filtrate flask was saved in a 40-ml muffled amber glass vial with a Teflon lined cap for measurement of dissolved organic carbon (DOC). The DOC and small plastic bottle samples were stored at 4 °C pending analysis.

3.8.3 Sample Extraction Methods

Extraction techniques for removal of 1,4-Dioxane from aqueous solutions include liquid-liquid extraction, solid phase extraction (SPE), trap and purge, and headspace injection. Head space and trap and purge methods have higher detection limits due to the low purge efficiency of 1,4-Dioxane (Draper *et al.*, 2000). Trap and purge methods are affected by matrix interferences and trap apparatus can be contaminated with 1,4-Dioxane (Park *et al.*, 2005). The detection limit for trap and purge is 3-20 $\mu\text{g L}^{-1}$ (Isaacson *et al.*, 2006). Solid phase extraction activated carbon disks eluted with acetone have proven successful in contaminated groundwater samples. High recovery and GC/MS detection limits (0.31 $\mu\text{g L}^{-1}$) were achieved with 80 ml sample volumes (Isaacson *et al.*, 2006). Various combinations of these methods have also been reported. Single contact liquid-liquid extraction followed by SPE and elution with acetonitrile provides 60-75 percent recovery in water samples (Song and Zhang, 1997). Continuous liquid-liquid extraction using 1.0 L samples produce extraction efficiencies of 70-75 percent and provides 0.2 $\mu\text{g L}^{-1}$ GC/MS detection limit (Draper *et al.*, 2000).

3.8.3.1 Liquid-Liquid Extraction

The Corning One-Step liquid-liquid extraction system was selected for the 1,4-Dioxane sample extraction based upon the history and level of acceptance by the U. S.

Environmental Protection Agency. The EPA method to quantitatively determine the presence of 1,4-Dioxane in liquid matrices utilizes continuous liquid-liquid extraction with methylene chloride as the extraction solvent. Solvents for extraction were pesticide grade. The one liter sample extract is concentrated to 1 ml with nitrogen evaporation.

The Corning Accelerated One-Step Extractor concentrator is approved for EPA Method 3520C for pesticides and PCBs with a 5.5 hour extraction time as identified in the U.S. Environmental Protection Agency documents: 1) Continuous Liquid-Liquid Extraction, SW-846 Method 3520C, Revision 3, December 1996 and 2) USEPA Contract Laboratory Program (CLP) Statement of Work (SOW) for Organics Analysis, Multi-Media, Multi-Concentration SOM01.1 - Exhibit D Semi-volatiles, May 26, 2005.

3.8.4 Liquid-Liquid Extraction Equipment Set-up

3.8.4.1 Jacketed K-D Concentrator

The extraction apparatus utilized a jacketed K-D concentrator heated with re-circulated water for boiling methylene chloride. The heat for the concentrator was supplied at 91 °C from a NESLAB Exacal EX200 re-circulating heater and a three-port manifold system.

The 91 °C water bath temperature produced a methylene chloride evaporation rate of 50 ml in 3.4 minutes as required per the Corning One-Step extractor manual.

3.8.4.2 Extractor Allihn Condenser

The extractor vapors were cooled with re-circulating chilled water in a jacketed Allihn condenser. The Allihn condenser had 5 °C circulating water from a NESLAB CFT-33 Series re-circulating chiller supplying 950 watts of cooling capacity (NESLAB, 1997).

3.8.4.3 Corning Extractor 1.0 L Vessel

The extractor vessels utilized a hydrophobic membrane to separate the water and DCM phases. The membrane was held in position between two Photoceram™ membrane supports and a Corning 3915 coupler assembly. The coupler assembly attached the extractor vessel bottom flange to the Corning extractor cup with the membrane and membrane supports between the two components.

Re-circulation of the extraction solvent was through a Snyder three ball sidearm connecting the extractor body to the K-D concentrator. The Snyder sidearm also connected the Corning extractor cup to the lower portion of the Snyder sidearm through a stopcock assembly sealed by Teflon coated silicone washers. Other connections in the system were sealed with Viton® O-rings.

The procedure for set up and operation of the Corning One-Step liquid-liquid extraction apparatus is contained in operating instruction supplied with the equipment.

3.8.4.4. Extractor Operation and Contaminant Sample Collection

The 1.0 L samples, after being added to the assembled Corning One-Step liquid-liquid extraction apparatus, were extracted for 6 hours using 100 ml methylene chloride. One ml of 1,4 dichlorobenzene d_4 (surrogate) was also added prior to each extraction.

After 6 hours of extraction, the K-D concentrator stopcock was closed and all but 3 ml of the methylene chloride in the concentrator was boiled off. The heated re-circulating water was stopped and the concentrator allowed to cool.

The concentrator was uncoupled from the Snyder sidearm and the remaining extract in the K-D condenser was evaporated to 1 ml volume using dry nitrogen. The 1 ml sample was removed from the condenser and transferred to a screw top GC vial utilizing a glass pipette. The 1 ml extract is a 1000 to 1 concentration factor from the 1 L sample. The capped vial, properly labeled with experiment and sample number and extraction date, was stored at -10°C until analyzed on gas chromatography equipment.

3.8.4.5 Extractor Efficiency and Variation

The single largest variation in analysis accuracy relates to the extraction efficiency (Zenker *et al.*, 2003). The extractor efficiency can be greatly impacted by matrix effects, membrane plugging, and rate of methylene chloride distillation. In this work, the 0.45 μm filtration step eliminated many matrix and clogging concerns. The use of KD jacketed condensers with adequate heat generating capacity and a condenser manifold system eliminated most extractor variability. In the laboratory study of Draper *et al.* (2000) an extraction efficiency of 70-75 percent was reported for 1,4-Dioxane.

The Corning One-Step extractor system from the Draper *et al.* (2000) laboratory study produced a 70-75 percent extraction efficiency using a 6.0 hour extraction time. The Corning extractor system consumed substantially less solvent volume than conventional Hershberg-Wolfe type extractors due to the hydrophobic membrane (Draper *et al.*, 2000).

The use of the hydrophobic membrane extractor eliminated the need to run the sample extract through a drying column containing anhydrous granular sodium sulfate.

Concentrating the sample extract to 1.0 ml volume was performed within the extractor set-up minimizing sample extract transfer and handling.

Chemicals utilized in the extraction process were PRA grade dichloromethane from Sigma-Aldrich Inc. (323993-4L). The surrogate was 1,2-Dichlorobenzene- d_4 .

3.8.5 1,4-Dioxane Measurements: Gas Chromatography / Flame Ionization Detection Methods

3.8.5.1 Gas Chromatography Analysis Procedures

Within twenty days of extraction, samples were analyzed on a Hewlett Packard (HP) 5790A gas chromatograph (GC) with a flame ionization detector (FID). For samples from experimental runs 1 and 2, the GC utilized a DB5 Column 30 meters long, 1.5 μm film thickness, and 0.53 mm diameter. The injection temperature was 200 $^{\circ}\text{C}$, detector temperature 300 $^{\circ}\text{C}$, and oven temperature 100 $^{\circ}\text{C}$. The N_2 gas pressure was 0.71 PSI. Samples were run in splitless mode.

The GC-FID measurements of 1,4-Dioxane were conducted in triplicate. The average peak area count was used to determine 1,4-Dioxane concentration. Each sample result file from the GC-FID integration software was saved on hard disk. The file consisted of a graphical summary of the plotted signal from the FID detector and the area percent report, as shown by example in Figures 3.21 and 3.22, respectively.

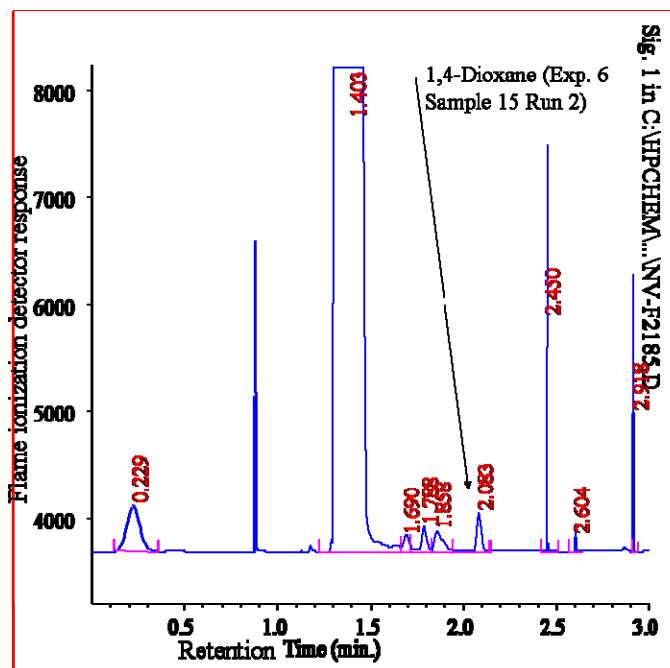


Figure 3.21. Typical GC Chromatogram Showing 1,4-Dioxane Peak Position at 2.083 minutes.

```

=====
                          Area Percent Report
=====
Data File Name   : C:\HPCHEM2\DATA\WARD\INV-F2185.D
Operator        : Ward                      Page Number   : 1
Instrument       : HP 5790                  Vial Number     :
Sample Name     :                          Injection Number:
Run Time Bar Code:                          Sequence Line  :
Acquired on    : 03 Sep 06 11:12 PM        Instrument Method: WJWSC1.MTH
Report Created on: 03 Sep 06 11:15 PM      Analysis Method : WJWSC1.MTH

Sig. 1 in C:\HPCHEM2\DATA\WARD\INV-F2185.D

```

Pk#	Ret Time	Area	Height	Type	Width	Area %
1	0.229	2104	438	BB	0.074	0.0120
2	1.403	1.74761E+007	2404726	BB S	0.120	99.9712
3	1.690	309	143	VV T	0.034	0.0018
4	1.788	462	229	VV T	0.031	0.0026
5	1.858	572	185	VV T	0.043	0.0033
6	2.083	683	365	VB T	0.029	0.0039
7	2.450	525	2413	BB	0.004	0.0030
8	2.604	47	183	BB	0.011	0.0003
9	2.918	339	1155	VV	0.012	0.0019

Total area = 1.74812E+007

Figure 3.22. Typical Area Percent report showing Detector Response Integrated Area Summary. The 1,4-Dioxane Peak is at 2.083 Minutes.

The 1,4-Dioxane concentration results were tabulated either separately or combined with other operating parameters, and used with volume discharge data to perform a mass balance analysis for each experimental run. Cumulative 1,4-Dioxane discharged mass from the tanks was established using both Tank 1 & 2 discharge samples as well as the Tank C & D samples taken just prior to pumping Tanks C & D to the respective ponds. In experimental runs 5 and 6, Tank 1 & 2 discharge samples and Tank C & D samples were collected at the same lapse time schedule. This sampling scheme permitted mass balance analysis comparisons based on the tank discharge grab samples and the time-integrated (composite) Tank C & D samples. These results are provided in Section 5.4.1.

Due to equipment gas flow failure and column degradation problems, experimental runs 3-6 utilized a new DB5 column installed on January 20, 2006. The new DB5 column was 30 meters long, 1.0 μm film thickness, and 0.252 mm diameter (Agilent Technologies 1225033 S/N US5261241H). The HP 5790A operating conditions were injection temperature 200 °C, detector temperature 300 °C, and oven temperature 100 °C. The N_2 gas pressure was 1.8 kg cm^{-2} with split vent flow of 11.4 ml min^{-1} and septum purge flow at 60 ml min^{-1} .

3.8.5.2 Gas Chromatography Operation

Three replicate injections of each sample were analyzed on the GC with the results averaged in determining the final constituent concentrations. The previously established

calibration standards and extraction standards were re-analyzed prior to a batch run of new samples.

Experiment number 5 GC samples were measured July 3, 2006. The HP 5790A GC operating conditions were injection temperature 200 °C, detector temperature 300 °C, and oven temperature 100 °C. The N₂ gas pressure was 1.8 kg cm⁻² with the split vent flow of 26 ml min⁻¹ and septum purge flow at 42.8 ml min⁻¹. These same operating conditions were utilized for the re-run of experiment number 4 samples on July 4, 2006 utilizing 2 µL injection volumes.

Experiment number 6 samples, and a re-run of experiment number 5 samples, was initiated September 3, 2006. The HP 5790A GC operating conditions were injection temperature 200 °C, detector temperature 300 °C, and oven temperature 100 °C. The N₂ gas pressure was 1.8 kg cm⁻² with split vent flow of 15 ml min⁻¹ and septum purge flow at 20 ml min⁻¹.

Method blanks were analyzed with each experimental run and indicated no presence of 1,4-Dioxane.

3.8.5.3 1,4-Dioxane Calibration Standard Curves

3.8.5.3.1 Dilution Calibration Standard Curves

The 1,4-Dioxane used in the experimental runs and for calibration standards was HPLC grade from Aldrich (D20,186-3). The 1,4-Dioxane standard curve, established with each batch of samples, consisted of six dilutions (1, 10, 100, 500, 1000, 5000 mg L⁻¹). A representative standard curve is shown in Appendix B.1.8, Figure B.3.

The 1,4-Dioxane standard curves, for all the experimental runs, averaged $r^2 = 0.997$ with the coefficient of variance for the slope below 30 percent. The calibration standard results demonstrated equipment sensitivity, detection limit, and linearity were similar for measurements taken from all the experimental runs. The variation in slope of the standard curves was resulting from: 1) changing of the column after experimental run 3, 2) shift from splitless flow to minimal control over septum purge, 3) lack of total flow control with replacement valve.

3.8.5.3.2 Extracted Calibration Standard Curves

In addition to conventional 1,4-Dioxane concentration standard curves, standard curves were also developed from extracted calibration standards. This calibration method accounted for the extraction efficiency and concentration without the need for individual sample result adjustment based on surrogate recovery. The method is valid if there is

minimal variation in extraction efficiency among sample types, including milli-Q water, Tank 1 discharge with tap water fed, and secondary effluent. To validate this methodology, standard curves were established with spiked extracted samples from each of these sample types. The tested spiked concentration of 1,4-Dioxane for each sample type was 0.1, 1.0, and 5.0 mg L⁻¹.

The solutions for the calibration spiked samples came from laboratory milli-Q water, Tank 1 discharge (tap water influent) and secondary effluent. The average slopes for the respective extracted calibration curves, from the various experimental run calibration set ups, were similar for the three water types: milli-Q = 0.00132, Tank 1 discharge = 0.000158, and secondary effluent = 0.000357 (mg L⁻¹/GC area).

3.8.5.3.3 1,4-Dioxane Concentrations Established by Extracted Standard Curves

The extracted calibration standard curves were utilized to establish the 1,4-Dioxane concentrations from the experimental run samples. A comparison between utilizing the 1,4-Dioxane in methylene chloride calibration curves, after adjusting for extraction efficiency and concentration factor, and the extracted calibration curves was conducted. The average difference between the two methods, adjusting for scale differences, was 4.1 percent.

The resulting calibration curve for 1,4-Dioxane extracted from various medium did not indicate significant matrix effects.

3.8.5.4 GC Equipment Constraints

3.8.5.4.1 Equipment Gas Flow Failure

The total flow valve failed on the HP 5790A GC and was removed leaving no means to control N₂ split flow or operate in splitless mode. This operating condition was not suitable for GC measurements and one in-line valve was added to provide minimal control of septum purge flow. The added valve directed a portion of the injected sample into the GC column. Samples from experimental runs 3-6 were measured using the modified flow control set-up.

3.8.5.4.2 Column Degradation Problems

The DB5 column used on the initial samples from experimental run #1 (August 5, 2005) adequately separated the DCM solvent, DCB surrogate, and 1,4-Dioxane peaks at lapse times 0.600, 0.748, and 0.841 min, respectively. The area count under the surrogate peak was around 160,000. This area reflects both the concentrating effect and efficiency of the extraction process.

In two months time, the DB5 column degraded such that the elution peaks for DCM and 1,4-Dioxane were reduced to 0.374 and 0.517 min, respectively, for samples from experimental run number 3 (October 30, 2005). The 1,4-Dioxane peak was contained within the tail of the DCM peak, precluding accurate determination of the integrated peak area. As a result of the column degradation, a new capillary column was purchased and put into service January 2006. The new column provided adequate elution separation between the solvent and 1,4-Dioxane peaks at 1.433 and 2.086 min, respectively.

3.8.5.4.3 Elution Timing Equipment Problems

Starting with experiment number 4 GC analysis, the manual start button on the HP 5790A would not make adequate electrical contact. Often several actuations of the start button were required to initiate the run timer. As a result, while the peak areas were easily distinguished, correlation to elution time was not as accurate.

3.8.5.5 Surrogate Operating Constraints

A surrogate was utilized in determining extraction efficiency from experimental run 1 samples. The surrogate was not found to increase accuracy and was not needed to improve the method detection level. Over a 30-60 day storage period, the surrogate appeared to degrade in the sample vials and became unsuitable for GC analysis correction.

A DCB surrogate standard of $0.20 \mu\text{g ml}^{-1}$ was used instead of the $20 \mu\text{g ml}^{-1}$ as recommended in a personal e-mail to Ultra Science technical service (Fitzgerald, E-Mail). This reduced concentration would offset the extractor 1000 X concentrating effects and the extraction efficiency. The extracted peak area of the $0.20 \mu\text{g ml}^{-1}$ surrogate was 59,955. A re-run of experiment number 1 samples on October 2, 2005 showed a significant reduction in the DCB surrogate peak area (mean = 69,683; std. deviation = 10,895) while the DCB surrogate standard reflected approximately the same area as the earlier result (54,885). Surrogate areas of samples from experimental run number 2 were significantly decreased (700-2,300) indicating a loss or degradation of the surrogate.

There was no surrogate peak on any sample in experimental run number 3 perhaps reflecting further degradation of the surrogate spiking solution. As a result, a new surrogate, 1,2-Dichlorobenzene- d_4 , was obtained and $0.20 \mu\text{g ml}^{-1}$ extraction concentrations were prepared. The new surrogate eluted at 1.399 minutes with a peak area of 60,032. The surrogate was unsuitable since it never separated from the solvent peak in any of the experiment 4, 5, or 6 samples.

The inability to accurately measure the surrogate peak area could have impacted the accuracy of the 1,4-Dioxane results. The surrogate typically resolves variations in extraction efficiency caused by matrix interference effects and extraction set-up and

operating conditions. Matrix effects did not pose a significant concern based on the results of the milli-Q, Tank 1 Discharge, and Secondary Effluent extracted calibration standards at 0.1, 1.0, and 5.0 parts per million concentrations.

3.8.5.6 Internal Standard Elution Problems

The fluorobenzene internal standard ($20 \mu\text{g ml}^{-1}$) consistently eluted at 0.748 min lapse time with a GC peak area of 31,000-34,000. No internal standards (IS) were added to the samples because the IS elution peak would overlap the 1,4-Dioxane elution peak resulting in sample measurement loss. Sample-to-sample injection volume variation was not significant, based on comparison of peak area counts.

External standards are superior to internal standards for low contaminant concentration samples with FID detectors because the 1,4-Dioxane and internal standard are not completely resolved (Draper *et al.*, 2000). The use of external calibration curves and extracted calibration curves provided accurate and repeatable results in the determination of 1,4-Dioxane concentration.

3.8.5.7 Impact of Bromide on 1,4-Dioxane Samples

A set of 1 mg L^{-1} 1,4-Dioxane extraction samples were analyzed on the GC-FID consisting of milli-Q water with and without bromide. The bromide concentration (80

mg L⁻¹) was the same utilized as a flow tracer for each experimental run. This analysis verified bromide presence did not negatively affect the extraction process and detection of 1,4-Dioxane by the GC-FID. The results showed no difference in peak area counts of 1 mg L⁻¹ 1,4-Dioxane spiked samples with and without bromide (80 mg L⁻¹).

3.8.5.8 Laboratory Contaminant Lower Detection Limit

The detection of 1,4-Dioxane with GC-FID is relatively straight forward with proper (functioning) equipment. The instrumental detection level of the HP 5790 used for the analysis of the sample extracts was 1 mg L⁻¹. With the liquid – liquid extraction concentration factor of 1000 to 1, the theoretical sample detection limit was 1 µg L⁻¹. With the equipment available, the level of quantitation, after extraction, of an experimental run sample was 0.2 mg L⁻¹.

3.8.5.9 Methods to Improve Lower Detection Limit

The Draper *et al.* (2000) study found using an isotope dilution procedure improved the accuracy by 10 percent and lowered the method detection limit by a factor of 4 fold (3.1 µg L⁻¹ to 0.72 µg L⁻¹). The isotope dilution step allows correction of the extractor efficiency (Draper *et al.*, 2000). The same study, using flame ionization detection, found calibration was superior with external standards because the 1,4-Dioxane and internal standard were not completely resolved (Draper *et al.*, 2000).

In another study of 1,4-Dioxane liquid-liquid extraction, Park *et al.* (2005) found the coefficient of variance to be 6.7 percent which is similar to extracted samples from the experimental wetlands.

3.8.6 Bromide Tracer, Turbidity, pH, Conductivity Methods

3.8.6.1 Sample Collection and Storage

For extraction designated samples (Arabic designation) a portion of the raw sample was set aside to conduct bromide tracer, turbidity, pH, and specific conductivity measurements. After the one-liter sample was removed from the 1.3 L amber glass jar sample, the remaining 0.3 liter portion of the sample was transferred to a smaller container and stored at 4 °C.

Non-extraction designated samples (Letter designation) were collected in 20 ml plastic containers and stored at 4 °C pending testing of bromide tracer, turbidity, pH, and conductivity.

3.8.6.2 Bromide Measurement

Bromide was measured with a Corning 315 portable pH/Ion meter with a Corning bromide ISE probe and a Corning AG/AGCI double junction reference electrode. The

reference probe (Corning P/N 476067) was checked for adequate content of 1.0 M KNO_3 and 3.0 M KCL in the outer and inner chambers, respectively. The Ion-Selective Electrode (ISE) bromide probe (Corning P/N 476128) was rinsed in milli-Q water and blotted dry with a lint-free paper towel. The reference junction probe was checked to ensure flow from the glass frit tip, rinsed in milli-Q water, and placed in a beaker of 1.0 M KNO_3 .

After solutions reached room temperature, 10 ml of each experimental run sample was transferred into separate clean 30-ml glass beakers. An equal amount of 0.2 m KNO_3 was added as buffer.

Prior to the analysis of each set of samples, bromide calibration standards (0.8, 8, 80, 800, 8000 mg L^{-1}) were measured to create a baseline and establish linearity and proper function of the bromide probe. Additionally, a calibration blank was measured. If the calibration was correct, the two probes were rinsed in milli-Q water and inserted into each sample and agitated briefly.

The Corning 315 portable Ion meter was set to read in milli-volts. After a couple of minutes, the ISE probe would stabilize and the meter would freeze the display value which was recorded for that sample. The ISE and reference junction probes were rinsed in milli-Q water and dried or placed back into the 1.0 M KNO_3 .

3.8.6.3 pH Measurement

Each sample was analyzed for pH using an Orion 210A Plus pH meter with an internal reference pH probe (Orion P/N 9105), and automatic temperature compensation (ATC) probe (Orion P/N 917005).

Both probes were rinsed in milli-Q water and blotted dry with lint free paper before taking readings of samples. Prior to running samples, the pH meter and probe would be sequenced through the 2-point automatic internal calibration procedure using 7 and 10 pH calibration buffers. The calibration procedure would establish the instrument internal conversion slope for the pH readings. The 7-10 calibration was utilized in lieu of the 7-4 calibration since most samples would be 7 or higher pH.

Utilizing the room temperature samples, 40.0 ml from each sample was decanted into separate clean 50-ml beakers. The two pH measurement probes were rinsed in milli-Q water and inserted into each sample and agitated briefly. After several minutes, the pH probe would stabilize and the meter would freeze the display value which was recorded for that sample. The two probes were rinsed in milli-Q water and placed in 7.0 pH buffer until used for the next sample.

3.8.6.4 Specific Conductivity Measurement

Each sample was analyzed for conductivity using an Orion conductivity meter (Orion 105A Plus) and probe (Orion P/N 011510). The meter/probe contained internal temperature compensation. The probe was rinsed in milli-Q water and blotted dry with lint free paper between samples.

Prior to analyzing samples, the probe was calibrated using a 1421 $\mu\text{S}/\text{cm}$ calibration standard and following the Orion calibration process. The ability of the temperature compensation to account for temperature variations was tested on several occasions by comparing room temperature and heated samples. A blank of milli-Q water was analyzed prior to running samples.

Utilizing the same samples and sample jars as for the pH measurements, the rinsed conductivity probe was inserted in a sample and agitated briefly. The probe was allowed to stabilize and the meter reading recorded. The probe was rinsed in milli-Q water and blotted dry with lint free paper prior to analyzing the next sample.

3.8.6.5 Turbidity Measurement

The remainder of each sample was utilized to measure turbidity. Turbidity measurements were conducted on a Hach Model 2100A Turbidimeter. Meter calibration utilized a

series of formazin secondary standards identified for a specific range and labeled with a calibration value specific to the equipment. For a specific range, the standard for that range was inserted in the photomultiplier detection chamber and the control adjusted so the meter read the specified value of standard.

After calibration, approximately 25 ml of each sample was decanted to a filling glass tube. The tube exterior was wiped with a dry paper towel and inserted into the detection chamber. The meter reading value was recorded for each sample. The sample was discarded and the glass tube rinsed in preparation for the next sample.

4.0 EXPERIMENTAL RESULTS – WETLAND TANK

HYDRAULIC CHARACTERIZATION

4.1 Introduction

The main objective of Chapter 4 is to characterize the wetland tank hydraulics and apply these results to explore implications for selected full-scale operating parameters. The pilot-scale wetland tanks received tap water during experiments 1, 2, and 3 conducted in the 2005 growing season and received secondary effluent during experiments 4, 5, and 6 conducted in the 2006 growing season. Bromide tracer tests were conducted to determine breakthrough and dwell detention time for the planted and control tanks. Tree growth was closely monitored during the six experimental runs to establish water uptake/transpiration rates which were then compared to historical results at CERF and other wetlands projects. Soil moisture was monitored to determine its impact on tree growth and to understand hydraulic limitations on contaminant availability for uptake by trees. Seasonal and diurnal variations in temperature, pH, specific conductivity, turbidity, and tree transpiration rate were measured and evaluated.

4.2 Characterization of Wetland Hydraulics

Several tracer tests were conducted to characterize the hydraulics of the two wetland tanks. A pre-experiment bromide tracer test was conducted from May 21, 2005 through

June 2, 2005. At this time the cottonwood trees had 10 months growth with heights from 2.0 to 3.5 meters. Each subsequent experimental run (1-6) also contained a bromide tracer commencing on July 18, 2005. The pre-experiment tracer study sampled 22 locations every 2 or 4 hours. The experimental run tracer was sampled at Tank 1 and 2 discharge ports every 12 hours.

4.2.1 Pre-Experiment Bromide Tracer Study

Prior to any experimental runs with the contaminant, a conservative tracer study was conducted using bromide to characterize the initial hydraulics of the system. The bromide tracer study established the hydraulic detention time, the initial break through lapse time, and also established the viability of mixing a spiked feed solution and make-up influent to feed the wetlands. The tracer study also identified the optimal timing for stopping and resuming Tank 1 & 2 discharge flow back to CERF, the sampling frequency for Tanks C and D, the adequacy of the tracer concentration used, and indicated the degree of dispersion through the system.

4.2.1.1 Tracer Study Results

The pre-experiment bromide tracer breakthrough curve results are shown in Figure 4.1 and Figure 4.2. At the discharge port of Tank 1 (planted), peak concentration of bromide was at 109 hours lapse time and at Tank 2 (control), it was at 97 hours lapse time. The

bromide tracer study lapse time for peak discharge concentration was similar to the estimated detention time of 113.4 hours as derived in Section 3.4.1. A point in time discharge outflow showed 43.2 L per hour for the planted tank and 49.9 L per hour for the unplanted tank. Initial bromide breakthrough occurred at 37 hours lapse time for both Tanks 1 and 2 (see Figure 4.1).

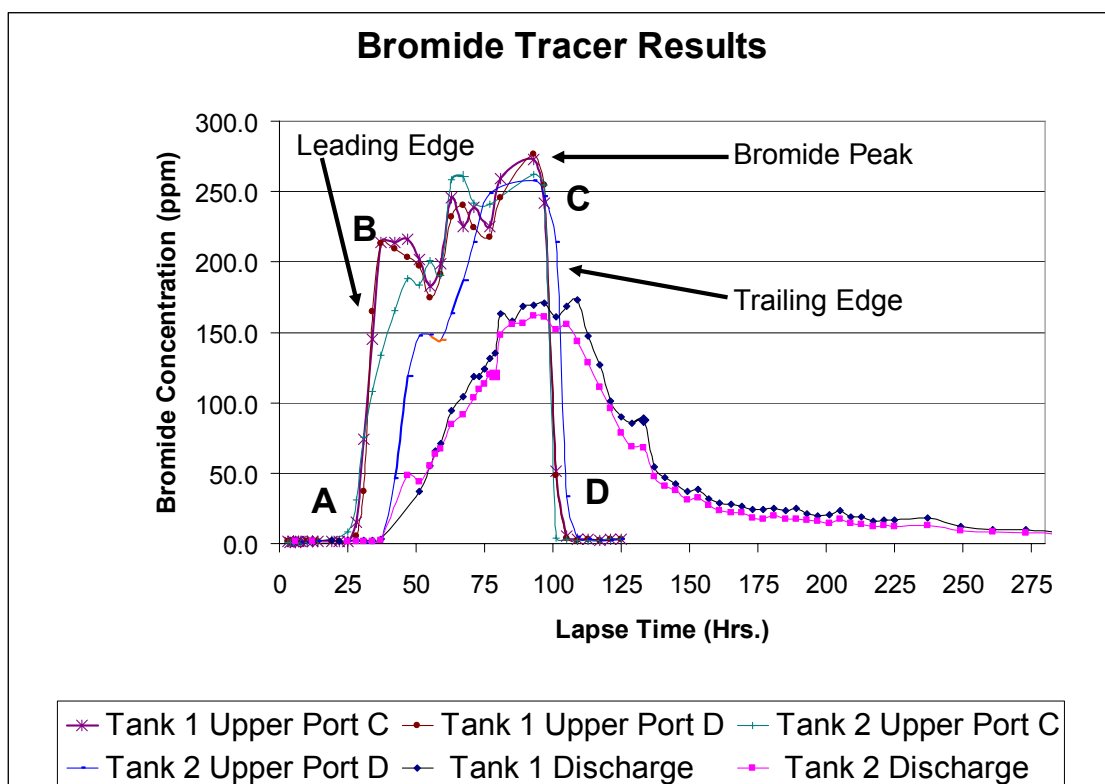


Figure 4.1. Bromide Tank Discharge Tracer Results.

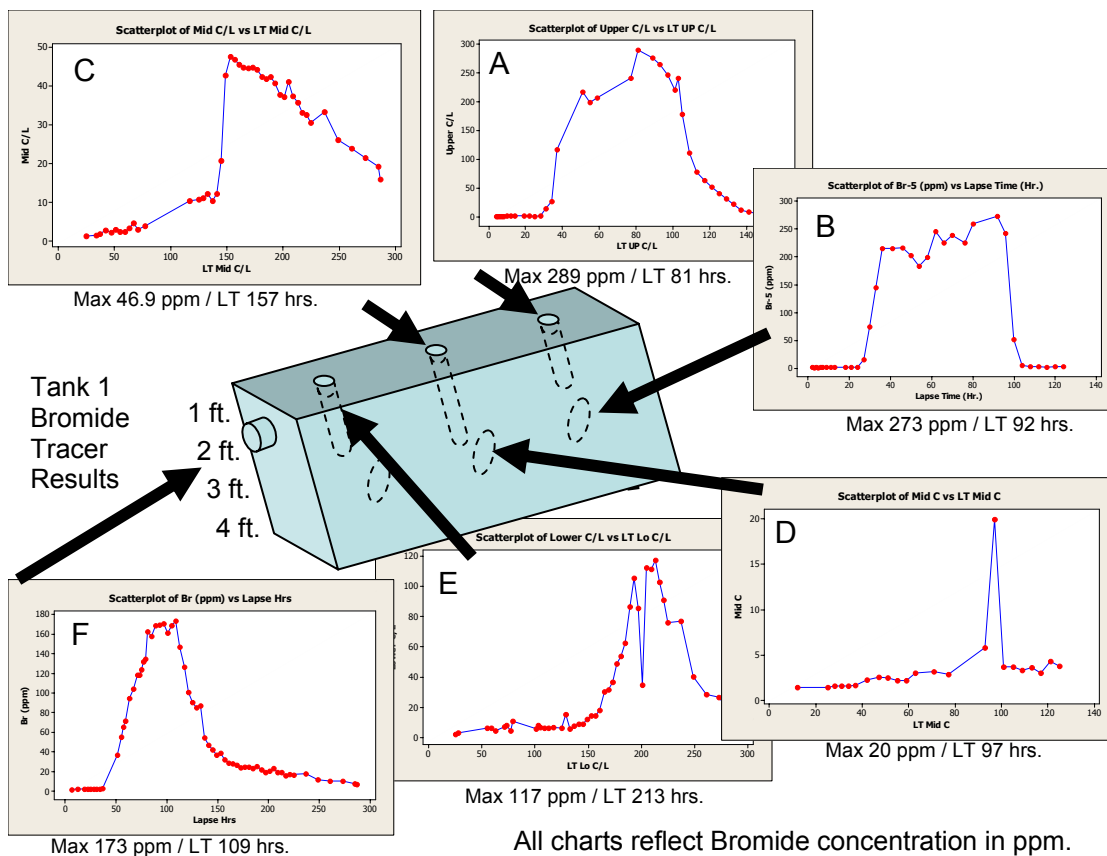


Figure 4.2. Tank 1 Pre-Experiment Bromide Tracer Study Results.

4.2.1.2 Quantitative Evaluation of Tracer Study Breakthrough Curve

As shown in Figure 4.2, the bromide transport through the Tank 1 porous media resulted in a variation of output concentration over time depending on the sampling point in Tank 1 and 2 as defined in Figure 3.12. This variation is attributed to heterogeneity of Tank 1 media that resulted in spatially variable three-dimensional flow patterns with preferential flow paths and dead zones (Schwarzenbach *et al.*, 1993). Tracer flow in a porous media is complex and difficult to assess from the measured longitudinal (one dimensional)

breakthrough curve data without an empirical correction factor that takes into account the three-dimensional structure of the flow (Schwarzenbach *et al.*, 1993). Taylor (1954) developed an expression for lengthwise solute pipe flow concentration variation that is widely used to model dispersion in streams and sub-surface aquifers (Singh and Beck, 2003). This expression, as shown below (Equation 4.1), utilizes a coefficient of longitudinal hydrodynamic dispersion (D) commonly known as a dispersion coefficient (Singh and Beck, 2003). The dispersion coefficient combines the effects of molecular diffusion, longitudinal dispersivity, and tortuosity plus the effects of transverse, turbulent, and vertical mixing (Schwarzenbach *et al.*, 1993). Molecular diffusion is mass flux resulting from a concentration gradient; tortuosity is the ratio of the real flow length path along the pores to the straight line between endpoints; and longitudinal dispersivity is the result of intrapore and interpore channel structure variations (Schwarzenbach *et al.*, 1993).

$$C(x,t) = \frac{M}{A\sqrt{4\pi Dt}} \exp\left[-\frac{(x_s - ut)^2}{4Dt}\right] \quad (4.1)$$

where

M = Mass of tracer injected at X = 0 and T = 0

A = Cross-sectional area of channel

u = Cross-sectional mean flow velocity

D = Coefficient of dispersion

C (x,t) = Concentration of tracer at Xs distance from fixed origin at time t

Equation 4.1 is applicable to open channel river or surface wetland flow. Sub-surface flow requires the equation be modified to reflect effective porosity of the media.

After flow has moved the tracer cloud an adequate distance from the tracer source (diffusion distance), allowing adequate mixing of tracer and pore water, the concentration distribution will reflect a Gaussian (normal) distribution per Equation 4.1 (Schwarzenbach *et al.*, 1993).

The accurate determination of the dispersion coefficient for a given sub-surface wetland or aquifer can aid in determining if early solute transport is dominated by flow advection or dispersion. The dispersion coefficient can aid in determination of solute concentrations at various locations along the flow path (Schwarzenbach *et al.*, 1993).

The longitudinal dispersion coefficient is a measure of rate at which a concentrated tracer mass spreads out along the flow path (Schwarzenbach *et al.*, 1993). Initial sub-surface flow from the tracer source does not generally have Gaussian distribution due to dead zones and other flow anomalies as demonstrated by the long tail on tracer study breakthrough curves (Field, 2002). To compensate for this early non-Gaussian behavior, Chatwin (1971) developed an alternate dispersion coefficient method based on Equation 4.1 (Field, 2002).

Chatwin (1971) rearranged Equation 4.1 as follows:

$$\left[t \ln \left(\frac{B}{c \sqrt{t}} \right) \right]^{1/2} = \frac{x_s}{2\sqrt{D}} - \frac{U}{2\sqrt{D}} t \quad (4.2)$$

Equation 4.2 provides a straight-line least squares regression solution when the left side of the equation is plotted against time on a natural graph. The graph has a y-intercept value equal to the first equation on the right side and a slope equal to the second equation (Field, 2002). The proportionality constant (B) is represented by Equation 4.3 which for symmetrical concentration distributions where can be rearranged where $\bar{C} = c_{\max} = B \sqrt{t \max}$. Rearranging the equation is shown as Equation 4.4 (Field, 2002).

$$B = \frac{M}{A \sqrt{4\pi D t}} \quad (4.3)$$

$$B = c \max \sqrt{t \max} \quad (4.4)$$

Equation 4.2 is the basis for the QTRACER2 shareware software developed by the U. S. Environmental Protection Agency. The QTRACER 2 software program is used for tracer breakthrough curve analysis for tests in karstic aquifers and other hydrologic systems. The software runs on personal computers and allows the user to input tracer study sub-

surface conditions and the time/concentration values from tracer test samples for a given measurement point (Field, 2002).

The Tank 1 and 2 sub-surface condition and tank discharge pre-experiment tracer study sample results were input to the QTRACER2 program. The program provided a graphical output of the left side of Equation 4.2 as shown in Figure 4.3 (Field, 2002).

The QTRACER2 program output for the Chatwin parameter shows the least squares regression line fitted to the early Tank 1 bromide tracer results with the straight line regression equation of $Y = 1132.81 + (- 10.4145)X$. The first value on the right hand side of the regression equation can be substituted for the y-intercept term in Equation 4.5. Equation 4.5 is the y-intercept function from Equation 4.2.

$$\text{y intercept} = \frac{X_s}{2\sqrt{D}} \quad (4.5)$$

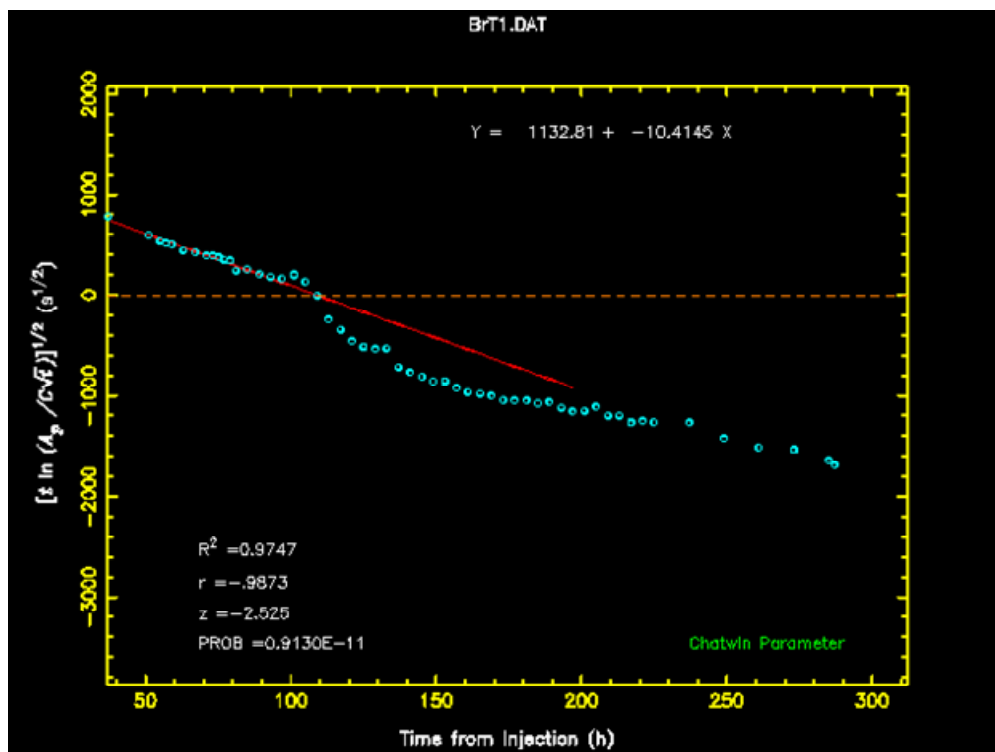


Figure 4.3. Tank 1 Bromide Tracer Study QTRACER2 Program Output.

Setting the y-intercept value equal to Equation 4.5, a determination of the dispersion coefficient (D) can be derived (Field, 2002). A dispersion coefficient of $0.0580 \text{ m}^2/\text{hr}$ was determined for Tank 1 based on the tracer study. Tank 2 dispersion coefficient from the tracer study was $0.0486 \text{ m}^2/\text{hr}$.

The calculated dispersion coefficients for Tanks 1 and 2 strongly depend on the scale of the aquifer (i.e. tank length, 9.1 m). As such, the specific dispersion coefficients should not be extrapolated to other systems such as short laboratory columns or long sub-surface flow wetlands (Schwarzenbach *et al.*, 1993).

The dispersion coefficient can be used in Equation 4.6 to determine the relative contribution of solute transport to advection or diffusion. Equation 4.6 establishes the Péclet number (Pe) which relates the effectiveness of solute transport by advection to the effectiveness of solute transport by diffusion (Field, 2002). The dimensionless Péclet number:

$$Pe = \frac{Ux}{D} \quad (4.6)$$

is obtained by dividing the mean tracer velocity times the distance between tracer inflow and sample point by the dispersion coefficient. Mean tracer velocity was established from the tracer time to peak. The Tank 1 pre-experiment tracer study Péclet number was 12.55 and the Tank 2 was 15.91.

As defined in the QTRACER2 documentation, Péclet numbers less than 0.4 indicate transport is diffusion controlled, 0.4 – 6.0 indicate suggest diffusion and advection are both important, and above 6.0 transport is through advection (Field, 2002).

4.2.1.3 Key Operating Parameters Established by Tracer Study

The Tank 1 & 2 pre-experiment tracer study results established initial breakthrough at 35 hours lapse time. Diverting flow to the evaporation ponds would prevent 1,4-Dioxane-spiked discharge from being sent to the sewage waste treatment plant. The tracer study

also established the 251 hour lapse time as the point to cease the collection of tank discharge at the ponds and to return the discharge from tanks 1 and 2 back to CERF or the sewer. The anticipated total discharge volume between 37 and 251 lapse time hours was used to establish the sizing of the evaporation ponds.

Based on the bromide tracer study the sampling window (83 – 107 lapse time hours) was utilized for experimental runs 1 and 2. The tracer study also established the process and procedure to enable mass balance analysis of bromide and 1,4-Dioxane from sampling of Tanks C and D. At 1.5 day intervals, beginning at 35 hours lapse time for each experimental run, the fluid volume in Tanks C & D was determined and samples were collected from both tanks, providing an integrated averaged concentration measurement for the previous 1.5 day discharge. This procedure facilitated a more accurate mass balance analysis on 1,4-Dioxane in tank discharge. The contents of the tanks were then transferred to the evaporation ponds.

4.2.1.4 Tracer Study Results From Upper Side Ports

The pre-experiment tracer results from Tank 1 and 2 upper side ports (Figure 4.2 – Graph B), samples 5 & 6 and 9 & 10, respectively, showed good uniformity of the mixture of sodium bromide and tap water. This uniformity validated the down tube and sliding channel disbursement apparatus that was utilized to feed the mixture into each tank. The upper side port maximum detected bromide concentration was 260 mg L^{-1} , versus the

calculated feed concentration of 230 mg L^{-1} during the spike, indicating complete mixing had not occurred. The tracer study revealed that a lower input concentration of bromide (80 mg L^{-1}) would be adequate to provide bromide measurements.

4.2.1.5 Tracer Study Results From Lower Side and Discharge Ports

Advection transport was evident in the other side port samples and Tank 1 & 2 discharge ports, indicating flow anomalies and dead zones (Figure 4.2 – Chart D). Tank 1 & 2 discharge bromide breakthrough curves (Figure 4.2 – Chart F) with steep fronts and long trailing edge tails are not uncommon. Wetlands typically exhibit non-uniform flow. A conservative tracer study conducted at the East polishing wetland system at the Sweetwater Wetlands in Tucson, Arizona (Vidales Contreras, 2001) showed similar non-uniform behavior. In this experiment the dimensionless Gaussian variance ratio (0.18) is reflective of lower dispersion. Higher dispersion causes the variance ratio to increase (Kadlec, 1994).

4.2.1.6 Tracer Study Tank Centerline Results

The advection transport effects from the tracer study were evident in the sample results of the delayed peaks for the downstream tank centerline pipes at 12 inches below ground level (Figure 4.2 – Chart E). For Tank 2 (unplanted) the bromide peak was at 165 hours lapse time (sample 22). Tank 1 (planted) bromide peak was at 209 hours lapse time

(sample 21). This same effect was observed in samples taken at 32-inch depth in the midstream of the tanks (Figure 4.2 – Chart C). Tank 2 peak was at 130 hours lapse time (sample 20) and Tank 1 peak was at 145 hours (sample 19). The highest point of a given bromide tracer curve is the peak as shown in Figure 4.1. This same effect was not observed with samples from the upstream centerline pipe at 12 inches below the tank surface (Figure 4.2 – Chart A). Samples 17 and 18 from Tank 1 & 2, respectively, showed rapid leading and trailing edge responses with peaks at 77 hours lapse time. Typical rapid leading and trailing edge response is shown in Figure 4.1 points A – B and C – D, respectively.

4.2.2 Experimental Run Bromide Tracer Results

4.2.2.1 Lapse Time Peak of Bromide Tracer and Contaminant

Due to the hydrophilic nature of 1,4-Dioxane, which is fully miscible in water, the breakthrough curves of the bromide tracer and 1,4-Dioxane added to each experimental run were expected to coincide very closely.

The experimental run tracer charts (Tables 4.1 & 4.2) show breakthrough and peaks for experimental runs 1-3 & 6 at the same lapse detention time for Tanks 1 & 2. Discharge concentrations of bromide as function of time are tabulated for each experiment in Tables

Table 4.1. Tank 1 Discharge Bromide Concentrations (mg L^{-1}) for Experimental Run 1-6 Lapse Time (Hr.).

Lapse Time (Hr.)	Exp Run 1	Exp Run 2	Exp Run 3	Exp run 4	Exp Run 5	Exp Run 6
0		6.8		9.0	2.2	17.7
12				7.3	2.3	11.1
24	5.9	4.9	6.4	6.7	1.9	11.1
35	6.1	4.2	5.0	6.0	2.2	5.7
47				10.1	2.1	6.0
59				27.2	10.1	10.5
71		22.7	21.4	33.8	21.8	18.8
83	32.0	31.6	26.8	47.6	20.8	19.7
95						31.7
107		25.3	19.7	51.5	22.5	44.4
119						41.7
131						58.6
143			15.7	41.1	21.2	50.7
167				32.2	17.1	36.7
179		10.5	11.8	22.3	11.5	32.7
191			8.2	21.8	13.0	24.1
203			4.9	19.4	9.0	24.7
227		7.1	8.2	15.4	4.7	23.6
239						22.9
251		7.1	4.9	11.8	4.3	24.5
275					6.6	27.1
287						16.0
299						21.2
311						23.9
323						20.4
347						17.9
371						21.9
395						16.3
419						14.5
443						14.4
467						14.2
491						12.7
539						11.1
611						7.3

Table 4.2. Tank 2 Discharge Bromide Concentrations (mg L^{-1}) for Experimental Run 1-6 Lapse Time (Hr.).

Lapse Time (Hr.)	Exp Run 1	Exp Run 2	Exp Run 3	Exp run 4	Exp Run 5	Exp Run 6
0		2.2	3.7	5.0	1.8	3.8
12				4.9	1.4	3.4
24	2.6	1.9	2.9	5.0	1.8	1.8
35	3.2	2.7	6.8	4.8	1.9	1.9
47				19.1	1.4	3.7
59				35.5	4.5	7.7
71	19.4	35.2	24.6	34.6	11.9	12.4
83	34.3	43.5	27.1	47.8	10.6	14.1
95						26.7
107		40.7	20.8	42.9	15.4	23.7
119						22.0
131						38.7
143			10.9	26.0	16.6	36.1
167				21.9	14.2	23.5
179		7.2	8.2	15.3	13.0	29.9
191				16.6	12.8	19.3
203				15.2	7.8	15.1
227		5.3	6.2	13.4	4.7	11.9
239						8.3
251		4.2	5.0	12.1	3.9	12.2
275					4.5	10.8
287						6.5
299						7.8
311						9.1
323						6.8
347						6.4
371						5.7
395						5.7
419						4.9
443						4.2
467						4.5
491						4.4
539						3.4
611						3.6

4.1 and 4.2 for Tank 1 and Tank 2, respectively. These experimental runs have rapid leading and trailing edges and a short (72) hour duration at peak mass. For experiment run # 4, Tank 2 peak was 83 hours lapse time while Tank 1 peak was 167 hours lapse time. The initial clogged discharge outlet may have been the primary factor for the delay. In experimental run # 5, the opposite condition existed where Tank 1 peak was 107 hours lapse time and Tank 2 was 143 hours lapse time. Experimental run 5 breakthrough curve, for Tank 1 & 2, reflected a higher degree of bromide transport by diffusion due to the lower peak concentration and curve shape as shown in Figure 4.4 and 4.5. This increased diffusion transport is also reflected in the lower Péclet number as shown in Table 4.3.

Table 4.3. Experimental Run 3 – 6 Péclet Number.

Experimental Run # / Tank Number	Chatwin y-intercept (s)^{1/2}	Longitudinal Dispersion Coefficient m²/Hr.	Péclet Number Dimensionless
3 Tank 1	880.38	0.0962	5.77
3 Tank 2	821.87	0.1103	6.22
4 Tank 1	961.61	0.0806	6.88
4 Tank 2	876.61	0.0970	8.08
5 Tank 1	813.96	0.1125	3.25
5 Tank 2	1026.88	0.0707	7.75
6 Tank 1	1228.68	0.0494	10.72
6 Tank 2	1289.91	0.0479	12.14

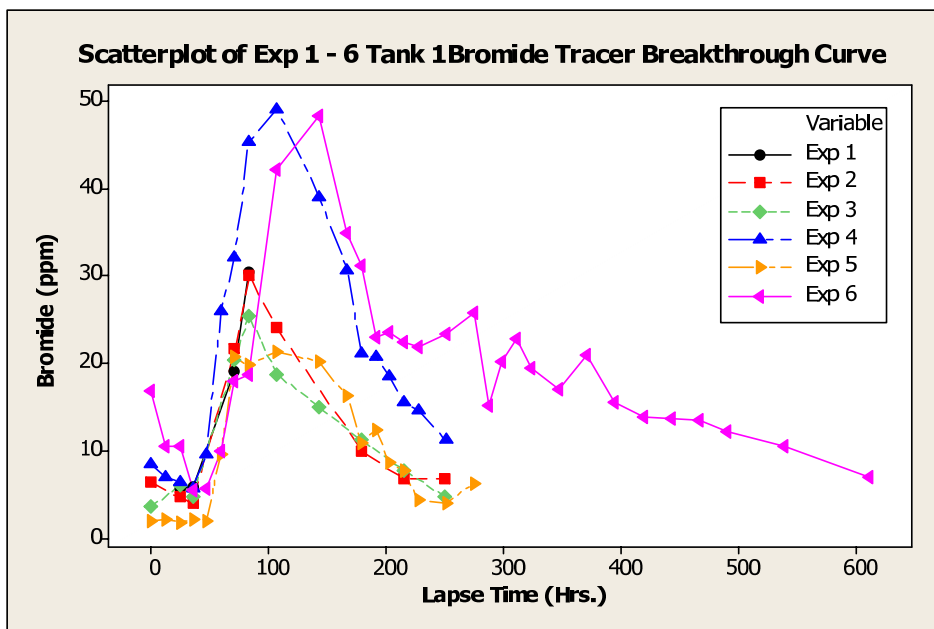


Figure 4.4. Bromide Tracer Breakthrough Curve Exp. Runs 1 – 6, Tank 1.

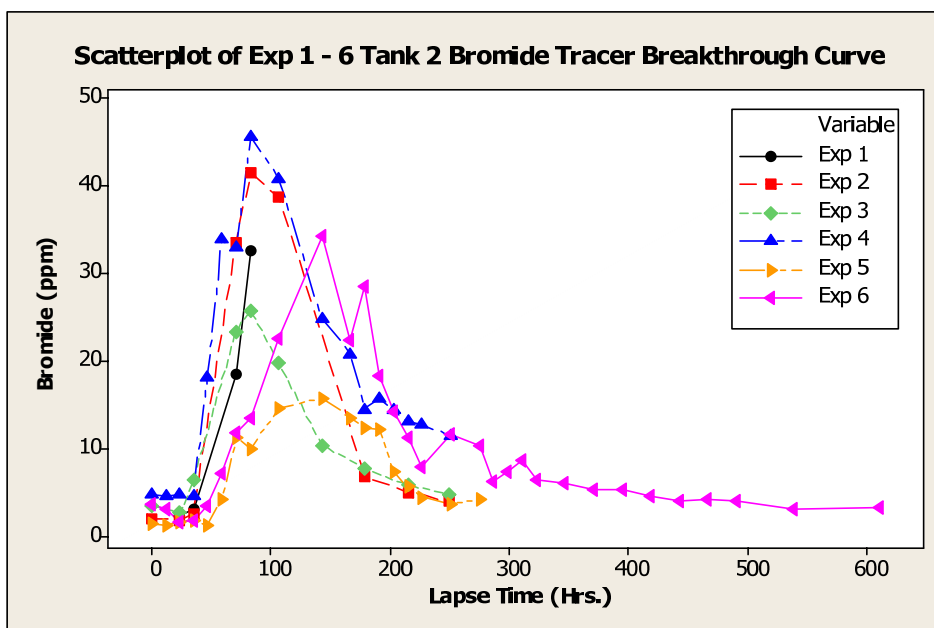


Figure 4.5. Bromide Tracer Breakthrough Curve Exp. Runs 1 – 6, Tank 2.

4.2.2.2 Total Mass Bromide Tracer Breakthrough

The lapse times for 25, 50, and 75 percent recovery in tank discharge of the input bromide mass during experimental runs 2-6 are shown in Table 4.4. The breakthrough lapse time values were determined from least square regression plots of bromide mass over measured lapse times. The applied bromide mass in each tracer test was 187.5 g.

Table 4.4. Bromide Breakthrough Lapse Times (Hrs).

Exp #	Tank 1			Tank 2		
	Percent Mass Breakthrough			Percent Mass Breakthrough		
	25%	50%	75%	25%	50%	75%
Exp # 2	84.5	132.2	179.6	51.2	105.1	160.1
Exp # 3	91.9	149.1	206.3	67.8	120.6	173.3
Exp # 4	91.9	136.9	181.9	71.4	105.7	140.1
Exp # 5	136.2	226.6	N/A	109.4	151.9	194.4
Exp # 6	114.7	156.3	184.7	104.4	142.4	180.5

(Exp # 5 maximum recovery was 50 % therefore 75% time is not applicable)

Comparison of the 25, 50, and 75 percent breakthrough curves for tanks 1 and 2 (Table 4.4) show longer lapse times for Tank 1 at the 50 percent bromide mass breakthrough.

The 25 percent breakthrough times increased from experiment 2-5 for Tanks 1 and 2.

Experiment 6 does not follow this pattern likely due to excessive rainfall.

4.2.2.3 Bromide and Contaminant Lapse Time Variation

In the first three experimental runs, the lapse time bromide peak for both tanks was at 82 hours. During experimental runs 4 and 5, using secondary effluent, the bromide peak

occurred at 107 hours for Tank 1. Tank 2 hours occurred at 83 and 143 hours, respectively. Experimental run 6 bromide peak lapse time for both tanks occurred at 131 hours. This is likely due to greater water uptake since the cottonwood trees were into the second growing season.

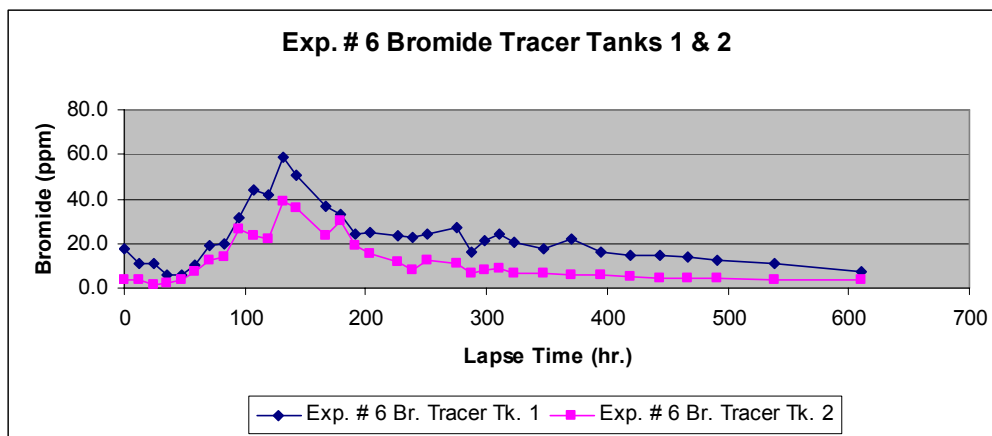


Figure 4.6. Experimental Run # 6 Tracer & 1,4-Dioxane.

4.2.2.4 Experimental Run Bromide Tracer Initial Breakthrough

The Tank 1 bromide tracer initial breakthrough for experimental runs 1-4 was at 35 hours lapse time. For experimental runs 5 & 6 the initial breakthrough increased to 47 hours. During experimental runs 5 and 6 the additional uptake by the trees resulted in zero discharge from Tank 1 during the hours of 2:00-7:00 p.m., impacting overall tank flow.

4.2.3 Experimental Run Bromide Tracer Longitudinal Dispersion

All experimental runs contained bromide tracer added concurrently with the spiked 1,4-Dioxane. Samples collected from Tank 1 and 2 discharge ports were analyzed for bromide concentration and breakthrough curves were established for experimental runs 3-6. Longitudinal dispersion coefficients and Péclet numbers were determined for Tanks 1 and 2 during experiments 3-6 using the Chatwin method and the QTRACER2 software program as described in Section 4.2.1.2. Results are shown in Table 4.3. Experimental run mean tracer velocity was calculated from the tank length (9.1 m) divided by the 50 percent breakthrough lapse time shown in Table 4.4.

The experimental run Péclet number results indicate predominant transport was by advection. The Péclet numbers showed a decreasing trend (greater diffusion) in later experimental runs. Greater diffusion may relate to the effects of secondary effluent and increased fine root structure of the cottonwoods. Experimental run 5 had the lowest mean tracer velocity due to higher cottonwood tree uptake. This lower tracer velocity resulted in a lower Péclet number (higher diffusion transport control) and a lower discharge bromide concentration as shown in Figures 4.4 and 4.5.

The change in longitudinal dispersion coefficient for experimental run 6 is likely due to the effect of a significant rainstorm event. Figure 4.7 summarizes significant rainfall events during the entire experimental time period. The bromide tracer results indicate

transport was controlled by longitudinal dispersion and are instructive in determining the amount of contaminant dispersion over the 9.1 meter tank length. As shown by the detailed initial bromide tracer study (Figure 4.2), there were spatial and temporal variations in contaminant concentration in Tank 1 which would have a direct impact on 1,4-Dioxane uptake in the cottonwood root zone.

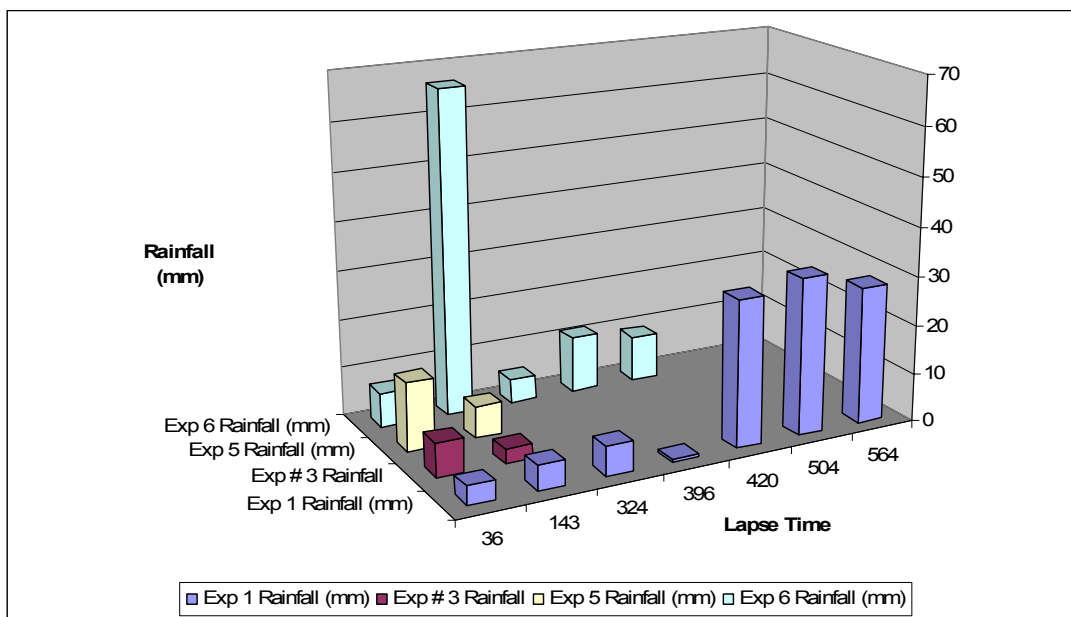


Figure 4.7. Rainfall Events During Experimental Runs 1 – 6.

4.2.4 Experimental Run Bromide Tracer Loss

4.2.4.1 Bromide Tracer Measurement

Tracer recovery was determined in experimental runs 1-6 by integrating the cumulative bromide mass in wetland effluent based upon samples taken from Tank C & D prior to

pumping discharge to the solar evaporation ponds. Discharge from Tanks 1 & 2 was allowed to collect in Tanks C & D, respectively, for 1.5 days at which point samples were taken and tank fluid depth was measured. These measurements provided the means to determine total volume collected and hence total bromide mass discharged from the wetland over the 1.5 day interval.

4.2.4.2 Plant Uptake of Bromide

Bromide is considered a conservative tracer and is used frequently in groundwater and wetland studies to characterize the hydraulics of a system. However, there are recent studies showing plant uptake of bromide. In a bromide tracer study at the Tres Rios Wetlands in Phoenix, Arizona, the average recovery from 12 separate wetland cells was 48 percent (Whitmer *et al.*, 2000). After eliminating the possibilities of seepage, measurement period, and analytical errors, a follow up analysis concluded the bromide tracer behaved non-conservatively and was taken up by the plants. A later laboratory study using *Typha latifolia* L. and *Phragmites australis* (Cav.) demonstrated uptake of bromide ($10 \mu\text{M L}^{-1} \text{ day}$) (Xu *et al.*, 2004). The uptake of bromide can be diminished by the addition of chlorine. A field experiment in Saskatoon, Canada, showed only a slight (0.08 mg g^{-1} dry plant material) uptake of bromide by Southern exposure poplar trees and a higher uptake (12.5 mg g^{-1} dry plant material) by sedge and smartweed (Parsons *et al.*, 2004).

4.2.4.3 Bromide Recovery Results

Bromide recovery from Tanks 1 and 2 for experiments 2-6 is summarized in Table 4.5. There was considerable variation in recovered amounts with Tank 1 (planted) showing bromide losses between 15 and 49 percent. It was hypothesized that the bromide loss from Tank 1 was due to precipitation of bromide on the upper soil surface during periods of high evaporation and possibly uptake by the cottonwoods. A white powder on the soil surface was observed at various locations throughout Tank 1 during the experimental runs. During the pre-experiment tracer study, bromide recovery from Tank 1 was 92.8 percent. During that time the pan evaporation averaged 9.8 mm day^{-1} . Discharge flow volume measurement methods were not as accurate during the tracer study which might account for the lower bromide loss in Tank 1. A positive correlation was found between pan evaporation measurements and the percent mass loss of bromide for experimental run 3-6 ($r^2 = 0.952$) as shown in Figure 4.8.

Table 4.5. Tank 1 and 2 Bromide Mass Recovery to Input For Experimental Runs 2-6.

Tank Recovery	Exp Run 2 Mass (mg) & (%)	Exp Run 3 Mass (mg) & (%)	Exp Run 4 Mass (mg) & (%)	Exp Run 5 Mass (mg) & (%)	Exp Run 6 Mass (mg) & (%)	Total Mass (mg) & (%)
Tank 1 Planted	114,828	156,537	182,704	86,844	174,133	715,046
Percent Recovery	(61.2)	(83.5)	(97.4)	(46.3)	(92.9)	(76.3)
Tank 2 Unplanted	195,833	186,094	249,245	172,331	187,048	990,551
Percent Recovery	(100.4)	(99.3)	(132.9)	(91.9)	(99.8)	(105.6)
Per Tank Input	187,500	187,500	187,500	187,500	187,500	937,500

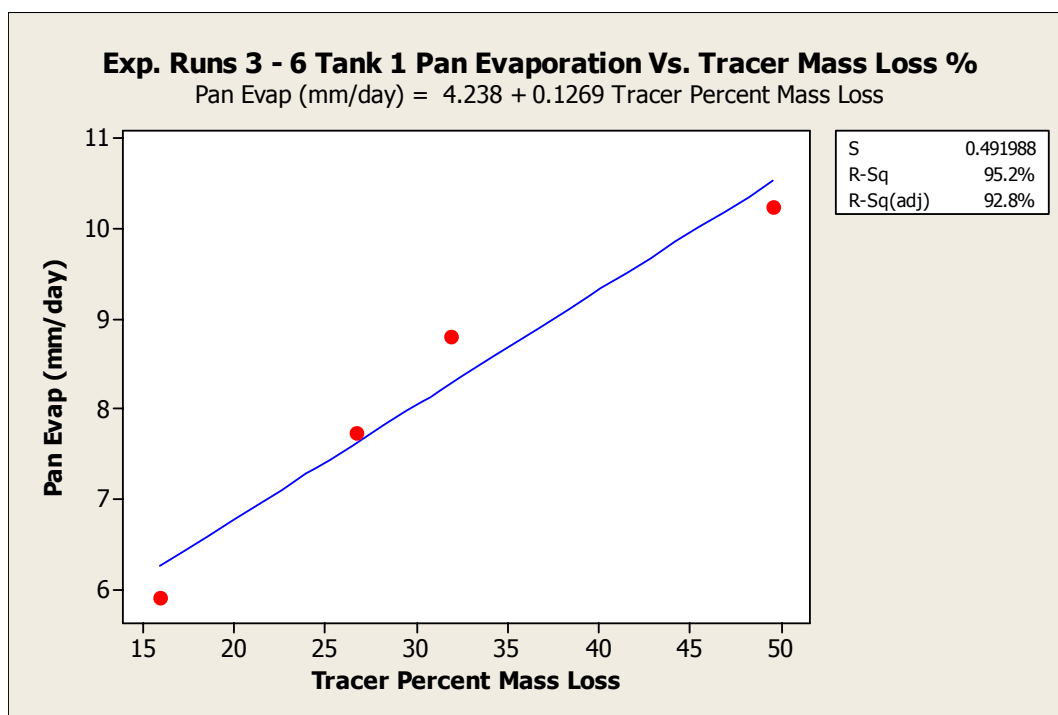


Figure 4.8. Exp. 3-6 Tank 1 Pan Evaporation to Percent Bromide Tracer Mass Loss.

4.2.4.4 Post Experimental Run Bromide Sampling

To test the proposed hypothesis for bromide loss from precipitation on soil, a bromide follow-up analysis was conducted after experiment # 6 (May 7, 2007) on three soil samples collected from Tanks 1 and 2. Soil samples (56 grams) were collected from the upstream, midstream, and downstream sections of the top 3-4 cm of soil in both tanks. Each soil sample was added to 200 ml milli-Q water, thoroughly mixed, and bromide concentration of the liquid was measured. All samples showed presence of bromide. The downstream samples from Tank 1 showed higher bromide levels, 80 mg L⁻¹ bromide, or 0.286 mg Br⁻ per g soil.

Assuming the same concentration of precipitated bromide was present in the top 5 cm of soil in the entire downstream one-third area of the tank, the mass of precipitated bromide would account for the Br⁻ missing in the experimental tank discharge. This was derived from each 56 g of soil equal to 16 mg bromide. The downstream soil volume (0.05 m • 3.0 m • 3.1 m), times the mass bulk density of 1.60 g cm⁻³, equals 781,200 g total soil mass. This mass times 0.286 mg Br⁻ per g soil equals 223.2 g bromide. The cumulative total bromide recovered in Tank 1 discharge during experimental runs 2-6 (715.046 g) plus the potential bromide mass remaining in the soil (223.2 g) equals 938.246 g. The total bromide input was 937.5 g.

4.2.4.5 Correlation of Bromide Mass Variation

The experimental runs where bromide cumulative mass exceeded input mass coincided with rainstorm or clogging events that may have re-dissolved precipitated bromide retained in the top soil surface.

4.2.4.5.1 Surface Saturation Correlation to Bromide Variation

The higher bromide mass from Tank 1 during experimental run # 4 was likely due to plugging of the outlet just prior to the start of the experiment. On April 24, 2006 (between experimental runs 3 and 4) 4.0 inches of standing water was observed at the downstream end of Tank 1. By April 29, 2006 the standing water extended throughout the entire length of the tank. Roots and dirt were removed from the tank drain and experimental run # 4 commenced May 1, 2006. Table 4.6 highlights key dates for the experimental runs. It is possible that standing water re-dissolved precipitated bromide from the upper soil surface into the tank discharge. Experimental run # 4 (Tank 2) showed bromide discharge mass in excess of the feed mass. Low flow rates and occasional rainstorms, during the winter stand down period between experimental runs # 3 and # 4 (November 18, 2005 – April 20, 2006), may have also re-dissolved precipitated bromide from the previous experimental runs.

Table 4.6. Experimental Run 1-6 Key Dates.

Experimental Run	Start Spiked Feed	Start Collection of Tank Discharge	Stop Spiked Feed	Stop Collection of Tank Discharge	Stop Data Collection
1	7/18/2005	7/20/2005	7/21/2005	7/29/2005	8/13/2005
2	9/12/2005	9/14/2005	9/15/2005	9/23/2005	10/8/2005
3	10/10/2005	10/12/2005	10/13/2005	10/21/2005	11/5/2005
4	5/1/2006	5/3/2006	5/4/2006	5/12/2006	5/27/2006
5	6/5/2006	6/7/2006	6/8/2006	6/16/2006	6/23/2006
6	7/24/2006	7/26/2006	7/27/2006	8/4/2006	8/19/2006

Note: spiked feed contained both Br⁻ and 1,4-Dioxane

4.2.4.5.2 Rainfall Correlation to Bromide Variation

The re-dissolution of precipitated bromide likely occurred during rain events. In experimental run # 6, a major rain storm (66.5 mm) occurred at 107 hours lapse time (Figure 4.7). The bromide breakthrough curve Tank 1 and 2 (Figure 4.6) shows increasing bromide concentrations at each rain event. The rain events occurred at 251, 347, and 383 hours lapse time, 5 mm, 11.5mm, 9.3 mm rainfall, respectively. The rain events correlate with increased bromide discharge concentrations likely the result of increased flow and reintroduction of bromide previously precipitated in surface soil.

4.3 Soil Moisture

4.3.1 Soil Moisture Balance

Experimental tank overall upper soil moisture variation was due to the balance of inflow (influent, rainfall) and outflow (discharge, evaporation, evapotranspiration) volumes.

Soil moisture variations of localized areas for each tank were the result of sub-surface dispersion and tree root density.

4.3.1.1 Wetland Tank Inflow Rate

The inflow rate into Tanks 1 and 2 during experimental runs 1-3 was regulated by drip emitters tied to both a peristaltic pump for the 1,4-Dioxane feed and tap water for a total of 52 L per hour. For experimental runs 4-6, using secondary effluent, the measured inflow rates are shown in Table 4.7. During non-experimental run periods, the inflow was controlled by an automatic watering timer tied to drip irrigation in the tanks. This resulted in simulated surge flow during experimental runs 1-3 as shown in Figure 4.9.

The inflow for Tanks 1 & 2 was nominally 52 liters per hour. However, occasional flow control perturbations would cause flow increases of short duration (spikes) for either or both of the wetland experimental tanks. Greater flow control was established during the

period of 1,4-Dioxane feed (lapse time 0-72 hours) due to use of peristaltic pumps. The only other inputs to the tanks were rain storm events as summarized in Figure 4.7.

Table 4.7. Influent Rate (L Hr⁻¹) Tanks 1 and 2 Experimental Runs 4, 5, and 6.

Lapse Time	Exp 4 L Hr ⁻¹ Tank 1	Exp 4 L Hr ⁻¹ Tank 2	Exp 5 L Hr ⁻¹ Tank 1	Exp 5 L Hr ⁻¹ Tank 2	Exp 6 L Hr ⁻¹ Tank 1	Exp 6 L Hr ⁻¹ Tank 2
0	51.31	50.86	54.22	52.94	54.22	52.94
12			53.57	54.22	54.22	54.22
24	51.14	50.56	53.57	53.57	54.22	56.25
36	51.14	49.45	53.57	53.57	51.72	52.94
47	51.14	56.25	52.94	54.22	51.72	52.94
59	54.88	51.14	54.22	52.33	50.56	51.72
71	56.25	52.33	128.57	118.42	52.33	51.14
83	47.87	42.86	50.00	46.39	56.25	47.37
95	47.37	45.92	47.37	100.00	45.00	47.37
107	44.55	45.45	48.91	47.37	62.50	51.72
119	45.45	47.37	47.37	48.91	45.00	47.37
131	48.39	51.72	42.86	48.39	45.00	54.22
143	40.91	42.06	42.86	48.39	45.00	45.00
155			42.86	60.00	39.82	40.91
167	47.87	47.37	47.87	48.91	100.00	33.33
179	47.37	47.87	52.94	48.39	42.86	56.25
191	42.06	42.86	56.25	48.91	55.56	42.86
203	50.56	47.37	51.14	49.45	60.00	42.86
215	51.31	50.86	51.14	48.39	40.54	40.91
227			56.25	48.39	47.37	39.13
239			50.00	46.88	47.37	40.91
251			48.91	47.87	54.22	52.94
Average	48.6	48.2	54.0	55.8	52.4	47.4

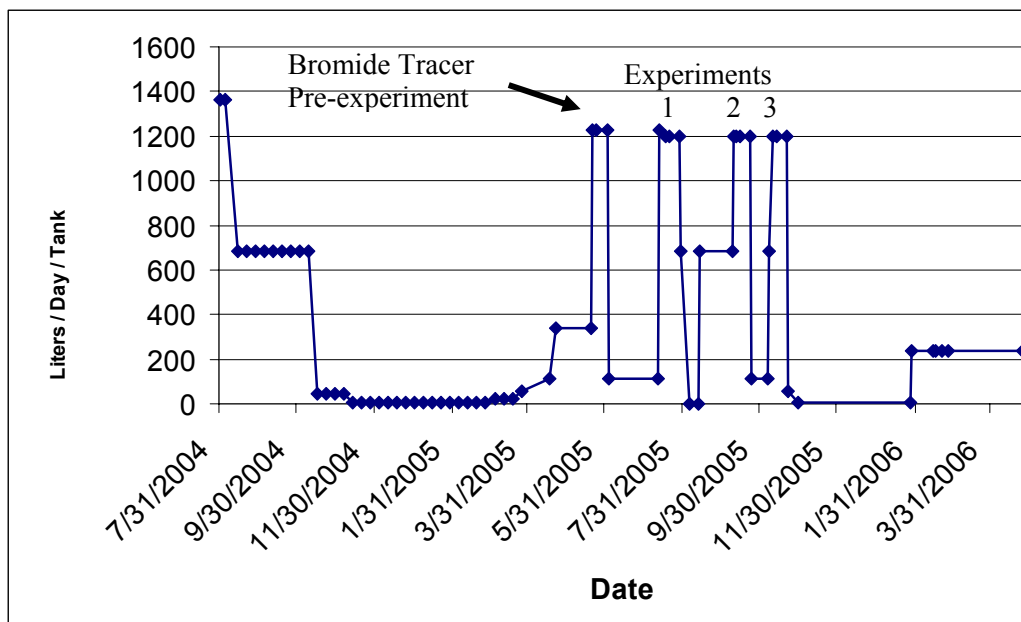


Figure 4.9. Experimental Runs 1-3 Surge Tank Flow.

4.3.1.2 Wetland Tank Discharge

The total discharge volume for each experiment (35-251 lapse time hours) from Tanks 1 & 2 is shown in Figure 4.10. Tank 2 discharge, with the exception of experimental run # 4, averaged 11,540 liters per experimental run. Experimental run # 4 had 23 percent lower discharge volume from Tank 2 due to lower influent volume after 191 hours. This reduced volume was the result of flow balance feed problems which were corrected by re-piping by the start of experimental run # 5. The discharge rates from experimental runs 4, 5, and 6 are shown in Table 4.8.

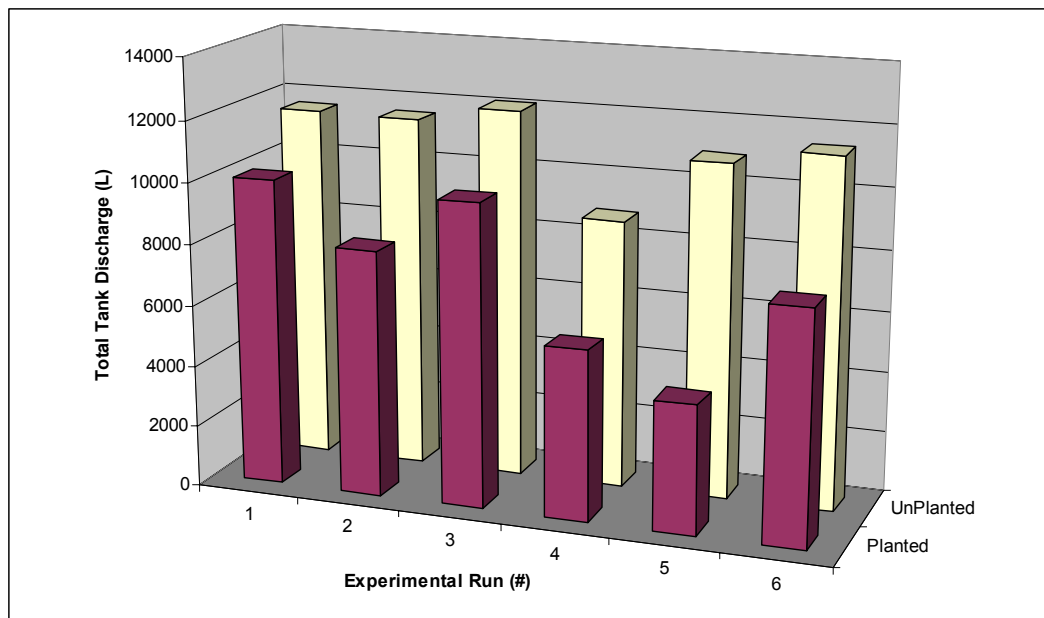


Figure 4.10. Wetland Tank Total Volume Discharge (L) for each Experiment.

The lower discharge from Tank 1 reflects the water losses to cottonwood evapotranspiration, with discharge flow rates approaching zero in the late afternoon hours. Before the beginning of experimental run # 6, the trees were significantly trimmed to reduce evapotranspiration and prevent a zero discharge flow condition. Experimental runs 1-3 showed average discharge rates of 43.3 L hr^{-1} and 54.5 L hr^{-1} for Tanks 1 and 2, respectively. For experimental runs 4-6, the average discharge rates were 27.3 L hr^{-1} and 51.8 L hr^{-1} for Tanks 1 & 2, respectively (excluding experimental run # 4). The significant reduction in Tank 1 discharge between the tap water and secondary effluent sets of experiments is reflective of the second year tree growth and the resulting increase in evapotranspiration. Variations in Tank 2 outflow (excluding flow control problems during experimental run 4) were minimal (1.9 L hr^{-1}).

Table 4.8. Discharge Rate (L Hr⁻¹) Tanks 1 and 2 Experimental Runs 4, 5, and 6.

Lapse Time	Exp 4 L Hr ⁻¹ Tank 1	Exp 4 L Hr ⁻¹ Tank 2	Exp 5 L Hr ⁻¹ Tank 1	Exp 5 L Hr ⁻¹ Tank 2	Exp 6 L Hr ⁻¹ Tank 1	Exp 6 L Hr ⁻¹ Tank 2
0	28.57	50.00	66.67	72.00	8.00	27.69
12	50.00	50.00	45.00	36.00	38.30	48.65
24	27.69	58.06	25.71	50.00	32.73	78.26
36	45.00	45.00	25.71	50.00	45.00	48.65
47	25.71	50.00	24.00	47.37	11.54	51.14
59	40.91	47.37	48.65	50.00	49.45	54.88
71	7.50	37.82	0.00	29.51	20.45	43.69
83	46.15	40.00	94.74	112.50	37.50	48.65
95	12.24	36.73				
107	40.91	38.14	24.06	25.14	47.37	14.40
119	9.23	40.00	0.00	54.55	150.00	70.31
131	40.00	45.00	13.33	15.65	28.00	64.29
143	9.09	37.50	8.00	29.03	21.18	45.00
155	38.30	38.30	33.33	60.00	7.69	42.86
167	3.24	40.00	0.00	40.91	14.17	40.91
179	17.14	13.33	30.20	47.37	100.00	32.14
191	4.92	17.14	0.00	41.86	0.00	38.30
203	38.30	37.50	32.73	50.00	26.87	39.13
215	4.26	36.73	40.00	51.43	20.69	36.00
227	42.86	34.62	50.00	45.00	24.00	39.13
251	40.00	31.58	21.18	45.00	32.73	39.13
263	0.18	26.87				
Average	26.01	38.71	27.78	47.30	35.98	45.87

4.3.2 Root Zone Soil Moisture

4.3.2.1 Soil Moisture and Contaminant Uptake

The status of soil moisture content in the root zone is a key parameter because contact between the roots, rhizosphere, and contaminant is required for wetland remediation to occur. Proper soil moisture range is critical for healthy plant growth.

In this study, soil moisture was measured at several depths within the root zone. This parameter was important in assessing the growth patterns of the cottonwoods in the constructed wetlands and provided verification that the root zone was maintained near saturation (maximum contact) thereby allowing maximum potential for remediation of the contaminant. A lack of soil moisture would impact the potential dispersion during rain infiltration and subsequent contaminant transport due to vertical flow. Also, water and contaminant flow are considerably slower in dryer zones (Yeh and Guzman-Guzman, 1995).

4.3.2.2 Time Domain Reflectometry Results

Volumetric soil moisture in both the planted and control tanks was monitored utilizing Time Domain Reflectometry (TDR). The TDR probes were installed prior to the start of experimental run 4. Volumetric water content data for Tank 1 midstream and downstream sections are shown in Figures 4.11 & 4.12. The water content data for Tank 2 midstream section is shown in Figure 4.13. Table 4.9 summarizes, for a given location, the average water content values during experimental runs 4-6.

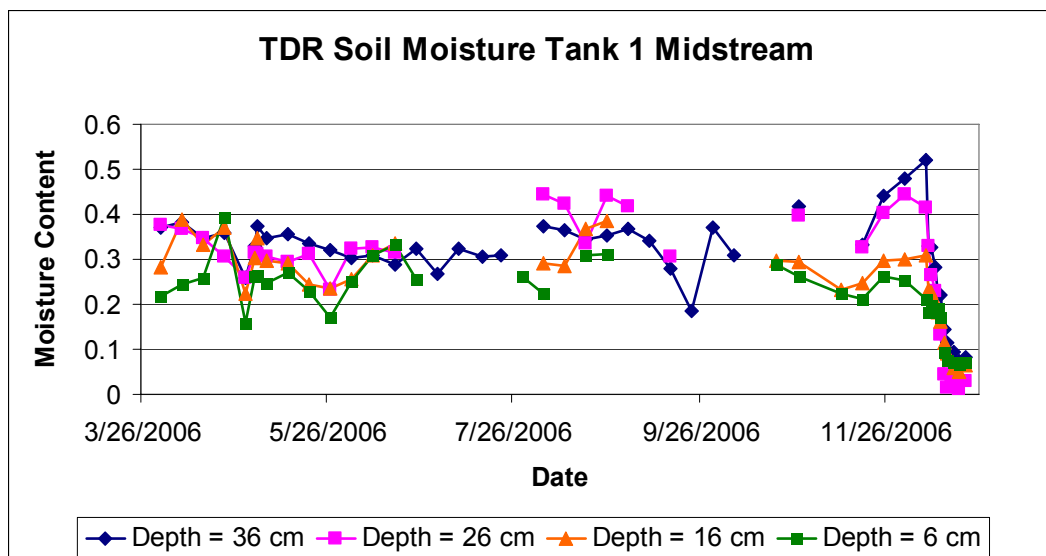


Figure 4.11. TDR Soil Moisture Tank 1 Midstream.

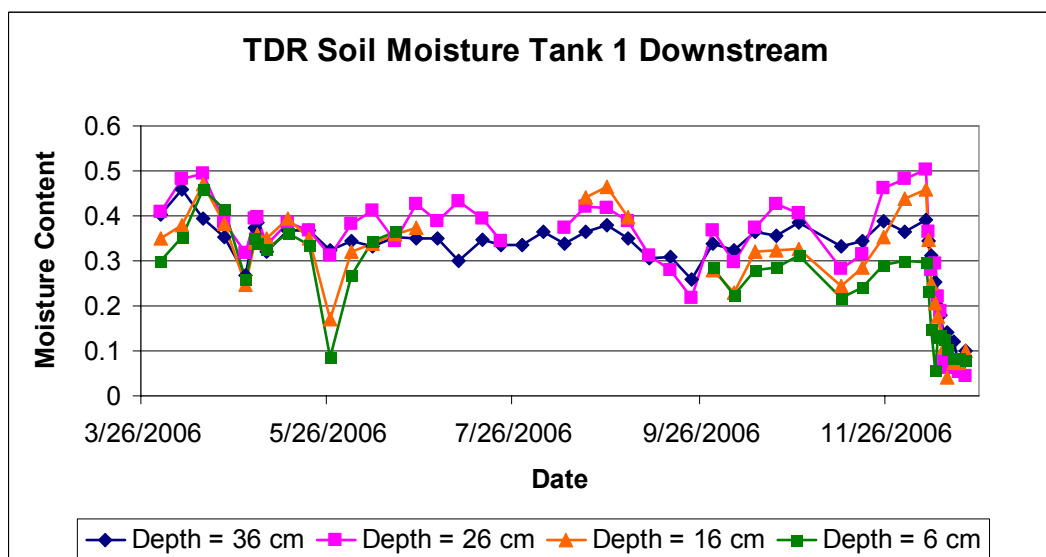


Figure 4.12. TDR Soil Moisture Tank 1 Downstream.

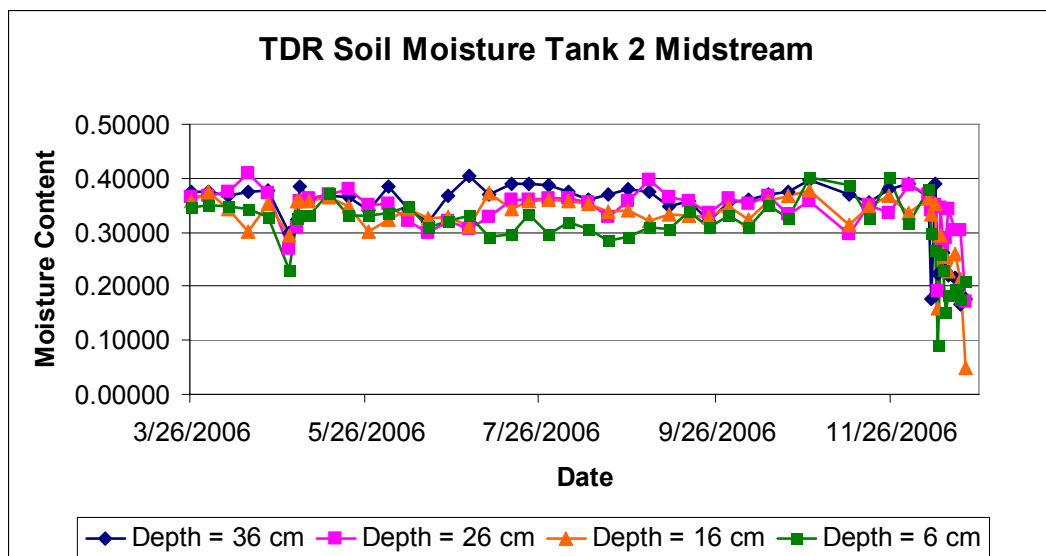


Figure 4.13. TDR Soil Moisture Tank 2 Midstream.

Table 4.9. TDR Average Soil Moisture Results.

Probe Position (cm depth)	Tank 1 Planted Volumetric Water Content (θ_v)	Tank 2 Un-Planted Volumetric Water Content (θ_v)
6	0.273	0.388
16	0.336	0.395
26	0.425	0.403
36	0.401	0.421

A 1.5-2.0 percent higher soil moisture was observed in the unplanted tank than in the planted tank for any given depth up to 36 cm. The most significant difference is soil moisture was between the lower and upper areas of the planted tank; the 6 cm depth had 15.2 percent lower soil moisture content than the 26 cm depth, indicating significant drying of the upper surface due to plant uptake. The control tank remained at or near saturation. The lower soil moisture in the upper 10 cm of soil had minimal impact to the

1-2 year old cottonwoods. The TDR probes measured higher soil moisture at 26 cm versus 36 cm depth. This may be reflective of the root pattern of the cottonwoods and the moisture distribution. It is also possible the anomaly is simply an artifact of probe installation. If soil and probe are not closely connected, the probe will reflect less soil moisture due to the air pockets.

4.3.2.3 TDR Measurement Problems

The TDR probes near the surface in Tank 1, due to increasing conductivity, would occasionally have the reflected signal completely attenuated. The reflected signal would not show an upswing when the impedance would change at the end of the probe. This problem created numerous gaps in data as shown in the charts for Tank 1 midstream and downstream TDR probe sets, Figures 4.11 and 4.12, respectively. However, the data set still provides the overall moisture content and relative trends which are informative. The TDR probe set in the midstream of Tank 2 did not experience conductivity problems and therefore provided a gap-free record of soil moisture as shown in Figure 4.13. In all TDR data sets, the lower probe number was positioned at 36 cm below soil surface with each succeeding probe number spaced 10 cm higher (26, 16, 6).

4.3.2.4 Significant Drying Events

Two significant drying periods can be seen for Tank 2 in Figure 4.13. The first drying period (May 2006) was the result of flow problems during the later portion of experimental run # 4. The flow problems were corrected by the start of experimental run # 5. The second drying period occurred at the termination of the experimental runs and was due to shut off of all flow to the experimental wetlands.

4.4 Tree Growth

4.4.1 Tree Height

A detailed growth record of the cottonwoods planted in Tank 1 is shown in Figure 4.14. Tree height measurements, using a steel measuring tape, were taken on a weekly basis from September 18, 2004 to December 9, 2006. Except for one early growth failure, 14 of the 15 trees remained healthy for the two-year duration of the experimental runs.

4.4.2 Tree Diameter at Breast Height

Diameter at breast height (DBH) measurements were taken from March 25, 2006 to August 26, 2006. There was a positive correlation ($r^2 = 0.964$) between tree height and diameter measurement as shown in Figure 4.15. Previous studies by Dr. Karpiscak have

shown a direct correlation between chest height cottonwood tree diameter and total height. This correlation was further validated by the tree diameter measurements taken from the experimental tank trees. This height to diameter correlation is consistent with numerous other studies showing similar correlations.

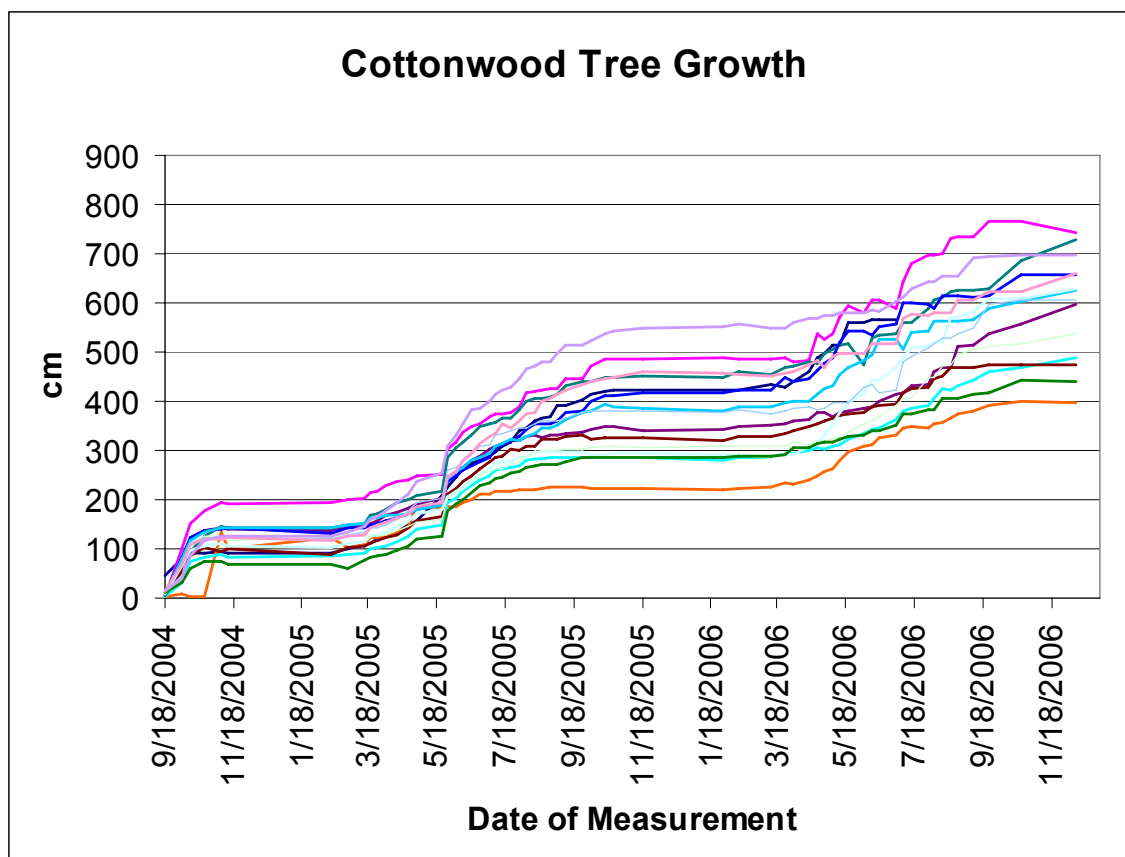


Figure 4.14. Cottonwood Tree Height (cm).

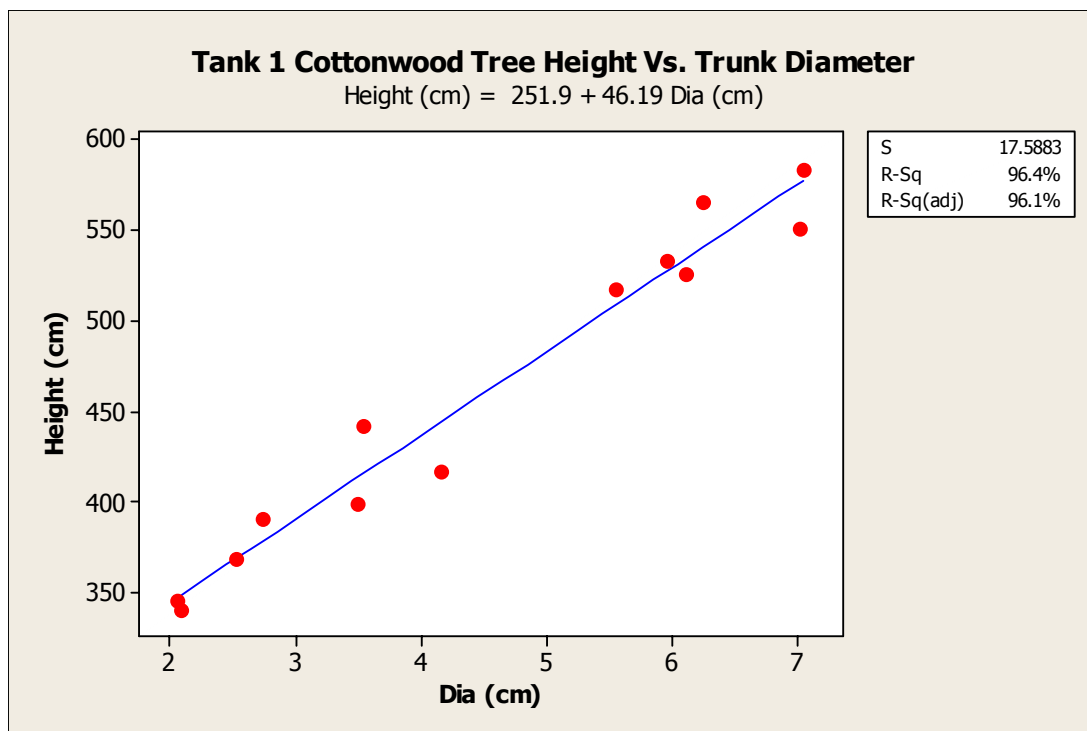


Figure 4.15. Correlation Cottonwood Tree Height and Chest Height Tree Diameter.

4.4.3 Tree Leaf Size and Color

During the first year experiments (2005) the cottonwood leaves were of moderate size for the age (1 yr.) of the trees with a bright medium green color during experimental runs 1-3 utilizing spiked tap water. The cottonwood leaves became significantly larger (2-3 times surface area) with a dark green color during experimental runs 4-6 (second growing season) utilizing spiked secondary effluent. The change in leaf size and color occurred over a 2-3 week period starting with the trees closest to the influent port and gradually progressing in series to all 15 trees. The color and growth changes were due to the added nutrients from the secondary effluent. Similar results have been observed in other plant

species irrigated with secondary effluent. Tree health did not appear to be impacted by the 1,4-Dioxane contaminant.

4.5 Discussion

4.5.1 CERF & AF Plant 4 Study Site Comparison

4.5.1.1 CERF Tree Height Measurements

Starting in 1991, five of the ponds were filled with gravel and planted with a variety of vegetation. Both black willow (*Salix nigra*) and cottonwood (*Populus fremontii*) were first planted in raceway # 1. In March of 1994 both tree species were also planted in raceways 2-5 along with bulrush, cattail and giant reed (Karpiscak *et al.*, 1999). A detailed record of tree height was maintained and is shown in Figure 4.16.

4.5.1.2 Correlation of CERF and Experimental Cottonwood Trees

On average, the growth rates of the CERF cottonwoods and the experimental tank cottonwoods were similar. Both tree groups achieved about 600 cm in height by the end of one year. Both records show growth during the summer months with minimal or no growth during the winter months. The growth spurts and dormant periods occurred in about the same time frame each year.

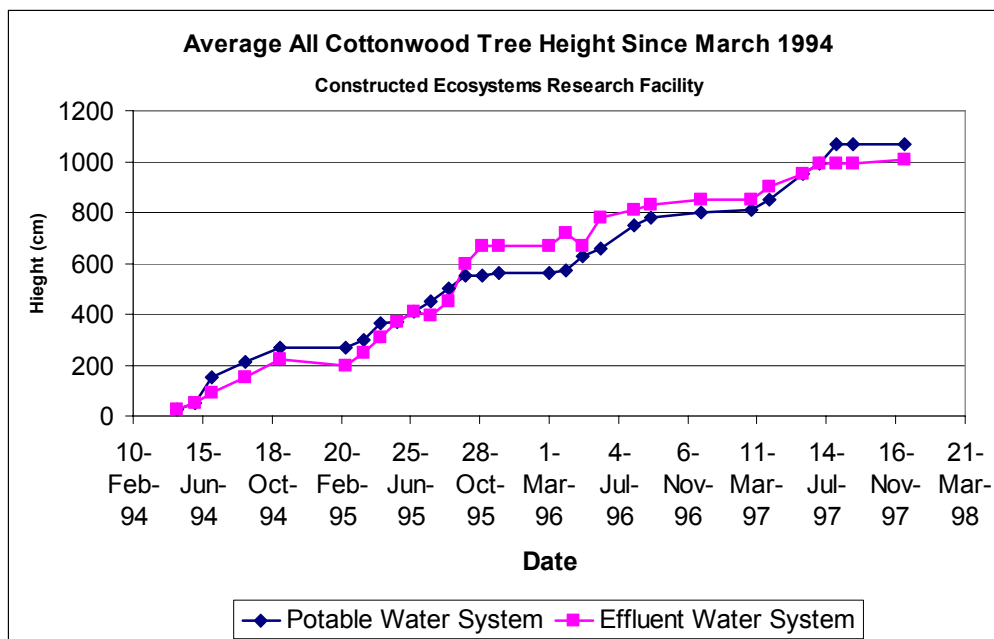


Figure 4.16. CERF Cottonwood Tree Height History.

4.5.2 Air Force Plant 4 Study - Cottonwood Growth

Air Force (A.F.) Plant 4 study utilized whip and caliper cottonwood tree plants in a field remediation project. This study had similar cottonwood tree growth results as the 1,4-Dioxane constructed wetland even though the planted spacing and locale were different.

4.5.2.1 A.F. Plant 4 Study Background

The A.F. Plant 4 study was a TCE contaminated site near Air Force Plant 4 in Fort Worth, Texas. Two 15 X 75 meter plantations perpendicular to the groundwater flow

were planted with 438 whips in first plantation and 224 caliper trees grown in 5 gallon buckets in the second plantation. Whip and caliper tree planted spacing was 2.88 m² and 5.76 m², respectively. The trees were planted in April 1996 and by the second growing season (1997) both whip and trees roots had reached the water table (275 cm) (Hendrick, 2006). In contrast, the 1,4-Dioxane constructed wetland planted 15 cottonwood cuttings in a tank 1.5 meters wide and 9.1 meters in length with plant spacing a 0.9 meters square. This high density spacing would not be adequate for long term growth and canopy closure of the trees over a 4-6 year period. However, for the duration of the planned constructed wetland, the high density planting provided maximum contaminant uptake potential for trees with 1-2 years growth.

4.5.2.2 Correlation of A.F. and Experimental Project Tree Height and Diameter

The A.F. project monitored the height and trunk diameter of the whips and caliper trees for a three-year period following planting. This data is shown in Figure 4.17 and Figure 4.18 (Hendrick, 2006). The tree height results are similar to both the CERF and the experimental tree height data. Tree diameter is difficult to compare since the experimental tank data was only operated for a short duration and the AF Plant 4 data does not indicate a relative position (chest height) for the trunk measurements. If the AF Plant 4 measurements were taken at chest breast height as were the experimental tank trees, then the experimental tank trees were significantly smaller in diameter (factor of 8).

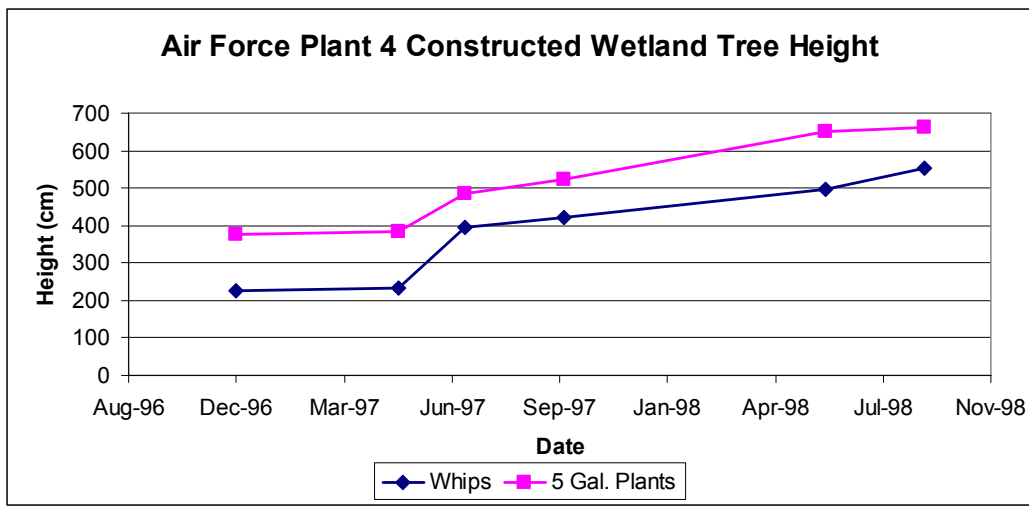


Figure 4.17. AF Plant 4 Whip and Caliper Tree Height.

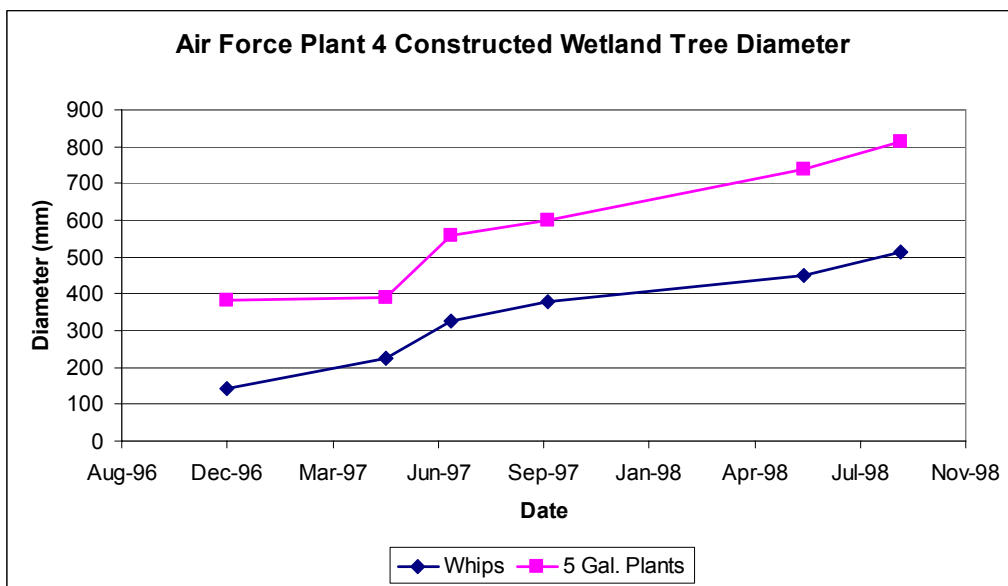


Figure 4.18. AF Plant 4 Whip and Caliper Tree Trunk Diameter.

Correlation of the tree height to diameter of whips and 5 caliper trees ($r^2 = 0.964$, $r^2 = 0.987$, respectively) in the AF Plant 4 study showed similar results to the experimental run ($r^2 = 0.964$). The overcrowded experimental tank planting may have had a negative

impact on trunk diameter. However, this impact would not have resulted in the large discrepancy to the A.F. study. The discrepancy is likely due to positional differences where tree height measurements were taken.

4.5.3 Transpiration Measurements

4.5.3.1 Transpiration

For the experimental runs 1-3 (first growing season) the trees had an average transpiration rate of $17.56 \text{ L day}^{-1} \text{ tree}^{-1}$. Each experimental run transpiration rate was calculated from the difference in outflow volume (L) of Tank 1 and 2 (lapse time 35 – 251 hours) divided by 24 hours per day and the quantity of trees (15). The transpiration rates ($\text{L day}^{-1} \text{ tree}^{-1}$) for experiments 1-3 were averaged. The experimental runs 4-6 (second growing season) the trees had an average $22.42 \text{ L day}^{-1} \text{ tree}^{-1}$ transpiration rate. These transpiration rates are based on the difference between average Tank C and D discharge rates during the experimental runs.

4.5.3.2 A.F. Plant 4 Study Tree Transpiration

The AF Plant 4 study established an average transpiration rate at one year for the whip and caliper trees as $4.274 \text{ L day}^{-1} \text{ tree}^{-1}$ and $7.8125 \text{ L day}^{-1} \text{ tree}^{-1}$, respectively. By the end of the second growing season the whip and caliper trees transpiration increased to $8.219 \text{ L day}^{-1} \text{ tree}^{-1}$ and $16.07 \text{ L day}^{-1} \text{ tree}^{-1}$, respectively (Hendrick, 2006). The

experimental run transpiration rates were roughly three times higher than the rate for the AF Plant 4 study.

4.5.3.3 Tree Transpiration Rate Correlated with Temperature

The cottonwood transpiration rate was found to be closely correlated with the average afternoon temperature, as shown in Figure 4.19 ($r^2 = 0.951$). While the AF Plant 4 study is a valid benchmark to compare tree growth, the comparison to transpiration rate and temperature is not valid. The lack of correlation to transpiration is due in part to operating and temperature differences. Between the two studies, there was a significant difference in depth to groundwater between the AF Plant 4 project and the experimental run (275 cm and 5 cm, respectively) and the daily high average air temperature (33.8 °C and 42.4 °C, respectively) (Griffiths, 1997). These two site specific factors account for most of the transpiration rate differences.

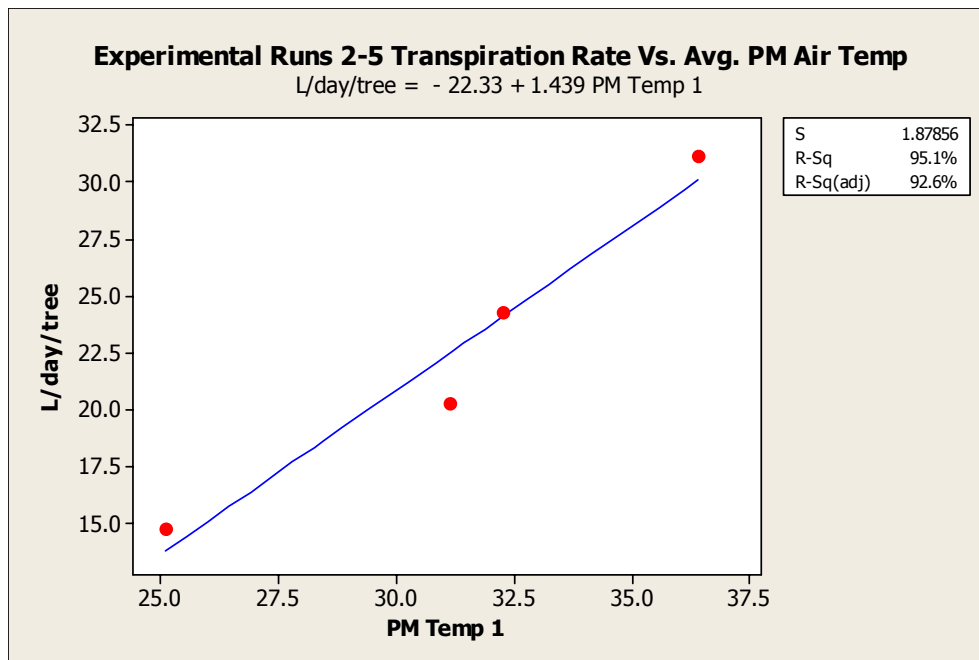


Figure 4.19. Experimental Run Transpiration Rate Vs. PM Air Temperature.

4.5.4 Temperature Measurements

4.5.4.1 Air Temperature Differences

Diurnal air temperature swings are significant in desert environments. Table 4.10 shows average air and subsurface temperature between morning (AM) and afternoon (PM) observed during experimental runs 1-6. Average AM temperature was the sum of hourly data logger temperature readings between midnight and 9:00 AM divided by 10 (number of hourly readings). The average PM temperature was the sum of hourly data logger temperature readings between 2:00 PM and 11:00 PM divided by 10 (number of hourly readings). Each data logger hourly reading was the numerical average of (4) automated

temperature measurements taken every 15 minutes. (Experimental runs 4 and 5 had an AM / PM average temperature difference of 14 °C.

Table 4.10. Exp. Runs 1 – 6 Air and Subsurface Average A.M. & P.M. Temperatures (°C) in Tanks 1 & 2.

A.M. Avg. Temp. Exp. Run No.	Air Temp.	Tank 1 Up- stream 15 cm sub- surface	Tank 1 Mid- stream 15 cm sub- surface	Tank 1 Down- stream 15 cm sub- surface	Tank 2 Up- stream 15 cm sub- surface	Tank 2 Mid- stream 15 cm sub- surface	Tank 2 Down- stream 15 cm sub- surface
1	25.90	27.70	28.30	27.69	27.67	27.39	27.58
2	20.91	23.87	24.22	23.90	22.42	20.98	21.78
3	14.24	18.17	19.02	19.24	16.54	15.37	16.32
4	20.96	23.62	22.80	22.06	20.60	20.51	20.76
5	26.56	28.11	27.05	26.50	24.11	23.76	24.33
6	25.02	27.28	26.37	26.10	24.72	23.79	24.22
P.M. Avg. Temp. / Exp. Run No	Air Temp.	Tank 1 Up- stream 15 cm sub- surface	Tank 1 Mid- stream 15 cm sub- surface	Tank 1 Down- stream 15 cm sub- surface	Tank 2 Up- stream 15 cm sub- surface	Tank 2 Mid- stream 15 cm sub- surface	Tank 2 Down- stream 15 cm sub- surface
1	34.19	29.58	29.72	28.98	29.54	30.77	30.33
2	32.29	26.09	25.89	25.31	23.63	23.29	23.43
3	25.09	19.80	20.27	20.35	17.55	16.98	17.60
4	31.15	24.74	23.41	23.44	22.23	23.77	23.71
5	36.43	29.48	27.68	27.71	26.04	26.75	26.99
6	31.29	29.35	27.25	26.94	26.30	25.28	25.54

4.5.4.2 Sub-Surface Temperature Differences

Subsurface temperatures in Tanks 1 and 2 are summarized in Table 4.10. The results show approximately a 4 °C lower sub-surface temperature in the Tank 2 during experimental run 3 and 5 compared to the respective Tank 1 temperature. This difference is due to the vegetation limiting heat loss during cooler nights. The temperature charts also reflect up to 4 °C higher daytime temperatures in a given tank than the night time temperatures. The higher temperature deltas primarily occur in the unplanted tank.

4.5.4.3 Impacts of Shading by Trees

Shading can significantly reduce the air and upper sub-surface temperature due to blocking direct radiation. The 15-cm upper sub-surface temperatures during the experimental runs are shown in Table 4.10. The average temperatures during the experimental runs reflect AM and PM values. This distinction is not as important in moderate climate regions, but in the Arizona southwest deserts, the difference can impact rhizosphere development or semi-volatile/volatile contaminant evaporation.

An example of shading impact is shown in the 15-day kiddie pool experiment conducted at the field site. Temperature was measured in two 113 L pools filled with secondary effluent to a depth of 15.2 cm. One pool was covered with a 10.2 cm air gap between the cover and the pool and the other pool remained uncovered. The results are shown in

Figure 4.20. The uncovered pool had significant swings in temperature where the covered pool fluctuation was moderate.

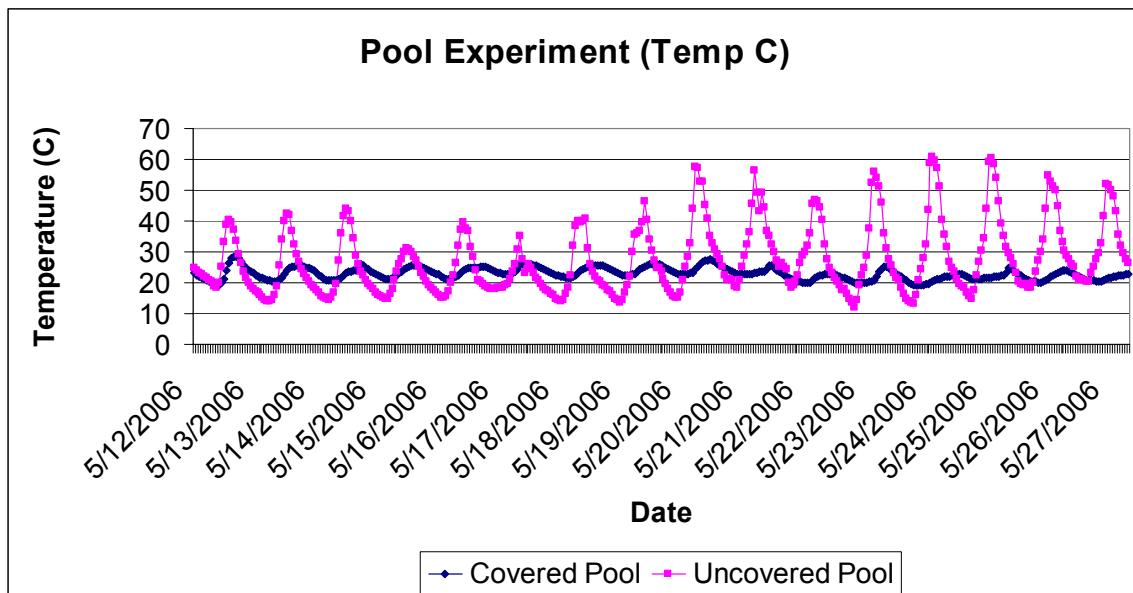


Figure 4.20. Water Temperature Readings from Covered and Uncovered Pools.

4.5.5 Seasonal Factors

Poplar trees are frequently utilized in phytoremediation projects due to their root structure, high level of transpiration, and ability to handle contaminants. The remediation potential of poplar and cottonwood trees fluctuates based on both diurnal and seasonal factors. The primary diurnal factor is transpiration. The seasonal physical factors include temperature, leaf loss (deciduous), rain, humidity, solar radiation, and soil moisture. Transpiration is also governed by a number of bio-physical factors including

size and density of stomata, degree of stomatal opening, hydraulics of water conducting tissue, size and density of canopy (Braatne, 1999). Studies have shown cottonwoods have the ability to highly regulate stomatal openings in response to a variety of environmental conditions (Gazal *et al.*, 2006).

4.5.5.1 Deciduous / Temperature

Both temperature and deciduous periods are important in developing and designing a phytoremediation system using cottonwood trees. If continuous inflow of contaminated water is feeding a cottonwood tree remediation wetland, then a secondary remediation means and contingency plans are needed during periods when the remediation potential of the cottonwood tree system is dormant (Tossell *et al.*, 1997). If contaminated water inflow volume varies, then a secondary water source is needed to maintain the cottonwood trees. Seasonal factors did impact flow rates in the pilot-scale experimental study.

In general, the growing season for poplars is April through October (Braatne, 1999). For the experimental tank cottonwood trees, the growing season was February through November given the specific location and site conditions. Several factors influence the annual leafing cycle of cottonwood trees. Leaf loss in winter and budding in spring are not solely linked to ambient air or sub-surface water temperature.

Experimental Tank 1 cottonwoods did not drop their leaves during the first winter season (1994-1995). This was due in part to the heat loss protection provided by the 3-foot freeboard of the steel tank. Protection from freezing was also provided by adding several strings of low wattage filament-type bulbs that offset freezing conditions.

The experimental tank cottonwoods first full growing season began January 22, 2005 when new growth was observed. At the end of the first full season, the experimental tank trees lost their leaves when the evening air temperature dropped to $-3.4\text{ }^{\circ}\text{C}$ on November 28, 2005. The corresponding 15.2 cm sub-surface temperature was $10.5\text{ }^{\circ}\text{C}$.

The cottonwoods started budding for the second full season growth on January 14, 2006 in response to daytime high temperatures of $29.6\text{ }^{\circ}\text{C}$. The corresponding 15.2 cm sub-surface temperature was $12.4\text{ }^{\circ}\text{C}$.

As seen in Figure 4.19, a direct correlation was found between cottonwood tree transpiration rate and temperature during the spring and summer season. However, when cottonwood trees drop their leaves, the transpiration rate goes to near zero as shown by the AF Plant 4 study data. Diurnal changes in transpiration rate at AF Plant 4 ranged from $9.1\text{ L tree}^{-1}\text{ day}^{-1}$ (June) – $1.6\text{ L tree}^{-1}\text{ day}^{-1}$ (October) for whips and $14.7\text{ L tree}^{-1}\text{ day}^{-1}$ (July) – $0.91\text{ L tree}^{-1}\text{ day}^{-1}$ (October) for caliper trees (Hendrick, 2006).

4.5.5.2 Experimental Run Rainfall Events

Rainfall during the experimental runs, as shown in Figure 4.7, created both soil moisture and discharge volume spikes. For short durations (24-48 hours), rainfall would also increase discharge from the planted tank not simply through direct input of moisture but also through reduced transpiration demand by the cottonwood trees. Following a rain event, the discharge from Tank 1 (planted) increased by 38-100 liters per hour where the direct rainfall input, based on surface square footage of the wetland tank, was 9.5 to 22 liters per hour. This transpired water from intercepted precipitation was accounted for in the water balance estimates for the AF Plant 4 project (Harvey, 2003). Rainfall during experimental runs was included in the Tank C & D discharge volume measurements and was factored out in calculating transpiration as the difference in total tank discharge volume.

In the Tucson, Arizona area, approximately 50 percent of the annual precipitation occurs in the winter months. Rainfall measurements at CERF support this observation (Figure 4.21). During the experimental time period (2005-2006) summer rainfall accounted for 57-58 percent of the annual total. A one-day rain event in July 2006 was 66.5 mm.

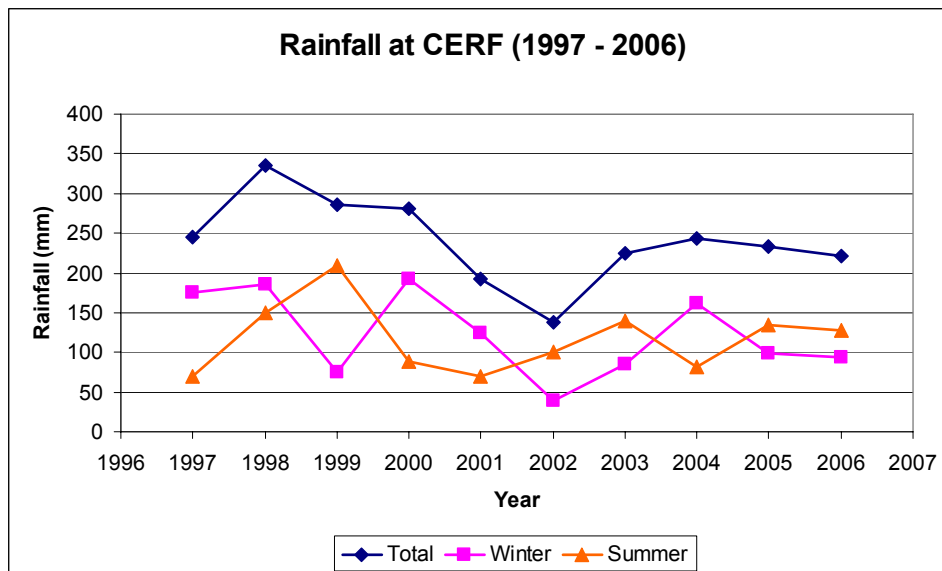


Figure 4.21. Monsoon and Winter Rainfall Measured at CERF from 1997 to 2006.

4.5.5.3 Humidity/ Solar Radiation

The effects of increasing solar radiation, larger tree diameter, and decrease in humidity (vapor pressure deficit) increase the transpiration rate of cottonwoods (Schnoor, 2002).

The humidity in the Tucson, Arizona area is typically very low (6-20 percent) except for July and August where relative humidity can exceed 90 percent. Monthly-averaged 2005 relative humidity data from CERF data records is shown in Figure 4.22.

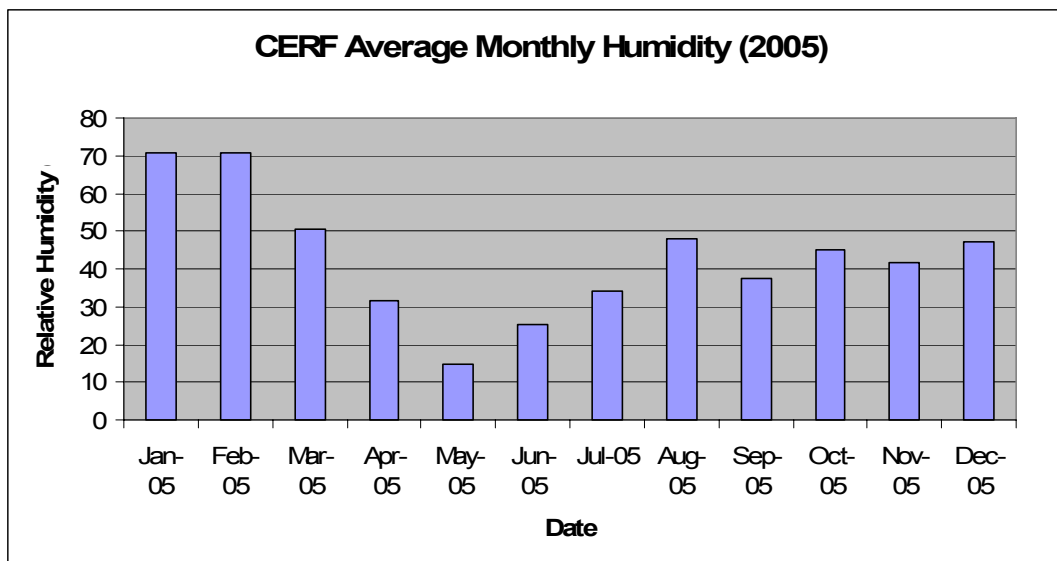


Figure 4.22. CERF Average Monthly Humidity (2005).

An inverse correlation was found between transpiration rate and occurrence of rainstorms or higher humidity. The calculated transpiration rates during experimental runs 1-3 were $13.62 \text{ L day}^{-1} \text{ tree}^{-1}$, $24.3 \text{ L day}^{-1} \text{ tree}^{-1}$, and $14.76 \text{ L day}^{-1} \text{ tree}^{-1}$, respectively.

Transpiration rates were calculated using the difference in outflow volume from tanks 1 and 2 (per day basis) divided by the number of trees in Tank 1 (15).

Experimental runs 1 and 3 had rainfall and higher humidity (August and October 2005; Figure 4.22). No rainfall occurred during experiment run number 2 and the humidity was lower at that time (September 2005; Figure 4.22). The outflows were based on cumulative volume measurements from Tank C and D for lapse times 35-251 (9 days).

An inverse correlation was also found for experimental run # 6 in 2006, again related to higher rainfall and humidity during that experiment.

Solar radiation intensity impacts both transpiration and cottonwood growth rates. Measurements taken at the experimental site showed UV radiation intensity was considerably lower in shade than in sun. Utilizing the same equipment for the one-day solar exposure measurement, full sun and shade (from the cottonwoods) measurements performed on June 17, 2006 were 9.44×10^{-4} watts cm^{-2} and 1.65×10^{-4} watts cm^{-2} , respectively. A solar-blind vacuum photodiode detector (IL 9ED240) was used with a research radiometer (IL 1700). The location of the sun reading was the influent point of experimental Tank # 2. The location of the shade reading was taken on the outer edge of Tank 1 in the midstream of the tank between the inflow and outflow ports. The readings were taken at 9:00 a.m. with a cloudless sky. Since solar radiation intensity is the most important parameter in determining evapotranspiration rate, cottonwoods in full shade would be expected to transpire four fold less water than cottonwoods in full sun, based on the observed difference in the shade and sun UV radiation measurements.

4.5.6 Edge Effects

It is not uncommon for plants at the edge of a field or wooded area to be larger and healthier than plants located more interior to the crop or forest. This edge effect is the summation of a plant's capability to utilize growth resources to its competitive advantage. The edge effect represents a competitive advantage by receiving greater solar radiation, water resources and/or nutrients. Often the competitive advantages are not

readily identified until further investigation reveals underlying physical, seasonal, diurnal, and biological advantages.

The cottonwood trees in the planted experimental tank experienced different growth rates based on their relative position in the tank as shown in Figure 4.23. In the figure, each tree was assigned to one of three growth rate groups (high, medium, low) based on height from one month after the date of planting. The same growth rate pattern continued throughout the first and second year growth cycles.

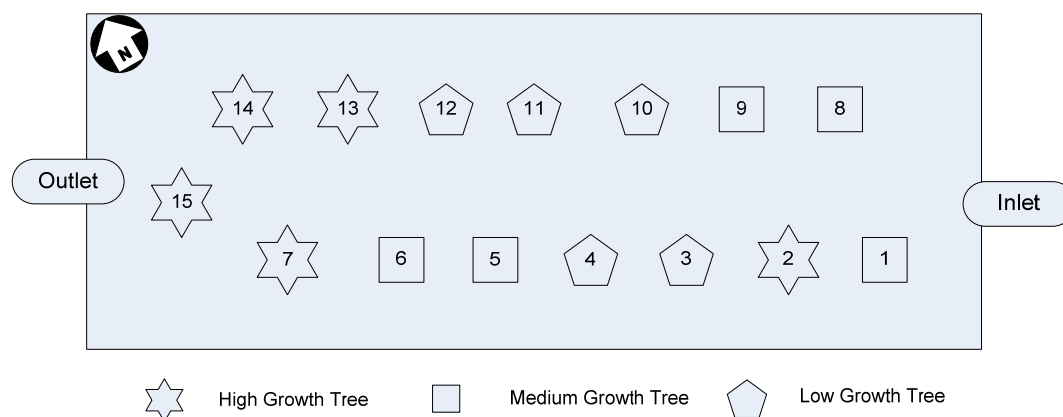


Figure 4.23. Tree Growth Height Pattern and Relative Position.

4.5.7 Hydrologic Effects

4.5.7.1 Experimental Wetland Tank Cottonwood Initial Growth Patterns

The initial growth patterns were attributed to local hydrologic conditions in the tank.

While sunlight or shading could have impacted growth rates, the larger trees were at both

ends of the tank while the smaller trees were in the midstream of the tank adjacent to the North or South side walls.

The drip irrigation scheme provided adequate soil moisture around the planted cutting. The tree root systems developed at 10-13 cm below the soil surface with a root bundle also 10-13 cm along the length of the cutting. The area below the root bundle was totally devoid of root growth.

As identified by the TDR soil moisture measurements, the midstream area of the unplanted tank in the upper 15.2-20.3 cm of soil contained 5-7 percent lower soil moisture than the upstream and downstream areas. This was under conditions when the tanks had an influent flow of 52 L hr^{-1} . The lower flow during the first six months after planting resulted in lower total soil moisture that negatively impacted early growth of the midstream plants. The plants at the downstream end of the tank received adequate soil moisture due to flow upwelling at the tank discharge and consequently exhibited faster growth rates.

4.5.7.2 Increased Flow Correlated to Increased Height of Higher Growth Trees

During the first year of the study, flow rate to the wetland tanks was reduced in between the individual experiments. Periods of higher flow, as shown in Figure 4.24, occurred four times from April through October 2005. These higher flows correspond to the pre-

experimental bromide tracer test and experiment runs 1, 2 and 3, respectively. A positive correlation is apparent between the higher flows and increased height of the taller trees.

The rate of change in tree height (cm) per day during April 12, 2005 and July 4, 2005 for trees in low, medium and high tree height categories was 1.287, 1.541, and 1.800, respectively. The rate of change in tree height (cm) per day during July 16, 2005 and September 25, 2005 for trees in low, medium and high tree height categories was 0.23, 0.62, and 0.88, respectively. These trees were able to capitalize on the increased flow where the less developed root system of the shorter trees could not. The inflow during this period of time was no longer through individual drip irrigation tubes to each individual plant but from flow distributed at the inlet of the tank. This flow scheme through soil water distribution provided additional moisture to trees near the tank inlet.

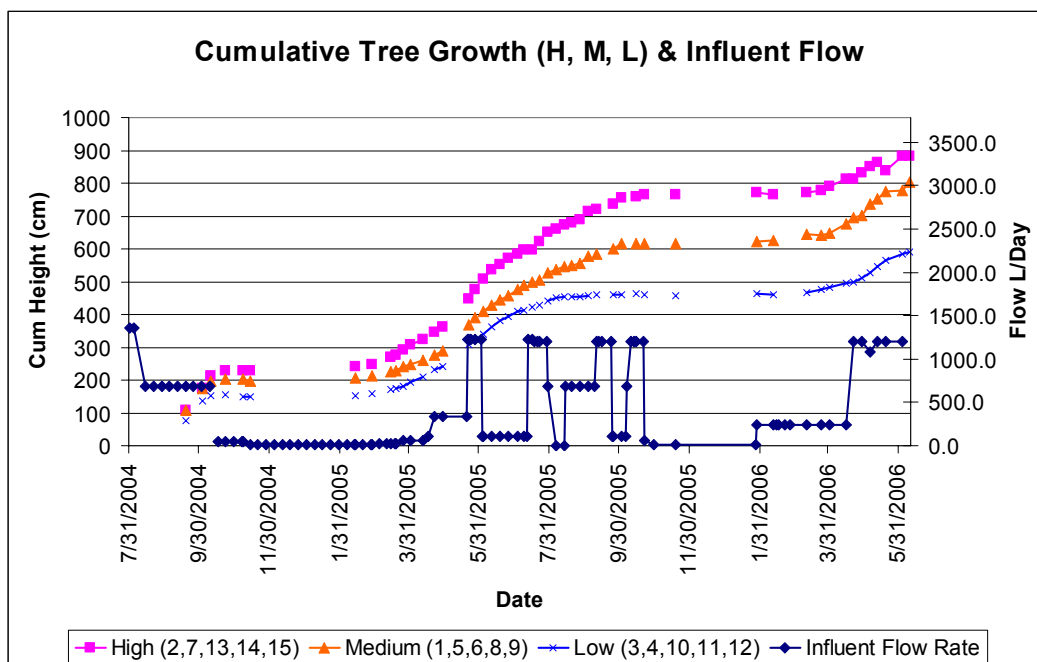


Figure 4.24. Average Tree Height by Category (H, M, L) and Influent Flow Rate.

4.5.7.3 Lower Soil Moisture and Growth of Midstream Plants

The midstream trees had less root development and were not able to capitalize on the surge flows even when the soil moisture was increased. Even under surge flow conditions, the midstream plants had less soil moisture in the upper 15.2-20.3 cm. The influent flow rate was held constant (52 L hr^{-1}) for the remainder of the experimental runs starting with the second growing season. The constant flow resulted in minimal soil moisture difference between the midstream and downstream tank areas. The higher growth plant continued a higher growth pattern through the third season as shown in Figure 4.24.

4.5.8 Sunlight/Shadow Effects

The orientation of the tank in relation to the position of the sun would provide an edge effect advantage to the trees at both ends of the tank and to the trees nearest the Southern exposure. Full shading of the Northern midstream trees (10, 11, 12) occurred during early morning and late afternoon providing a continuing disadvantage to the smaller trees. Previous measurement of solar energy in full sun and shade of cottonwood trees showed a four fold intensity difference ($9.44 \times 10^{-4} \text{ watts cm}^{-2}$, $1.65 \times 10^{-4} \text{ watts cm}^{-2}$, respectively).

Some of the highest solar energy influx rates are found in the Sonoran and Mohave desert regions. Mid latitude deserts can receive 250 watts m^{-2} mean solar energy in a 24-hour period (Cohen, 2002). Prior to the beginning of the experimental runs, a full-sun UV exposure measurement was taken several times over a three-month period in 2004 as shown in Figure 4.25. Section 3.7.1.2 provides detail on the UV detector and filters used. For most of the experimental runs, there were clear skies with full sun exposure. The shadowing of interior (midstream) trees resulted in significantly reduced growth rates for trees 3, 4, 10, 11 and 12 as shown in Figure 4.23.

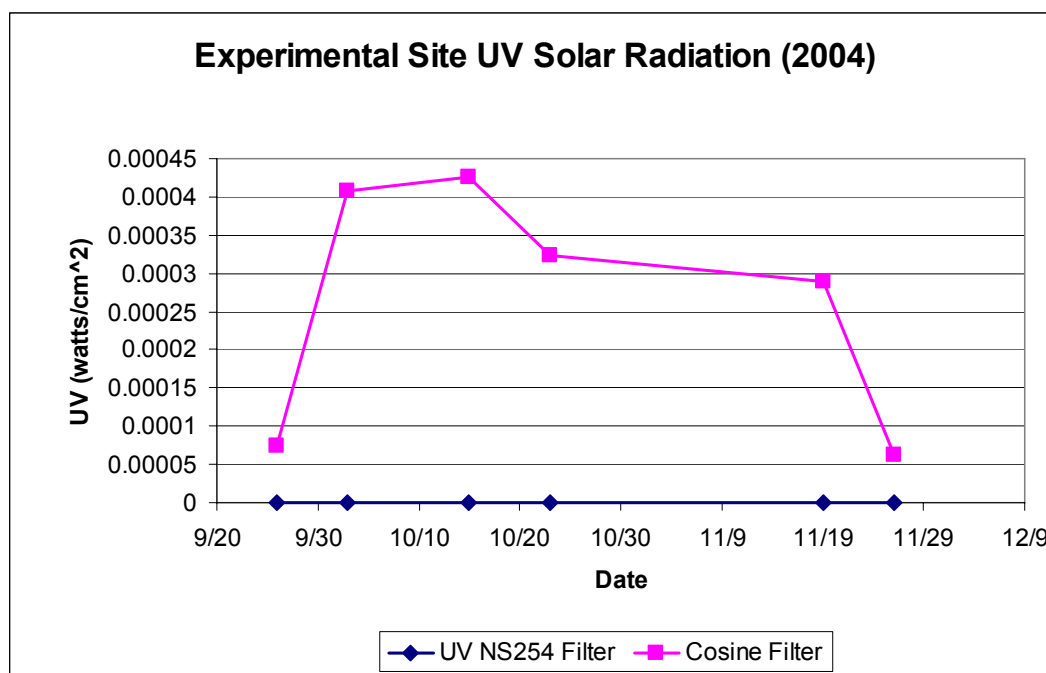


Figure 4.25. Experimental Site UV Solar Radiation Measurements Conducted in 2004 at the Field Site.

4.5.9 Longitudinal Dispersion Effects

Mixing during subsurface transport in Tanks 1 & 2 was controlled by longitudinal dispersion according to the Péclet numbers calculated for both the pre-experiment tracer study and the experimental run tracer breakthrough curves. The dispersion was primarily influenced by heterogeneities in the porous media.

Where average fluid velocity was reduced by increased transpiration uptake (experiment # 5), molecular diffusion became more important in the spreading of the bromide tracer, resulting in a lower Péclet number, a lower mean tracer velocity, and a lower peak tracer concentration. The impact of the increased transpiration rate during experiment # 5 on contaminant removal is discussed in Chapter 5.

The detailed breakthrough curves (Figure 4.2) from the tracer study showed non-flow zones or slow flow areas within the cottonwood root zone in Tank 1 that contained significantly lower tracer concentrations at extended lapse times. The preferential flow patterns during transport in the planted tank had a negative impact on the ability of the cottonwood tree to take up the 1,4-Dioxane contaminant (Section 5.6.2.3).

4.6 Conclusions

The hydraulic and tree growth characterization data from the pilot-scale wetland project support specific guidelines to facilitate operation of full-scale remediation wetlands.

4.6.1 Pilot-Scale to Full-Scale Wetland Considerations

Site characteristics and plant selection are key parameters in developing a successful phytoremediation project. Numerous booklets exist that spell out most of the design and development steps. One very important factor which is not included in many constructed wetlands design guides is the need to conduct a pilot-scale study to test the many assumptions taken for granted in during the wetland design.

Operation of the pilot-scale experimental wetlands utilizing the steel Tanks 1 & 2 provided insights on a number of flow control, soil moisture, plant growth, and transport mechanism variations which should be resolved prior to implementing a full-scale wetland remediation project.

Some of the physical conditions and constraints in the pilot-scale wetland such as sub-surface heterogeneity will be difficult to overcome. Flow control and dispersion can be improved through wetland design by increasing flow length and reducing flow velocity.

Plant growth variations from edge effects and soil moisture will require placement and flow analysis.

A tracer study is an invaluable tool in assessing whether design changes are needed prior to moving from a pilot-scale to a full-scale wetland project.

4.6.2 Simulate Full-Scale Operating Factors for Pilot-Scale Wetlands

The pilot-scale test conditions should be closely aligned with the full-scale operation. This may be viewed by some as a significant waste of time and resources. The successes are easily found in the literature and rarely are startup problems even addressed in the final papers. This is unfortunate in that the real lesson learned, in developing and implementing constructed wetlands, is identifying and avoiding similar problems. Often constructed wetland failures (or failures that required re-engineering) are not readily identifiable until a period of on-site operation has occurred. Shortly after project implementation, an array of publications will highlight the wetlands project as a complete success. Correcting the numerous design flaws will be left up to others.

4.6.3 Full-Scale Example Without a Pilot-Scale Project

Where a valid pilot-scale project has been conducted prior to full-scale development, many of the implementation and operational problems will be identified and resolved at a

significantly reduced cost. One example where a full-scale project failed primarily due to lack of a pilot-scale project is the AF Plant 4 project. The AF project planted hundreds of trees and conducted numerous engineering studies. At the end of the final cost benefit analysis report, in a small section indicating that a post audit of the project had been performed, the results show 50 percent of the trees had died prior to full canopy closure. The cause was both animal and human interference. The audit projected that 90 percent of the remaining trees would likely die due to the lowering of the ground water table beyond the ability of the trees to withdraw from the underground aquifer. There are likely many other significant events that could not have been anticipated with this project and a full reporting is beyond the scope of this summary.

4.6.4 Experimental Pilot-Scale Project Benefits to Full-Scale Implementation

The experimental runs conducted with the pilot-scale constructed wetland identified numerous operational and design concerns that would need to be addressed prior to full-scale implementation at a contaminated site or where a constructed wetlands would be treating pumped water or effluent. One lesson from the pilot-scale experimental effort is to identify and test all hydraulic assumptions and to validate the results are as expected. The understanding of diurnal and seasonal impacts on plant uptake and transpiration is not automatic and needs to be addressed in a pilot-scale study. Pilot-scale implementations should be conducted in the field where a full array of nature and man-made variables can interact with the engineered system. A laboratory-scale project is not a valid substitute for field efforts.

Due to the competitive nature of plants and animals to survive, small differences in operating conditions or site parameters can create significant changes in the final outcome. In this project, it was anticipated that all trees would have similar growth rates in a large tank. The initial causation for significant differences in later growth patterns (edge effects, shading, and soil moisture) seemed trivial at the onset. The pilot-scale wetlands have helped to identify several initially insignificant factors that, in fact, need additional attention prior to a full-scale implementation.

Based on rainfall and temporary storage challenges from the experimental wetland, designing full-scale wetland systems need a 2.0-2.5 times flow rate capacity safety margin to handle unanticipated events. Additionally, the design should anticipate operating parameter extremes and develop redundancy or capability to address rapidly changing conditions that were present in the experimental wetland.

4.6.5 Recommendations to Improve Experimental Wetlands Study

The experimental wetlands instrumentation and operating parameters were adequate to meet planned objectives. In retrospect, improved discharge measurement and improved influent mixing/volume control would have provided better time/discharge-based correlations and reduced variation, respectively. Tank discharge continuous volumetric flow meter measurements would better correlate with other time based results and better define flow anomaly cause and effects.

Measurement of cottonwood tree water uptake volume would further validate experimental results. Sap flow velocity in the conducting xylem of each cottonwood tree could be measured using heat dissipation methods. Extracting one liter samples from the cottonwood xylem flow, without causing permanent damage to the tree, would be required.

5.0 EXPERIMENTAL RESULTS – SUBSURFACE WETLAND TREATMENT

5.1 Introduction

The primary objective of this research was to determine the effectiveness of cottonwood trees in a constructed wetland to uptake the contaminant 1,4-Dioxane from either tap water or secondary effluent. The simultaneous testing of a planted tank and an unplanted tank provided the ability to quantify the role of cottonwood trees to remediate 1,4-Dioxane contaminated sites. The set-up and operating parameters selected for the experiment provided realistic conditions, simulating a full-scale sub-surface-flow constructed wetland. The impact of the trees on the soil, discharge volume, and surrounding environment during the experimental runs was evaluated.

5.1.1 Contaminant Contact Time

Of several key wetland operating conditions, detention time is a primary factor in determining remediation capability. Adequate detention time of the contaminated water with the tree root mass is necessary for uptake to occur. In these experiments, the tank dwell time was three days at the 52 L per hour per tank flow rate, providing the tree roots with near saturation soil moisture conditions, maximizing the potential for uptake to occur. These conditions were validated through the measurement of soil moisture and

conservative tracer analyses in the experimental tanks as described in Chapter 4 Sections 4.2 and 4.3.

5.1.2 Evapotranspiration

Solar radiation, ambient air temperature, and water temperature are among the key environmental factors that determine the overall water uptake rate (remediation potential) of cottonwood trees. Cottonwood trees respond rapidly to changing environmental conditions. The most direct change is the rate of water uptake and transpiration. Various environmental conditions were measured throughout the experimental runs including sub-surface temperature at several depths, air temperature, relative humidity, and pan evaporation rate. Conducting the experiments during the summer months provided optimal conditions for maximizing plant uptake. The local area of the field site (Sonoran desert) experiences high ambient temperatures during the hottest time of the day ($43.3 \pm$ °C) with low humidity ($< 6\%$) during most of the summer months (May-September). Environmental conditions were measured throughout the experimental runs either through on-site sensors or from sensors at the nearby CERF facility. In addition, reference evapotranspiration data were obtained from the AZMET website for the experimental time period. The temperature, pan evaporation, evapotranspiration, and relative humidity measurements were tested for correlation with the Wetland tank discharge results.

The volume of water uptake (transpiration) by the cottonwood trees in the planted tank (Tank 1) was calculated as the difference in total discharge volumes from the planted and unplanted tanks. Water depth measurements in the discharge collection tanks (Tanks C and D) were recorded prior to pumping the collected discharge volumes to the evaporation Ponds. Depth measurements were converted to discharge volumes based upon the known diameters of the round tanks. An average per tree evapotranspiration rate in Tank 1 was calculated based on the total uptake volume divided by the total number of trees (15).

5.1.3 Cottonwood Tree Growth

Season, cottonwood tree maturity, and tree health are key factors that have significant impact on water uptake rates and wetland remediation potential. Wetland tank experimental runs 1-3 were conducted after the plants had been in the ground about one year. Experimental runs 4-6 were conducted during the summer months of the second growing season. The cottonwood trees had very fast growth rates and achieved 3-4.5 meters height by experimental run number 2 and 4-6 meters height by experimental run number 5. Experimental tree root mass was not measured. The tree roots were intertwined by the end of the experimental runs. This was discovered while removing sensors at the end of the experiments. In comparing the tree growth data to other studies of cottonwood tree growth, tree growth did not appear to be hindered in these experiments. However, the trees were approaching an overcrowded condition that would

have effected growth or health over a third growing season. Tree height and diameter at breast height measurements were taken weekly throughout the growing season and experimental runs. This data was found to be comparable with other cottonwood growth studies with similar tree ages. Tree cuttings in other published laboratory experiments have demonstrated the ability to up-take 1,4-Dioxane with newly developed roots. The one-year and two-year old maturing cottonwoods in the experimental runs would also have had this root uptake capability.

5.1.4 Discharge Measurements

In addition to 1,4-Dioxane measurements and operational, environmental, and tree growth parameters, a number of soil and water quality parameters were measured to explore possible relationships with 1,4-Dioxane uptake and remediation potential of constructed wetlands. Turbidity, specific conductivity, and pH measurements were conducted on the discharge samples collected throughout each experimental run in accordance with pre-established schedule and sample identification sheets. Dissolved organic carbon (DOC) measurements were conducted on the discharge samples from experimental runs 5 and 6. These sheets, found in Appendix A, provided the consistent timing intervals for sample collection from the planted and control tanks during the experimental runs. The results from these measurements were tested for correlation with various operating, environmental, and tree parameters to identify relationships that would aid in understanding 1,4-Dioxane results and other variations in recorded data. Sample

results for DOC, pH, conductivity, turbidity and 1,4-Dioxane were initially recorded in writing in the lab log book or the sample identification sheet for that experimental run. Results were then transferred to electronic spreadsheets as are shown in Appendix A.

5.2 Wetland Tank Key Parameter Results

5.2.1 Specific Conductivity

Specific conductivity is an indirect measure of the amount salts or ions in solution. Increased specific conductivity measurement reflects higher total dissolved solids (salts) in solution. The influent specific conductivity for tap water from the spiked feed (Tank A) averaged $615 \mu\text{S cm}^{-1}$ and the secondary effluent spiked feed averaged $1,053 \mu\text{S cm}^{-1}$. Baseline discharge specific conductivity of Tank 1 and 2 for tap water feed averaged $1,100$ and $555 \mu\text{S cm}^{-1}$, respectively. The baseline discharge specific conductivity of secondary effluent feed averaged $1,385$ and 980 for Tanks 1 and 2, respectively.

Specific conductivity of the control tank (Tank 2) discharge for experimental runs 1-3 averaged $575 \mu\text{S cm}^{-1}$ and for experimental runs 4-6 the average was $1,050 \mu\text{S cm}^{-1}$. The planted tank (Tank 1) discharge specific conductivity averaged $870 \mu\text{S cm}^{-1}$ for tap water fed experimental runs and $1,250 \mu\text{S cm}^{-1}$ for secondary effluent fed experimental runs. A 3-4 times higher variation was observed in the initial lapse time specific conductivity results of Tank 1 as compared to Tank 2.

Tank 1 discharge had higher electrical conductivity values than influent (Figure 5.1). In experimental runs 1-4, Tank 1 conductivity ranged 300 – 600 micro Siemens per centimeter ($\mu\text{S cm}^{-1}$) higher than Tank 2. For runs 5 and 6, Tank 1 conductivity was 1500 $\mu\text{S cm}^{-1}$ higher than Tank 2.

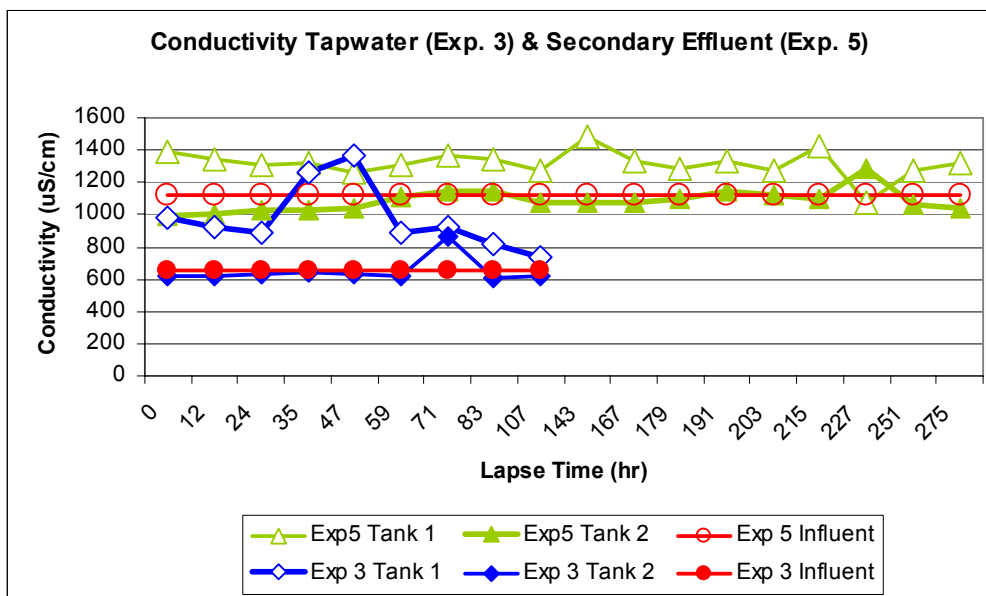


Figure 5.1. Influent & Discharge Conductivity during Exp. 3 (Tap Water) & Exp. 5 (Secondary Effluent).

For experimental runs 3, 4, 5 and 6 discharge volume measurements and tank discharge samples were taken at 71, 107, 147, 179, 215, and 251 lapse time hours from both Tank 1 and Tank 2. The discharge samples were analyzed for specific conductivity and numerically averaged for each experiment as shown in Table 5.1. Total discharge and influent volumes are shown in Table 5.1. The influent volume was derived from daily flow rate samples (L hr^{-1}) which were averaged for this same lapse time period multiplied

by the total lapse time hours. Experimental runs 1 and 2 were excluded from the analysis because detailed inflow and discharge measurements were not taken over the same lapse time period. Pan evaporation rates were averaged from the CERF data log readings for the respective experimental lapse time periods.

Table 5.1. Specific Conductivity and Total Volume (Influent/Discharge) for Exp. 3-6 Tank 1 & 2 for Experimental Lapse Time Hours 71-251.

Total Influent and Discharge Volumes & Avg. Specific Conductivity	Experimental Run Number			
	3	4	5	6
Tank 1 Avg. Influent Cond. ($\mu\text{S cm}^{-1}$)	649	1,150	1,123	1,140
Tank 1 Avg. Discharge Cond. ($\mu\text{S cm}^{-1}$)	988	1,211	1,344	2,053
Tank 1 Total Influent Volume (L)	12,500	10,105	11,610	12,079
Tank 1 Total Discharge Volume (L)	9,899	5,568	4,209	7,590
Tank 2 Avg. Influent Cond. ($\mu\text{S cm}^{-1}$)	658	1,144	1,120	1,139
Tank 2 Avg. Discharge Cond. ($\mu\text{S cm}^{-1}$)	632	1,055	1,117	1,010
Tank 2 Total Influent Volume (L)	12,500	10,019	12,599	12,595
Tank 2 Total Discharge Volume (L)	12,120	8,804	10,947	11,428

Specific conductivity of Tank 2 discharge was positively correlated to pan evaporation rate (Figure 5.2) for experimental runs 3-6. This correlation was the result of surface evaporation from Tank 2. Tank 1 discharge conductivity was positively correlated to

transpiration rate. The difference in flow volume (influent – discharge) from experimental runs 3, 4, and 5 was used in the analysis (Figure 5.3). Experiment 6 was excluded from the analysis as the conductivity significantly increased due to a 66 mm rain storm. Experiment 6 also reflected discharge increases in turbidity, DOC, and bromide tracer concentration as a result of the rainstorm.

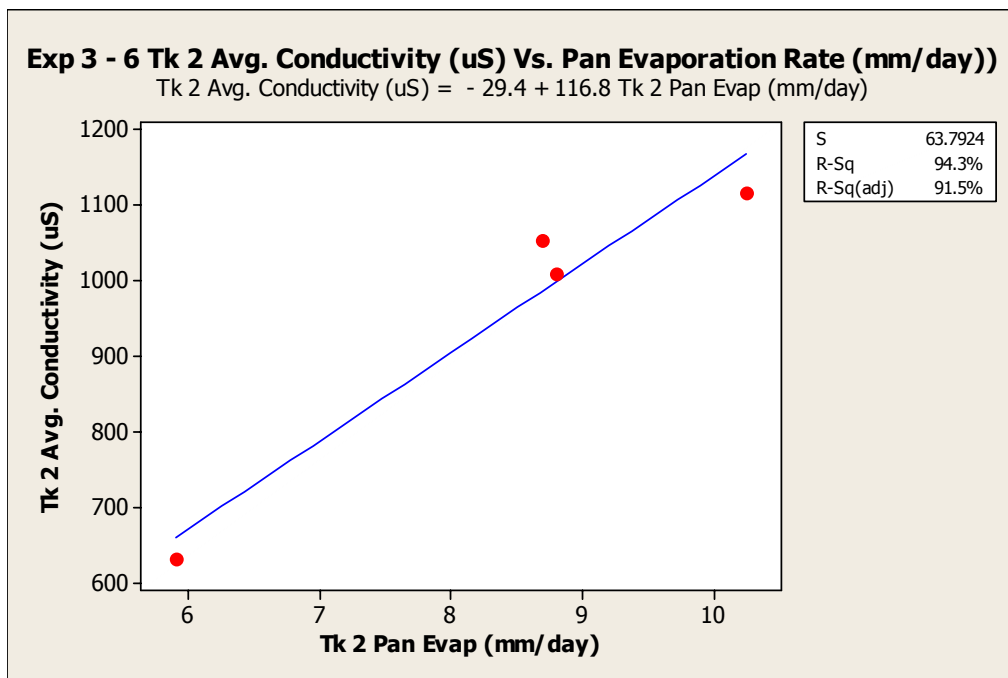


Figure 5.2. Correlation Tank 2 Discharge Conductivity to Pan Evaporation Rate.

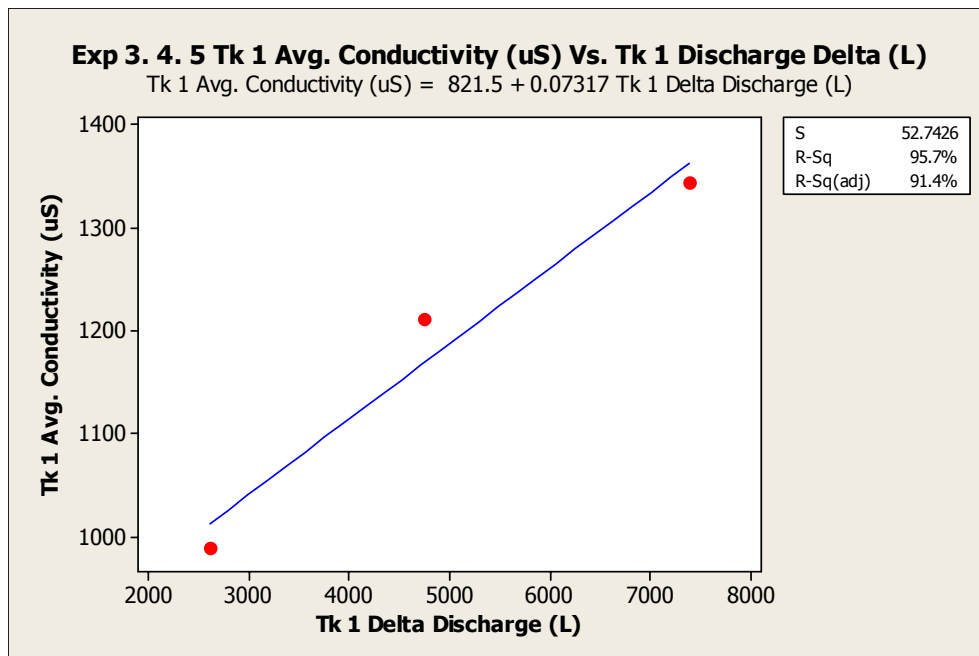


Figure 5.3. Correlation of Tank 1 Discharge Conductivity to Total Transpiration Volume.

Tank 1 and 2 difference in conductivity (discharge – influent) and discharge difference showed no correlation ($r^2 = 0.0 - 0.05$). Tank 1 and 2 conductivity values and discharge differences are shown in Table 5.1.

5.2.2 pH

5.2.2.1 Discharge pH Measurements

The pH of soil and pore water can impact plant growth and microbial populations. A neutral pH (6-8) provides optimal growth conditions (LaGrega *et al.*, 1994). The flow discharge pH values from both experimental tanks, for all runs and lapse times, ranged

between 7.0-8.6. Therefore there would have been minimal negative impact on cottonwoods or microbes. For experimental runs 1-4 the pH of Tank 2 discharge was consistently higher than from Tank 1 (0.8 pH). In experimental runs 5 & 6, pH of the discharge from both tanks was similar.

5.2.2.2 Discharge Tanks pH Peaks

In comparing the time series pH values of the Tank C and Tank D samples from all experimental runs, each sample reflecting a 1.5 day discharge accumulation, two peaks were noted in several of the experimental runs. The peaks occurred at 143 and 215 hours lapse time (Figure 5.4). The peaks were more evident in Tank D (unplanted) discharge than in the planted Tank C discharge.

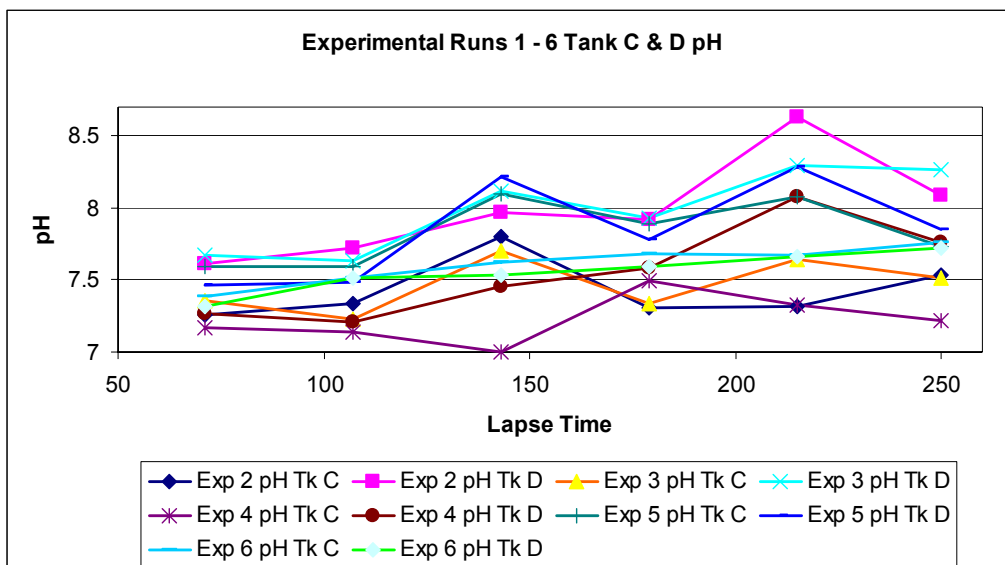


Figure 5.4. Tank C & D pH for Experimental Runs 1-6.

5.2.2.3 Time Correlation of pH Peak and Spiked Feed

The time lag between the two pH peaks is 72 hours which corresponds to the duration of the bromide and 1,4-Dioxane spiked feed to the tanks. The first pH spike also occurs at 72 hours after the spiked feed had stopped. Seventy-two hours is also near the theoretical tank residence time. Based on the timing of the first pH peak and its occurrence in both the planted and control tank, it first appeared the peak could be related to the presence of the bromide and/or 1,4-Dioxane. The timing would indicate changes in the sub-surface environment during the bromide and 1,4-Dioxane dwell time (0-71 hours) with a lag time of 60 hours.

5.2.2.4 True Cause of pH Peak in Discharge Collection Tanks

Upon further analysis, the timing of the pH peaks was found to correspond with the afternoon sampling of Tanks C & D. Tanks C & D were sampled every 1.5 days. The 5:00 P.M. sampling time at 143 and 215 hours lapse time provided two days of sunlight exposure on the tank where sampling at 5:00 A.M. (107, 179, 551 hours lapse time) allowed only one day of exposure. The 143 and 215 hour lapse time pH peaks in the Tank C and Tank D samples are most likely the result of a doubling of sunlight exposure prior to sampling. The additional sunlight promoted algae growth, which produced a corresponding increase in pH. The sampling and exposure timeline is shown in Figure 5.5. Tank C & D pH (Figure 5.4) values increased during an experimental run.

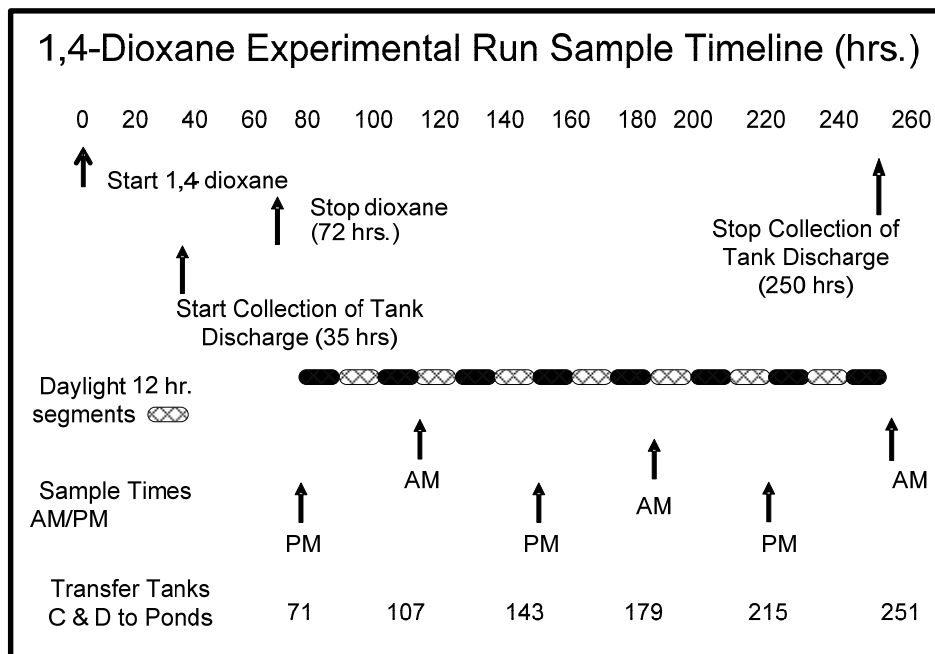


Figure 5.5. 1,4-Dioxane Experimental Run Sample Timeline.

5.2.3 Turbidity

Turbidity is a measure of the total suspended solids in an aqueous solution. Increased turbidity in streams is typically associated with added solids from rainfall runoff and bottom sediment re-suspension from increased flow rates. Turbidity was measured in Tank 1 and 2 discharge at specific lapse times in accordance with the schedule and sample identification plan for each experimental run as shown in Appendix A.

Tank discharge turbidity results from all experiments are shown in Figure 5.6 and 5.7.

Higher turbidity readings were almost all associated with Tank 1 discharge and occurred

during periods of increased flow. A transient increase in influent flow occasionally occurred due to equipment problems or during re-establishment of influent flow rate during the changeover from spiked flow (72 hours lapse time). The influent flow increases were of short duration (1-2 hrs.) which likely translated to similar duration for turbidity increases. Rainfall events also caused periods of increased flow. During periods of increased flow, sediment and/or biological materials were mobilized, resulting in increased turbidity in tank discharge. Following a high flow event, Tank 1 discharge turbidity would return to similar levels as in Tank 2 discharge (0.45 - 0.65 NTU). The periods of increased turbidity did not appear to impact other parameters during the experimental runs.

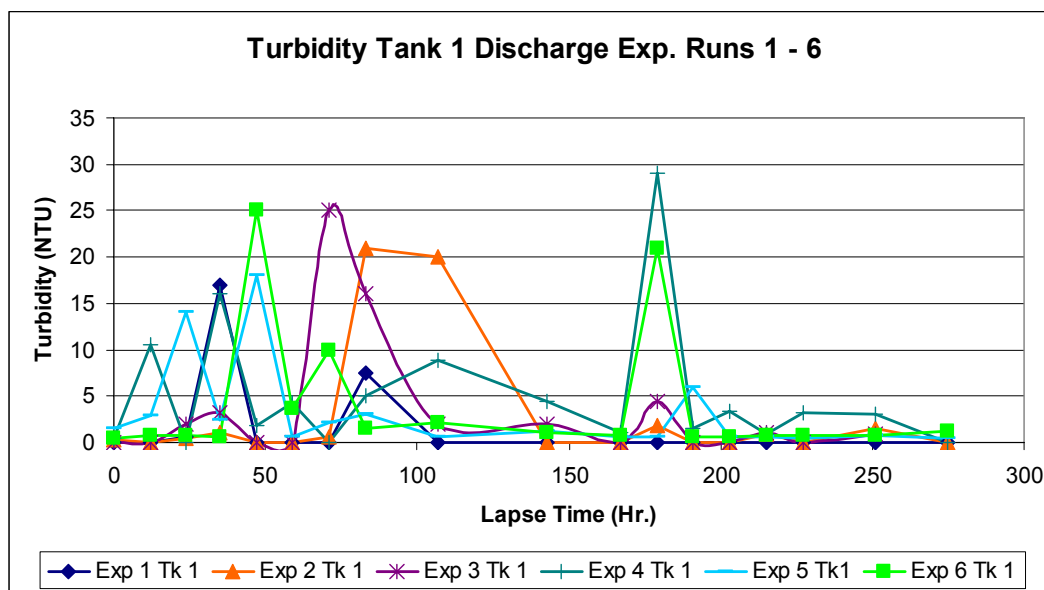


Figure 5.6. Experimental Run 1 – 6 Turbidity Results Tank 1 Discharge.

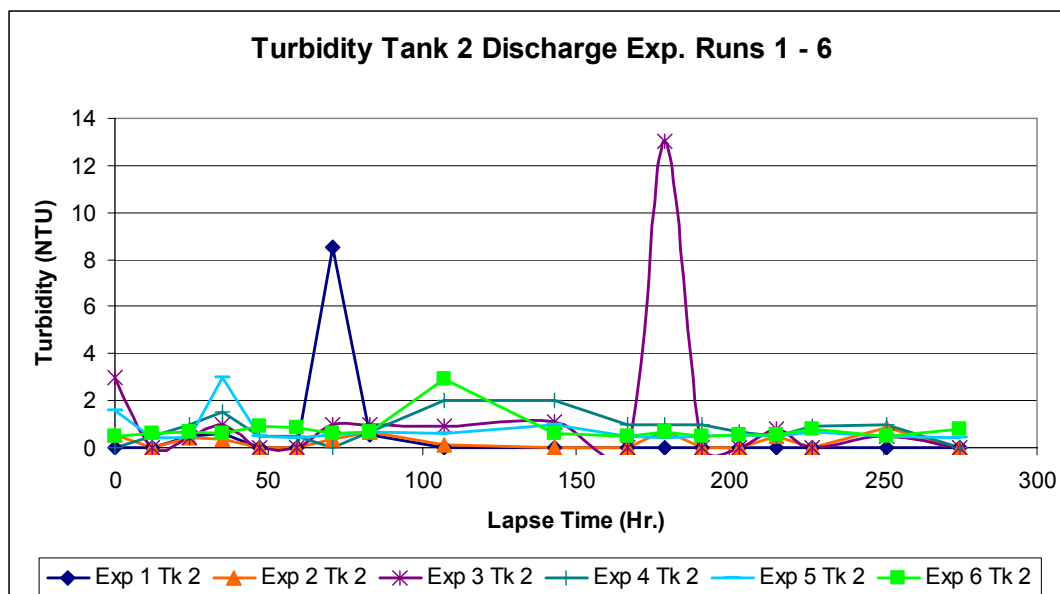


Figure 5.7. Experimental Run 1 – 6 Turbidity Results Tank 2 Discharge.

5.2.4 Dissolved Organic Carbon

Dissolved organic carbon (DOC) in wetland effluent includes residual biological and root material of wetland origin. The DOC concentration in secondary effluent can be reduced during wetland treatment by a combination of aerobic and anoxic degradation processes.

DOC analysis was conducted on influent and Tank 1 and 2 discharge samples obtained during experimental run 5. In experimental run 5, influent DOC concentrations were 15.0 mg L^{-1} . Discharge concentrations from Tanks 1 & 2 were 17.8 mg L^{-1} and 14.7 mg L^{-1} , respectively (Figure 5.8). Based on the limited samples, it appears the cottonwood

trees had minimal impact on DOC values (Figure 5.8). The elevated DOC from Tank 2 discharge may have reflected ongoing washout of soil DOC during the experiments.

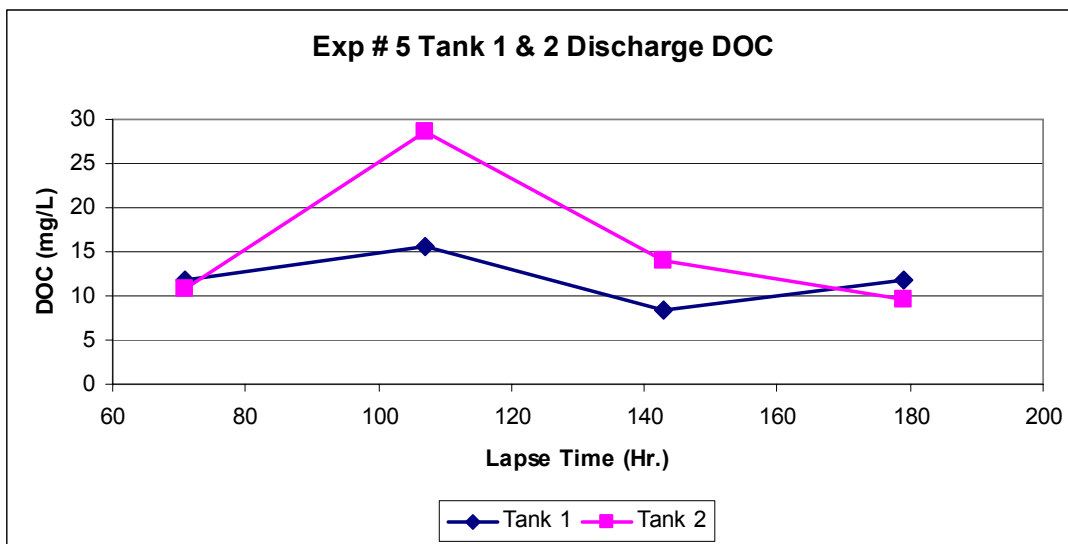


Figure 5.8. DOC Concentration in Discharge From Tank 1 and 2 (Experiment # 5) - Influent DOC averaged 15 mg/L.

5.3 1,4-Dioxane Results

5.3.1 Wetland Tank Influent

Influent samples from Tanks 1 and 2 were taken at 0.0, 35, and 59 hour lapse times during each experimental run. The sample volume was measured and timed to validate influent flow rate (52 L hr^{-1}). The samples were extracted and 1,4-Dioxane was measured (GC-FID). Results from experiments 3 – 6 are summarized in Table 5.2.

Table 5.2. Measured 1,4-Dioxane Influent Concentrations (mg L^{-1}) During Experimental Runs 3-6.

Lapse Time (Hrs.)	Exp. Run 3		Exp. Run 4		Exp. Run 5		Exp. Run 6	
	Tank 1	Tank 2						
0.0	3.56	5.56	6.09	5.47	4.35	5.95	6.60	4.04
35	4.66	4.79	5.03	5.15	6.76	5.50	5.18	5.38
59	4.77	5.23	5.05	5.46	5.74	4.96	4.91	4.47

The initial influent lapse time samples, at time zero, consistently had $1\text{-}2 \text{ mg L}^{-1}$ difference in feed concentration from the concentration target (5.2 mg L^{-1}). This variation was not evident in the influent samples taken at 35 and 59 hours lapse times. Variances from targeted feed concentrations could be the result of inadequate mixing from the feed Tank (A), variances in pump volume, or inadequate mixing from the drain channel fed mechanism. Further analysis showed little or no variation in pumping volume and the drain channel mixing was unmodified for all samples collected. Additionally, there was no piping or physical tank bias present which could have affected the initial feed concentration. The time zero influent concentration variation was likely due to incomplete mixing of the stock solution in Tank A. This inadequate mixing would have been for only a short duration (1-2 hours) and would not have significantly impacted the overall rate of 1,4-Dioxane addition to the tanks during an experiment.

5.3.2 Wetland Tank Effluent

5.3.2.1 Planted and Control Wetland Tank Results

Samples from the discharge pipes of Tanks 1 and 2 were taken at 71, 107, 143, and 179 hours lapse time for experimental runs 3-6. An additional sample for experimental run 5 was taken at 275 hours lapse time. In experimental run 6, additional samples were taken at 47, 59 and 275 hours lapse time. The 1,4-Dioxane tank discharge concentrations are shown in Table 5.3. Due to preferential flow patterns and sub-surface heterogeneity, the point-in-time discharge concentrations had considerable variation. Some planted tank (Tank 1) samples showed greater contaminant concentration than in the control tank (Tank 2) samples.

Table 5.3. 1,4-Dioxane Wetland Tank Discharge Concentrations (mg L^{-1}) During Experimental Runs 3-6.

Lapse Time	Exp. Run 3		Exp. Run 4		Exp. Run 5		Exp. Run 6	
	Tank 1	Tank 2						
47	-		-		-		0.24	0.24
59	-		-		-		0.41	0.46
71	2.71	3.09	2.87	2.76	4.24	2.17	0.89	0.71
107	2.25	3.20	4.36	4.32	5.21	2.68	1.39	1.78
143	1.75	1.73	4.15	2.43	3.73	3.10	3.25	3.04
179	1.51	0.90	2.13	1.41	1.99	3.27	1.64	2.25
275					0.57	0.68	0.59	0.61

5.3.3 Discharge Collection Tanks

Experimental run samples were also taken from Tanks C and D at lapse times 71, 107, 143, 179, 215 and 251 prior to pumping the tanks to their respective evaporation ponds (Table 5.4). Tanks C and D would collect 1.5 days of discharge from Tanks 1 and 2, respectively, before the tanks would be full and need to be pumped to the ponds. The temporary (1.5 days) discharge storage in Tanks C and D provided the ability to accurately measure the total discharge volume and a more representative (composite) contaminant concentration. Experiment Run 3 was excluded from Table 5.4 since sampling was only from Tank 1 or 2 discharge.

Table 5.4. 1,4-Dioxane Discharge Collection Tank Concentrations (mg L^{-1}) During Experimental Runs 4 – 6.

Lapse Time (Hr.)	Exp. Run 4 (mg L^{-1})		Exp. Run 5 (mg L^{-1})		Exp. Run 6 (mg L^{-1})	
	Tank C	Tank D	Tank C	Tank D	Tank C	Tank D
71	-	-	-	-	0.89	0.072
107	3.95	3.58	3.31	1.25	1.42	0.97
143	3.55	2.50	2.16	1.68	2.48	1.80
179	2.86	1.94	1.32	3.01	2.09	1.93
215	-	-	-	-	1.63	1.61
251	-	-	-	-	1.01	0.79

5.4 Experimental Run 1,4-Dioxane Mass Breakthrough

The lapse times for 25, 50, and 75 percent breakthrough of 1,4-Dioxane mass, relative to mass applied in wetland influent (19,387 g), during experimental runs 3-6 are shown in Table 5.5. The breakthrough lapse time values were determined from least squares regression plots of contaminant mass over measured lapse times. The longer lapse time breakthrough in Tank 1 is reflective of cottonwood tree uptake.

Table 5.5. 1,4-Dioxane Breakthrough Lapse Times (Hrs.).

Exp. #	Tank 1			Tank 2		
	Percentage Mass Breakthrough			Percentage Mass Breakthrough		
	25%	50 %	75 %	25%	50 %	75 %
Exp # 3	84.2	143.5	N/A	68.3	94.8	141.4
Exp # 4	86.4	143.1	N/A	75.1	106.9	132.2
Exp # 5	91.3	N/A	N/A	88.5	155.6	191.5
Exp # 6	126.3	173.5	N/A	106.8	138.0	176.4

(Tank 1 maximum recovery less than 75 percent (50% Exp. 5) therefore time is not applicable)

Comparison of the bromide and 1,4-Dioxane breakthrough times for 25, 50, and 75 percent mass recovery showed bromide (Table 4.4) had slightly longer residence time than 1,4-Dioxane. The difference in breakthrough times may be related to sampling frequency and/or timing differences between bromide and 1,4-Dioxane.

5.4.1 Mass Balance Overview

Mass balance analyses on 1,4-Dioxane were conducted for experimental runs 3-6. The mass balance assessment can provide insight on the fate of a contaminant during a treatment process. Since 1,4-Dioxane does not adsorb to soil, and is known to transpire readily from cottonwood trees, the outputs in a wetland are the discharge mass and the transpired mass. In conducting 1,4-Dioxane mass balances of the planted and control tanks, an assessment of the total mass transpired (taken-up) in experiments 3-6 was determined. This assessment reflects the capability of the constructed wetland to remove the contaminant mass given similar conditions in full-scale wetlands.

The mass balance analysis of 1,4-Dioxane was conducted with results from experimental runs 3-6. Experimental runs 1 and 2 did not have sufficient sampling to adequately determine mass of contaminant discharged and are not included in the mass balance analyses. Experimental run number 4 was conducted immediately after the winter shutdown. Roots and silt had clogged the outflow of Tank1 just prior (2 days) to the start of experimental run 4. Both tanks experienced low discharge flows throughout experimental run 4 with occasional increases in discharge turbidity. These variations in operating conditions limited the ability to utilize the results from experimental run 4 to establish meaningful correlations with other experimental runs. The bromide tracer results from experimental run 4 as shown in Section 4.2.4.5.1 also reflect discharge anomalies.

5.4.2 Mass Balance Approach

The total input of 1,4-Dioxane to each wetland tank for an experiment was 19,387 mg. This was based on the density of 1,4-Dioxane ($1,034 \text{ mg ml}^{-1}$) times the spiked volume (37.5 ml) added to the feed Tank A, giving the total influent mass of 38,775 mg. One-half this mass was added to each tank (19,387 mg).

Total 1,4-Dioxane mass in the planted and control tank (Tank 1 and Tank 2) discharge was determined in experimental runs 3-6 by integrating the cumulative 1,4-Dioxane mass in wetland effluent based upon samples taken from Tanks 1 and 2 or from Tanks C & D prior to pumping discharge to the solar experimental ponds. Discharge from Tanks 1 & 2 would collect in Tanks C & D, respectively, for 1.5 days between sampling events. The total volume and concentration measurements provided the means to determine 1,4-Dioxane mass in tank discharge over time.

5.4.2.1 Comparison of Wetland Tank Mass Discharge Results

Cumulative 1,4-Dioxane mass discharge using data from Tanks 1 and 2 and also from Tanks C and D, as a function of time, is shown in Tables 5.6-5.9 for experiments 3-6, respectively. The data indicate recovery of 1,4-Dioxane mass from Tank 2 discharge exceeded 100 percent in 3 of the 4 experiments. The 1,4-Dioxane mass recovered from

Tank 1 discharge was similar for experiments 4, 5, and 6. A further confounding factor for experimental runs 3 and 4 mass calculation is the use of both Tank 1 and 2 and Tank C and D concentration measurements. Sampling of Tanks 1, 2, C, and D was not performed at the same lapse time. Experimental runs 5 and 6 had separate discharge sample sets for Tanks 1, 2, C, and D.

Tanks C and D mass discharge were derived in the same manner as the Tanks 1 and 2 except the 1,4-Dioxane concentrations were from the Tanks C and D samples. The same approach of using discharge volumes multiplied by the measured concentrations of 1,4-Dioxane was utilized to determine the cumulative discharge mass in a given experiment.

The cumulative mass discharge for experimental runs 3-6 are shown in Tables 5.6 – 5.9.

Table 5.6. Cumulative 1,4-Dioxane Mass (mg) in Discharge from Tanks 1 & 2 and Tanks C & D during Experiment 3.

Lapse Time (Hr)	Tank 1	Tank C	Tank 2	Tank D
71	3,509	3,509	5,407	5,407
107	7,032	7,032	11,868	11,868
143	9,642	9,642	14,845	14,845
179	12,337	12,337	16,674	16,674
191	14,134	12,957	19,011	17,445
250	15,901	13,280	21,417	17,839
Input Mass (mg)	19,387	19,387	19,387	19,387

Table 5.7. Cumulative 1,4-Dioxane Mass (mg) in Discharge from Tanks 1 & 2 and Tanks C & D during Experiment 4.

Lapse Time (Hr)	Tank 1	Tank C	Tank 2	Tank D
71	2,937	2,937	4,287	4,287
107	7,863	7,402	10,850	9,724
143	10,629	9,767	14,408	13,387
179	12,756	12,630	16,739	16,589
191	13,680	13,092	18,411	17,425
250	13,894	13,306	18,667	17,681
Input Mass (mg)	19,387	19,387	19,387	19,387

Table 5.8. Cumulative 1,4-Dioxane Mass (mg) in Discharge from Tanks 1 & 2 and Tanks C & D during Experiment 5.

Lapse Time (Hr)	Tank 1	Tank C	Tank 2	Tank D
71	3,784	2,479	3,758	2,480
107	10,417	6,711	9,828	5,311
143	11,526	7,354	14,206	7,684
179	12,852	8,233	20,392	13,378
191	13,299	8,680	20,394	16,791
250	13,735	9,115	21,602	18,000
Input Mass (mg)	19,387	19,387	19,387	19,387

Table 5.9. Cumulative 1,4-Dioxane Mass (mg) in Discharge from Tanks 1 & 2 and Tanks C & D during Experiment 6.

Lapse Time (Hr)	Tank 1	Tank C	Tank 2	Tank D
71	956	956	1,276	1,276
107	3,273	3,322	5,124	4,341
143	6,991	6,157	11,598	9,633
179	10,271	10,329	16,270	13,639
191	11,556	11,613	18,798	16,167
250	12,493	12,551	20,174	17,543
Input Mass (mg)	19,387	19,387	19,387	19,387

5.4.3 Wetland 1,4-Dioxane Mass Removal

5.4.3.1 1,4-Dioxane Mass Removal in the Planted Wetland

Percent removals of 1,4-Dioxane mass by the planted wetland were calculated for each experimental run. The mass reduction was derived from the total 1,4-Dioxane mass input to the tank (19,387 mg) minus the Tank 1 (or Tank C) cumulative discharge mass (mg), divided by the input mass. This fraction was multiplied by 100 to express a percentage mass reduction attributable to the constructed wetland cottonwood treatment. Results indicate a significant removal of 1,4-Dioxane from the planted tank (Figure 5.9). The 1,4-Dioxane percentage reductions from the Tank C mass discharge calculations more

accurately reflect wetland performance since the data is based on integrated 1.5 day sample of discharge contaminant concentration.

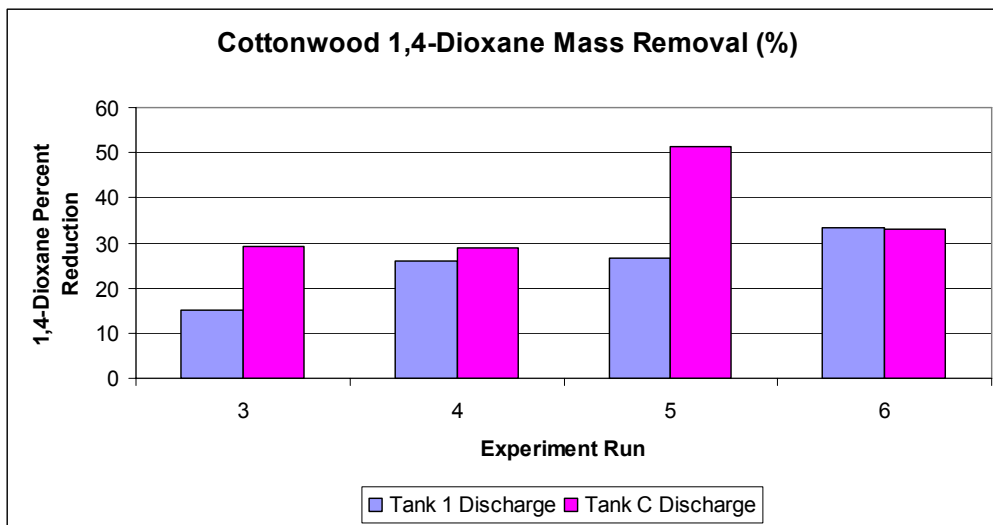


Figure 5.9. 1,4-Dioxane Mass Removal from Tank 1 / Tank C Discharge Mass Balance Calculations.

5.4.3.2 1,4-Dioxane Mass Removal in the Unplanted Wetland

Based on the Tank 2 discharge measurements, 1,4-Dioxane mass discharged exceeded the total applied mass during experiments 3-6 by an average of 9.1 percent (Tables 5.6 – 5.9). Tank D underestimated 1,4-Dioxane mass discharge by 3.8 and 10.8 percent for experimental runs 4 & 6 and 3 & 5, respectively. The Tank 2 overestimation may have been the result of point-in-time sampling at the end of Tank D 1.5 day discharge collection period. Using a similar approach as Tank C mass removal, Tank D discharge indicated a 4.0-6.4 percent loss of 1,4-Dioxane. This loss may be attributable to

remaining residual contaminant in the wetland that was unmeasured after the last sample (251 hours lapse time) was taken. Experimental run 5 also had 9.1 percent bromide tracer remaining after 251 hours lapse time. However, experimental runs 3, 4 and 6 bromide residual (after 251 hours lapse time) was near 1.0 percent.

The loss of 1,4-Dioxane from Tank 2 is likely the result of evaporation either from the soil surface and/or during detention of discharge in Tank D. Based on the TDR soil moisture measurements at 6 cm depth, the planted tank soil moisture was an average 15.2 percent lower than in the unplanted tank, which remained at or near saturation (Section 4.3.2.2). Losses of 1,4-Dioxane by evaporation from the control tank surface were likely greater than evaporative losses from the planted tank, resulting from differences in soil moisture near the surface in the two tanks. As such, the 1,4-Dioxane loss by evaporation from the control tank (Tank 2) was not used as an adjustment in mass balance analyses on the planted tank (Tank 1).

5.5 Correlation of 1,4-Dioxane Uptake to Environmental Factors

The uptake of 1,4-Dioxane by cottonwoods is evident from comparison of the contaminant mass reductions in Tanks 1 and 2 during experiments 3-6 (Figure 5.9). Tank 2 mass reductions (Figure 5.10) were attributed to near surface saturation of soil which did not occur in Tank 1 as evidence by lower TDR soil moisture measurements in Tank 1.

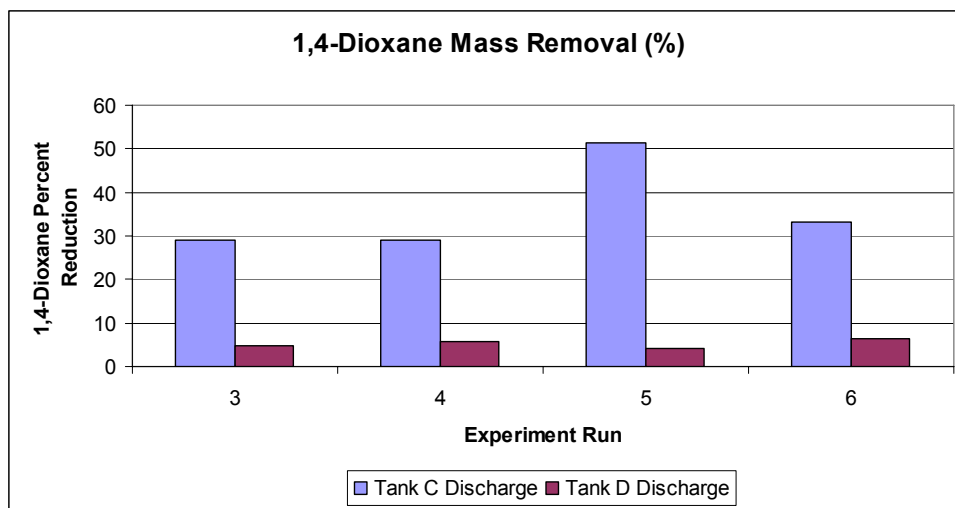


Figure 5.10. 1,4-Dioxane Mass Removal from Tank C and Tank D Discharge Mass Balance Calculations.

5.5.1 Transpiration Correlation to 1,4-Dioxane Uptake

With 1,4-Dioxane being fully miscible in water, the contaminant removal rate from the planted tank was expected to be highly correlated with water removal (transpiration) rate by the cottonwoods. A correlation analysis was conducted between the evapotranspiration rate and the total 1,4-Dioxane mass uptake in the planted tank. The total 1,4-Dioxane uptake mass for an experiment was calculated from 1,4-Dioxane Tank C input mass minus the cumulative contaminant discharge mass (Tables 5.6-5.9). For experimental runs 3, 5, and 6, there is a strong positive correlation ($r^2 = 0.998$) between the Tucson AzMET station ETo evapotranspiration data and 1,4-Dioxane planted tank uptake for the respective time periods (Figure 5.11). The Tucson AzMET station ETo is derived from the Penman-Monteith equation as outlined in the Standardized Reference

Evapotranspiration booklet (Az1324) (Brown, 2005). The AzMet ETo value used in the correlation was the average from the daily readings over the same time period as the experimental run discharge sample collections.

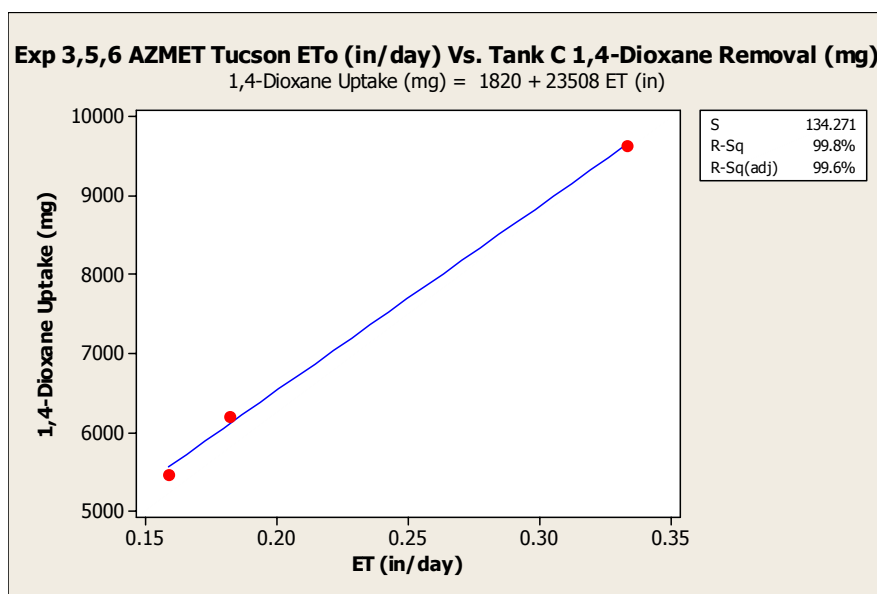


Figure 5.11. Experimental Runs 3, 5, and 6 Planted Tank 1,4-Dioxane Uptake to ETo (in/day).

Experimental run 4 was excluded from the uptake correlation analysis because of clogging as described previously in Section 5.4.

5.5.2 Planted Tank 1,4-Dioxane Uptake Correlation to Maximum Air Temperature

Experimental runs 3, 5, and 6 showed a positive correlation ($r^2 = 0.91$) between the planted tank 1,4-Dioxane uptake and the maximum daily air temperature (Figure 5.12).

This correlation is consistent with plant transpiration since a primary factor of plant transpiration is air temperature.

As shown in Figure 4.19, a strong positive correlation was found between transpiration rates in Tank 1 and average afternoon air temperature. The transpiration rate was determined as the difference in volume discharge between Tank 1 and 2. A correlation analysis between 1,4-Dioxane planted tank uptake and maximum air temperature during the respective experimental runs was conducted as shown in Figure 5.12. The maximum daily air temperature was utilized as being closely associated with transpiration rate.

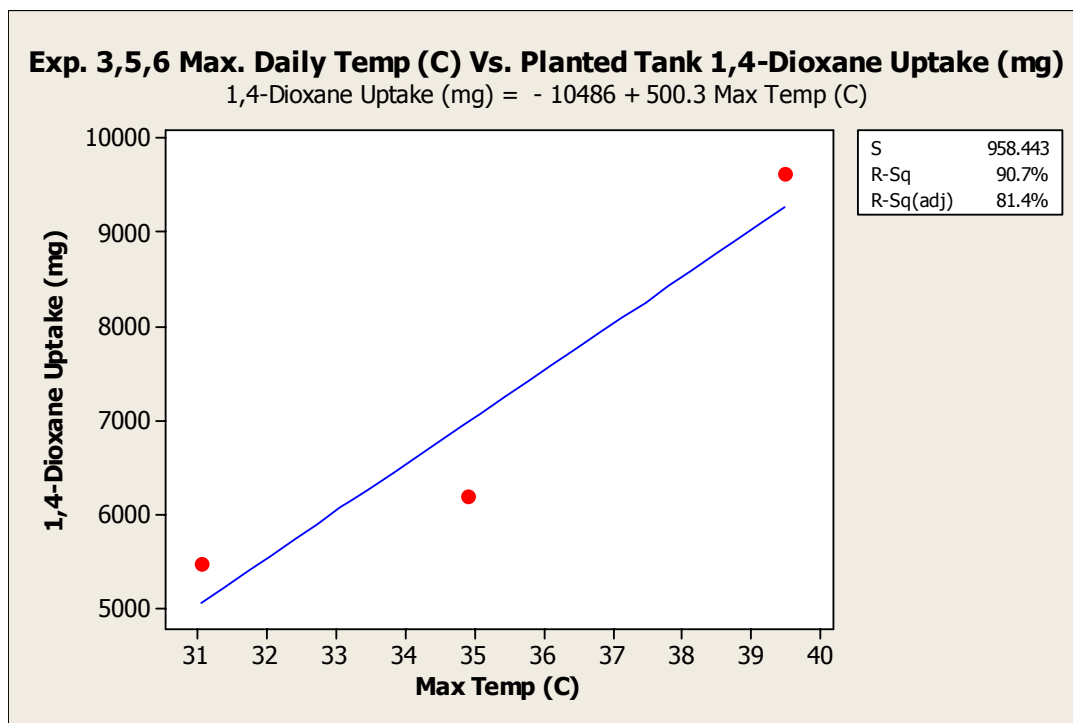


Figure 5.12. Experimental Runs 3, 5, and 6 Planted Tank 1,4-Dioxane Uptake to Maximum Daily Temperature (°C).

5.6 Determination of 1,4-Dioxane Uptake Efficiency

The efficiency of 1,4-Dioxane uptake by the cottonwoods during experimental runs 3, 4, 5, and 6 was determined. The difference in total 1,4-Dioxane discharge mass from Tank 1 during an experiment was attributed to cottonwood tree uptake. The 1,4-Dioxane cumulative uptake mass (mg) (Table 5.6-5.9 Tank C cumulative input – discharge mass) for each experiment was divided by the measured discharge time period (216 hrs) to derive the uptake rate (mg hr^{-1}). The uptake rates for experiments 3, 4, 5 and 6 are listed in Table 5.10.

Table 5.10. Experimental Runs 3-6 1,4-Dioxane Uptake Rates.

Experiment Run No.	3	4	5	6
Aqueous Phase Conc. (mg L^{-1})	5.2	5.2	5.2	5.2
Uptake Rate (mg Hr^{-1})	28.27	28.15	47.56	31.65
Transpiration Rate (L Hr^{-1})	9.17	15.05	31.34	17.85
TSCF Factor	0.59	0.36	0.29	0.34

Total cottonwoods transpiration volume was derived from the difference between the cumulative discharge volume from Tank C and Tank D. This difference in volume was divided by the total discharge measurement time period (216 hrs) to derive the total transpiration rate (L hr^{-1}). Since 1,4-Dioxane is fully miscible in water, it was expected

that tree uptake of water would carry with it the same concentration as was applied to the wetland tank, i.e. 5.2 mg L^{-1} .

The physical factors in the experimental wetlands produced considerable variation in the contaminant uptake rates as shown in Table 5.11. The planted tank had high capacity for 1,4-Dioxane removal as shown by the 7.88 mg L^{-1} uptake during lapse time 71-107 hours for experimental run 3. The higher uptake rates for experimental run 3 indicate a potential tap water advantage since experimental runs (4-6) utilized secondary effluent.

Table 5.11. Planted Tank Exp. Runs 3-6 Lapse Hr. 1,4-Dioxane Uptake Rates (mg L^{-1}).

Lapse Time (Hr)	Experiment Number			
	3	4	5	6
71	5.38	3.24	0.25	0.63
107	7.88	3.76	-1.14	1.98
143	2.79	2.04	1.74	2.96
179	-3.57	0.96	4.35	2.44
215	0.88	0.69	2.12	1.87
250	0.20	0.30	0.76	0.70

5.7 Discussion

The experimental wetlands attempted to establish operating conditions that would be instructive for future full-scale implementations. The pilot-scale contaminant

concentration and dwell time were designed to be similar or scalable to a full-scale implementation. The experimental wetland operating parameters were a balance between anticipated full-scale conditions, available equipment, and evaporation capability for the contaminated discharge. The results and subsequent analyses, show the experiment was successful in representing potential full-scale operating conditions.

The target 1,4-Dioxane influent concentration was 5.2 mg L^{-1} for the pilot-scale experimental wetland and was based upon consideration of the detection limits of available analytical equipment and to provide a sufficient remaining concentration in wetland effluent during the follow-on solar remediation experiments in the evaporation ponds. The target concentration was also based upon conditions from a local contaminated aquifer site. The Tucson Airport Area Remediation Project (TARP) has reported 1,4-Dioxane in groundwater monitoring wells very distant from the contamination source at 57 parts per billion (Karura, 2002). It is very likely the contamination level at the source is around 5 mg L^{-1} . A cottonwood-based remediation wetland would be capable of receiving concentrations of 1,4-Dioxane greater than 5 mg L^{-1} for example, Aitchison *et al.* (2000) reported that cottonwoods should not experience toxicity at a concentration of 23 mg L^{-1} . At the Pall Corporation, Gelman remediation site in Ann Arbor, Michigan, the average influent concentration was 3.5 mg L^{-1} 1,4-Dioxane (Fatouhi and Brode, 2003).

The pilot-scale experimental wetland influent flow rate was 52 liters per hour which is similar to the GAC treatment flow rate from Stanford's Linear Accelerator former solvent underground storage tank remediation project. The GAC treatment groundwater remediation concentration was $1,000 \text{ mg L}^{-1}$ and ex-situ treatment flow rate was 26 L Hr^{-1} (Sabba and Witebsky, 2003).

The contaminant concentration in a full-scale implementation would likely vary based on location of extraction wells in relation to contaminant source for on-site wetland treatment. The influent contamination concentration could be maintained within a target range by mixing feed from several extraction wells. Based upon the initial influent concentration differences of the spiked feed for the experimental wetland, the distribution of 1,4-Dioxane could be problematic without adequate dispersion. While 1,4-Dioxane is highly miscible in water, the experimental wetland did not achieve sufficient distribution as shown by the tracer analysis (Chapter 4).

5.7.1 Comparison of Experimental Wetlands to Laboratory Studies

Transpiration is a key variable that determines the potential rate of chemical uptake and is dependent on the plant type, leaf area, nutrients, soil moisture, solar radiation, temperature, and wind conditions (Schnoor, 1997). Contaminant uptake efficiency depends on a variety of physical properties, the specific chemical properties, and the plant root and transport properties (Schnoor, 1997).

A strong positive correlation was found for 1,4-Dioxane uptake rates and transpiration rates in the planted tank. However, overall 1,4-Dioxane uptake rate was significantly lower than observed in a laboratory study by Atchinson *et al.* (2000). The primary mechanism of 1,4-Dioxane removal was via transpiration, in agreement with a laboratory study that demonstrated a high correlation between 1,4-Dioxane transpiration rate (as measured based on recovery from carbon traps) and total transpiration rate (Aitchison *et al.*, 2000). Their laboratory experiment, using soil planted cuttings, showed that 34.3 ± 6.4 percent of 1,4-Dioxane was transpired from the leaves with 18.8 ± 7.9 percent remaining in soil solution and 35.0 ± 6.0 percent unaccounted (Aitchison *et al.*, 2000).

Aitchison *et al.* (2000) used sealed reactors of cottonwood cuttings and spiked hydroponic solution to demonstrate complete (100%) uptake of 1,4-Dioxane, based on measurements of the solution. The same experimental setup with sealed reactors containing contaminated soil achieved uptake efficiency between 20 and 50 percent.

The variation in reactor uptake in soil versus the hydroponic solution lends insight to results obtained in the experimental wetlands. In the laboratory study, soil moisture was readjusted to 80 percent field capacity every four days. Potential variations included incomplete mixing and variable saturation conditions. The water additions would have also diluted the 1,4-Dioxane concentration in the reactors and the plant roots would not have had 100 percent contact with the saturated soil. The reactor study indicated that

uptake efficiency is dependent upon the plant uptake capacity, the specific chemical properties, and perhaps more importantly, the soil-plant physical properties.

The cumulative uptake rates were considerably less than what was derived in the hydroponic laboratory study of Aitchison *et al.* (2000). The laboratory study (1,4-Dioxane and Cottonwood cuttings) derived a removal rate of 22.1 mg L⁻¹ transpired. 1,4-Dioxane-contaminated soil in planted reactors (cottonwood cuttings) in Aitchison *et al.* (2000) laboratory study determined the 1,4-Dioxane transpiration stream concentration factor (TSCF) was 0.72. This TSCF indicates 1,4-Dioxane contaminant moves freely with water into the plants (Aitchison *et al.*, 2000). The TSCF (dimensionless) accounts for the partial uptake of contaminant that is typically lower than water due to membrane barriers at the root surface (Schnoor, 1997). For 1,4-Dioxane, the laboratory study TSCF indicates other pathways (lateral root emergence) may be present (Aitchison *et al.*, 2000). The 0.72 TSCF factor is further described in Section 2.3.2.2. The uptake rate is given by the following equation.

$$U = (\text{TSCF}) (T) (C) \quad (5.1)$$

where U = uptake rate of contaminant (mg Hr⁻¹)

TSCF = transpiration stream concentration factor, dimensionless

T = transpiration rate of vegetation (L Hr⁻¹)

C = aqueous phase concentration in influent (mg L⁻¹)

The experimental run conditions $C = 5.2 \text{ mg L}^{-1}$, $T = 21.0 \text{ L hr}^{-1}$ avg., and the TSCF = 0.72 from Aitchison *et al.* (2000) using Equation 5.1 established a potential uptake rate of 78.62 mg Hr^{-1} . This uptake rate is higher than what was measured for experimental runs 3 – 6. Using Equation 5.1 and the known uptake and transpiration rates (Table 5.10), TSCF factors were calculated for experimental runs 3-6. The TSCF factors from the experimental data indicate the 1,4-Dioxane contaminant uptake rate by the cottonwoods in the planted tank was significantly lower than water uptake (Table 5.10). The TSCF factor assumes evenly distributed aqueous phase concentration to vegetation root systems.

5.7.2 Experimental Run Uptake Rate Compared to Previous Laboratory Study

The laboratory study of Aitchison *et al.* (2000) placed cottonwood cuttings into flasks with a 1,4-Dioxane spiked nutrient solution. Both the fluid transpired and removed 1,4-Dioxane were measured over time. A plot of these results showed one-half of the 1,4-Dioxane (2.27 mg) was removed when one-half of the solution (100 ml) had been removed (Aitchison *et al.*, 2000). The same study using contaminated soil in the planted reactors resulted in constant removal rates over time with 20-50 percent removed in the same period of time (Aitchison *et al.*, 2000).

When uptake efficiency is less than 100 percent, the wetland discharge can be evapoconcentrated. Evapoconcentration occurs where the water transpiration is greater

in proportion than contaminant uptake resulting in a higher contaminant concentration. Evapoconcentration is a potential concern for phytoremediation of ground-water plumes or constructed wetlands where the discharge stream can have a higher concentration (Ucisik, 2007).

The potential for evapoconcentration of the contaminant is evident with a transpiration stream concentration factor less than 1.0 as shown in Table 5.10. However, the experimental wetlands 1,4-Dioxane discharge concentration (Table 5.3 and 5.4) did not reflect consistently higher contaminant concentrations from Tank 1 than Tank 2. The apparent lack of evapoconcentration in the planted tank indicates a potential of cottonwood trees to uptake higher concentrations. Minor differences between Tank 1 and 2 bromide tracer breakthrough curves (Figure 4.6) suggest evapoconcentration impact was minimal.

The average uptake rate (33.9 mg hr^{-1}) of 1,4-Dioxane was lower (57 percent on average) than what was observed in a bench-scale laboratory study using poplar cuttings (Aitchison *et al.*, 2000). The laboratory study determined a TSCF factor (0.72) from experimental results for 1,4-Dioxane uptake efficiency that equates to a projected 78.62 mg hr^{-1} uptake rate when applied to Equation 5.1 with average experimental wetland transpiration rates (L hr^{-1}) and aqueous phase concentration of 5.2 mg L^{-1} . Lower uptake rates in this field study were expected since the contact time (3.5 days) and input 1,4-Dioxane concentration (5.2 mg L^{-1}) were lower than in the laboratory study (14 days and

23 mg L⁻¹, respectively). The higher soil moisture content in the laboratory study would also have enhanced contaminant uptake. The experimental study dispersion and preferential flow pathways in the tanks circumvented tree root mass and reduced uptake.

The 1,4-Dioxane uptake rate differences can be resolved by comparing key parameters between the experimental laboratory study and the pilot-scale experimental constructed wetlands. As shown in Table 5.12, of the various parameters evaluated below, the contact time and sunlight difference between the experiments would likely offset the 16-fold higher 1,4-Dioxane uptake of the hydroponic laboratory study.

Table 5.12. Comparison of Experimental Factors Related to Variable 1,4-Dioxane Uptake.

Site	Contact Time	1,4-Dioxane Concentration	Sub-Surface Temperature	Full Sunlight (hrs.)	Soil Moisture
Pilot-Scale Experimental Wetlands (this study)	36-50 Hours	5 mg L ⁻¹ (diluted with back-mixing)	22 – 23 °C	4-6 hrs. per day (150 μmol m ⁻² •s in shade)	70 % Field Capacity (specific area variations)
Hydroponic Laboratory Study (Aitchison <i>et al.</i> 2000)	217 Hours	22.7 mg L ⁻¹ (no replenishment)	24 – 29 °C	16 hrs day ⁻¹ (110–165 μmol m ⁻² •s)	80 % Field Capacity

Adequate contact time is a key feature in any wetlands remediation effort. Without contact with root surfaces, no uptake is possible. As shown in Table 5.12, a five-fold contact time difference has a direct impact on the contaminant uptake rate.

As shown in Table 5.12, a nearly five-fold concentration factor difference would also contribute to a difference in total mass transpired. The pilot wetlands were under continuous flow that added contaminant-free influent immediately following the three days of spiked influent. Due to non-ideal plug flow conditions, such as back-mixing, the contaminant concentration at portions of the root zone may have been lower than the target concentration.

In addition to contaminant concentration differences between the experiments, both subsurface and air temperature would also impact transpiration rate as well as the hours of full sunlight.

As shown in Table 5.12, the hydroponic experiment plants were exposed to photosynthetic light for 16 hours per day. Additionally, the sub-surface temperature in the hydroponic experiment was 2-6 °C higher than the wetland sub-surface temperature. The difference in temperature would also impact the amount of 1,4-Dioxane uptake.

The TDR soil moisture measurements indicated that the root zone of the constructed wetland would have periods of upper surface drying. This drying would limit the amount

of contaminant available for uptake by the cottonwoods. Where the soil was maintained near saturation (maximum moisture content), the maximum uptake of the contaminant by cottonwoods would occur. However, as noted in the bromide tracer analysis in Section 4.2.3, the concentration of bromide (and contaminant) were not evenly distributed in the upper 30.5 cm depth of Tank 1 even though the soil was saturated. As shown in Table 5.12, the hydroponic experiment plants had a consistent and higher level of soil moisture content where the planted experimental wetland experienced localized drying in the upper soil surface.

5.7.3 Experimental Run 1,4-Dioxane Discharge Variations in Wetlands Tanks

The discharge mass recovery of 1,4-Dioxane varied considerably throughout the various experimental runs as shown in Figure 5.13. The variations, while ultimately linked to transpiration for Tank 1, are a combination of temperature, humidity, rainfall, soil moisture, solar radiation and tree age.

The cumulative discharge mass results from Tank D for experimental runs 3-6 (Figure 5.13) are approximately 95 percent 1,4-Dioxane recovery. Experimental runs 3, 4 and 6 Tank C cumulative discharge mass results are approximately 70 percent (Figure 5.13). Experiment run 5 results for Tank C cumulative discharge mass is 48 percent. The variations in contaminant cumulative discharge mass percentages over time for experiments 5 and 6 are linked to specific environmental events.

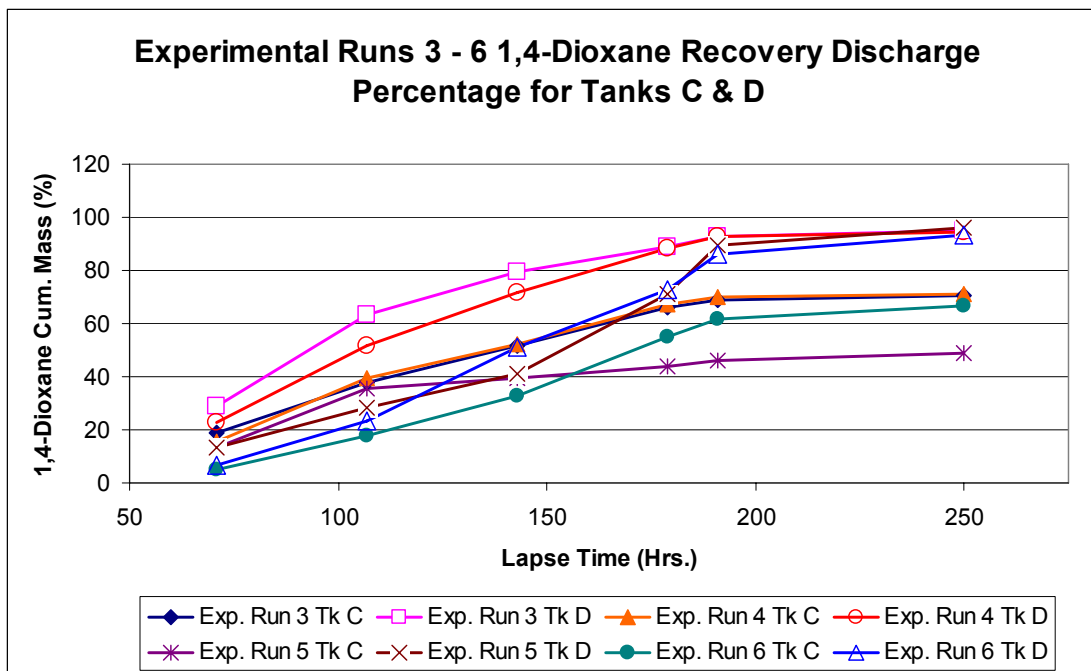


Figure 5.13. 1,4-Dioxane Cumulative Mass Recovery Percentage During Experimental Runs 3 - 6 From Tanks C and D.

Experimental run # 6 had excessive rainfall at 107 hours lapse time (66 mm). The rain event does coincide with a higher 1,4-Dioxane mass being discharged following the rainstorm in experimental run # 6 Tank 2. Experimental run # 5 experienced 8 °C higher 15.2 cm sub-surface temperatures. A lower 1,4-Dioxane discharge mass in Tank C, after 150 hours lapse time, does coincide with higher air and sub-surface temperatures resulting in higher uptake from trees.

The rainfall and temperature events assist in understanding 1,4-Dioxane discharge mass variations. Similar results were observed in the bromide tracer cumulative discharge mass results for experiment 6 Tank 2 (Figure 5.14). The tracer results also reflect a lower

bromide mass discharged for experiment 5 Tank 1. This result reflects an increase in bromide precipitating from solution due to soil surface drying in Tank 1 (Figure 5.14).

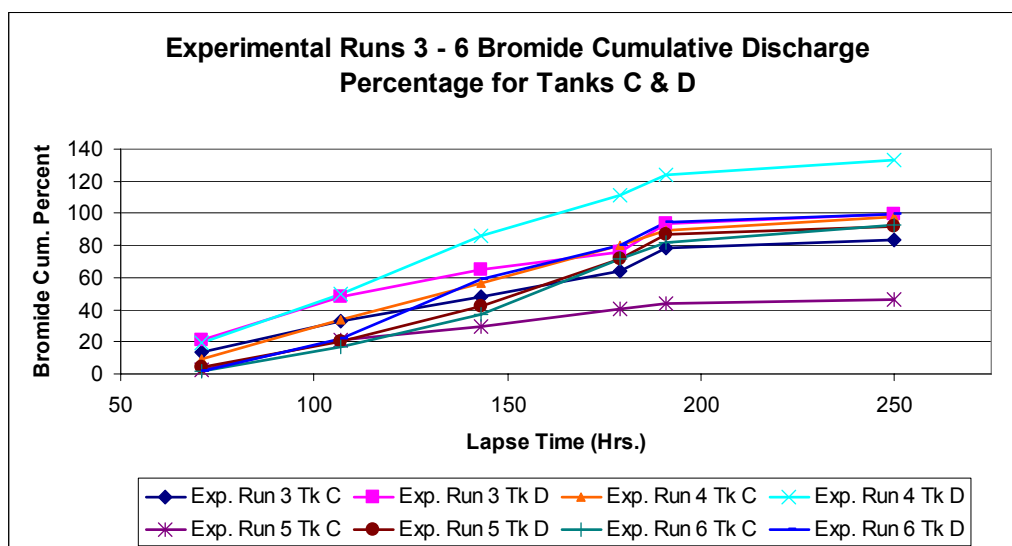


Figure 5.14. Bromide Cumulative Recovery Percentage During Experimental Runs 3-6 From Tanks C and D.

Surprisingly, considerable variation exists in the results from 1,4-Dioxane Tank 2 discharge. Temperature variations and rainfall events, while not related to cottonwood tree variations, would impact the mass of contaminant and bromide tracer being discharged. The bromide tracer cumulative recovered mass from Tank 2 experiment 4 was greater than the input mass. This was due to the turn-on after winter shut down between experiments 3 and 4 re-introducing precipitated bromide from the soil surface.

5.7.4 Control Tank 1,4-Dioxane Removal Rate Due to Evaporation

The Tank 2 1,4-Dioxane percentage loss for experimental runs 3, 4, and 6, had a positive correlation ($r^2 = 0.986$) to the CERF pan evaporation data (Section 5.2.1) for the respective time periods (Figure 5.15).

Volatilization of 1,4-Dioxane was higher in the control tank than the planted tank due to higher surface moisture in the near surface soil. Unplanted Tank 2 contaminant mass loss averaged 5.3 percent from experimental runs 3-6 (Figure 5.9). Influent flow rate (52 L hr^{-1}) fully saturated Tank 2 resulting in surface puddles for short periods of time. Tank 1 influent flow of 52 L hr^{-1} , due to the tree uptake, would have short periods of zero discharge. 1,4-Dioxane can readily volatilize from surface water as demonstrated by the experimental results of the surface evaporation ponds (Chapter 6). Throughout all experimental runs, the Tank 1 upper surface soil moisture was considerably lower as shown by TDR measurements.

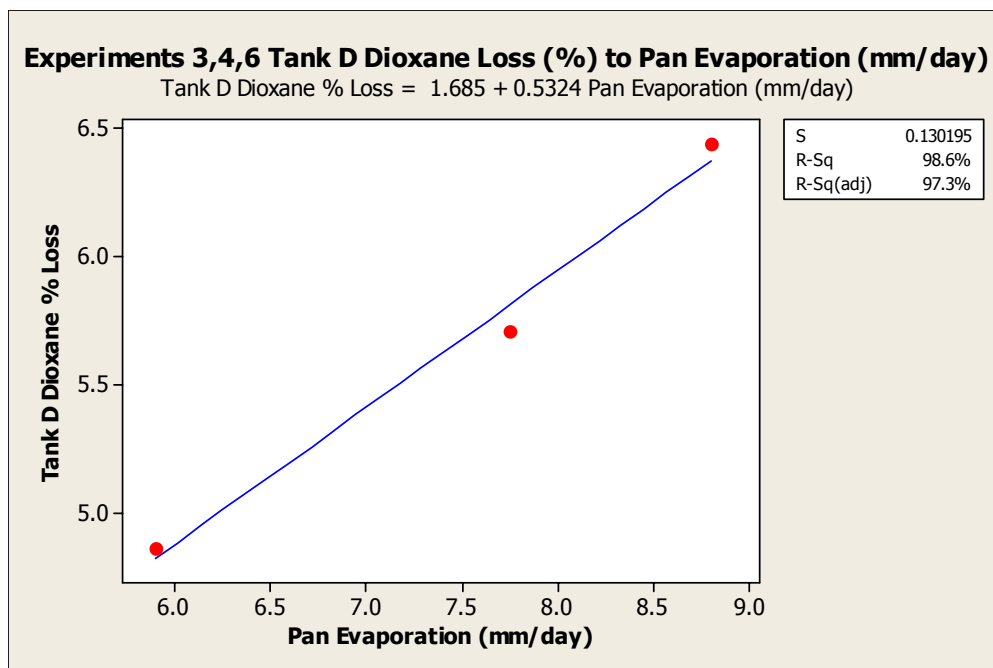


Figure 5.15. Tank D 1,4-Dioxane Mass Loss (%) Vs Pan Evaporation (mm/day) for Experimental Runs 3, 4, 6.

The soil moisture in the planted and control wetland tanks at the 5 cm depth was an average (9 months 2006) of 0.223 and 0.388, respectively. The higher moisture content in the control tank allowed higher surface evaporation and contaminant volatilization than in the planted tank.

The TDR moisture measurements (0.223 & 0.388) were taken in the early morning when the planted tank had maximum soil moisture content. Due to transpiration, the near surface soil moisture in the planted tank decreased significantly in the afternoon. The lower moisture content resulted in a lesser volatilization rate than in the unplanted tank

(Tank 2). It was therefore assumed volatilization losses from Tank 1 were insignificant and were not considered in determination of Tank 1 uptake rate calculations.

5.7.5 Comparing Tap Water and Secondary Effluent Experimental Runs

5.7.5.1 Experimental Run 3 (Tap-Water) and Run 4 (Secondary Effluent)

Experimental run 3 and 4 has similar 1,4-Dioxane discharge mass recoveries as shown in Figure 5.13. The influent for experimental run 3 was spiked tap water and for experimental run 4 was spiked secondary effluent. A six month lag time separated experimental runs 3 and 4.

Surprisingly, contaminant mass recovery outflow differences between experiments 3 and 4 were minimal, given the winter shutdown and influent change between the experimental runs. However, while the 1,4-Dioxane total mass discharges was similar, almost no other environmental factor was the same (Table 5.13).

Table 5.13. Experimental Runs 3 and 4 Environmental Factor Comparison.

Exp #	Tree Age (Mo.)	Rainfall Amount	Maximum Air Temp. (°C)	Transpiration Tank 1 (Liters)	Average Daily Pan Evaporation (mm day⁻¹)	Conductivity (µS cm⁻¹)
3	14	Trace	31.0	2222	5.90	977
4	21	None	36.4	3238	7.75	1224

5.7.5.2 Experimental Run # 4 Operational Factors

Experimental run # 4 should have had greater uptake of 1,4-Dioxane based upon previous correlations showing increased 1,4-Dioxane uptake with increase in maximum temperature and pan evaporation. Experiment 4 did have increased transpiration but without a similar increase in 1,4-Dioxane uptake. Two operational factors may have contributed to the lack of contaminant uptake. These factors were discharge port clogging and tank infiltration rate. The occasional clogging and low discharge flow from both Tank 1 and 2 could have impacted the overall contaminant uptake and tree transpiration by providing varying soil moisture content during the experimental run.

From April 24, 2006 to April 29, 2006, the discharge port from Tank 1 was totally clogged with roots and silt which resulted in 10.2 cm of standing secondary effluent at the downstream end of Tank 1. This clogging was resolved by removing a large mass of tree roots that encased the screened discharge port and extended down the inside of the vertical discharge pipe. New screening was added to the port with new sand being packed around the port to the same density as the rest of the tank.

The problems of clogging continued into experimental run # 5 that commenced May 1, 2006. Throughout the experimental 5 run, the morning discharge volumes from both Tanks 1 and 2 would occasionally be 50-65 percent lower than normal. These occasional

low flows likely indicate experimental run 4 also experienced infiltration rate problems in the tanks due to the added rhizosphere material available from the winter period.

The lower uptake of 1,4-Dioxane in experimental run 4 may have been attributable to a number of operational factors. The tank clogging and standing secondary effluent may have put some of the trees under stress due to the flooded conditions. Cottonwoods can withstand from 2-3 weeks in submerged conditions. However, the flood event will stress the root system and result in altered transpiration. The digging up and removing some of the roots from trees 7, 14, and 15 to clear the clogged piping would also have induced some stress on the tree and likely impacted uptake and transpiration.

Influent salt content impacts plant water use by an osmotic effect. The higher salt content increases the energy with which water is held in the soil which results in lower water uptake by plants (Blaylock, 1994). Cottonwood trees are moderately salt sensitive and did not appear to be impacted (transpiration) by the increase conductivity in Tank 1 as shown in Table 5.13.

5.7.6 Pilot-Scale and Full-Scale Wetland Contaminant Removal

The experimental pilot-scale wetland is reflective of the degree of contaminant removal that can be expected in a full-scale implementation.

In the pilot-scale experimental wetland, the fifteen trees in the planted tank were significantly overcrowded with 0.93 square meters per tree. The depth from soil surface to discharge outflow was 0.30 meters. The trees were probably already in a crowded condition at the end of the first year as shown in Figure 5.16. The crowded conditions likely slowed tree and root growth.

The hybrid poplar whips and caliper trees planted in the Air Force Plant 4 full-scale remediation study allowed 2.88 sq. meters and 5.76 sq. meters, respectively. The intention of the higher density whip plantation was to conduct thinning out (50 percent) as the trees matured. Canopy closure was modeled to be at year twelve in the AF Plant 4 study. At that time, the tree transpiration rate was predicted to equal 50-90 percent of the groundwater flow (Eberts *et al.*, 1999). The depth to groundwater in the AF study was 2.5 to 4 meters (Harvey, 2003).

In comparing the pilot-scale to full-scale wetland, the overall transpiration rate was three times the rate as the AF Plant 4 trees as discussed in Sections 4.5.1.1 and 4.5.1.2. A full-scale wetland with a planting density of 4 sq. meters per tree will likely achieve the same level of transpiration in about 2 years when the trees reach 6 m in height. The pilot-scale wetland did have an advantage in that the secondary effluent greatly increased the size of the leaves on the cottonwoods by a factor of 2 - 3. The added nutrients are assumed to have stimulated root growth as well.



Figure 5.16. Experimental Wetland Cottonwood Tree Growth (1 yr).

5.7.7 Fate of Contaminant

5.7.7.1 No Biodegradation of 1,4-Dioxane

Based on the near 100 percent Tank 2 mass recovery of 1,4-Dioxane (Figure 5.13), no biodegradation of the contaminant occurred. This may be due in part to the very short

duration (72 hrs) of the spiked feed. The lag phase for efficient microbial degradation may take weeks or months depending on the environmental conditions and the species, numbers, and adaptability of specific degrading microorganisms (Maier, 2003). A number of microbial degraders of 1,4-Dioxane such as *Amycolata sp.* CB1190 (Kelley *et al.*, 2001) have been identified. In laboratory studies, 25 percent of the 1,4-Dioxane added to CB1190-augmented soil (10 mg kg⁻¹) was mineralized. The soil augmentation was 10⁷ cells per gram of soil. When a planted reactor was utilized, transpiration removed 33 percent of the contaminant and 17 percent was mineralized to CO₂ over the 18-26 day test period.

5.7.7.2 Fate of 1,4-Dioxane After Tree Uptake

The experimental constructed wetlands study did not address the fate of 1,4-Dioxane after uptake by the cottonwood trees. Several studies (Platz *et al.*, 1997, Geiger *et al.*, 1999, Maurer *et al.*, 1999) have shown 1,4-Dioxane is readily transpired from the leaves to the atmosphere at which point the half life is 6-18 hours (Section 2.1.1.2).

5.7.8 Sampling Frequency

Due to the high cost of materials and length of extraction time (6 hours per sample), the number of samples collected during the experimental runs was constrained. In experimental runs 1 & 2, the two data points of Tank 1 & 2 discharge concentrations

were inadequate to conduct a mass balance or determine peak contaminant values. For experimental runs 3-6, the number of 1,4-Dioxane samples collected from Tanks 1 & 2 and Tanks C & D was increased to six to enable mass balance analyses and correlation analyses with operating parameters. In a full-scale wetlands implementation, based on increased flows and regulatory requirements, more frequent sampling will be required. The sampling frequency and subsequent reporting will need to occur within a timeframe that allows appropriate response to changing operating conditions before exceeding regulatory thresholds.

5.7.9 Discharge Tank Sampling Concerns

There exist the potential that samples not taken directly from the experimental tank discharge port can be altered or subject to other environmental factors. This situation was evident in the pH peaks from Tanks C & D thought to be related to additional sunlight exposure in the open Tanks (C & D). While the possibility for sampling concerns exists, it was thought the Tank C and D sample results would provide a better reflection of the constructed wetland remediation potential as shown in Table 5.4. In conducting 1,4-Dioxane mass balance calculations, the results from using both sets of samples were compared.

5.8 Conclusions

The pilot-scale constructed wetland successfully demonstrated the ability of cottonwood trees to take up and transpire 1,4-Dioxane in tap water and secondary effluent. The results from experimental runs 1 through 6 showed a significant increase in 1,4-Dioxane reduction in the planted versus control tanks (18-48 percent). This removal is attributed to the uptake of the contaminant by the cottonwood trees.

The results show a strong correlation between 1,4-Dioxane removal and cottonwood tree transpiration rate. The percentage reductions in the experimental tanks are considered minimal compared to a mature full-scale wetlands. This assessment is based on the age of the trees and crowded conditions which limited crown development. It is also based on the limitations of the root mass and the potential for preferential flow pathways.

Key correlations were established between operating parameters and 1,4-Dioxane removal by the wetlands. The correlations help validate other researchers experimental study results while providing a better understanding of 1,4-Dioxane removal by cottonwood trees.

5.9 Future Research

Two distinct areas need further research in the determination and successful implementation of full-scale constructed wetlands for 1,4-Dioxane remediation.

5.9.1 Treatment and Disposal of Trace Level Contaminated Discharge

The first area needing further research is handling, treating, and disposing of wetland effluent that after treatment contains trace levels of contaminant. With biological compounds, a polishing step is incorporated into the treatment process that removes remaining harmful microorganisms prior to the effluent being discharged. The contaminant 1,4-Dioxane is very recalcitrant in nature and being fully miscible in water will likely not be degraded with a simple polishing step following wetland treatment. Research is needed to identify and qualify a process which will remediate 1,4-Dioxane contaminated waters to below regulatory action limits following wetland treatment.

5.9.2 Atmosphere Degradation Pathways for 1,4-Dioxane

The second area of research is to further identify the degradation pathways of 1,4-Dioxane transpired to the atmosphere. This research would look at both the secondary chemical compounds created as well as the overall reaction mechanisms.

6.0 EXPERIMENTAL RESULTS – OPEN POND TREATMENT

A separate experimental study, utilizing the contaminated discharge from each experimental wetland run, was conducted in open ponds to examine 1,4-Dioxane elimination during open storage. The influent to the open ponds was from the discharge collection tanks. Pond samples were measured for bromide concentration, conductivity, turbidity, pH, DOC, and 1,4-Dioxane. Sample preparation and analysis was as described previously. Algae type was identified from pond samples utilizing the key published by G. W. Prescott.

Several side experiments, both in the laboratory and at the experimental wetland site, were conducted to evaluate the potential of using solar and UV light to degrade 1,4-Dioxane. The side experiments provided valuable insight into possible secondary treatment options to degrade residual 1,4-Dioxane.

6.1 Pond Volume Measurement: Method Comparison

Comparing the pond volume results from the direct measurement method and the adjusted method (Section 3.3.4), the adjusted measurement method provided a smaller volume for both the ponds from experimental run 4 and Pond 1 from experimental run 5. The opposite condition exists for both the ponds from experimental run 6 and Pond 2 from experimental run 5. The difference from experiment 6 Pond 2 (adjusted volume

higher) was the result of a significant rainstorm. The difference from experiment 5 Pond 1 (adjusted volume lower) was the result of higher pan evaporation rate. The direct measurement method provided better volume measurement accuracy and was utilized in all subsequent analyses.

6.2 Temperature Measurement

Accurate air and pond water temperature measurements were required in order to assess temperature impact on contaminant concentration and mass over time.

6.2.1 Average Pond Temperature

Pond average temperatures were determined as shown in Table 6.1. The pond A.M. average temperatures were summarized from the 12 midnight to 9 A.M. daily hourly readings. The pond P.M. average temperatures were summarized from the 2 P.M. to 11 P.M. daily hourly readings.

The average pond temperature range during the various experimental runs was 10 °C. There was minimal temperature variation between Pond 1 & 2 for each experimental run.

Table 6.1. Average Pond & Air Temperatures (°C).

Exp #	Avg. Pond Temp		Avg. AM Temp		Avg. PM Temp		Air Temp	
	Pond 1	Pond 2	Pond 1	Pond 2	Pond 1	Pond 2	Air AM	Air PM
1	30.1	29.4	26.1	25.6	33.2	32.6	25.9	34.2
2	25.5	25.9	19.6	20.4	28.9	29.2	21.0	32.3
3	19.6	19.8	15.9	15.8	22.8	22.9	14.2	25.1
4	26.3	24.4	16.5	16.0	31.3	29.9	20.9	31.1
5	29.6	28.1	21.4	22.0	32.1	31.1	26.6	36.4
6	30.5	30.7	25.3	25.3	32.6	32.8	25.0	31.3

Average air temperatures (Table 6.1) were derived from a reference temperature probe located between Tank 1 and 2. Differences in air temperature for experimental runs did not correlate with corresponding pond fluid temperature differences (Table 6.1). Due to specific heat capacity of water, the ponds would act as temporary heat storage given the influx of long & short wave radiation, energy flux, and convection and conduction according to the basic energy balance equation of Gates, 1962 (Patten and Smith, 1975).

6.2.2 Pond Diurnal Temperature Variations

Pond fluid temperatures fluctuated due to daytime heating as shown in the example from experimental run # 4 in Figure 6.1. Shading or a top cover can significantly dampen the diurnal variations as shown in Figure 4.16. The diurnal temperature variations from a

covered and uncovered pool side experiment (Figure 4.16) highlight the dampening impact of the cover. The fluid depth was similar for the pool side experiment and the experimental ponds.

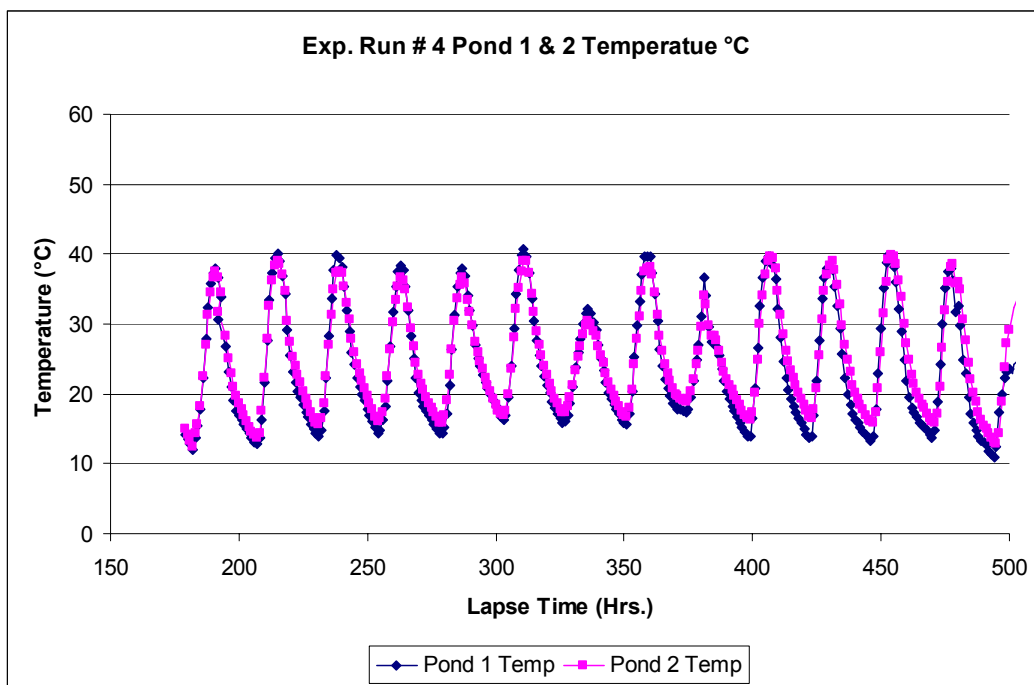


Figure 6.1. Water Temperature in Ponds 1 and 2 during Experimental Run # 4 (typical diurnal temperature variation).

6.3 1,4-Dioxane Reduction in Ponds

6.3.1 1,4-Dioxane Discharged to Ponds

Discharge from the Wetland tanks was gravity fed into the discharge collection tanks (Tanks C and D). Manual operation of the dedicated pumps in Tanks C and D transferred the accumulated 1.5 day discharge to Ponds 1 and 2, respectively. Wetland discharge

from the planted and control tanks to the respective open pond was a simple process that consisted of temporary staging of fluid in open stock tanks (1.5 days) and subsequent transfer by dedicated electric pumps and piping. This operational processing resulted in different total masses of 1,4-Dioxane being discharged to Ponds 1 and 2 in a given experiment. Pond 1 total mass was lower than Pond 2 due to the removal of 1,4-Dioxane by transpiration in Tank 1 as shown in Figure 5.10. The total mass of 1,4-Dioxane delivered to the ponds is shown in Table 6.2. Experiments 4, 5 and 6 pond volume was accurately established by direct measurement. Consequently, only these experiments were utilized for further analyses.

The total mass of 1,4-Dioxane delivered to the ponds (Table 6.2) was based on the sum of mass established by Tank C and D samples collected just prior to pumping accumulated discharge into Ponds 1 and 2. Tank C and D samples were collected every 1.5 days between experimental run 71-257 lapse time hours.

Table 6.2. Total Mass of 1,4-Dioxane Delivered to Pond 1 & 2 During Experimental Runs 4-6.

Experimental Run #	1,4-Dioxane Pond 1 (mg)	1,4-Dioxane Pond 2 (mg)
4	13,305	17,680
5	9,115	17,999
6	12,550	17,543

6.3.1.1 Pond Sampling Schedule

To determine the fate of 1,4-Dioxane during detention of discharge in the ponds, samples were collected at regular time intervals. At the time of the initial pond sample (191 hour lapse time), discharge contaminant masses at 71, 107, 143, and 179 hours lapse times would have had environmental exposures for the preceding 120 hours. The next pond sampling was at 263 hours lapse time and subsequently every 90-100 hours thereafter. This sampling schedule was utilized for experimental runs 1-5. During experimental run # 6, the planned sampling schedule was modified due to the excessive rainfall at 107 hours lapse time. The excessive rainfall required transfer of pond liquid to separate emergency overflow storage containers designated for Pond 1 and 2. The diverted water was reintroduced to the ponds at 251 hours lapse time. As such, pond experimental run # 6 was an anomaly in that overflow storage from Pond 1 was temporarily stored in a sealed container while the other storage (Pond 2) was stored in a third open air pond. Minimal 1,4-Dioxane removal occurred in the closed container during the overflow storage time frame as compared to the open pond emergency overflow storage. The difference in storage conditions resulted in Pond 1 having a higher starting contaminant mass than Pond 2 at 251 hour lapse time (Table 6.3).

Table 6.3. Mass of 1,4-Dioxane in Pond 1 & 2 in Experimental Run 4 – 6 at 191 hour lapse time.

Experimental Run #	1,4-Dioxane Pond 1 (mg)	Percent Reduction*	1,4-Dioxane Pond 2 (mg)	Percent Reduction*
4	4,749	64	5,198	70
5	1,342	85	5,576	69
6**	2,689	78	2,551	85

* Percent reduction of 1,4-Dioxane at 191 hr lapse time, relative to the total mass delivered to the ponds (Table 6.2).

** Experiment 6 sample taken at 251 hour lapse time due to rainstorm.

6.3.1.2 1,4-Dioxane Initial Pond Sample Compared to Discharge Starting Mass

The total contaminant mass in the ponds during experiments 4, 5 and 6 was calculated using the pond sample concentration measurements at 191 hour lapse times multiplied by the measured pond volumes (Table 6.3). The measured results reflect a 64-85 percent reduction in total mass from the total contaminant mass discharged from Tanks C and D prior to the initial sample taken from Pond 1 and 2. This decrease in contaminant mass is likely the result of enhanced opportunity for volatilization and UV degradation because of the shallow water depth in the ponds. The first pumping at 71 hours lapse time resulted in a pond depth of 1.9 centimeters. Contaminant loss may have occurred from Tank C & D during the lapse time (1.5 days) between volume transfers to the respective ponds. The tank evaporation was not a component of the reduction shown in Table 6.3 since Tank C & D samples were taken just prior to the volume transfer. Tank C & D

contaminant mass loss, due to 1.5 days evaporation, would be accounted for in contaminant concentration measured from Tank C & D samples.

6.3.1.3 Comparison of Contaminant Mass Reduction and Pond Volume Evaporation

The remaining contaminant in the ponds is shown in Figure 6.2 for experimental runs 4 – 6. Except for experimental run # 6, the initial 1,4-Dioxane reductions for samples taken at 191 hour lapse time and 263 hour lapse time are a combination of two additional Tank 1 & 2 discharge volume additions and the volume in Pond 1 & 2 having 3 additional days solar/UV exposure. A rapid reduction of the 1,4-Dioxane mass in the ponds occurred in the initial 120-hour time frame from the last Tank 1 and 2 discharge addition (263 hours lapse time). In each subsequent 80 – 120 hour time period the reduction in mass diminished from the preceding time period.

The pond volume loss due to evaporation (Figure 3.11) was consistent for the duration of each experimental run. The 1,4-Dioxane mass reduction (Figure 6.2) compared to the consistent evaporation loss of water (Figure 3.11), indicate the 1,4-Dioxane was eliminated at a faster removal rate than the water evaporation rate throughout a given experimental run. For experimental run 4, during lapse time hours 179-263, the Pond 1 & 2 concentration reduction was 52.0 and 34.0 percent, respectively while both ponds volume loss was 21.0 percent. Experimental runs 5 and 6 had similar results with

experiment 6 Pond 1 & 2 concentration reduction of 66.0 and 57.0 percent and both ponds volume reduction was also 21.0 percent.

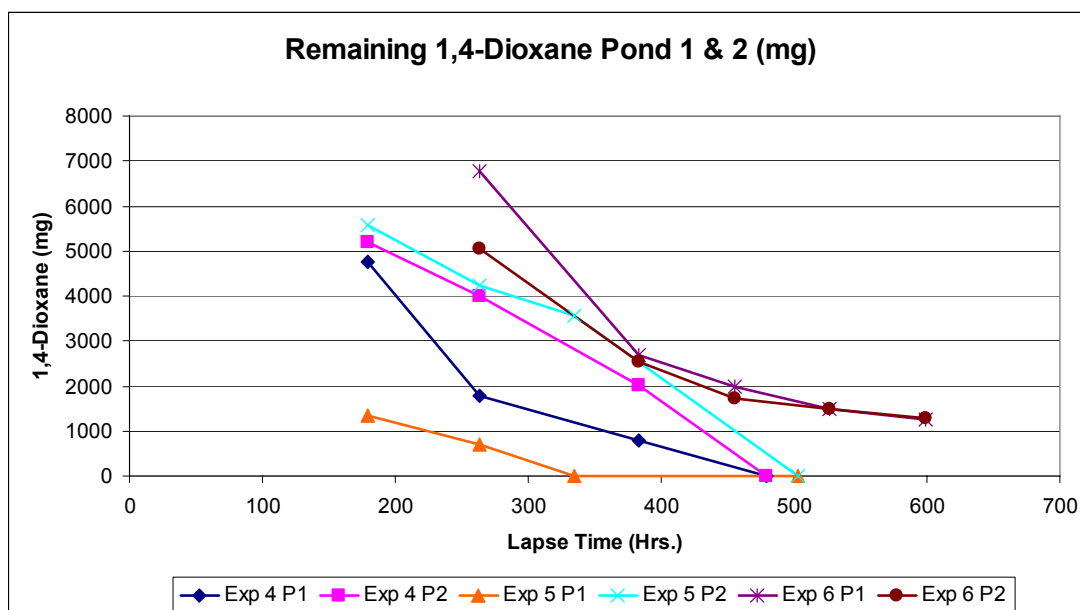


Figure 6.2. 1,4-Dioxane Remaining in Ponds (mg).

6.3.2 Calculating 1,4-Dioxane Removal Rate

The removal of the contaminant from the ponds over the approximate 430-hour sampling time frame (191-623 hr. lapse time) in a given experiment, demonstrated that one or more processes related to the ponds also reduced the mass of 1,4-Dioxane. For experimental runs 3-6, a 72-hour lapse time occurred between the first and second pond samples. For all but experimental runs 5 and 6, after the second pond sample, a 120 hour lapse time was between subsequent samples. Experimental runs 5 and 6 continued with 72 hour

lapse times between all pond samples. The pond samples reflected 1,4-Dioxane concentration remaining (mg L^{-1}). For experimental runs 4, 5 and 6, pond depth measurements were taken at the same time as samples. Based upon volume to depth conversion tables previously developed for each pond, the depth measurements during the experimental runs were converted to volume. The volume in the pond multiplied by the pond contaminant concentration at the sampling lapse time would establish the total contamination concentration remaining (mg). The difference in total contaminant mass divided by the difference in lapse time hours provided an assessment of the contaminant reduction rate (mg hr^{-1}).

6.3.3 1,4-Dioxane Removal Rate Kinetics

For experimental runs 4, 5 & 6 from both Pond 1 & 2, the rate of 1,4-Dioxane removal was correlated to the concentration as shown in Figure 6.3. As the concentration in the ponds decreased from 1.4 to 0.3 mg L^{-1} , the rate of reduction decreased from 40 mg hr^{-1} to 5 mg hr^{-1} . At 0.1 mg L^{-1} and below, the reduction of 1,4-Dioxane was minimal. This correlation between concentration and contaminant removal rate indicates the removal process kinetics are first order since the rate depends linearly on the concentration.

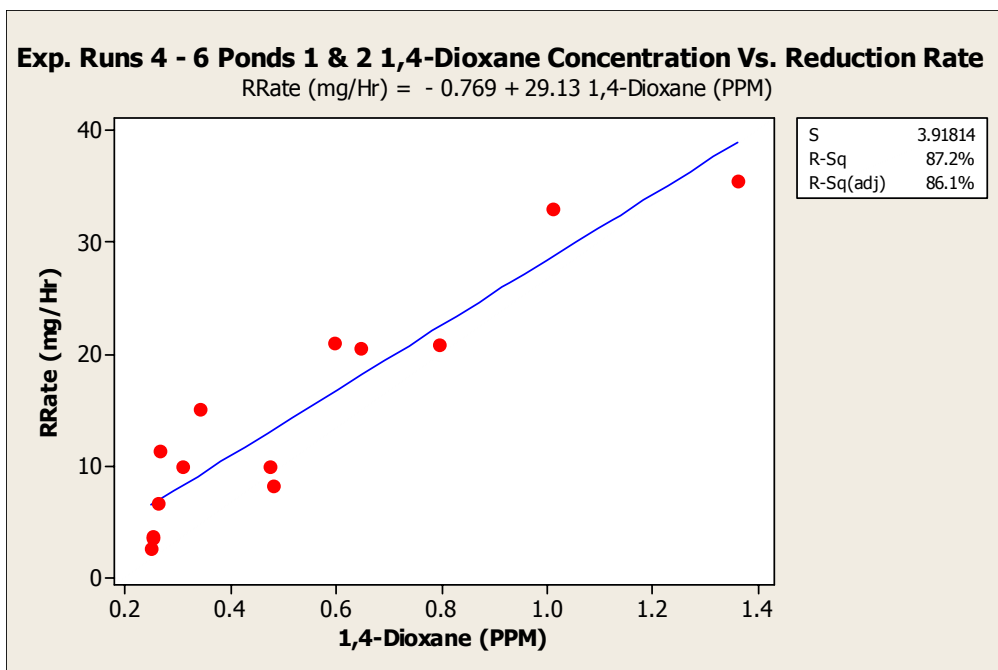


Figure 6.3. 1,4-Dioxane concentration correlated to contaminant reduction rate.

6.3.4 Determination of First Order Loss Rate Constants and Half Lives

First order rate constants were determined for Pond 1 and 2 for experimental runs 2-6 (Table 6.4). The mathematical formula for a first order process is $dC/dt = -K_e C$. The rate of elimination of a contaminant (dC/dt) is directly proportional to the contaminant concentration (C) based upon an elimination rate constant (K_e) (Schwarzenbach *et al.*, 1993). The rate constant is the fraction of the remaining contaminant that is eliminated per unit-time. The units for the rate constant are time⁻¹. The minus sign in the first order equation indicates the contaminant transport occurs from large to small concentrations.

Table 6.4. Experimental Runs 2-6 Ponds 1 and 2 First Order Rate Constants.

Exp. Run	Pond 1 Rate Constant (Hour⁻¹)	R- Sq. %	Pond 2 Rate Constant (Hour⁻¹)	R- Sq. %
# 2	0.002536	76.1	0.003161	81.3
# 3	0.002105	93.3	0.002189	94.4
# 4	0.01511	91.3	0.002686	89.7
# 5	0.0452	79.0	0.003153	77.6
# 6	0.001546	96.4	0.001415	75.7

The rate constants in Table 6.4 were determined from the characteristic kinetic plot of each experimental run data set for Ponds 1 and 2. The characteristic first order plot shows a straight line when the natural log of the contaminant concentration is plotted against time. The slope of a first order kinetic plot is K_e . An example of an individual regression plot (experimental run 3 Pond 2) is shown in Figure 6.4.

The higher Pond 1 rate constants for experiment 4 and 5 are the result of lower starting pond volumes of 3,486 and 2,000 (L), respectively. Starting pond volume for experiment 6 Pond 1 was 7,817 L. Starting pond 2 volumes for experiments 4, 5, & 6 were 5,247, 6,721, and 8,319 L, respectively. Lower pond volumes had higher contaminant concentrations (Figure 6.2) and higher liquid temperatures (Exp. 5) - subsequently higher first order rate constants.

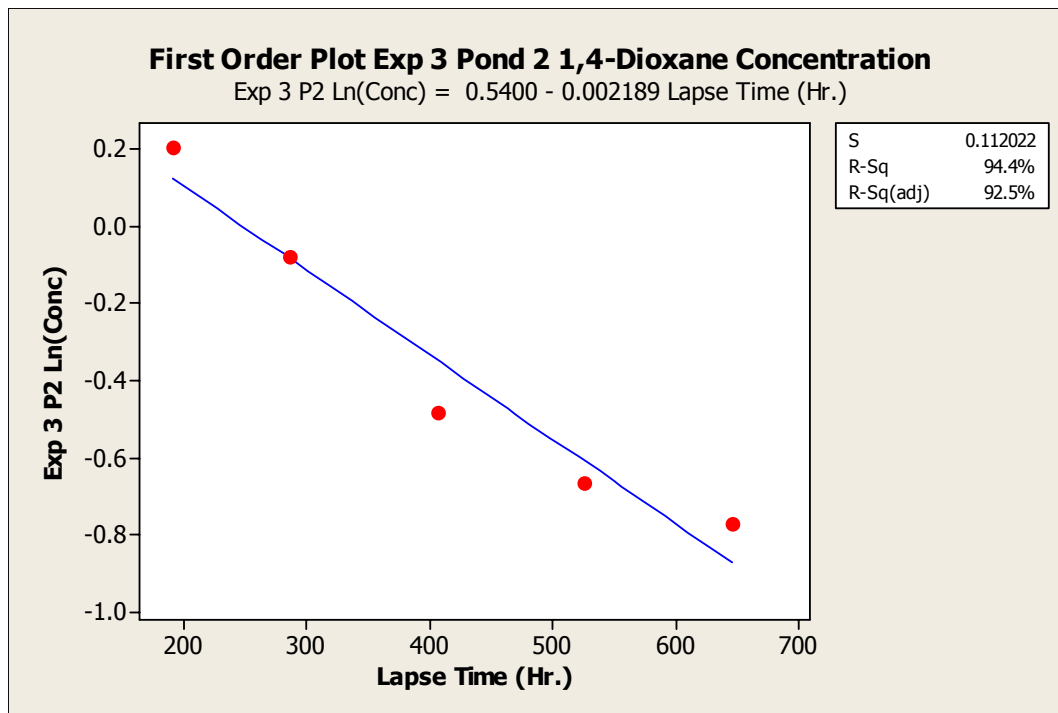


Figure 6.4. Characteristic Kinetic Plot of Exp 3 Pond 2 1,4-Dioxane Elimination.

The results from Pond 1 and 2 experimental runs indicate the elimination process is first order with the process rate constants reflecting half-life reductions of the contaminant as shown in Table 6.5.

A difficulty in establishing the half-life of the contaminant concentration in the ponds is the multiple additions from the discharge tanks over a period of time. The half-life calculations assume pond start time (0.0) is at 191 hours experimental lapse time.

Table 6.5. Experimental Runs 2-6 Ponds 1 and 2 Contaminant Half-Life.

Experimental Run	Pond 1 Half-Life Hrs. (Days)	Pond 2 Half-Life Hrs. (Days)
# 2	273 (11.8)	219 (9.1)
# 3	329 (13.7)	316 (13.2)
# 4	45 (1.8)	258 (10.7)
# 5	15 (0.6)	219 (9.1)
# 6	448 (18.6)	489 (20.3)

6.4 Determination of 1,4-Dioxane Removal Mechanism: Side Experiment

Results

6.4.1 Grey Tub Side Experiment Results

In an attempt to identify the 1,4-Dioxane removal mechanism observed in the ponds as either volatilization or photo degradation, a side experiment was established adjacent to the ponds during experimental run 3 utilizing two grey tubs. The side experiment methods are detailed in Section 3.7.2.

The 1,4-Dioxane concentration in the uncovered tub decreased by 54 percent after 9 days, where as a 19.8 percent loss occurred in the covered tub over that time. Samples taken at

18 days lapse time showed similar 1,4-Dioxane reductions (75-78 percent) in both tubs (Figure 6.5). No further sampling was conducted on the grey tubs.

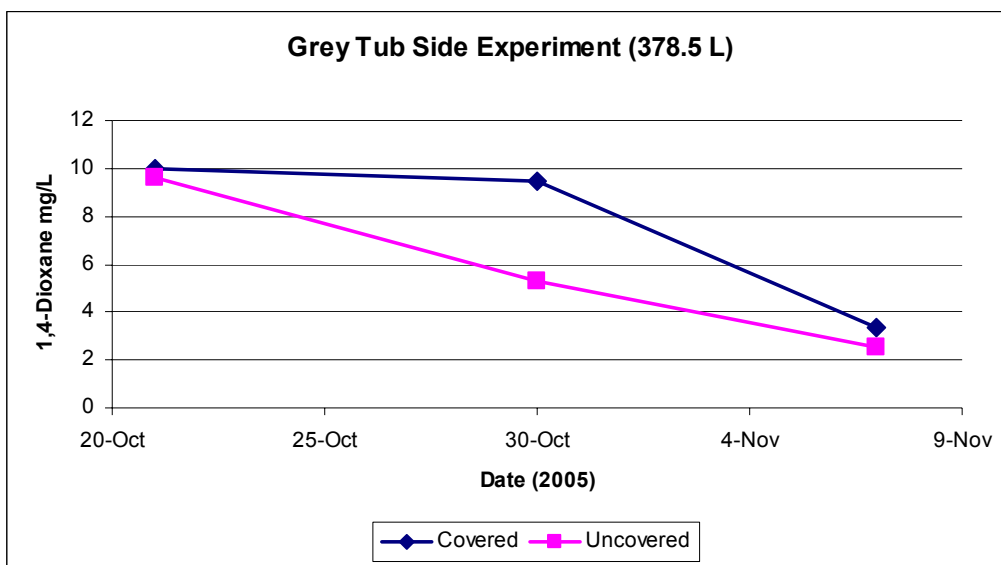


Figure 6.5. First Solar/UV and Evaporation Side Experiment (one tub was covered).

6.4.2 Pool Side Experiment Results

A second trial of the volatilization/photodegradation side experiment was conducted in early May 2006. The results from the second trial (Figure 6.6) were similar to the grey tub side experiment. The covered pool had a slight delay in reduction of 1,4-Dioxane concentration. At the end of 15 days, the difference in concentration of the pool experiment was 0.814 mg L^{-1} which was the same difference in the previous grey tub experiment with an ending concentration of 0.818 mg L^{-1} . Water temperature readings

were taken from the covered and uncovered pool side experiment as shown in Figure 4.20.

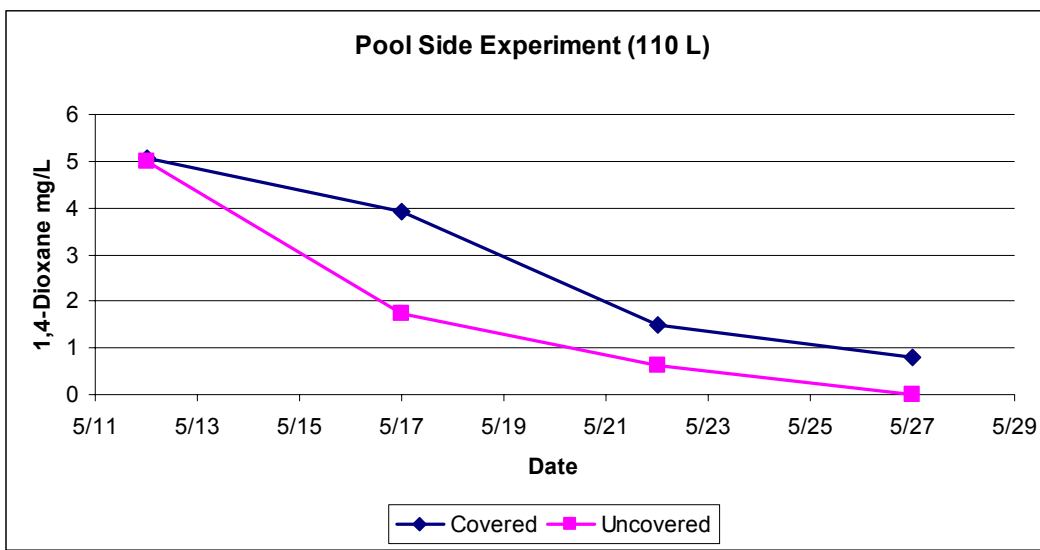


Figure 6.6. Second Trial of Solar/UV Side Experiment (one tank covered).

6.4.3 Remaining Contaminant in Grey Tub and Pool Side Experiments

The remaining contaminant mass in (mg) in the grey tub and pool side experiments is shown in Figure 6.7. This contaminant remaining mass was determined from the sample concentration times the remaining volume. This volume was calculated from depth measurements taken every day during the side experimental runs.

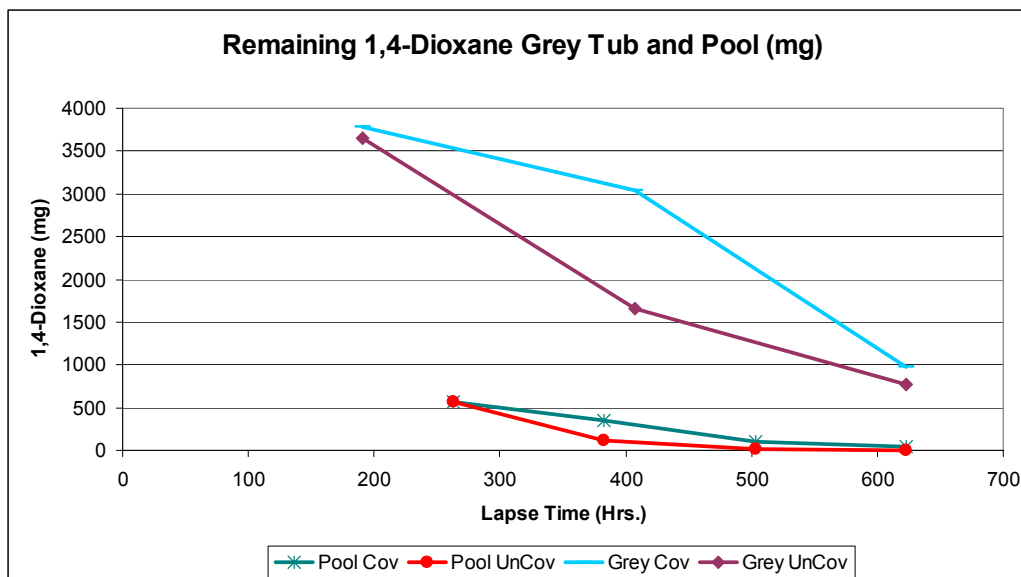


Figure 6.7. Remaining 1,4-Dioxane in Grey Tub and Pool Side Experiments (mg).

6.4.4 Grey Tub and Pool Elimination Rate Constant Comparison

Characteristic kinetic plots of each side experimental data set were developed to compare the covered and uncovered rate constants containing spiked tap water and secondary effluent, grey tub and pool side experiments, respectively. Rate constant comparisons between the two side experiments are valid even though the grey tub covered and uncovered containers were spiked with 10.0 mg L^{-1} 1,4-Dioxane while the pool containers were spiked at 5.3 mg L^{-1} . The exponential rate constant is independent from the initial concentration.

The rate constants for the grey tub and pool side experiments are shown in Table 6.6. For a given test condition, the side experiment (grey tub and pool) rate constants were similar. However, the un-covered rate constants were substantially higher than the covered rate constants for a given experiment (grey tub and pool) suggesting sunlight exposure was an important factor in 1,4-Dioxane removal rates. It is also possible that volatilization rates were reduced by the covers.

Table 6.6. First Order Rate Constants Derived from the Grey Tub and Kiddie Pool Side Experiments (18 days).

Side Experiment	Covered		Un-Covered	
	Rate Const.	r ² (%)	Rate Const.	r ² (%)
Pool (5.3 mg L ⁻¹)	0.005108	96.1	0.02543	80.4
Grey Tub (10 mg L ⁻¹)	0.002546	78.8	0.01648	98.5

6.5 Pond and Pool Side Experiments 1,4- Dioxane Mass Flux

The field side experiment first order rate constants (covered) were similar to the open pond rate constants (Exp 2-6 Pond 2). The uncovered side experiment first order rate constants were similar to Experiment 4 and 5 Pond 1 rate constants. The first and second side experiments were run coincident with experimental runs 3 and 4, respectively, starting at 191 hours experimental lapse time. The solar and environmental exposure was nearly identical for the ponds and the open tubs. The starting and ending 1,4-Dioxane mass (mg) at the specific lapse times in Experiments 4-6 for Ponds 1 and 2 are shown in

Table 6.7. The difference in mass divided by the lapse time duration (hr) and surface area (m²) gives the 1,4-Dioxane mass flux (mass of contaminant diffusing through a unit area per unit time).

Table 6.7. Comparison of pond / pool / grey tub mass flux of 1,4-Dioxane.

Experiment	Duration Lapse Time (hrs)	Pond 1 & 2		Surface Area Sq. Meters	Mass Flux mg / M ² -hr
		Starting Mass (mg)	Ending Mass (mg)		
Exp. Run 4	191 – 383	P1 – 4749	P1 – 780	39.34	0.52
		P2 – 5198	P2 – 2026	34.51	0.48
Exp. Run 5	191 – 335	P1 – 1342	P1 – 0.0	39.34	0.24
		P2 – 5576	P2 – 3549	34.51	0.41
Exp. Run 6	251 – 599	P1 – 6770	P1 – 1242	39.34	0.40
		P2 – 5044	P2 – 1296	34.51	0.31
Tub Experiment	250 – 670	O – 3644	O – 770	0.56	12.23
		C – 3785	C – 967	0.56	11.98
Pool Experiment	263 – 503	O – 569	O – 13	1.82	1.45
		C – 574	C – 102	1.82	1.23

(Note: Pond 1 = P1, Pond 2 = P2, Open = O, Covered = C)

6.5.1 Key Differences of Experimental Ponds and Side Experiments

The side experiment mass flux results support the German Chemical Society – Advisory Committee’s contention that a significant fraction of 1,4-Dioxane discharged to the environment transfers to the gas phase and into the atmosphere (Full Public Report, 1998). The normalized contaminant flux rates (water to air) in mg/m²-hr were almost three orders of magnitude higher in the first side experiment (grey tub tap water) than in the experimental run 4-6 ponds with secondary effluent (Table 6.7). A significant difference also occurred between the second side experiment (kiddie pools) and

experimental run 4-6 ponds both using secondary effluent. Key functional differences between the side experiments and the ponds were sodium bromide concentration, contaminant concentration, temperature, and amount of algae growth causing pH increase.

The gray tub and pool side experiments did not receive sodium bromide additions. The grey tub and kiddie pool starting concentration of 1,4-Dioxane was 10.0 and 5.3 mg L⁻¹, respectively while the starting concentrations at 191 hours lapse time for Experiment 4 and 5 Pond 1 was 1.36 and 0.67 mg L⁻¹, respectively. Experiment 6 starting concentration of 1.01 mg L⁻¹ for Pond 1 started at 251 hours lapse time. Pond 2 starting concentration at 191 hours lapse time for Experiments 4, 5, and 6 was 1.25, 1.12, and 0.79 mg L⁻¹, respectively.

The grey tub covered and uncovered did not have visible evidence of algae. The pool (secondary effluent) uncovered container had slight traces of visible algae while the covered container did not. Ponds 1 and 2 in all experimental runs had significant algae blooms as determined by sight.

Temperature differences between the ponds for each experimental run were impacted by air temperature and total pond volume (Table 6.1). Temperature differences between the ponds and the kiddie pool existed due to volume differences (Figure 4.20).

6.5.2 Aqueous Solubility Influence on Contaminant Air Water Partition Coefficient

At the 1,4-Dioxane concentrations in the ponds, a number of factors can influence the air water partition coefficient including aqueous activity coefficient, inorganic salts, and organic particulates (Schwarzenbach *et al.*, 1993).

Compound solubility is 10-50 percent lower in sea water (NaCl 35 mg L⁻¹) than in pure water (Schwarzenbach *et al.*, 1993). In these experiments, sodium bromide (NaBr 80 mg L⁻¹) was added to the wetland influent as a conservative tracer. The addition of NaBr and its further concentration, due to evaporation and transpiration in the ponds, likely increased the 1,4-Dioxane volatilization flux rate by lowering the aqueous solubility (“salting out” effect). One study showed aqueous solubility of benzene in water was reduced with the addition of NaBr (1 to 1) (Schwarzenbach *et al.*, 1993). No data on similar studies using 1,4-Dioxane have been identified.

6.6 Algae Growth and Effect on Pond pH

Pond pH measurements were performed in order to help understand pond chemistry changes that would have an impact on contaminant concentration and mass change over time. An example of typical pond pH during an experiment is shown in Figure 6.8. The

pond pH increased from 7.5-8.0 up to 10.0 during the first 400 hours of water detention in the ponds, coinciding with the development of algae blooms in the ponds.

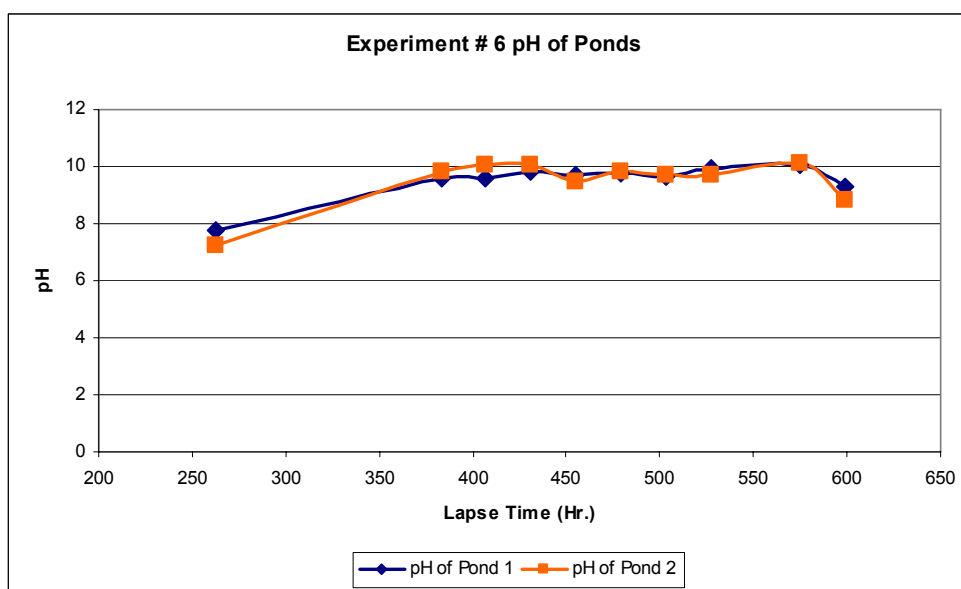


Figure 6.8. Experimental Run # 6 Pond pH

6.6.1 Algae Blooms

6.6.1.1 Qualification of Algae Volume

Algae samples were collected from the ponds during experimental runs 4, 5 and 6 in order to identify algae species. Samples for algae identification (15-20 ml) were decanted from the raw Pond 1 and 2 extraction samples into wide-mouth 30-ml sample jars. After sample filtration, the trapped residuals and filters (3 μm and 0.7 μm) were added to the respective decanted sample jar and the jars capped with Teflon® coated jar

lid seals. The sample jars were stored at 4 °C prior to algae identification. As the pond temperature increased (Table 6.1), the volume of algae also increased. Experimental pond algae increase was noted through visual observation of the pond surface and the overall volume of algae residue remaining on the filters after 3 and 0.7 µm filtration of the 1-liter samples. There was a high association between visual pond algae increase and the quantity of 3 and 0.7 µm filters required to filter a one-liter sample.

6.6.1.2 Algae Identification

Algae identification was made possible by assistance from Dr. Martin Karpiscak. One form of alga in both Ponds 1 and 2 was identified as *Chlorella* M. Beijerinck. The identification was made utilizing the taxa key of Prescott (Prescott, 1970). The *Chlorella* alga is a single spherical shaped cell 2-12 µm in diameter. It has a very high growth rate producing four daughter cells in less than 24 hours (Siver, 2007) and the highest chlorophyll content of any known organism (28.9 g kg⁻¹). *Chlorella* has been researched for use in sewage waste purification (Siver, 2007).

6.6.1.3 Impact of Algae on 1,4-Dioxane Fate

The hydrophilic nature of 1,4-Dioxane likely precludes volatilization reduction based on pond algae. The pond algae may have increased the water-to-air diffusion boundary layer thickness. This increase in thickness increases the diffusion path length caused by the

presence of a solid phase. Increasing the diffusion path length may slow down the 1,4-Dioxane transport across the diffusion water boundary layer (Schwarzenbach *et al.*, 1993).

6.6.2 Pond Carbonate System Change on Contaminant Concentration

The partial pressure of CO₂ is buffered by the carbonate system in the oceans. Henry's Law constant for CO₂ is dependant on pH through the hydronium ion concentration (Brune, 2007). At pH from 2-6.5 the Henry's constant for CO₂ is 0.034 M/atm. At a pH of 8, the Henry's constant is 1.4 M atm⁻¹. The change in Henry's Law constant would likely change the overall carbonate and bicarbonate equilibrium constants of 4.7×10^{-11} and 4.3×10^{-7} K(M), respectively (Brune, 2007). The change in CO₂ flux or changes in the bicarbonate equilibrium constant could negatively impact the flux of 1,4-Dioxane from the pond to the air by reducing the contaminant available water to air interface area (Schwarzenbach *et al.*, 1993).

6.7 1,4-Dioxane Laboratory Photo-oxidation Experiment

In order to better understand the role of sunlight on reduction of 1,4-Dioxane in ponds, a series of laboratory experiments were conducted using a sealed reactor in which one-liter solutions of 1,4-Dioxane in milli-Q water were recirculated and exposed to light.

6.7.1 UV-B / Solar Sun Light Side Experiment Exposure

During a laboratory experiment with UV-B light, only a fraction of the 1-liter solution was exposed to UV light at any given moment which equated to 70 percent less UV-B light than from natural sunlight UV-B over the same time period. The 70 percent factor was derived from the measured exposure output of the UV-B lamp at the distance from the light source to the circulating fluid ($0.00402 \text{ W cm}^{-2}$). The sample chamber provided 10 cm^2 of exposure area per 5 ml fluid, or 0.0402 W/5ml . Using a 1-liter sample and a flow rate of 5 ml sec^{-1} , each 5 ml was exposed for one second out of every 200 seconds or 432 exposure events per day. The total exposure in a 24-hour period was 17.4 W cm^{-2} , equivalent to 25 percent of the average solar UV-B exposure of 61.5 W cm^{-2} per day. The 75 percent less UV-B exposure from the lamp was partly offset by the continuous 24 hours per day run time. A full 24-hour day lamp exposure equated to 70-85 percent effective UV-B solar exposure.

6.7.2 UV-B / Visible Light 1,4-Dioxane Reduction

The 1,4-Dioxane reductions during the visible/UV light experiments are shown in Table 6.8. The 1.0 and 2.5 day UV-B experiments validity is uncertain due to the equipment set up used; the exposure well (Figure 3.15) allowed air into the closed system. The 1,4-Dioxane reductions from the visible light (solar sun lamp) were 8-6 percent for 1.0 and

2.5 days lapse time, respectively, and increased to 14 percent with exposure duration of 5 days. A 17 percent reduction occurred during the 5 day UV-B exposure. The experimental control showed no reduction in 1,4-Dioxane over 1, 2.5, and 5 days.

Table 6.8. UV/Solar Light Side Experiment 1,4-Dioxane Percentage Reduction

Experiment	Percentage Reduction		
	1-day	2.5-days	5-days
Control	0.0	0.0	0.0
Solar	8.2	6.2	13.9
UV-B	*	*	17.8

* Validity of result uncertain due to failure of experimental set-up.

Other research efforts have shown success using UV light to degrade 1,4-Dioxane in combined with semiconductor materials such as titanium dioxide (Maurino *et al.*, 1997).

Without the semiconductor, the required energy to break ether bonds is inadequate.

6.8 Discussion

6.8.1 Experimental Pond, Grey Tub, and Pool Contaminant Elimination

6.8.1.1 Determination of First Order Reaction Process

The rate of contaminant loss from the experimental ponds was found to be a first order process, meaning the elimination rate was a function of the contaminant concentration as shown by the straight line characteristic kinetic plots from the experimental run results (Figure 6.4). Since sedimentation and biotransformation were not expected to be factors

in 1,4-Dioxane reduction in the ponds, it was hypothesized that volatilization was the dominant mechanism accounting for loss of 1,4-Dioxane. To confirm this hypothesis, additional side experiments were performed to investigate the roles of temperature and exposure to UV/visible light on 1,4-Dioxane loss rate.

The field side experiments utilized tall grey tubs and shallow kiddie pools. In the tall grey tubs the temperature difference between the covered and un-covered containers was not significant and the reduction difference after 18 days was minimal (Table 6.7). The derived loss rate constant (Table 6.6) for the covered container was $0.002546 \text{ hour}^{-1}$ and the un-covered container loss rate constant was $0.01648 \text{ hour}^{-1}$ indicating 1,4-Dioxane loss occurred about 6 times faster in the presence of sunlight.

The laboratory UV-B and solar sun visible light side experiment, while showing some 1,4-Dioxane reduction from milli-Q water, would likely have minimal impact on the contaminant reduction in the experimental ponds due to the lower water quality. The most likely process for the contaminant degradation over the observed time span is volatilization.

6.8.2 Volatilization as Pond Contaminant Elimination Process

6.8.2.1 1,4-Dioxane in Ponds Volatilization Factors

The experimental results from the ponds highlighted several parameters that impact solute mass transfer and Henry's Law partitioning. These factors include contaminant concentration, temperature, pH, and bromide concentration. All of these factors contributed to the rate of 1,4-Dioxane reduction from the ponds.

Volatilization involves multiple processes where a number of factors relating to the contaminant, the water body containing the contaminant, and the surrounding atmosphere impact the total mass of contaminant movement from water to air. Factors affecting volatilization rate include aqueous solubility, vapor pressure, Henry's law constant, and diffusivity (Schwarzenbach *et al.*, 1993). Factors related to the water body include depth, flow rate, turbulence, water temperature, and other constituents which would reduce contaminant velocity across the boundary layers (Schwarzenbach *et al.*, 1993). General atmosphere factors which impact volatilization include wind speed, air turbulence, and air temperature.

6.8.2.2 Contaminant Chemical Properties Indicative of Volatilization

With a moderate vapor pressure (37 mm Hg @ 25 °C), volatilization of 1,4-Dioxane is possible. However, the low Henry's law constant ($2.8 \times 10^{-6} \text{ atm}\cdot\text{m}^3 \text{ mol}^{-1}$) indicates

minimal transfer will occur by diffusion from water to air (Mohr, 2001). Conversion to the dimensionless Henry's air water constant (K_{aw}), for 1,4-Dioxane gives 1.130×10^{-4} , indicating minimal contaminant will be present in the gas phase in a closed system at equilibrium. In the dimensionless form, K_{aw} , equals concentration in air (C_a) divided by concentration in water (C_w). As an example, at equilibrium, with 1 mg L^{-1} 1,4-Dioxane in the pond water, the concentration in the air would be $1.130 \times 10^{-4} \text{ mg L}^{-1}$ at 298 degrees Kelvin. Temperature can significantly impact the Henry's constant. However, the concentration in the air would still remain minimal at the average temperature of the ponds. The diffusion constant in air for 1,4-Dioxane is $0.229 \text{ cm}^2 \text{ sec}^{-1}$ according to EPA air emission modeling tables (U.S. EPA, 1994). Matrix effects can lower the solubility of compounds in water and subsequently increase their volatility. For 1,4-Dioxane matrix effects are not a plausible explanation to conclude volatilization was solely responsible for the observed losses from the ponds (Mohr, 2001).

6.8.2.3 Henry's Law Level of Contaminant Volatilization in Contrast to Fugacity Models

A number of research studies on the fugacity of 1,4-Dioxane contend minimal partitioning to air. A level 1 MacKay fugacity model (Full Public Report, 1998) indicated 1,4-Dioxane partitions to water and air at 91 and 9 percent, respectively. Under near equilibrium conditions with relatively pure solvent (water) and solute (1,4-Dioxane), mass transfer from water to air would be minimal. This would apply for fugacity models, which relate intrinsic chemical properties of the solute, temperature, and partial pressure

(Valsaraj, 1995), or gradient-flux models, which relate molecular diffusion and boundary layer transfer rate (Schwarzenbach *et al.*, 1993). This is in stark contrast to the German Chemical Society – Advisory Committee claim that the major portion of 1,4-Dioxane discharged to the environment goes directly into the atmosphere. The committee further stated that, based on the Henry's Law constant, 1,4-Dioxane discharged into surface water will transfer from water to air via volatilization (Full Public Report, 1998).

6.8.3 Temperature Dependency of Elimination Rate Constant

As shown in Figure 6.2, there was a significant reduction of contaminant mass from the pond water over time. This reduction is attributed primarily to mass transfer of the contaminant from water to air by the volatilization process with photodegradation being of much less importance.

6.8.3.1 Diffusion Coefficient Key to Volatilization Process

The volatilization process is driven by a concentration gradient which drives the transfer of the contaminant by molecular diffusion through the water-to-air boundary layer. The rate of transfer is dependent on the phase exchange coefficients that reflect various properties of the process such as temperature, flow velocity, depth, and turbulence (Schwarzenbach *et al.*, 1993). Diffusion is a thermally active process whose rate is defined by phase exchange coefficients, also known as diffusion coefficients. The

diffusion coefficient is a measure of the mobility of the diffusing species through a specific boundary. The diffusion coefficient (D) is related to temperature and activation energy by an Arrhenius type equation (Schwarzenbach *et al.*, 1993).

6.8.3.2 Pond Experimental Results Correlated to Volatilization Process

To determine if the observed 1,4-Dioxane loss rates from the ponds followed an Arrhenius relationship, plots were made of the natural log of the loss rate constants obtained from Pond 1 and Pond 2 1,4-Dioxane measurements (Table 6.4) to the reciprocal of the average pond temperature from each experiment in °K. No correlation was indicated for plots of Pond 1 and Pond 2 experimental runs 2-6 data sets in determining an Arrhenius relationship. Removing the experiment 6 data point, from both data sets, greatly strengthened the correlation ($r^2 = 0.70$) and ($r^2 = 0.927$) as shown in Figure 6.9 and 6.10, respectively.

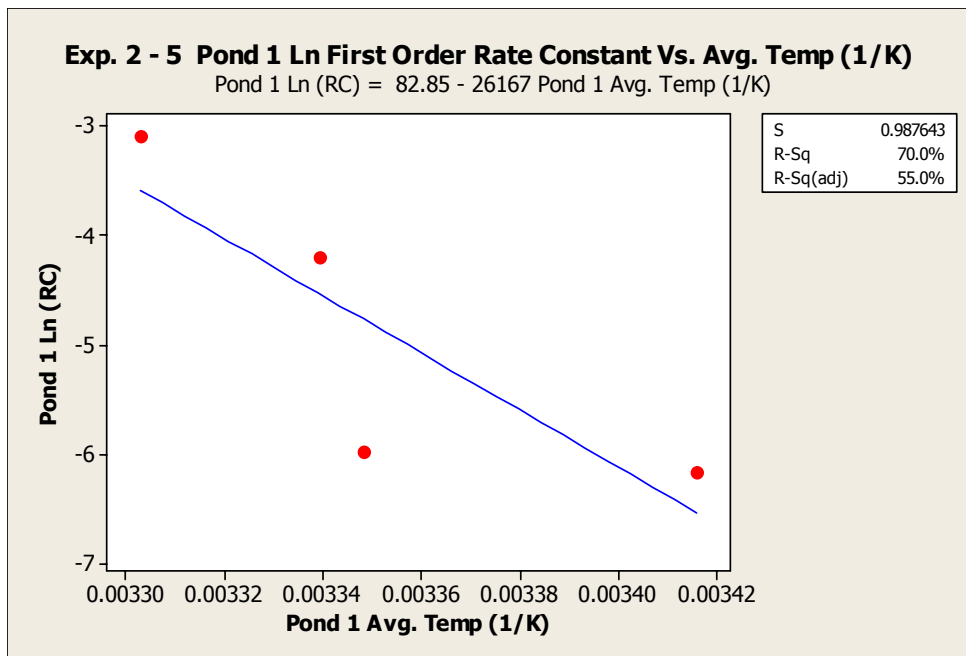


Figure 6.9. Correlation Test for Arrhenius Relationship on Experimental Run 2 - 6 Pond 1 1,4-Dioxane Reduction Rate and Avg. Pond Temperature (°K).

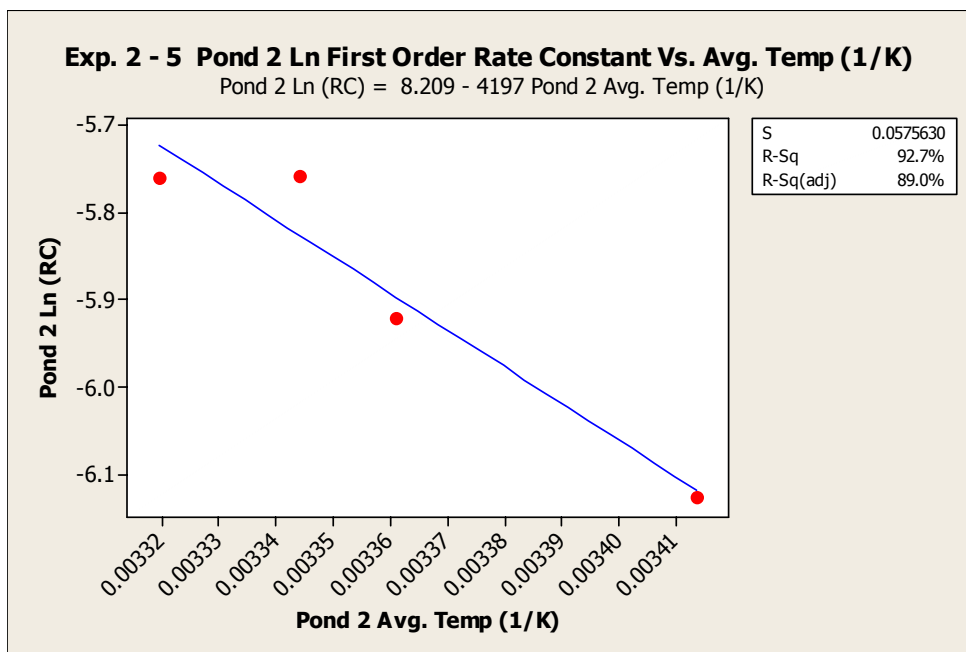


Figure 6.10. Correlation Test for Arrhenius Relationship on Experimental Run 2 - 6 Pond 2 1,4-Dioxane Reduction Rate and Average Pond Temperature (°K).

Data from experimental run 6 was excluded from the correlation analysis based on the input of rainfall that occurred during the experiment. Rainwater addition to ponds in experiment 6 resulted in lower 1,4-Dioxane concentrations. A lower pond contaminant concentration would result in a lower first order rate constant. The lower rate constant (concentration per unit time) would result in a lower flux of 1,4-Dioxane diffusing across the pond surface (concentration gradient) based on mass conservation where a change in concentration with respect to time is equal to a change in flux with respect to position (Schwarzenbach *et al.*, 1993). Excluding experiment 6 data from the correlation analysis in Figures 6.11 and 6.12 was based on the lower Pond 1 and 2 rate constants of 0.001546 and 0.001415, respectively (Table 6.4) resulting in poorly correlated natural log of the rate constants. The rate of diffusion of 1,4-Dioxane is proportional to the concentration gradient and is temperature dependent (Schwarzenbach *et al.*, 1993).

6.8.3.3 Experimental Reduction Results Infer Multiple Elimination Processes

Disregarding experimental run 6 Pond 1 and 2 data, a significant correlation was found between the 1,4-Dioxane reduction rates in the ponds and pond temperature, per the Arrhenius relationship. This finding indicates the elimination process was controlled by diffusion. The Arrhenius function correlation would be in agreement with diffusion related to the pure contaminant vapor pressure data of 3.9 kPa and 4.9 kPa at 20 °C and 25 °C, respectively (Full Public Report, 1998) and the effect of temperature on Henry's constants for most chemicals. The effect of temperature on the Henry's constants tracks

closely with changes in vapor pressure (Valsaraj, 1995). The aqueous activity coefficients of similar compounds increase with increase in temperature. For chloroform, the activity coefficient is 700 and 850 for 5 °C and 25 °C, respectively (Schwarzenbach *et al.*, 1993).

6.8.4 Experimental Side Studies

6.8.4.1 Significant Contaminant Reduction Without Sunlight Exposure

The field-based experimental side studies (utilizing open and covered containers) clearly established 1,4-Dioxane concentration reduction occurred without direct sunlight exposure (Table 6.7). While both side studies showed significant lag time for the covered solution, this result was likely due to water temperature differences between experiments. The greater lag time (9 days) in the first side experiment was experienced using the 68.6-cm deep tub whereas the 15.2-cm deep tub used in the second side experiment produced a much shorter lag time (3-5 days).

6.8.4.2 1,4-Dioxane Mass Flux Water to Air Transfer

The 1,4-Dioxane mass flux from Ponds 1 and 2 was consistent between Experiments 4 – 6 except for Experiment 5 Pond 1 with a 50 percent reduced rate. This reduced rate is attributed to Exp. 5 Pond 1 starting concentration (0.67 mg L^{-1}) being 50 percent lower

than experiments 4 and 6 Pond 1 and the significantly lower lapse time due to lower total water volume.

The higher mass flux from the side experiments is attributed to the higher starting concentration in the grey tub and kiddie pool of 10.0 and 5.0 mg L⁻¹, respectively versus 1.0 mg L⁻¹ or less for the experimental ponds.

6.8.4.3 Environmental Factors Influencing Contaminant Air Water Partition Coefficient

Bromide concentration, temperature, algae growth, and pH were key environmental differences between the side experiments and experimental ponds that would impact 1,4-Dioxane transfer from water to air.

Increased concentration of NaBr likely increased the volatilization flux rate. Due to lower Pond 1 volumes for experiments 4 and 5, the higher bromide concentration would create a salting-out of the 1,4-Dioxane that would account for the higher rate constants (Table 6.4). Salting out of 1,4-Dioxane using sodium sulfate is part of the USEPA CRL Method 624 dated March 25, 1997.

Water temperature of ponds would increase due to volume reduction when rainstorm events would require use of temporary storage white tank or Pond 3. A typical example of pond temperature increase was experiment 1 having similar air temperatures two days

before and after a volume transfer that reflected a 1-3 °C increase in Pond 1 & 2 temperature with the lower pond volumes.

Algae growth in the experimental ponds likely increased the water to air diffusion path length and potentially reduced the overall mass transfer. The total mass transport of a contaminant from the water source to air is a series of rate limiting diffusion boundaries. While the water diffusion thickness may increase due to algae, the rate limiting boundary most impacting contaminant removal rate may not necessarily be impacted by algae growth (Schwarzenbach *et al.*, 1993). Although the algae created extensive blooms in the ponds, it does not appear the algae had a direct impact on 1,4-Dioxane fate. Other research has shown little impact on ammonia volatilization in algae or duckweed (*Lemna gibba*) ponds (Zimmo *et al.*, 2003). Consequently, algae growth reducing experimental pond contaminant transport was not fully established.

Increase in pond pH due to algae growth was significant (7.7-10.0 pH) over the Pond 1 and 2 experimental lapse time. The increase in pH may have altered the pond chemistry where the available water to air interface area for 1,4-Dioxane was reduced. This reduction in unoccupied boundary area would account for reduced mass transfer rate from the ponds verses side experiment rates with containers that did not have algae.

6.8.4.4 UV / Solar Sun Side Experiments Demonstrate Contaminant Removal Potential

The laboratory UV/visible light side experiment results, as shown in Figure 6.6, demonstrated the potential for UV and solar light to photo oxidize 1,4-Dioxane. The faster reductions observed in the uncovered containers in the field side experiments support this finding.

The limited number of samples obtained from the laboratory side experiment precludes a statistical analysis and are presented as a starting point for further study.

6.9 Conclusions

At the beginning of the UV/solar light experiment, minimal volatilization of 1,4-Dioxane from the ponds was expected based on the very low Henry's Law constant for 1,4-Dioxane. Photo-oxidation of 1,4-Dioxane was expected to occur based on previous studies showing success using UV light in conjunction with advanced oxidation processes, ultrasonic transducers, or semiconductor materials (titanium dioxide). UV light alone has shown a slight potential for degradation of 1,4-Dioxane (Hill *et al.*, 1997); it was anticipated solar radiation would contribute to a reduction of contaminant level in the ponds.

Current research literature and the scientific foundation of water/air flux mass transport processes indicated a potential for greater partitioning of 1,4-Dioxane to air. This potential was enhanced with higher desert air temperatures and lower humidity. However, the Henry's constant for 1,4-Dioxane indicated the contaminant would volatilize by slow molecular diffusion through air. The gas-phase resistance would dominate the liquid phase resistance and would be the overall diffusion rate limiting step.

6.9.1 1,4-Dioxane Degradation Potential

Volatilization of the contaminant was found to be the primary removal mechanism given the vapor pressure, air-water partitioning of the contaminant, and phase transfer dynamics. Mass balance assessment showed 1,4-Dioxane removal after 120 hours lapse time was 64-85 percent.

6.9.2 Experimental Results Verify First Order Process

The contaminant reduction rate was found to be a first order process and rate constants were established from characteristic kinetic plots of each experimental run data set for Ponds 1 and 2.

6.9.3 Experimental Results Suggest Diffusion Temperature Dependency

Established volatilization principles show that diffusion is a thermally activated process whose rate is defined by a diffusion coefficient. The 1,4-Dioxane loss rates from the ponds did not show a high degree of correlation to the temperature dependent diffusion process (Arrhenius type function). As a result of this lack of correlation, it was difficult to assess if the total mass removed from the pond was solely related to the mass exported by gas exchange.

6.9.4 Various Operational Conditions Impact Diffusion Processes

The lack of correlation strength may be related to the varying physical parameters of the time period of experimentation. These variations included diurnal temperature changes, unintended pond volume increases due to rainfall, the dynamic algae and pH conditions. Further, due to rainstorms during the experimental runs and the limited storage capacity of the ponds, it was sometimes necessary to transfer 1,800 L of pond water pumped to a holding tank during which time contaminant volatilization did not occur over the holding period of 2 or 3 days. The transfer would also lower the depth of water remaining in the ponds by approximately 6 cm. These volume changes accounted for additional fluctuations in pond temperature that impacted pond elimination rate.

6.9.5 Diffusion Plus Other Contaminant Elimination Processes

Additional elimination processes such as photo oxidation (UV and solar) degradation may account for the lack of correlation to a single diffusion process.

6.9.5.1 UV / Solar Grey Tub and Pool Experimental Site Side Experiments

Side experiments were performed to isolate UV/Solar degradation from other mechanisms. These experiments indicated a higher elimination rate constant in un-covered versus covered containers. This higher elimination may be related solely to temperature increase but could also have a solar degradation component as was shown in the laboratory UV-B and visible light side experiments. The grey tub and pool side experiment elimination rates were similar to what was determined for the ponds.

Removal rate was not impacted by influent source water quality (tap water or secondary effluent).

6.9.5.2 UV / Solar Light Laboratory Side Experiments

The possibility exists that some level of photo degradation occurred in the ponds during the experimental runs. This was observed in the kiddie pool side experiment where the elimination rate in the un-covered container rate was 15 percent higher (Table 6.7). The increased rate ($1.45 \text{ mg/m}^2\text{-hr}$) would be the result of temperature increase and solar

elimination. The single data point, for the UV-B degradation side experiment, highlights the potential that 17 percent elimination from UV-B light is possible. This potential reduction warrants further research.

6.9.6 Open Pond Treatment for Full-Scale Wetland Operation

Given the limited number of samples taken per pond, it was difficult to adequately characterize a highly dynamic process under dynamic operating conditions as was experienced during the pond experimental runs. The experimental results from the pilot-scale pond treatment indicate open pond staging prior to treatment would result in reduced concentration of 1,4-Dioxane.

6.9.6.1 Constraints of Contaminant Remediation Using Open Ponds

The use of open ponds for 1,4-Dioxane remediation has several limitations. The open ponds can become a breeding ground for various insects that are direct or indirect vectors of viruses such as the West Nile. Open ponds attract other wildlife, such as birds, which introduce various pathogens. Open ponds require additional maintenance to ensure algae blooms and water chemistry are within operational constraints and open water quality standards.

6.10 Future Research

Two areas of further research were identified from the pond experimental results.

Determination of the UV and solar light degradation of 1,4-Dioxane from open ponds is the first identified area needing further research. The side experimental results indicate UV and/or solar light were contributing factors in the 1,4-Dioxane reduction from the ponds. These initial results could be validated with further research.

Additional research is needed to quantify the impact of algae on the 1,4-Dioxane elimination rates from open ponds. This research would include water-air boundary exchange impacts for variations in boundary thickness and pond water pH.

7.0 SUMMARY

This chapter summarizes the results and conclusions of this research. This research focused on the emerging contaminant 1,4-Dioxane, which is considered a probable human carcinogen. Its continued use in consumer products and its worldwide presence as a contaminant in groundwater and surface water pose potential health and environmental risks, particularly in light of new research showing genotoxic effects on mice from chromosomal breakage. The lack of existing cost effective remediation methods, and recent laboratory studies showing the potential of phytoremediation, provided the impetus to perform a field-based study of phytoremediation for 1,4-Dioxane contaminated site clean-up and evaluate open pond treatment via UV photo oxidation/evaporation to treat 1,4-Dioxane contaminated water. These treatment techniques, validated in this field research, are applicable to remediation of 1,4-Dioxane contaminated sites as well as contaminated water sources.

The phytoremediation research consisted of three experiments using tapwater and three experiments using secondary effluent. In each experiment, wetland influent was spiked with 1,4-Dioxane and then fed to the planted and unplanted wetland tanks. The efficacy of phytoremediation was determined by performing mass balance analyses on 1,4-Dioxane.

Prior to conducting the six wetland experimental runs, the tank hydraulics and operating parameters were characterized. The operating parameters of flow rate and duration coupled with environmental conditions of temperature, solar radiation, and subsurface preferential flow, resulted in negative impacts to wetland plant growth and contaminant availability.

In the open pond storage experiments, discharge from the planted and unplanted wetland tanks was stored in open ponds where UV/solar light exposure and evaporation would occur. Contaminant loss rates were determined by sampling the ponds over time.

Chapter 4 provides the experimental operating parameters and the array of results from varying environmental conditions. The quantitative evaluation of the pre-experimental-run bromide tracer study demonstrated the planted and control tank flow was controlled by advection-dispersion. In comparing the experimental wetland tree growth and transpiration rates to other published cottonwood wetland studies, the impacts of lower soil moisture, sunlight/shading, and longitudinal dispersion reduced the transpiration potential of the experimental planted tank. Conclusions from the hydraulic characterization research, for the established environmental and operating conditions, highlighted the value of tracer studies, the competitive nature of plants to capitalize growth with seemingly trivial environmental advantages, and the need for pilot-scale studies prior to implementing full-scale wetland systems. The hypothesized benefit of pilot-scale studies was validated by the wetland results.

Chapter 5 addressed the efficiency of 1,4-Dioxane uptake by comparison of planted and control tank discharge volumes, contaminant concentrations, and water quality parameters of the experimental runs. Discharge sample measurements for turbidity (showing total suspended solids), pH (impact on microbial and plant growth), and conductivity (showing total dissolved solids) established basic water quality parameters. Each experimental run included a bromide tracer to compare against the baseline pre-experimental results and consistency between the planted and control tanks.

To establish the uptake efficiency by the cottonwood trees, a mass balance methodology was utilized. Measurements of 1,4-Dioxane inflow and discharge concentration were multiplied by the volume of influent or discharge, respectively. The difference between the mass input and the mass output in the planted tank gave the remaining mass that was attributed to tree uptake and transpiration.

The mass balance analysis from the phytoremediation research study showed 1,4-Dioxane was taken up by the trees. Correlation and comparison analysis was conducted to determine the mechanism and efficiency of the contaminant uptake. There was a positive correlation between contaminant uptake rate and local reference evapotranspiration rate (AZ MET ETo rate). Contaminant uptake rate was related to the single mechanism of plant transpiration rate, given that the control tank showed minimal

1,4-Dioxane loss. Temperature, a key factor in the ETo rate, was also positively correlated with 1,4-Dioxane uptake rate.

The efficiency of the 1,4-Dioxane uptake in the planted tank was established by determining a transpiration stream concentration factor (TSCF) for each experiment. The TSCF is a measurement of the fractional efficiency of 1,4-Dioxane uptake relative to water uptake. The TSCF in experiment 3, utilizing tap water, was 0.59. The TSCFs in the three experiments utilizing secondary effluent were 0.36, 0.29, and 0.34. A previous laboratory study showed a higher TSCF (0.72) for pure water with nutrient solution. The lower TSCFs observed in this research are attributed to the tank advection-dispersion flow, preferential pathways in planted tank soil, and impact of water quality.

The phytoremediation research showed the pilot-scale wetland system was successful to remediate 1,4-Dioxane contaminated tap-water and secondary effluent. This research is applicable for remediation of 1,4-Dioxane contaminated sites where recovery of water is not a concern. However, contaminant concentration may increase after wetland treatment in a closed system where the effective TSCF factor is less than 1.0.

Chapter 6 summarized the research results of evaporation and solar (UV) degradation experiments of 1,4-Dioxane in open ponds. The very low Henry's Law constant for 1,4-Dioxane suggested there would be minimal volatilization of 1,4-Dioxane from aqueous solution. On the other hand, photo-oxidation of 1,4-Dioxane has been shown using UV

light in conjunction with advanced oxidation processes, ultrasonic transducers, or semiconductor materials (titanium dioxide).

The research hypothesis focused on solar (UV) degradation, but anticipated moderate volatilization based on current research literature. The scientific foundation of water/air flux mass transport processes indicated a potential for greater partitioning of 1,4-Dioxane to air, particularly with higher desert air temperatures and lower humidity.

A mass balance method was again utilized to establish the 1,4-Dioxane loss from the ponds. Experimental runs showed a nominal six percent reduction per day in 1,4-Dioxane mass in the ponds occurred prior to an evaporative reduction in pond water volume. A positive correlation between 1,4-Dioxane removal rate and concentration was established. The kinetics of pond contaminant removal were determined to be a first order process.

First order rate constants were determined and utilized to derive the theoretical half-life of the contaminant in each pond experiment. The pond contaminant loss kinetics were shown to be temperature dependent.

Several side-experiments at the field site and in the laboratory were conducted to determine if exposure to UV/visible light contributed to the measured contaminant removal or if the removal was strictly by volatilization. The experimental site side-

experiments showed slightly greater removal of 1,4-Dioxane occurred in the presence of sunlight. A laboratory side experiment was performed to test whether visible or UV light were effective in oxidizing 1,4-Dioxane. The laboratory side-experiment indicated that exposure to UV or visible light promoted some degradation of 1,4-Dioxane.

The results from the open pond research demonstrated that 1,4-Dioxane elimination was predominately by volatilization with a potential UV and solar component. The objective of the experimental study was validated by showing treatment of 1,4-Dioxane contaminated water was possible in open ponds. The research also established open pond treatment of 1,4-Dioxane contaminated water would result in significantly lower concentration of contaminant prior to a significant water loss from evaporation.

7.1 Future Study Recommendations

7.1.1 General

The research identified topics related to the health impacts, chemical isolation, and remediation of 1,4-Dioxane needing further study.

Current toxicology studies establishing toxicity and health concerns of 1,4-Dioxane could be augmented with newer analytical methods showing gene sequence and protein expression change after contaminant exposure. Improved toxicity knowledge would increase regulation of 1,4-Dioxane.

1,4-Dioxane contaminated water wetland treatment could include soil augmented bioremediation. Bioremediation research is needed for 1,4-Dioxane degraders such as toluene monooxygenase expressing bacteria.

7.1.2 Specific

Liquid-liquid extraction methods for 1,4-Dioxane contaminated water samples have extraction solvent quantity, health, and safety concerns. Solid phase extraction research could offer an effective minimal solvent extraction technique.

The experimental wetlands instrumentation and operating parameters were adequate to meet planned objectives. In retrospect, improved discharge measurement and improved influent mixing/volume control would have provided better time/discharge-based correlations and reduced variation.

Measurement of cottonwood tree water uptake volume would further validate experimental results. Sap flow velocity in the conducting xylem of each cottonwood tree could be measured using heat dissipation methods.

The handling, treating, and disposing of wetland effluent, after wetland treatment, contains trace levels of contaminant. With biological compounds, a polishing step is

incorporated into the treatment process that removes remaining harmful microorganisms prior to the effluent being discharged. This polishing step would likely not degrade the remaining 1,4-Dioxane and research is needed to identify and qualify a process which will remediate 1,4-Dioxane contaminated waters to below regulatory action limits.

Research to further identify the degradation pathways of 1,4-Dioxane transpired to the atmosphere is needed. This research would look at both the secondary chemical compounds created as well as the overall reaction mechanisms.

The side experimental results indicate UV and/or solar light were contributing factors in the 1,4-Dioxane reduction from the ponds. These initial results could be validated with further research.

The impact of algae on 1,4-Dioxane elimination rates from open ponds needs further research. This research would include water-air boundary exchange impacts for variations in boundary thickness and pond water pH.

APPENDIX A. SCHEDULE AND RECORDED MEASUREMENTS
EXPERIMENTAL RUNS 1-6

Table A.1. Schedule and Recorded Measurements – Experimental Run # 1.

Lapse Time (Hrs)	Sample Designator	pH	Cond $\mu\text{S cm}^{-1}$	Turbidity NTU	Bromide mV	GC Area 1,4-Dioxane	GC Area Surrogate
			20.2C				
			0.02		185.5		
		4pH	1341	Stds	52.3 80 mg L^{-1}		
					56.2 80 mg L^{-1}		
0	Baseline	7.28	596	0.35	64.9		
24	A	7.11	970	0.55	133.2	NA	
	B	7.09	550	0.5	154.1	NA	
35							
	C	6.81	1,018	17	132.5	NA	
	D	7.03	536	0.62	148.7	NA	
71							
72	E	7.01	879	8.5	102.8	NA	
	F	7.03	534	0.6	100.1	NA	
83	1	6.67	633	5.8	82.2	13,625	162,689
	2	6.57	623	2	81.2	15,088	168,852
	3	6.67	611	1.95	68	19,588	195,923
	4	6.97	604	2	77.7	15,281	199,500
	5	6.64	792	7.5	90.1	7,393	128,746
	6	6.8	544	0.56	88.3	11,607	162,367
	7	6.46	712	4.2	76.8	15,356	192,317
	8	6.88	626	12	77.1	15,521	190,129
105	9	6.9	821	4.9	91.5	7,519	126,030
	10	7.13	543	1.5	90.3	10,843	141,831
191	11	8.64	970	2	86.9	498	149,446
	12	9.11	706	1.5	88.1	479	125,673

Table A.2. Schedule and Recorded Measurements – Experimental Run # 2.

Lapse Time (Hrs)	Sample Designator	pH	Cond $\mu\text{S cm}^{-1}$	Turbidity NTU	Bromide mV	GC Area 1,4-Dioxane	GC Area Surrogate
	Calibration Standard	7	1422		72		
0							
0							
	Base F	7.98	1,067	0.31	31.1		
	Base 1	6.94	1,243	0.35	129.5		
	Base 2	7.55	506	0.55	158.6		
24							
	A	6.74	1,156	0.5	138		
	B	6.97	477	0.42	161.8		
35							
35							
	C	6.72	1,082	1	141.7		
	D	7.24	503	0.39	153.4		
71							
71							
	E	7.26	1,835	0.51	96.2		
	F	7.61	674	0.62	85.7		
	G	7.79	952	0.55	98.8		
	H	7.7	659	0.35	87.6		
83							
	1	6.99	746	12	77.7	19,255	302
	2	7.15	761	4.75	78.1	23,427	320
	3	7.29	701	0.9	72.4	21,968	738
	4	7.25	680	1.75	73.4	14,916	557
	5	7.72	2,250	21	90.4	13,069	1192
	6	7.57	680	0.65	82.2	20,667	1272
	7	7.23	996	8.5	75	20,960	1182
	8	7.6	696	0.56	78.3	18,245	938
107							
107							
	I	7.34	1,000	0.37	112.6		
	J	7.72	592	0.54	104		

Lapse Time (Hrs)	Sample Designator	pH	Cond $\mu\text{S cm}^{-1}$	Turbidity NTU	Bromide mV	GC Area 1,4-Dioxane	GC Area Surrogate
	9	7.78	1,436	20	96.1	11,920	1,240
	10	7.72	666	0.12	83.9	22,966	1,372
143							
	K	7.8	1,119	0.66	95.3		
	L	7.97	646	0.53	92.7		
179							
	M	7.31	881	0.58	109.2		
	N	7.92	618	0.97	116		
	M1	7.3	865	1.89	118.5		
	N1	7.67	617	0.72	128.3		
191							
	11	8.47	1,352	4.6	94.1	3,756	1,085
	12	9.07	733	1.35	91.2	5,807	1,542
215							
	O	7.32	832	0.49	122.6		
	P	8.63	634	0.8	127.7		
	O1	7.35	815	0.92	128.4		
	P1	7.89	672	0.46	135.8		
250							
	Q	7.53	818	0.53	127.2		
	R	8.09	662	1	136.5		
	S	7.75	809	1.5	128.7		
	T	7.7	657	0.84	141.7		
264							
	13*			1.2			
	14*			0.67			
265							
	13	8.69	1,238	0.62	97.1	852	952
	14	9.16	734	0.8	94.9	1,644	1,258
384							
	15	8.94	1,390	0.87	94.2	763	1,965
	16	8.93	866	2.5	94.5	865	857
504							
	17	7.3	1,599	5.1	88.6	185	x
	18	8.65	956	7.2	81.7	435	x
624							
	19	7.41	2,05	3.7	81.5	65	x
	20	7.8	1068	6.8	83.7	159	x

Table A.3. Schedule and Recorded Measurements – Experimental Run # 3.

Lapse Time (Hrs)	Sample Designator	pH	Cond $\mu\text{S cm}^{-1}$	Turbidity NTU	Bromide mV	GC Area 1,4-Dioxane	GC Area Surrogate
		7- Apr	1,405		67.9		
			2.3		182.3		
0							
0							
0							
	Base F	7.27	1,038	0.5	34.4		
	Base 1	x	x	x	x		
	Base 2	7.3	623	3	145.5		
	1	7.21	654	0.65	87.6	12,625	x
	2	7.3	654	0.6	85.4	20,494	x
24							
	A	7.13	980	2	131.1		
	B	7.5	614	0.4	151.4		
35							
35							
	C	7.11	925	3.2	137.4		
	D	7.61	620	1	129.8		
	25	7.67	642	0.5	87.1	16,949	x
	26	7.71	649	0.5	82.3	17,457	x
71							
71							
	E	7.36	912	0.5	111.6		
	F	7.67	665	x	105.5		
	3	7.07	890	25	100.4	9,304	x
	4	7.24	629	1	96.8	10,796	x
	23	7.53	653	0.2	83.3	17,392	x
	24	7.53	673	0.5	81.8	19,952	x
83							
	G	7.25	952	2.4	99.2		
	H	7.7	642	0.5	96.4		

Lapse Time (Hrs)	Sample Designator	pH	Cond $\mu\text{S cm}^{-1}$	Turbidity NTU	Bromide mV	GC Area 1,4-Dioxane	GC Area Surrogate
	5	7.15	1,265	16	94.6	9,951	x
	6	7.46	641	1	94.3	10,320	x
107							
107							
	I	7.23	1,255	1.9	96.5		
	J	7.63	642	0.4	94.4		
	7	7.21	1,361	2	102.5	7,511	x
	8	7.51	630	0.9	101.1	11,211	x
143							
143							
	K	7.7	1,038	2	101.4		
	L	8.12	638	0.5	102.1		
	9	7.43	887	2	108.2	5,542	x
	10	7.6	617	1.1	117.5	5,445	x
179							
179							
	M	7.34	985	2	104.9		
	N	7.93	620	0.6	117.9		
	11	7.53	923	4.5	115.6	4,600	x
	12	7.56	864	13	124.8	2,211	x
191							
	13	7.61	1,070	14	104.5	2,947	x
	14	7.53	681	0.5	104.4	3,457	x
215							
	O	7.64	972	2.4	108.3		
	P	8.29	614	0.6	126.4		
	Q	7.38	822	1	124.8		
	R	7.72	610	0.8	132		
250							
	S	7.51	769	2.6	132		
	T	8.27	615	0.9	132.6		
	U	7.37	740	0.95	137.8		
	V	7.74	618	0.5	137.4		
286							
	15	7.87	966	1	109.6	1,809	x
	16	7.79	694	0.45	107.1	2,288	x
384							

Lapse Time (Hrs)	Sample Designator	pH	Cond $\mu\text{S cm}^{-1}$	Turbidity NTU	Bromide mV	GC Area 1,4-Dioxane	GC Area Surrogate
	17	7.61	963	2	107.6	1,093	x
	18	x	761	6.5	105.1	1,080	x
504							
	19	7.31	1,034	1.8	104.1	364	x
	20	7.77	812	0.6	102.4	678	x
624							
	21	7.95	1,113	1.4	101.5	385	x
	22	7.46	887	1	100	464	x

Table A.4. Recorded 1,4-Dioxane GC Measurements – Experimental Run # 3.

Sample #	Run 1	Time	Run 2	Time	Run 3	Time	Avg. Area
1	12,554	0.518	12,219	0.517	13,103	0.517	12,625
2	19,925	0.517	20,409	0.517	21,147	0.52	20,494
3	8,831	0.518	9,637	0.516	9,443	0.522	9,304
4	11,487	0.507	10,734	0.513	10,167	0.519	10,796
5	9,886	0.513	9,551	0.515	10,416	0.519	9,951
6	10,750	0.511	9,458	0.518	10,752	0.517	10,320
7			7,342	0.517	7,679	0.52	7,511
8	11,382	0.519	10,935	0.517	11,316	0.516	11,211
9	5,593	0.518	5,230	0.516	5,803	0.519	5,542
10	5,243	0.517	5,755	0.516	5,337	0.512	5,445
11	4,526	0.514	4,674	0.514			4,600
12	2,215	0.514	2,101	0.519	2,318	0.518	2,211
13	2,962	0.513	2,834	0.515	3,045	0.518	2,947
14	3,214	0.516	3,487	0.515	3,670	0.515	3,457
15	1,876	0.52	1,710	0.518	1,840	0.517	1,809
16	2,255	0.516	2,237	0.517	2,372	0.521	2,288
17	1,049	0.515	1,132	0.518	1,098	0.519	1,093
18	1,137	0.513	1,033	0.517	1,071	0.517	1,080
19	352	0.518	344	0.517	395	0.521	364
20	687	0.52	683	0.521	665	0.521	678
21	402	0.521	402	0.518	352	0.521	385
22	439	0.523	490	0.522	462	0.52	464
23	16,425	0.516	17,548	0.515	18,204	0.519	17,392
24	19,472	0.519	19,267	0.514	21,117	0.517	19,952
25	17,165	0.52	17,471	0.516	16,210	0.519	16,949
26	16,786	0.517	17,931	0.517	17,654	0.516	17,457

Table A.5. Schedule and Recorded Measurements – Experimental Run # 4.

Lapse Time (Hrs)	Sample Designator	pH	Cond $\mu\text{S cm}^{-1}$	Turbidity NTU	Bromide mV	GC Area 1,4-Dioxane
		7	1,421	x	66.9	x
		x	X	x	173.2	x
0						
0						
0						
	Base F	7.24	1,062	2.9	128	
	Base 1	7.07	1,386	0.50	122.6	
	Base 2	7.32	975	x	137.3	
	1	7.17	1,145	5.5	72.2	51,536
	2	6.98	1,147	3.5	71.1	45,962
12						
	W	6.89	1,404	10.5	127.9	
	X	7.2	972	0.5	138.1	
24						
	A	6.89	1,359	x	129.9	
	B	7.16	977	1.0	137.7	
35						
35						
	C	6.91	1,235	16.0	133	
	D	7.16	976	1.5	138.5	
	25	7.66	1,150	3.3	65.5	41,949
	26	7.67	1,139	3.6	64.4	43,074
47						
	Y	7.07	1,281	1.9	119.5	
	Z	7.19	1,039	0.5	103.3	
59						
59						
	AA	6.97	1,273	4.3	94.2	
	BB	7.31	1,059	0.5	87.4	
	23	7.44	1,156	3.5	64.1	42,176

Lapse Time (Hrs)	Sample Designator	pH	Cond $\mu\text{S cm}^{-1}$	Turbidity NTU	Bromide mV	GC Area 1,4-Dioxane
	24	7.3	1,146	3.0	64.1	45,873
71						
71						
71						
	E	7.17	1,274	x	104.6	
	F	7.27	1,074	2.0	96.7	
	3	6.68	1,222	1.6	88.7	22,431
	4	7.34	1,023	x	88.1	21,378
83						
	G	6.93	1,245	5.0	79.9	
	H	7.35	1,059	0.7	79.8	
107						
107						
	5	7.14	1,232	8.5	82.6	32,263
	6	7.21	1,071	1.5	84.9	28,838
	7	6.9	1,210	8.8	77.9	35,877
	8	7.05	1,037	2.0	82.6	35,547
143						
143						
	29	7	1,251	high	71.5	28,591
	30	7.45	1,052	1.0	79.2	19,092
	9	6.96	1,159	4.5	83.7	34,004
	10	6.94	1,038	2.0	95.4	18,410
167						
	I	7.3	1,155	1.0	89.9	
	J	7.31	1,051	1.0	99.8	
179						
179						
	27	7.49	1,175	10.0	80.4	22,359
	28	7.58	1,040	1.0	91.9	13,977
	11	6.72	1,144	29.0	99.3	15,692
	12	7.08	1,012	1.0	109	9,202

Lapse Time (Hrs)	Sample Designator	pH	Cond $\mu\text{S cm}^{-1}$	Turbidity NTU	Bromide mV	GC Area 1,4-Dioxane
191						
	13	7.92	1,750	15.0	74.4	8,764
	14	7.72	1,311	9.0	83.6	7,794
191						
	K	7.34	1,147	1.5	99.9	
	L	7.32	1,057	1.0	106.8	
203						
	M	6.98	1,160	3.3	102.8	
	N	7.25	1,056	0.7	109.1	
215						
	CC	7.33	1,173	1.1	94.8	
	DD	8.08	1,041	1.1	103.4	
215						
	Q	7.24	1,145	0.9	107.1	
	R	7.35	1,056	0.5	111.7	
227						
	O	6.95	1,153	3.2	108.8	
	P	7.28	1,054	0.9	112.3	
251						
251						
	S	7.22	1,164	2.0	109.1	
	T	7.76	1,054	0.7	111.3	
	U	7.07	1,144	3.0	115.6	
	V	7.36	1,053	1.0	114.9	
263						
	15	8.52	1,820	8.0	75.1	2,267
	16	8.89	1,247	5.0	85.8	3,835
287						
	EE					
	FF					

Lapse Time (Hrs)	Sample Designator	pH	Cond $\mu\text{S cm}^{-1}$	Turbidity NTU	Bromide mV	GC Area 1,4-Dioxane
311						
	GG					
	HH					
335						
	II					
	JJ					
359						
	KK					
	LL					
383						
	17	8.88	3,060	10.0	59.5	769
	18	7.85	1,881	37.0	75.6	1,824
407						
	MM	9.13	3,860		49.7	
	NN	9.59	1,650		67.4	
431						
	OO	9.13	4,770		41.5	
	PP	9.31	1,787		67.7	
455						
	QQ	9.32	6,630		30.9	
	RR	9.23	1,971		61.1	
479						
	SS	7.77	1,1230		15.5	
	TT	9.97	2,550		51.8	
479						
	19	9.32	9,580	30.0	21.5	672
	20	9.14	2,150	26.0	62.7	145
527						
	UU					
	VV	9.63	2,990		49.4	

Lapse Time (Hrs)	Sample Designator	pH	Cond $\mu\text{S cm}^{-1}$	Turbidity NTU	Bromide mV	GC Area 1,4-Dioxane
551						
	WW					
	XX					
		9.41	1,694		59.7	
575						
	YY					
	ZZ	8.99	4,510		38.1	
599						
	AAA					
	BBB	8.76	5,980		30.7	
623						
	21	x	X	DRY	x	DRY
	22	8.62	6,960	53.0	27.3	10
Pool Study Pool 1 - Covered & Pool 2 - Uncovered						
263						
	31	7.57	1,089	x	130	32,470
	32	7.52	1,127	x	x	73,029
383						
	33	7.49	1,207	x	x	24,467
	34	9.51	1,230	x	x	8,906
503						
	35	7.91	1,344	x	x	7,155
	36	9.44	2,480	x	x	792
623						
	37	8.03	2,000	x	x	2,248
	38	x	X	x	x	DRY

Table A.6. Recorded 1,4-Dioxane GC Measurements – Experimental Run # 4.

Sample #	Run 1	Time	Run 2	Time	Run 3	Time	Avg. Area
1	53,452	2.172	47,375	2.166	53,782	2.183	51,536
2	42,374	2.167	46,474	2.181	49,038	2.175	45,962
3	21,018	2.182	25,005	2.172	21,271	2.183	22,431
4	22,560	2.169	19,897	2.17	21,677	2.174	21,378
5	32,227	2.176	32,234	2.176	32,327	2.185	32,263
6	29,176	2.174	29,341	2.167	27,996	2.159	28,838
7	35,846	2.163	37,986	2.183	33,799	2.173	35,877
8	36,032	2.168	35,074	2.167	35,534	2.161	35,547
9	31,001	2.181	35,936	2.18	35,074	2.17	34,004
10	18,144	2.165	17,723	2.186	19,363	2.169	18,410
11	15,788	2.182	15,468	2.179	15,820	2.17	15,692
12	9,470	2.18	8,717	2.181	9,420	2.182	9,202
13	8,441	2.139	8,712	2.182	9,140	2.173	8,764
14	7,990	2.163	7,674	2.109	7,719	2.164	7,794
15	2,364	2.136	2,149	2.156	2,289	2.16	2,267
16	3,359	2.159	3,762	2.132	4,383	2.169	3,835
17	754	2.151	816	2.174	737	2.157	769
18	1,814	2.162	1,809	2.162	1,848	2.142	1,824
19	927	2.13	597	2.147	492	2.119	672
20	131	2.168			159	2.181	145
21							
22	14	2.158	5	2.162			10
23	44,962	2.187	40,933	2.148	40,632	2.155	42,176
24	41,176	2.171	49,536	2.167	46,908	2.162	45,873
25	42,796	2.153	39,472	2.172	43,578	2.15	41,949
26	41,976	2.169	45,389	2.181	41,856	2.177	43,074
27	20,772	2.17	21,928	2.155	24,376	2.156	22,359
28	14,428	2.176	14,581	2.161	12,921	2.166	13,977
29	25,628	2.157	29,813	2.168	30,332	2.174	28,591
30	18,806	2.149	19,437	2.166	19,033	2.15	19,092
31	32,283	2.166	30,339	2.172	34,788	2.187	32,470
32	73,802	2.147	79,549	2.177	65,736	2.169	73,029
33	24,384	2.172	24,223	2.16	24,793	2.181	24,467
34	8,757	2.167	9,211	2.175	8,750	2.173	8,906
35	6,988	2.176	7,561	2.17	6,916	2.185	7,155
36	728	2.171			855	2.176	792
37	2,717	2.162	1,982	2.174	2,045	2.164	2,248

Table A.7. Schedule and Recorded Measurements – Experimental Run # 5.

Lapse Time (Hrs)	Sample Designator	DOC mg L ⁻¹	pH	Cond μ S cm ⁻¹	Turbidity NTU	Bromide mV	1,4-Dioxane mg L ⁻¹
			7.10	1,419		83.3	x
				1.3		192.5	x
0							
0							
0							
	Base F		7.55	1,053	1.6	162	
	Base 1		7.34	1,385	2.6	158.9	
	Base 2		7.3	992	0.46	164.3	
	1	13.49	7.2	1,132	1.5	94.2	4.350
	2	15.15	7.35	1,127	1.6	93.4	5.950
12							
	W		7.25	1,342	2.9	156.9	
	X		7.42	1,005	0.42	169.7	
24							
	A		7.33	1,303	14	162.1	
	B		7.48	1,023	0.45	163.2	
35							
35							
	C		7.32	1,316	2.5	157.9	
	D		7.32	1,025	3	162.7	
	25	16.56	7.5	1,134	1.3	91.8	6.760
	26	15.39	7.89	1,120	1.4	90.6	5.500
47							
	Y		7.42	1,259	18	159.3	
	Z		7.5	1,038	0.47	169.5	
59							
59							
	AA		7.32	1,305	0.66	119.4	
	BB		7.33	1,112	0.4	140.3	
	23		7.56	1,105	1.1	90.5	x
	24	15.94	7.44	1,113	1.4	90	5.080

Lapse Time (Hrs)	Sample Designator	DOC mg L ⁻¹	pH	Cond μ S cm ⁻¹	Turbidity NTU	Bromide mV	1,4-Dioxane mg L ⁻¹
71							
71							
71							
	E		7.59	1,285	3.3	135.1	
	F		7.46	1,152	0.52	140.6	
	3	11.89	7.43	1,363	2.2	99.9	4.240
	4	10.71	7.47	1,146	0.54	115.3	2.170
83							
	G		7.22	1,338	3	101.1	
	H		7.37	1,142	0.7	118.4	
107							
107							
	5	12.09	7.59	1,341	3	103.1	3.310
	6	20.36	7.48	1,172	0.75	117.8	1.250
	7	15.61	7.37	1,272	0.65	99.1	5.210
	8	28.52	6.82	1,076	0.6	108.7	2.680
143							
143							
	29	14.95	8.1	1,345	3	91.6	2.160
	30	9.99	8.22	1,094	1.9	102.3	1.680
	9	8.46	7.13	1,482	1.2	100.6	3.730
	10	14.01	7.52	1,073	1	106.8	3.100
167							
	I		7.26	1,328	0.65	106.1	
	J		7.3	1,073	0.49	110.8	
179							
179							
	27	12.97	7.89	1,407	3.7	99.7	1.320
	28	25.93	7.78	1,116	1.3	101.8	3.010
	11	11.8	7.8	1,283	0.56	116.2	1.990
	12	9.67	6.97	1,094	0.45	113	3.270
191							
	13	36.8	9.37	2,270	2.1	85.4	0.671

Lapse Time (Hrs)	Sample Designator	DOC mg L ⁻¹	pH	Cond μ S cm ⁻¹	Turbidity NTU	Bromide mV	1,4-Dioxane mg L ⁻¹
	14	26.91	9.52	1,202	3.5	101.2	1.115
191							
	K		7.48	1,326	5.9	113	
	L		7.19	1,139	0.5	113.5	
203							
	M		7.16	1,274	0.56	122.4	
	N		7.31	1,118	0.55	126.1	
215							
	31	13.34	8.08	1,331	3.2	111.4	1.390
	32		8.28	1,096	4	115.4	x
215							
	Q		7.29	1,426	0.6	124.9	
	R		7.4	1,099	0.5	132.8	
227							
	O		7.36	1,077	0.5	139.3	
	P		7.25	1,285	0.65	139	
251							
251							
251							
	CC		9.69	3,830	1.1	69.5	
	DD		10	1,284	2.9	105.7	
	S		7.73	1,359	3.5	134.2	
	T		7.85	1,074	3	136.9	
	U		7.45	1,272	0.69	141.6	
	V		7.48	1,059	0.48	144	
263							
	15	57.68	9.92	3,140	2.8	77.5	0.474
	16		10.04	1,269	3.6	109.7	0.665
275							
	33	28.92	7.67	1,318	0.46	130.3	0.572
	34	10.8	7.51	1,040	0.45	140.3	0.677

Lapse Time (Hrs)	Sample Designator	DOC mg L ⁻¹	pH	Cond μ S cm ⁻¹	Turbidity NTU	Bromide mV	1,4-Dioxane mg L ⁻¹
287							
	EE		9.63	4,280	1.4	66.7	
	FF		10.08	1,291	4.6	103.9	
311							
	GG		10.16	6.02	5.2	56.2	
	HH		11.08	1,419	4.5	94.3	
335							
	17	68.83	9.9	9,920	3	41.1	ND
	18	45.44	10.15	1,456	8	97.6	0.661
359							
	II		10.1	17,320	3.5	24.3	
	JJ		10.99	15.9	2.1	96.2	
383							
	KK		9.65	3,900	23	-8	x
	LL		10.95	1,695	5	87.9	x
407							
	MM		x	X	x	x	
	NN		10.85	1,723	2	94.5	
431							
	OO		x	X	x	x	
	PP		10.77	1,763	1.6	93.8	
455							
	QQ		x	X	x	x	
	RR		10.82	1,939	2.5	112.9	
479							
	SS		x	X	x	x	
	TT		10.79	2,060	2.4	93.7	
503							
	19		x	X	x	x	x
	20		9.98	2,160	1.5	87.9	x

Lapse Time (Hrs)	Sample Designator	DOC mg L ⁻¹	pH	Cond μ S cm ⁻¹	Turbidity NTU	Bromide mV	1,4-Dioxane mg L ⁻¹
527							
	UU		x	X	x	x	
	VV		10.57	2,320	2.3	90.2	
551							
	WW		x	X	x	x	
	XX		10.45	2,520	1.8	81.4	
575							
	YY		x	X	x	x	
	ZZ		10.19	2,780	1.5	82.4	
599							
	AAA		x	x	x	x	
	BBB		x	x	x	x	
623							
	21		x	x	x	x	x
	22		9.3	2,770	1.4	79.8	x

Table A.8. Recorded 1,4-Dioxane GC Measurements – Experimental Run # 5.

Sample #	Run 1	Time	Run 2	Time	Run 3	Time	Avg. Area
1	21,113	2.044	23,541	2.04	24,619	2.04	23,091
2	33,377	2.039	32,390	2.038	29,357	2.042	31,708
3	22,287	2.038	21,139	2.04	22,832	2.04	22,086
4	11,051	2.039	10,160	2.037	11,814	2.039	11,008
5	20,431	2.04	15,101	2.036	15,472	2.045	17,001
6	3,782	2.049	4,275	2.042	5,105	2.042	4,387
7	19,954	2.042	18,278	2.044	24,912	2.04	31,572
8	11,423	2.045	12,837	2.043	15,377	2.04	13,212
9	18,818	2.046	18,104	2.042	16,223	2.047	17,715
10	17,865	2.047	15,182	2.041	15,730	2.038	16,259
11	6,068	2.042	7,860	2.041	6,648	2.041	10,288
12	13,855	2.047	13,969	2.037	16,442	2.04	14,755
13	2,062	2.041	1,770	2.044	2,023	2.041	1,952
14	4,113	2.041	5,355	2.042	3,370	2.044	4,279
15	533	2.042	491	2.042	736	2.039	587
16	3,250	2.035	3,521	2.036	3,146	2.039	3,306
17	ND		ND		33	2.035	33
18	1,291	2.044	1,368	2.039	1,333	2.043	1,331
19							0
20	214	2.039	180	2.041	177	2.039	190
21							0
22	37	2.043	39	2.04	32	2.04	36
23	21,431	2.041	20,084	2.037	21,985	2.039	21,167
24	23,229	2.044	27,509	2.043			25,369
25							0
26							0
27	4,559	2.039	4,879	2.041	3,875	2.041	4,438
28	14,090	2.045	13,379	2.044	14,452	2.046	13,974
29	8,261	2.045	8,289	2.047	8,266	2.042	8,272
30	7,051	2.043	6,699	2.041	6,386	2.041	6,712
31	4,734	2.045	4,918	2.047	4,795	2.044	4,816
32	8,026	2.044	8,366	2.04	10,252	2.036	8,881
33	1,318	2.041	1,289	2.047	1,206	2.042	1,271
34	1,366	2.044	1,521	2.043	1,485	2.045	1,457

Table A.9. Schedule and Recorded Measurements – Experimental Run # 6.

Lapse Time (Hrs)	Sample Designator	DOC mg L ⁻¹	pH	Cond μ S cm ⁻¹	Turbidity NTU	Bromide mV	1,4-Dioxane mg L ⁻¹
			7.10	1,423		78.1	
				186		253.9	
						Chg Ref Probe	
						57.9	
0							
0							
0							
	Base F		6.92	1,053	1.5	149.5	
	Base 1		7.33	2,580	0.5	105.2	
	Base 2		7.29	981	0.5	144.4	
	1	164.804	7.51	1,154	2.7	72.2	6.604
	2	99.32068	7.53	1,157	2	71.5	4.043
12							
	W		7.51	2,340	0.7	117	
	X		7.35	1,001	0.6	147.7	
24							
	A		7.25	3,620	0.8	117.2	
	B		7.01	1,014	0.65	163.4	
35							
35							
	C		7.22	2,040	0.6	134.1	
	D		7	1,021	0.6	162.7	
	25	105.2349	7.8	1,142	2.7	71.7	5.183
	26	24.45616	7.74	1,136	4.1	71.7	5.379
47							
	35	73.27198	8.21	1,559	25	132.9	0.237
	36	50.65318	7.7	1,002	0.9	145.3	0.236
59							
59							
	37	73.17928	7.65	1,931	3.6	118.5	0.411
	38	60.31252	7.64	1,155	0.85	126.6	0.460
	23	69.21172	7.82	1,126	2.5	72.6	4.911
	24	64.31716	7.66	1,125	2.05	72.2	4.469

Lapse Time (Hrs)	Sample Designator	DOC mg L ⁻¹	pH	Cond $\mu\text{S cm}^{-1}$	Turbidity NTU	Bromide mV	1,4-Dioxane mg L ⁻¹	
71								
71								
71								
	E		7.39	1,885	1	134.6		
	F		7.32	1,134	0.5	143.3		
		3	81.42958	7.96	1,760	10	103.6	0.892
		4	100.6926	7.33	1,123	0.6	114.2	0.725
83								
	G		7.23	2,050	1.5	102.5		
	H		7.11	1,117	0.7	111		
95								
	Y		7.73	1,742	1.1	90.3		
	Z		7.37	1,140	0.6	94.7		
107								
107								
		5	106.3288	7.51	1,898	6.1	93.3	1.420
		6	51.09814	7.51	1,042	0.7	103.2	0.969
		7	128.0762	7.35	2,830	2.2	81.7	1.391
		8	58.99618	7.3	899	2.9	97.7	1.783
119								
	AA		7.61	1,956	1.4	83.3		
	BB		6.54	902	1	99.6		
131								
	AAA		7.27	2,010	1	74.6		
	BBB		7.06	1,024	0.6	85.2		
143								
143								
		29	82.0414	7.62	2,160	1.8	81.3	2.483
		30	156.6464	7.53	938	1.25	95.1	1.805
		9	63.1306	7.77	1,844	1	78.3	3.255
		10	114.5976	7.32	1,054	0.6	87	3.037

Lapse Time (Hrs)	Sample Designator	DOC mg L ⁻¹	pH	Cond μ S cm ⁻¹	Turbidity NTU	Bromide mV	1,4-Dioxane mg L ⁻¹
167							
	I		7.42	1,817	0.8	86.6	
	J		7.22	1,008	0.5	97.9	
179							
179							
	27	79.74244	7.68	2,040	2	81.3	2.087
	28	108.3682	7.59	937	1.2	91.4	1.928
	11	71.90002	7.38	2,190	21	89.5	1.641
	12	145.2257	7.57	1,031	0.7	91.8	2.248
191							
	K		7.44	2,230	0.6	97.3	
	L		7.16	1,056	0.5	103	
203							
	M		7.51	2,240	0.63	96.7	
	N		7.18	1,059	0.55	109.3	
215							
	31	65.67058	7.67	2,170	1	86	1.636
	32	48.65086	7.66	1,039	1.2	95	1.608
227							
	O		7.45	2,260	0.7	97.8	
	P		7.28	1,043	0.55	115.4	
239							
	AAAA		7.43	2,240	0.7	98.6	
	BBBB		7.21	893	0.8	124.6	
251							
251							
	13	71.23258	7.76	2,170	1	89.5	1.010
	14	100.7853	7.72	971	1.2	115.6	0.795
	Cir A		7.52	2,150	0.8	96.9	
	Cir B		7.42	1,014	0.5	114.6	

Lapse Time (Hrs)	Sample Designator	DOC mg L ⁻¹	pH	Cond μ S cm ⁻¹	Turbidity NTU	Bromide mV	1,4-Dioxane mg L ⁻¹
263							
	Q		7.78	2,160	0.7	104	
	R		7.25	983	0.82	124.8	
275							
	33	64.29862	8.05	2,010	1.2	94.3	0.590
	34	39.17692	7.21	972	0.8	117.8	0.607
287							
	S		7.14	2,170	2	107.8	
	T		7.39	982	0.5	130.6	
299							
	Cir C		7.52	2,110	1	100.6	
	Cir D		7.31	966	0.5	126.2	
311							
	CCC		7.19	2,130	0.5	97.5	
	DDD		7.03	948	0.5	122.1	
323							
	Cir E		7.63	2,130	0.75	101.6	x
	Cir F		7.35	937	0.5	129.8	x
347							
	Cir G		7.63	2,030	0.6	104.9	
	Cir H		7.31	945	0.5	131.3	
371							
	Cir I		8.39	2,240	1.5	99.7	
	Cir J		7.41	941	0.5	134.1	
383							
	15	102.2871	9.57	1,510	0.7	87.1	0.344
	16	70.89886	9.8	881	0.4	94.1	0.342
395							
	Cir K		7.75	2,020	0.9	107.3	
	Cir L		7.33	932	0.5	134.1	

Lapse Time (Hrs)	Sample Designator	DOC mg L ⁻¹	pH	Cond $\mu\text{S cm}^{-1}$	Turbidity NTU	Bromide mV	1,4-Dioxane mg L ⁻¹
407							
	MM		9.61	1,557	0.6	84.9	
	NN		10.04	931	0.5	93.5	
419							
	Cir M		7.62	1,945	1.5	110.3	
	Cir N		7.54	943	0.7	137.9	
431							
	OO		9.81	1,604	0.9	83.6	
	PP		10.04	941	0.3	91.1	
443							
	Cir O		7.78	1,927	1	110.4	
	Cir P		7.54	938	0.6	141.7	
455							
	17	127.9094	9.7	1,674	0.8	83.2	0.306
	18	82.83862	9.47	948	0.4	91.2	0.263
467							
	Cir Q		7.58	1,955	1.1	110.8	
	Cir R		7.55	945	0.6	140.1	
479							
	QQ		9.79	1,701	0.6	81.5	
	RR		9.8	975	0.4	89.9	
491							
	Cir S		7.44	1,830	3	113.6	
	Cir T		7.54	948	0.5	141	
503							
	SS		9.65	1,712	0.9	79.6	x
	TT		9.73	968	0.3	88.3	x
527							
	19	129.7077	9.92	1,778	0.5	78.2	0.262
	20	82.5976	9.71	998	0.45	86.8	0.252

Lapse Time (Hrs)	Sample Designator	DOC mg L ⁻¹	pH	Cond μ S cm ⁻¹	Turbidity NTU	Bromide mV	1,4-Dioxane mg L ⁻¹
539							
	Cir U		7.11	1,782	3.4	117	
	Cir V		7.08	950	0.4	147.5	
575							
	UU		10.04	1,861	0.5	77.6	
	VV		10.11	1,061	0.5	82.6	
599							
	21	191.0566	9.27	1,892	0.8	77.6	0.250
	22	98.61616	8.85	1,064	1	87.1	0.247
611							
	Cir Y		7.14	1,574	4.5	127.7	
	Cir Z		7.33	955	0.6	146.1	

Table A.10. Recorded 1,4-Dioxane GC Measurements – Experimental Run # 6.

Sample #	Run 1	Time	Run 2	Time	Run 3	Time	Avg. Area
1	37,328	2.042	41,781	2.04	36,175	2.042	38,428
2	21,457	2.104	23,481	2.104	23,995	2.1	22,978
3	4,129	2.104	3,992	2.103	3,793	2.102	3,971
4	2,797	2.103	2,700	2.103	3,397	2.099	2,965
5	7,564	2.094	7,026	2.096	6,881	2.097	7,157
6	4,388	2.095	4,198	2.094	4,721	2.095	4,436
7	6,517	2.089	7,126	2.088	7,291	2.089	6,978
8	8,987	2.092	9,929	2.089	9,124	2.091	9,347
9	19,829	2.089	18,962	2.082	15,895	2.089	18,229
10	16,420	2.084	16,441	2.086	17,869	2.083	16,910
11	8,460	2.089	8,192	2.086	8,811	2.093	8,488
12	13,553	2.084	11,452	2.085	11,445	2.085	12,150
13	4,985	2.082	4,447	2.085	4,614	2.083	4,682
14	3,657	2.082	3,165	2.085	3,325	2.081	3,382
15	687	2.085	683	2.083	622	2.085	664
16	530	2.076	521	2.082	902	2.067	651
17	430	2.083	459	2.083	406	2.079	432
18	184	2.054	171	2.056	164	2.056	173
19	164	2.055	164	2.053	184	2.052	171
20	120	2.051	98	2.054	102	2.052	107
21	87	2.055	108	2.053	92	2.051	96
22	70	2.044	82	2.053	82	2.047	78
23	29,586	2.046	25,556	2.048	29,500	2.048	28,214
24	27,883	2.048	24,308	2.052	24,455	2.055	25,549
25	24,884	2.053	33,315	2.039	31,376	2.051	29,858
26	30,645	2.043	28,402	2.041	34,068	2.04	31,038
27	11,272	2.038	10,812	2.041	11,449	2.038	11,178
28	9,902	2.034	9,815	2.041	10,933	2.037	10,217
29	14,016	2.033	12,696	2.043	13,985	2.033	13,566
30	9,218	2.035	9,447	2.035	9,761	2.032	9,475
31			8,167	2.027	8,744	2.035	8,456
32	8,888	2.035	7,430	2.04	8,546	2.034	8,288
33	2,044	2.037	2,249	2.038	2,156	2.039	2,150
34	2,346	2.039	2,169	2.036	2,242	2.039	2,252
35	18	2.032	18	2.03	23	2.035	20
36	16	2.044	17	2.043	9	2.043	14
37	1,206	2.036	963	2.039	1,039	2.039	1,069
38	1,454	2.034	1,289	2.045	1,343	2.039	1,362

APPENDIX B. CALIBRATION AND DATA VALIDATION

B.1 Equipment Calibration

B.1.1 Calibration Solutions

To ensure consistency and accuracy of measurements, calibration of equipment was conducted at the beginning of each experimental run. The calibration utilized previously prepared or industry created standards. These standards were utilized prior to the actual sample measurements to validate equipment functionality. Current calibration results were compared with previous calibration curves to validate consistency. For 1,4-Dioxane measurement, each experimental run or GC equipment set up had a separate calibration curve created. The calibration curve of the pure chemical (1,4-Dioxane) in solvent was generated in addition to extracted calibration curves from milli-Q, Tank 1 discharge, and secondary effluent spiked standards. Other equipment calibration, such as turbidity and conductivity, were calibrated with traceable standards available with the equipment. The DOC and bromide tracer calibration was made through a series of prepared concentrations. All raw materials and prepared standards were stored in accordance with recommended procedures as outlined in various laboratory standard methods with were used.

B.1.2 Bromide Tracer Calibration

Bromide was measured with a bromide ion specific electrode (ISE) utilizing a double junction reference electrode. In order to calibrate the instrument/probes to reflect accurately the bromide concentration, a series of 5 standards were prepared in Milli-Q ultrapure water. The standards (8000, 800, 80, 8 and 1 mg L⁻¹) were measured and recorded as milli-volt readings. Bromide calibration curves are shown in Figure B.1.

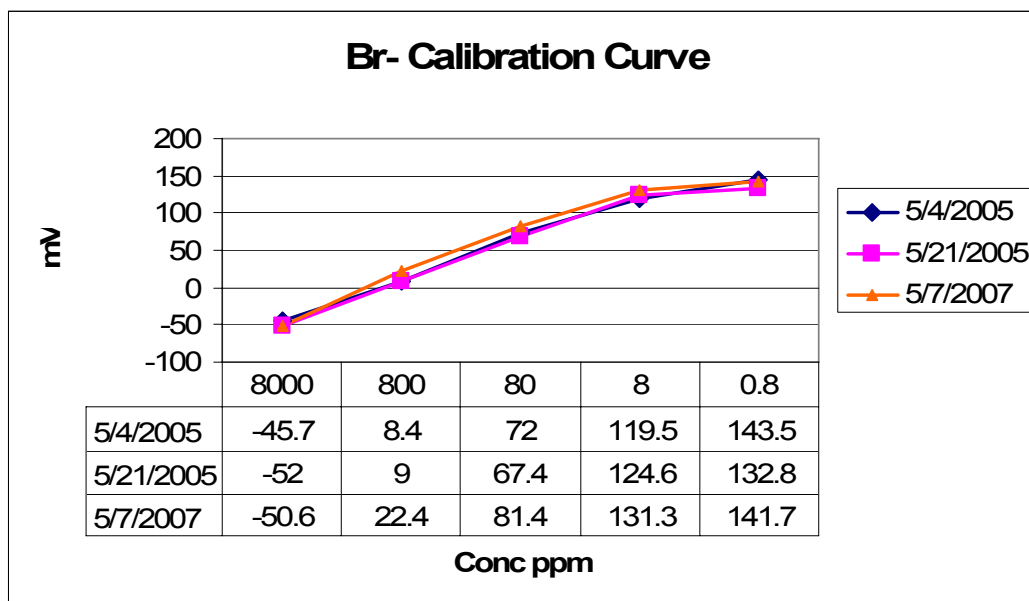


Figure B.1. Bromide Tracer Calibration Curve.

The calibration curve has a slope of -58.8 with a y-intercept of 178.6. The concentration of bromide was calculated as ($\text{mg L}^{-1} = 10^{eV-178.6/-58.8}$). Ion selective electrodes give log response to activities of ions rather than concentration. A 50 % buffer (KNO₃) was added

to each sample to bring all samples to the same ionic strength (activity coefficient being equal). The ionic strength is a function of charge and concentration of all ions present. If the buffer was not used, as concentration increases there would be increasing interaction (Debye-Huckel) which would change the ionic strength (Rundle, 2000). For Bromide, as ionic strength increases, bromide ion activity coefficient decreases. In general, mV measurements increase for cations and decrease for anions with increasing concentration. In the case of bromide ISE measurements, lower concentrations allow more ions to pass through the ion-selective membrane and thus a higher magnitude of voltage potential is developed across the electrode. As the ions become more closely packed, their movement is impeded by inter-ionic interactions and less potential is developed.

An 80 mg L^{-1} bromide measurement was made prior to sample measurements for each experimental run. The various 80 mg L^{-1} mV reading standard deviation was 2.339 with a mean of 67.717. The measurement accuracy (standard deviation divided by mean) converted to percent was 3.5 with a 95 percent confidence interval.

Over the course of the experimental runs, the double junction reference probe would occasionally have insufficient flow of electrolyte through the porous frit or the filling solutions would become contaminated. The double junction electrode is used to prevent gradual contamination of the test solution with electrolyte ions. The outer solution provides a conductive path between the inner reference system and the sample. This

outer solution does not contaminate the sample with ions that would impact the measured results (Rundle, 2000). To fix an unstable reference junction probe, the porous frit tip was boiled in milli-Q water for 15 minutes and the inner and outer solutions were removed and replaced. On occasion the ISE probe itself would need to be reconditioned by lightly rubbing the end of the probe with toothpaste followed by a thorough cleaning. These activities would typically require a re-run of the calibration curve.

B.1.3 pH Calibration

The pH meter provided a semi-automated calibration process where a two or three buffer solution calibration could be selected. The internal processor of the meter would indicate which solution to insert the probe and require operator response when the reading stabilized. At the end of the calibration sequence, the probe would display the change in slope reading based on temperature. If the slope reading was greater than 92 percent, the calibration was successful. This slope factor is a percentage difference of the theoretical value (59.16 mV/pH at 25 °C) to the measured value. An automatic temperature compensation probe (± 2 percent) was connected to the meter so the slope difference was minimal based on good electrode condition and accurate temperature measurement. Fresh calibration buffers (7-10) were utilized for meter/probe calibration.

The pH measurement captures the electrical potential across the probe membrane surface. This electrical potential requires a reference potential to be in the measurement circuit.

The reference potential was supplied by the combination probe utilized to measure pH. The combination probe contains both the pH probe (membrane) and the reference probe in one unit. The relationship between the ionic concentration and the electrode potential of the pH probe is described by the Nernst equation which is $E_{\text{measured}} = E_{\text{reference}} + (2.3 RT/nF) \log a_h$. The $E_{\text{reference}}$ is the reference potential or the sum of all the liquid junction potentials in the probe, the $\log a_h$ is the logarithm of the response of the pH probe, R = gas constant law, F = Faraday's constant, n = the charge on the ion, and T = temperature. The slope of the calibration curve is defined as $2.3 RT/nF$ and the y-intercept is the $E_{\text{reference}}$ (Rundle, 2000).

For each experimental run, prior to taking sample measurements, a calibration procedure was initiated and saved on the pH meter. This re-calibration, along with the automatic temperature compensation probe, ensured accurate readings of pH ($\pm 3\%$).

B.1.4 Conductivity Calibration

The conductivity calibration was similar to the pH calibration in that the meter electronics and firmware offered a semiautomatic calibration sequence for the meter/probe combination. Conductivity calibration standards were available at the CERF lab and the conductivity meter was calibrated prior to running samples for each experimental run. In the case of the conductivity meter, the 4 conductor probe had automatic temperature compensation built in and required only one conductivity standard

to establish calibration. The standard most commonly utilized for the experimental runs was 1421 uS/cm^{-2} . A calibration standard reading was taken at the start and during measuring experimental samples. The reading was typically within 2-5 μS of the calibration value. The experimental run calibration standard deviation was $6.75 \mu\text{S}$ with a mean of $1418.5 \mu\text{S}$. The measurement accuracy (standard deviation divided by mean) converted to percent was 0.5 with a 95 percent confidence interval.

B.1.5 Turbidity Calibration

Turbidity measurement of experimental run samples was conducted on a photomultiplier tube type turbidimeter. The meter had 5 selectable ranges (0-0.2, 0-1.0, 0-10, 0-100, 0-1,000 nephelometric turbidity units (NTU)). The accuracy of the instrument was ± 2 percent. Calibration of the turbidimeter consisted of inserting the specific turbidity standard, for the range of interest, in the photomultiplier cell holder assembly and selecting the range with the front rotary switch. Each calibration standard had been previously tested by the manufacturer and the measured value was provided with the standards for use on that specific piece of equipment. Accuracy of secondary turbidity standards was $\pm 5\%$. After selecting the appropriate range for the calibration standard, the meter pointer would be positioned to that standard's pre-determined value on the turbidimeter.

The standard would be removed and an experimental run sample, decanted to a test vial, would be inserted into the photomultiplier cell holder assembly. The sample reading would then be recorded from the meter pointer. If the current or following sample reading was not within the current scale setting, the sample would be removed and a new range and its associated calibration standard would be selected. The re-calibration process would occur as above with a new setting adjustment required with the standardize potentiometer.

The calibration standards were Gelex secondary standards from the manufacturer. Most primary turbidity standards are made from formazin. However, formazin is relatively unstable at low concentrations for extended periods (weeks). The Gelex standards, not having the same light scattering characteristics as formazin, must be specifically formulated for the turbidity model they will be used with. This is a slight disadvantage but the Gelex standards have an almost indefinite shelf life and stable turbidity value. The specific measured value for the Gelex standards was 675 NTU for the 1,000 range, 75.5 NTU for the 100 range, 6.45 NTU for the 10 range and 0.77 NTU for the 1 range.

Due to the wide variation of the NTU values of the experimental run samples, re-calibration of the turbidimeter would occur on an almost every other sample basis.

B.1.6 TDR Probe Calibration

The twelve TDR probes were calibrated in accordance with the procedures established by the Utah State University WinTDR software program. The WinTDR calibration utilizes de-ionized water to establish the effective length of the probe not the physical length. This calibration sequence is similar to the USDA TACQ program that uses open air measurements for calibration. The moisture content standard deviation of the probes immersed in milli-Q pure water was $0.0153 \theta_v$ with a mean of $0.8058 \theta_v$. The measurement accuracy (standard deviation divided by mean) converted to percent was 1.9 with a 95 percent confidence interval. Probe soil moisture content measurements were adjusted based on the calibration readings.

After a stabilization period following probe installation, initial measurements from the center probe set in the planted tank are showing percent volumetric water contents of 17.6, 23.2, 30.9, and 29.3 θ_v at depths of 5, 15, 25, and 36 cm below grade, respectively. Additional samples over a period of time are required to assess potential impacts or conclusions of this soil moisture variability.

B.1.7 Dissolved Organic Carbon Calibration

Dissolved Organic Carbon (DOC) calibration standards were prepared with potassium hydrogen phthalate in milli-Q pure water at 5, 30, and 100 mg L^{-1} concentrations. The

standards were pH adjusted (2-2.5 pH) with 2M HCL and analyzed within 48 hours of preparation on a Shimadzu TOC – Vcsh Analyzer with the oven temperature at 680 °C and purified air flow of 150 ml min⁻¹. A total of 3-5 injections were performed on each standard sample to achieve the statistical accuracy specified (Standard Deviation 0.1 – Confidence Value 2.0 percent). Blank samples were inserted before and after the calibration standards. The DOC calibration curve is shown in Figure B.2.

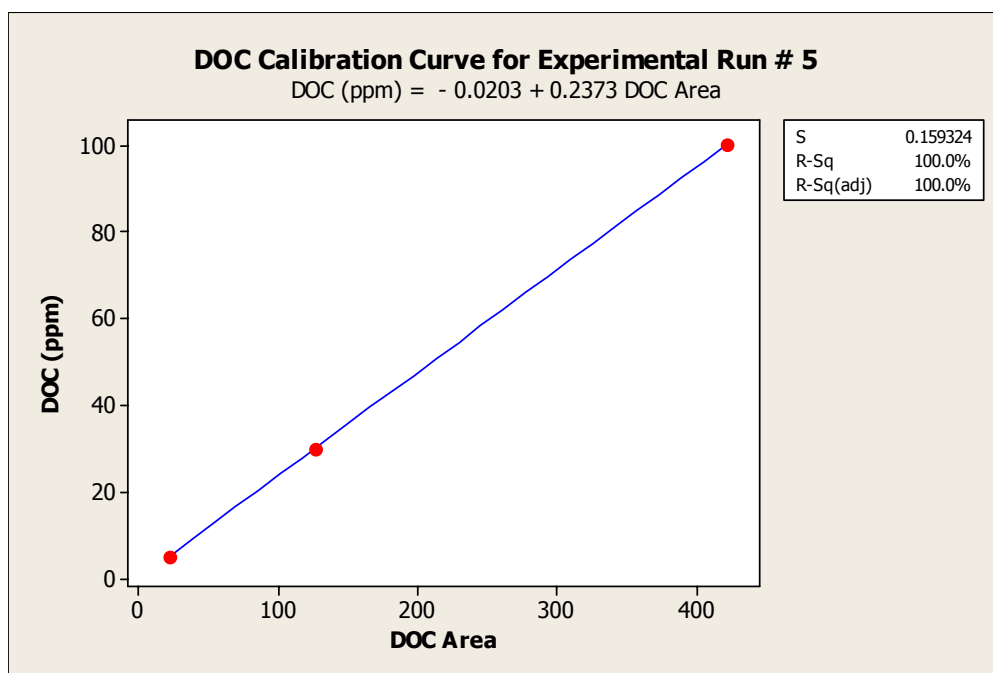


Figure B.2. DOC Calibration Curve.

B.1.8 1,4-Dioxane Calibration

The 1,4-Dioxane measurements were conducted on an HP 5790 GC – FID. To establish the sensitivity, linearity, and detection limit of the equipment, a set of pesticide-grade

1,4-Dioxane calibration standards in methylene chloride was created on June 14, 2005. The standards were 1, 10, 100, 500, 1,000 and 5,000 mg L⁻¹. The standards were stored in dark glass vials with PTFE-lined septa at -10 +/- 2 °C. Due to the variation of the equipment, prior to each experimental run sampling on the GC, a new set of calibration standards would be established. The GC operating procedure established separate baselines for each set of samples and the equipment sensitivity, limits and linearity prior to evaluating experimental samples.

Using the standards, a typical 1,4-Dioxane standard curve was established as shown in Figure B.3. In calibration standards, solvent and 1,4-Dioxane only, the eluting time for the solvent and contaminant was 0.536 and 0.739 minutes, respectively. The standard curve shown in Figure B.3 was created with the GC configured to splitless flow with an Agilent Technologies DB-Wax mega bore 30 meter column.

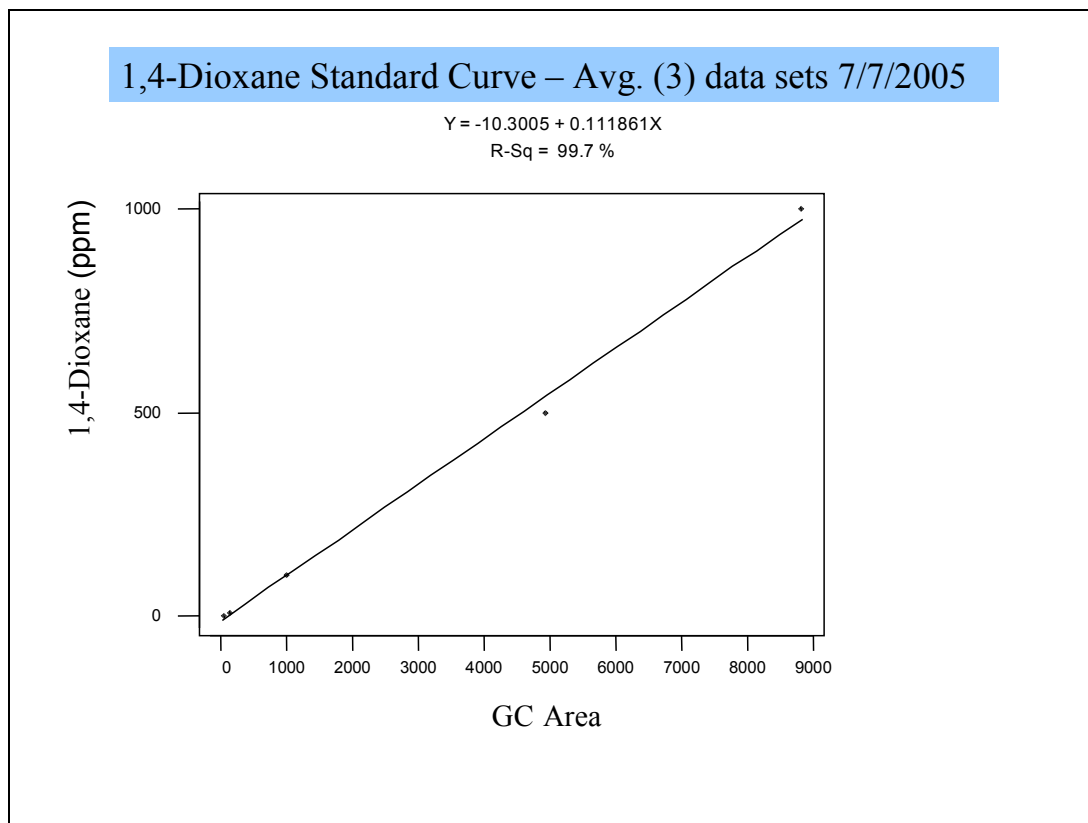


Figure B.3. Initial GC 1,4-Dioxane Standard Curve.

In addition to the 1,4-Dioxane calibration standards created, extracted calibration standards were also developed for 0.1, 1.0, and 5.0 mg L⁻¹ concentrations in milli-Q water, discharge water (where influent was tap water) from Tank 1, and secondary effluent from feed source. One liter samples for each concentration were prepared from the three water sources and extracted for six hours. Following GC/FID analysis of the extracted calibration standards, calibration curves were developed and utilized to determine the concentrations of 1,4-Dioxane in the various experimental run samples. For the Tank 1 discharge, extraction efficiency was 43, 45, and 48 percent for the 0.1,

1.0, and 5.0 mg L⁻¹, respectively. Secondary effluent extraction efficiencies were 5-9 percent less than the Tank 1 discharge extraction efficiencies.

B.1.9 Calibration Results

Values for the calibration standards and method blanks are also shown on the electronic spreadsheets. Least squares regression analysis and statistical parameters were performed using MINITAB Student Release 14 statistical software. The results from the regression analysis are shown in Table B.1.

Table B.1. 1,4-Dioxane Standard and Extracted Calibration Curve Slopes and r² Values.

Exp. Run	Slope Cal. Curve	R-Sq. %	Extracted Solution	Slope Extracted Standard Curve	R-Sq. %
1	.1119	95.5	Milli-Q	.001331	95.5
2	.06447	98.3	Milli-Q	.001309	90.4
3	.08466	100.0	TK1 Disch	.000165	98.7
3	.08466	100.0	S.E. Disch	.000400	98.2
4	.05170	100.0	TK1 Disch	.000087	98.6
4	.05170	100.0	S.E. Disch	.000216	98.2
5	.05715	99.9	TK1 Disch	.000096	99.0
5	.05715	99.9	S.E. Disch	.000238	97.9
6	.1072	99.7	TK1 Disch	.000207	99.9
6	.1072	99.7	S.E. Disch	.000387	97.6

Surrogate recovery methods, based on the variation in extraction efficiency, have been shown to improve result accuracy in other published research papers (Draper *et al.*, 2000). Surrogate recoveries from experimental run # 1 showed the coefficient of

variance for all samples of 8.03 percent. Replicated samples show the majority of variance could be attributed to inconsistency of the equipment and not significant differences in extraction efficiency.

Replicated GC analysis sampling variability is often correlated to slight differences in the injection volume. This is more pronounced when manual injections are made as was done for all the experimental runs. Experimental run # 4 was analyzed on the GC-FID with both 1 μL and 2 μL injection volumes. Based upon the equipment operating parameters and the bulk of the sample being purged, the 1,4-Dioxane area results for each sample were nearly identical. With minimal variation in 1,4-Dioxane areas at 2X the sample volume, it would be unlikely the variations in surrogate areas were the result of minor differences ($\pm 0.05\mu\text{L}$) in injection volumes.

A comparison of the GC integrated areas for the concentrations of 100, 1,000, and 5,000 mg L^{-1} from the 1,4-Dioxane standard curve to the 0.1, 1.0 and 5.0 mg L^{-1} extracted calibration curve area is shown in Table B.2. The consistency in ratios across experimental runs (1-6) between the standard curve and extracted calibration curves supports the use of the extracted calibration curves for determination of contaminant concentration.

An initial GC analysis of experimental run number 4 samples was conducted with the injection volume of 1.0 μL . All other experimental run analysis was conducted with injection volumes of 2.0 μL based on the recommendations in the GC operating manual. At a later date, a re-run of experimental run number 4 samples was conducted with an injection volume of 2.0 μL . The peak areas for 1,4-Dioxane 2.0 μL injections were closely aligned with the peak areas of the 1.0 μL injections. With the lack of GC flow and purge control, the operating conditions provided a minimal volume of any sample going through the column and the remaining sample volume purged. These operating conditions minimized the impact of sample volume and injection errors on the final peak areas. As such, the inability to utilize an internal standard to compensate for such errors had minimal effect on the 1,4-Dioxane results.

Evaluating impact of bromide on 1,4-Dioxane extraction and GC area measurements, two replicate samples (1 mg L^{-1}) in milli-Q pure water were measured. The resulting GC area standard deviation for separate extractions with multiple GC injections was 208.16 with a mean of 5,410.8. The measurement accuracy (standard deviation divided by mean) converted to percent was 3.85 with a 95 percent confidence interval. This overall extraction and measurement accuracy reflected optimal operating conditions with minimal extraction matrix effects and prior to equipment H_2 flow problems. Tank 1 discharge extracted (1 mg L^{-1} calibration standard) GC area measurements for the May and June 2006 time frame had standard deviation of 420.5 with a mean of 3,812.7. The

measurement accuracy (standard deviation divided by mean) converted to percent was 11.0 with a 95 percent confidence interval.

Table B.2. 1,4-Dioxane Standard Curve Ratio to Extracted Calibration Curves for 100, 1000, and 5000 mg L⁻¹ (0.1, 1.0, and 5.0 extracted).

Milli-Q Extracted	Exp 1 Cal Std.	Exp 2 Cal Std	Exp 3 Cal. Std.	Exp 4 Cal. Std.	Exp 5 Cal. Std.	Exp 6 Cal. Std.
0.1	0.40	0.36	0.37			
1.0	0.24	0.29	0.22			
5.0	0.59	0.59	0.64			
Tk 1 Extracted						
0.1		0.39	0.38	0.34	0.37	0.48
1.0		0.20	0.19	0.17	0.17	0.18
5.0		0.48	0.52	0.51	0.56	0.52
S.E. Extracted						
0.1		0.34	0.34	0.24	0.26	0.44
1.0		0.36	0.36	0.37	0.36	0.40
5.0		0.22	0.23	0.22	0.24	0.29

Table B.3. Experiment Run 3 Calibration Standard Results.

HP GC 5790 Calibration Standards 10/30/2005 (Experiment # 3)						
DB5 Column 30 m, 1.5um .53 mm.						
Injection temp 200 C, Detector Temp 300 C, Oven 100 C.						
Gas pressure set at .71 PSI						
Injection split/splitless and purge valve removed from system.						
Injection Volume 2.0 µL						
Conc/	1 PPM	10 PPM	100 PPM	500 PPM	1000 PPM	5000 PPM
Readings	Area	Area	Area	Area	Area	Area
	13	121	1,156	5,821	11,314	59,523
	14	113	1,249	6,290	12,338	58,772
	13.5	117	1,202.5	6,055.5	11,826	59,147.5
Exp 3 Std Curve = - 15.07 + 0.08466 Dioxane Area						
0.1 PPM 1,4-Dioxane Extracted 100 ml DCM for 6 hrs conc. to 1 ml volume.						
Sample vacuum filtered with 0.7muffled glass & .455 PVDF Vericel filters						
	Milli Q	Tank 1	Secondary Effluent			
	Area	Area	Area			
	460	458	406			
	432	457	432			
Avg	446	457.5	419			
1.0 PPM 1,4-Dioxane Extracted 100 ml DCM for 6 hrs conc. to 1 ml volume.						
Sample vacuum filtered with 0.7muffled glass & .455 PVDF Vericel filters						
	Milli Q	Tank 1	Secondary Effluent			
	Area	Area	Area			
	2,579	2,259	4,192			
	2,753	2,288	4,465			
			4,389			
Avg	2,666	2,273.5	4,349			

5.0 PPM 1,4-Dioxane Extracted 100 ml DCM for 6 hrs conc. to 1 ml volume.
Sample vacuum filtered with 0.7muffed glass & .455 PVDF Vericel filters

	Milli Q Area	Tank 1 Area	Secondary Effluent Area
	35,958	28,923	12,837
	39,028	28,830	13,295
	30,490	28,031	13,021
Avg	35,159	28,595	13,051

10/30/2005

**Milli Q Extracted compared with Calibration
Standards**

.1 ppm	446	100	1,202.5	0.370894
1 ppm	2,666	1,000	11,826	0.225435
5 ppm	35,159	5,000	59,147.5	0.594429

10/30/2005

**Tk 1 Discharge Extracted compared with Calibration
Standards**

.1 ppm	457.5	100	1,202.5	0.380457
1 ppm	2,273.5	1,000	11,826	0.192246
5 ppm	2,8595	5,000	59,147.5	0.483452

Exp 3 Tk1 Extract = $0.3154 + 0.000165 \text{ Tk 1 Area}$

10/30/2005

**Secondary Effluent Extracted compared with Calibration
Standards**

.1 ppm	419	100	1,202.5	0.348441
1 ppm	4349	1,000	11,826	0.367749
5 ppm	13051	5,000	59,147.5	0.220652

Exp 3 SE Extract = $-0.3413 + 0.000400 \text{ SE Area}$

Table B.4. Experiment Run 4 Calibration Standard Results.

HP GC 5790 Calibration Standards 7/05/2006 (Re Run Experiment # 4)						
DB5 Column 30 m, 1.0um .252 mm. (Agilent Tech. 1225033 S/N US5261241H)						
Injection temp 200 C, Detector Temp 300 C, Oven 100 C.						
Gas pressure set at 1.8 kg/cm2 PSI						
Split Vent 20 ml 1 min 45 sec						
Septum Purge 25 ml 25 sec						
Sample injection volume 2.0 µL						
Conc/	1 PPM	10	100	500	1000	5000 PPM
		PPM	PPM	PPM	PPM	
Readings	Area	Area	Area	Area	Area	Area
1			1,983	10,424	18,851	93,040
2			2,175	10,844	20,379	10,1258
3			2,079	10,634	19,615	97,149
Exp 4 Dioxane = - 23.63 + 0.05170 Std. Curve Area						
0.1 PPM 1,4-Dioxane Extracted with 100 ml DCM for 6 hrs and conc. to 1 ml volume.						
Sample vacuum filtered with 0.7muffled glass and .455 PVDF Vericel micron filters						
		Tank 1	Secondary Effluent			
		Area	Area			
1		714	420			
2		718	584			
Avg		716	502			
1 PPM 1,4-Dioxane Extracted with 100 ml DCM for 6 hrs and conc. to 1ml volume.						
Sample vacuum filtered with 0.7muffled glass and .455 PVDF Vericel micron filters						
		Tank 1	Secondary Effluent			
		Area	Area			
1		3,630	7,686			
2		3,416	6,975			
Avg		3,523	7,331			
5.0 PPM 1,4-Dioxane Extracted with 100 ml DCM for 6 hrs and conc. to 1 ml volume.						
Sample vacuum filtered with 0.7muffled glass and .455 PVDF Vericel micron filters						
		Tank 1	Secondary Effluent			
		Area	Area			
1		49,441	21,324			
2		50,565	22,190			
Avg		50,003	21,757			

7/4/2006

Tk 1 Discharge Extracted compared with Calibration

Standards

.1 ppm	100 ppm	716	2,079	34.43963	65.56037
1 ppm	1,000	3,523	19,615	17.96074	82.03926
5 ppm	5,000	50,003	97,149	51.47042	48.52958

Cal Curve $y = .310198 + .0000874 (X)$ (98.6%)

Exp 4 Tk 1 Extract = $0.3154 + 0.000087$ Tk 1 Area

7/4/2006

Secondary Effluent Extracted compared with Calibration

Standards

.1 ppm	100 ppm	502	2,079	24.14622	75.85378
1 ppm	1,000	7,331	19,615	37.37446	62.62554
5 ppm	5,000	21,757	97,149	22.3955	77.6045

Cal Curve $y = .43 + .00021 (X)$ (98.2%)

Exp 4 SE Extract = $-0.3413 + 0.000216$ SE Area

Table B.5. Experiment Run 5 Calibration Standard Results.

HP GC 5790 Calibration Standards 7/03/2006 (Experiment # 5)						
DB5 Column 30 m, 1.0um .252 mm. (Agilent Technologies 1225033 S/N US5261241H)						
Injection temp 225 C, Detector Temp 300 C, Oven 100 C.						
Gas pressure set at 1.8 kg/cm2 PSI						
Split Vent 20 ml 1 min 45 sec						
Septum Purge 25 ml 25 sec						
Injection volume 2.0 µL						
Conc/	1 PPM	10 PPM	100 PPM	500 PPM	1000 PPM	5000 PPM
Readings	Area	Area	Area	Area		
		78	1,914	9,456	15,919 20,379	87,836
Exp 5 Std Curve = - 45.65 + 0.05715 Dioxane Area						
0.1 PPM 1,4-Dioxane Extracted with 100 ml DCM for 6 hrs and conc. to 1 ml volume. Sample vacuum filtered with 0.7muffled glass and .455 PVDF Vericel micron filters						
		Tank 1	S. E.			
		Area	Area			
1		712	420			
2		718	584			
Avg		715	502			
1 PPM 1,4-Dioxane Extracted with 100 ml DCM for 6 hrs and conc. to 1ml volume. Sample vacuum filtered with 0.7muffled glass and .455 PVDF Vericel micron filters						
		Tank 1	S. E.			
		Area	Area			
1		3,458	7,686			
2		3,748	6,975			
3		3,630				
4		3,416				
Avg		3,563	7,331			
5.0 PPM 1,4-Dioxane Extracted with 100 ml DCM for 6 hrs and conc. to 1 ml volume. Sample vacuum filtered with 0.7muffled glass and .455 PVDF Vericel micron filters						
		Tank 1	S. E.			
		Area	Area			
1		49,441	21,324			
2		48,898	22,190			
3		50,565				
Avg		49,635	21,757			

10/30/2005

Tk 1 Discharge Extracted compared with Calibration Standards

.1 ppm	100 ppm	715	1,914	.37356
1 ppm	1,000 ppm	3,563	20,379	.17483
5 ppm	5,000 ppm	49,634.67	87,836	.56508

Tank 1 Extract = $0.2761 + 0.000096$ Tk 1 Area

10/30/2005

Secondary Effluent Extracted compared with Calibration Standards

.1 ppm	100 ppm	502	1,914	.26227
1 ppm	1,000 ppm	7,330.5	20,379	.35970
5 ppm	5,000 ppm	21,757	87,836	.24770

SE Extract = $-0.3120 + 0.000238$ SE Area

Table B.6. Experiment Run 6 Calibration Standard Results.

HP GC 5790 Calibration Standards 9/03/2006 (Experiment # 6)						
DB5 Column 30 m, 1.0um .252 mm. (Agilent Technologies 1225033 S/N US5261241H)						
Injection temp 200 C, Detector Temp 300 C, Oven 100 C.						
Gas pressure set at 1.8 kg/cm2 PSI						
Split Vent 15 ml/min						
Septum Purge 20 ml /min						
Injection volume 2.0 µL						
Conc/	1 PPM	10 PPM	100 PPM	500 PPM	1000 PPM	5000 PPM
Readings	Area	Area	Area	Area		
	7	95 110	1,033	5,269	11,893	46,685
Exp 6 Std Curve $y = -59.22 + 0.1072(x)$ (99.7%)						
0.1 PPM 1,4-Dioxane Extracted with 100 ml DCM for 6 hrs and conc. to 1 ml volume.						
Sample vacuum filtered with 0.7muffled glass and .455 PVDF Vericel micron filters						
		Tank 1	S. E.			
		Area	Area			
1		556	402			
2		452	515			
3		482	474			
Avg		497	464			
1 PPM 1,4-Dioxane Extracted with 100 ml DCM for 6 hrs and conc. to 1ml volume.						
Sample vacuum filtered with 0.7muffled glass and .455 PVDF Vericel micron filters						
		Tank 1	S. E.			
		Area	Area			
1		1,909	4,511			
2		2,163	5,218			
3		2,583	4,530			
Avg		2,218	4,753			
5.0 PPM 1,4-Dioxane Extracted with 100 ml DCM for 6 hrs and conc. to 1 ml.						
Sample vacuum filtered with 0.7muffled glass and .455 PVDF Vericel micron filters						
		Tank 1	S. E.			
		Area	Area			
1		24,179	14,207			
2		24,272	11,609			
3		24,719	14,791			
Avg		24,390	13,536			

9/3/2006

Tk 1 Discharge Extracted compared with Calibration Standards

.1 ppm	100 ppm	496.6667	1,033	0.4808
1 ppm	1,000	2,218	11,893	0.186496
5 ppm	5,000	24,390	46,685	0.522438

Cal Curve $y = -.05387 + .000207(X)$
(99.9%)

9/3/2006

Secondary Effluent Extracted compared with Calibration Standards

.1 ppm	100 ppm	463.6667	1,033	0.448854
1 ppm	1,000	4,753	11,893	0.399647
5 ppm	5,000	13,535.67	46,685	0.289936

Cal Curve $y = -.3845 + .000387(X)$ (97.6%)

REFERENCES

- Abe, A. 1999. Distribution of 1,4-dioxane in relation to possible sources in the water environment. *The Science of The Total Environment*. **227**(1): 41-47.
- Ahn-Ercan, G., Krienke, H., and Schmeer, G. 2006. Structural and dielectric properties of 1,4-dioxane - water mixtures: New Highlights of Solution Chemistry: Diffraction, Simulation and Theoretical Studies - Invited Contributions Dedicated to Professor Gabor Palinkas on Occasion on his 65th Birthday. *Journal of Molecular Liquids*. **129**(1-2): 75-79.
- Aitchison, E.W., Kelley, S.L., and Alvarez, P.J.J. 2000. Phytoremediation of 1,4-dioxane by hybrid poplar trees. *Water Environment Research*. **72**(3): 313-321.
- Ashby, J. 1994. The genotoxicity of 1,4-dioxane. *Mutation Research/Genetic Toxicology*. **322**(2): 141-142.
- Beckett, M.A. and Hua, I. 2003. Enhanced sonochemical decomposition of 1,4-dioxane by ferrous iron. *Water Research*. **37**(10): 2372-2376.
- Black, R.E., Hurley, F.J., and Havery, D.C. 2001. Occurrence of 1,4-dioxane in cosmetic raw materials and finished cosmetic products. *Journal of AOAC International*. **84**(3): 666-670.
- Blaylock, A.D. 1994. Soil Salinity, Salt Tolerance, and Growth Potential of Horticultural and Landscape Plants. B-988. College of Agriculture - Department of Plant, Soil, and Insect Sciences. University of Wyoming Cooperative Extension Service. Laramie, Wyoming.
- Braatne, J.H. 1999. Biological Aspects of Hybrid Poplar Cultivation and Floodplains in Western Northern America - A Review. EPA Document Number 910-R-99-002. Assistant Professor University of Washington. U. S. Environmental Protection Agency. Seattle, Washington.
- Briggs, G.G., Bromilow, R.H., and Evans, A.A. 1982. Relationships between lipophilicity and root uptake and translocation of non-ionised chemicals by barley. *Pesticide Science*. **13** : 495-504.
- Brown, P. 2005. Standardized Reference Evapotranspiration: A New Procedure for Estimating Reference Evapotranspiration in Arizona. AZ1324. University of Arizona College of Agriculture and Life Sciences. College of Agriculture and Life Sciences - Cooperative Extension. Tucson, Arizona.

- Brune, W.H. 2007. Chemistry of the Atmosphere - Aqueous Phase Chemistry. Penn State College of Earth & Mineral Sciences. University Park, PA.
- Calza, P. and Pelizzetti, E. 2001. Photocatalytic transformation of organic compounds in the presence of inorganic ions. *Pure & Applied Chemistry*. **73**(12): 1839-1848.
- Cermax 1998. Cermax Lamp Engineering Guide. Perkin Elmer Optoelectronics. Sunnyvale, Ca.
- Chatwin, P.C. 1971. On the interpretation of some longitudinal dispersion experiments. *Journal of Fluid Mechanics*. **48**(04): 689-702.
- Christian, V. 2003. Survey of 1,4-Dioxane Occurrence at Solvent Release Sites in the San Francisco Bay Area. In: 1,4-Dioxane and Other Solvent Stabilizer Compounds in the Environment. The Ninth Symposium in GRA's Series on Groundwater Contaminants. Groundwater Resources Association. Sacramento, California.
- Cohen, R.R.H. 2002. ESGN 513 Limnology: Light and Energy Balance to Lakes. Colorado School of Mines.
- Collins, C., Fryer, M., and Grosso, A. 2006. Plant Uptake of Non-Ionic Organic Chemicals. *Environmental Science & Technology*. **40**(1): 45-52.
- Cron, M. 2005. Second Five Year Review Report - Bally Ground Water Contamination Superfund Site. PAD061105128. EPA Region III. U. S. Environmental Protection Agency. Philadelphia, Pennsylvania.
- Dahab, M.F. and Surampalli, R.Y. 2001. Subsurface-flow constructed wetlands treatment in the plains: five years of experience. *Water Science & Technology*. **44**(11-12): 375-380.
- Dietz, A.C. and Schnoor, J.L. 2001. Advances in phytoremediation. *Environmental Health Perspectives* . **109**(Supplement 1163 - 168).
- Draper, W.M., Dhoot, J.S., Remoy, J.W., and Perera, S.K. 2000. Trace-level determination of 1,4-dioxane in water by isotopic dilution GC and GC-MS. *Analyst*. **125**(8): 1403-1408.
- Eberts, S.M., Schalk, C.W., Vose, J., and Harvey, G. 1999. Hydrologic Effects of Cottonwood Trees on a Shallow Aquifer Containing Trichloroethene. Special Issue 4th USA/CIS Joint Conference . U. S. Geological Survey, US Forest Service, USAF . American Institute of Hydrology. San Francisco, California.
- Eden, S., Gelt, J., Megdal, S., Shipman, T., Smart, A. and Escobedo, M. 2007. Artificial Recharge: A Multi-Purpose Water Management Tool. *Arroyo*. **Winter**: 1-12.

Ellman, E.D. 1997. Groundwater Quality Effects and Operational Considerations of an Unlined Constructed Wetland Treating Raw Sewage. Master of Science Thesis. Department of Hydrology and Water Resources. University of Arizona. Tucson, Arizona.

Evet, S.R. 2000. The TACQ Computer Program for Automatic Time Domain Reflectometry Measurements: 1. Design and Operating Characteristics. *Transactions of the ASAE*. **43**(6): 1939-1946.

Fatouhi, F. and Brode, J. 2003. Managing a Significant Release of 1,4-Dioxane into a Complex Glacial Depositional Environment; the Integration of Hydrogeology, Remedial Engineering and Politics. In: 1,4-Dioxane and Other Solvent Stabilizer Compounds in the Environment. The Ninth Symposium in GRA's Series on Groundwater Contaminants. Groundwater Resources Association. Sacramento, California.

Field, M.S. 2002. QTracer Program for Tracer-Breakthrough Curve Analysis for Karst and Fractured-Rock Aquifers. EPA/600/R-98/156a. U.S. Environmental Protection Agency. National Center for Environmental Assessment. Washington Office, Washington, DC.

Fitzgerald, Ed. 2005. Ultra Scientific . Recommended internal standard and surrogate. E-Mail. To: Ward, W. J.

Full Public Report 1998. 1,4 Dioxane Priority Existing Chemical No. 7. *National Industrial Chemicals Notification and Assessment Scheme*.

Gazal, R.M., Scott, R.L., Goodrich, D.C., and Williams, D.G. 2006. Controls on transpiration in a semiarid riparian cottonwood forest. *Agricultural and Forest Meteorology*. **137**(1-2): 56-67.

Gearheart, R.A. 2006. Constructed Wetlands for Natural Wastewater Treatment. *Southwest Hydrology*. **5**(1): 16-17.

Geiger, H., Maurer, T., and Becker, K.H. 1999. OH-initiated degradation mechanism of 1,4-dioxane in the presence of NO_x. *Chemical Physics Letters*. **314**(5-6): 465-471.

Gelt, J. 1997a. Constructed Wetlands: Using Human Ingenuity, Natural Processes to Treat Water, Build Habitat. *Arroyo*. **9**(4): 1-12.

Gelt, J. 1997b. Constructed Wetlands Treating More of Arizona's Wastewater. *Arizona Water Resource* . **6**(1): 1-2.

Gerba, C.P., Thurston, J.A., Falabi, J.A., Watt, P.M., and Karpiscak, M.M. 1999. Optimization of Artificial Wetland Design for Removal of Indicator Microorganisms and Pathogenic Protozoa. *Water Science and Technology*. **40**(4-5): 363-368.

- Gersberg, R.M., Lyon, S.R., Brenner, R., and Elkins, B.V. 1987. Fate of viruses in artificial wetlands. *Appl. Environ. Microbiol.* **53**(4): 731-736.
- Green, C. and Hoffnagle, A. 2004. Phytoremediation Field Studies Database for Chlorinated Solvents, Pesticides, Explosives, and Metals. Student Papers. Environmental Careers Organization / University of Arizona. U. S. Environmental Protection Agency. Washington, D.C.
- Griffiths, J.F. 1997. Texas Climatic Bulletin. Volume 10 Number 8. Office of the Texas State Climatologist, Texas A&M University. Austin, Texas.
- Guy, R.D. 2003. Analytical Spectroscopy and Separations. Dalhousie University, Halifax, Nova Scotia, Canada.
- Harvey, G.J. 2003. Phytoremediation of Groundwater at Air Force Plant 4, Carswell, Texas. EPA/540/R-03/506. U. S. Air Force. U. S. Environmental Protection Agency - Superfund Innovative Technology Evaluation. Cincinnati, Ohio.
- Hauser, V.L., Gimon, D.M., and Horin, J.D. 1999. Draft Protocol for Controlling Contaminated Groundwater by Phytostabilization. Prepared for Air Force Center for Environmental Excellence. Mitretek Systems. Mitretek Systems, San Antonio, Texas. Brooks AFB, Texas.
- Heathman, G.C., Starks, P.J., and Brown, M.A. 2003. Time Domain Reflectometry Field Calibration in the Little Washita River Experimental Watershed. *Soil Sci Soc Am J.* **67**(1): 52-61.
- Hendrick, R.L. 2006. In Situ Remediation of a TCE-Contaminated Aquifer using a Short Rotation Woody Crop Groundwater Treatment System. CU 9519. Warnell School of Forestry and Natural Resources. U. S. Department of Defense - Environmental Security Technology Certification Program. Arlington, Virginia.
- Hill, R.R., Jeffs, G.E., and Roberts, D.R. 1997. Photocatalytic degradation of 1,4-dioxane in aqueous solution. *Journal of Photochemistry and Photobiology A: Chemistry.* **108**(1): 55-58.
- Isaacson, C., Mohr, T.K.G., and Field, J.A. 2006. Quantitative Determination of 1,4-Dioxane and Tetrahydrofuran in Groundwater by Solid Phase Extraction GC/MS/MS. *Environ. Sci. Technol.* **40**(23): 7305-7311.
- Italia, M.P. and Nunes, M.A. 1991. Gas chromatographic determination of 1,4-dioxane at the parts-per-million level in consumer shampoo products. *Journal of the Society of Cosmetic Chemists.* **42**(2): 97-104.

- Jain, A.K. and Srivastava, R.K. 1996. Ab-initio studies on electroosmotic separation: separation of 1,4-dioxane in water solution. *Journal of Membrane Science*. **112**(1): 41-46.
- Jones, S.B., Wraith, J.M., and Or, D. 2002. Time domain reflectometry measurement principles and applications. *Hydrological Processes*. **16**: 141-153.
- Kadlec, R.H. 1994. Detention and mixing in free water wetlands. *Ecological Engineering*. **3**(4): 345-380.
- Kamath, R., Schnoor, J.R. and Alvarez, P.J.J. 2004. Effect of Root-Derived Substrates on the Expression of nah-lux Genes in *Pseudomonas fluorescens* HK44: Implications for PAH Biodegradation in the Rhizosphere. *Environmental Science and Technology*. **38**(6): 1740-1745.
- Karpiscak, M.M., Wass, R.D., Freitas, R.J. and Hopf, S.B. 1999. Constructed Wetlands in Southern Arizona. *Arid Lands Newsletter*. **45**.
- Karura, C.J. 2002. May - June 2002 1, 4 - Dioxane Results. ADEQ WQARF Annual Report. ADEQ. Arizona Department of Environmental Quality.
- Kawata, K., Ibaraki, T., Tanabe, A., and Yasuhara, A. 2003. Distribution of 1,4-Dioxane and -Dimethylformamide in River Water from Niigata, Japan. *Bulletin of Environmental Contamination and Toxicology*. **70**(5): 876-882.
- Kelleners, T.J., Seyfried, M.S., Blonquist, J.M.Jr., Bilskie, J., and Chandler, D.G. 2005. Improved Interpretation of Water Content Reflectometer Measurements in Soils. *Soil Sci Soc Am J*. **69**(6): 1684-1690.
- Kelley, S.L., Aitchison, E.W., Deshpande, M., Schnoor, J.L., and Alvarez, P.J.J. 2001. Biodegradation of 1,4-dioxane in planted and unplanted soil: effect of bioaugmentation with amycolata sp. CB1190. *Water Research*. **35**(16): 3791-3800.
- Kitchin, K.T. and Brown, J.L. 1994. Dose-response relationship for rat liver DNA damage caused by 49 rodent carcinogens. *Toxicology*. **88**(1-3): 31-49.
- Klecka, G.M. and Gonsior, S.J. 1986. Removal of 1,4-dioxane from wastewater. *Journal of Hazardous Materials*. **13**(2): 161-168.
- Knight, P. 1996. A Primer on Mass Spectrometers. Volume 1 Number 2 Newsletter. U.S. Environmental Protection Agency. Manchester Laboratory . Manchester, Washington.

- Kosaka, K., Yamada, H., Matsui, S., and Shishida, K. 2000. The effects of the co-existing compounds on the decomposition of micropollutants using the ozone/hydrogen peroxide process. *Water Science & Technology*. **42**(7-8): 353-361.
- LaGrega, M. D., Buckingham, P. L. and Evans, J. C. 1994. Hazardous Waste Management. McGraw-Hill, Inc., New York, N.Y.
- Lee, H. 2006. Aerobic Degradation of Selected Environmental Pollutants. University of Guelph. Ontario, Canada.
- Li, H., Betterton, E.A., Arnold, R.G., Ela, W.P., Barbaris, B., and Grachane, C. 2005. Convenient New Chemical Actinometer Based on Aqueous Acetone, 2-Propanol, and Carbon Tetrachloride. *Environ. Sci. Technol.* **39**(7): 2262-2266.
- Littlewood, A. B. 1970. Gas Chromatography Principles, Techniques, and Applications. Academic Press, New York.
- Mahendra, S. and Alvarez-Cohen, L. 2006. Kinetics of 1,4-Dioxane Biodegradation by Monooxygenase-Expressing Bacteria. *Environ. Sci. Technol.* **40**(17): 5435-5442.
- Maier, R. 2003. Personal Communication. *Professor Biochemistry University of Arizona*.
- Maurer, T., Hass, H., Barnes, I. and Becker, K.H. 1999. Kinetic and Product Study of the Atmosphere Photooxidation of 1,4-Dioxane and its Main Reaction Product Ethylene Glycol Diformate. *Journal Physics Chemistry A*. **103**: 5032-5039.
- Maurino, V., Calza, P., Minero, C., Pelizzetti, E., and Vincenti, M. 1997. Light-assisted 1,4-dioxane degradation. *Chemosphere*. **35**(11): 2675-2688.
- McFee, A.F., Abbott, M.G., Gulati, D.K., and Shelby, M.D. 1994. Results of mouse bone marrow micronucleus studies on 1,4-dioxane. *Mutation Research/Genetic Toxicology*. **322**(2): 145-148.
- Mueller, R. and Goswami, D. 2003. Technical and Regulatory Guidance for Constructed Treatment Wetlands. Interstate Technology Regulatory Council (ITRC).
- Modeer, D.V. 2002. Minute Levels of 1, 4 - Dioxane Detected in TCE Plume. *The Water Connection*.
- Mohr, T.K.G. 2001. Solvent Stabilizers. *Santa Clara Valley Water District*. **Pre-Publication Copy**: 1-52.

National Plant Data Center 2002. Windbreaks and Woodland Tree and Shrub Characteristics. FOTG Section I. NRCS. USDA. North Dakota.

NESLAB 1997. CFT Series Recirculating Chiller Instruction and Operation Manual. NESLAB Instruments, Inc.

Odah, M. 2003. In Well Air Stripping for 1,4-Dioxane Removal: Dynamic Subsurface Circulation Technique. In: 1,4-Dioxane and Other Solvent Stabilizer Compounds in the Environment. The Ninth Symposium in GRA's Series on Groundwater Contaminants. Groundwater Resources Association. Sacramento, California.

OEHHA 2003. Air Chronic Reference Exposure Levels Adopted by OEHHA . Chronic Toxicity Summary for 1,4-Dioxane. California EPA. California Office of Environmental Health Hazard Assessment. Sacramento, California.

Oppelt, T.E. 1998. Advanced Photochemical Oxidation Processes. EPA /625/R-98/004. National Risk Management Research Laboratory. U. S. Environmental Protection Agency - Office of Research and Development - Center for Environmental Research Information . Cincinnati, Ohio.

Or, D., Jones, S.B., VanShaar, J.R., Humphries, S., and Koberstein, L. 2004. WinTDR Version 6.1 Users Guide. Fall 2004. Utah State University Soil Physics Group. Utah State University. Utah .

Ouyang, Y. 2002. Phytoremediation: modeling plant uptake and contaminant transport in the soil-plant-atmosphere continuum. *Journal of Hydrology*. **266**(1-2): 66-82.

Parales, R.E., Adamus, J.E., White, N., and May, H.D. 1994. Degradation of 1,4-dioxane by an actinomycete in pure culture. *Applied Environmental Microbiology*. **60**(12): 4527-4530.

Park, Y.-M., Pyo, H., Park, S.-J., and Park, S.-K. 2005. Development of the analytical method for 1,4-dioxane in water by liquid-liquid extraction. *Analytica Chimica Acta*. **548**(1-2): 109-115.

Parsons, D.F., Hayashi, M., and van der Kamp, G. 2004. Infiltration and solute transport under a seasonal wetland: bromide tracer experiments in Saskatoon, Canada. *Hydrological Processes*. **18**: 2011-2027.

Patten, D. T. and Smith, E. M. 1975. Environmental physiology of desert organisms. Halsted Press, New York, NY.

Payne, F., Suthersan, S., Molnaa, B., and Davis, S. 2003. Developing In-situ Reactive Zone Strategies for 1,4-Dioxane Treatment. In: 1,4-Dioxane and Other Solvent Stabilizer Compounds in the Environment. The Ninth Symposium in GRA's Series on Groundwater Contaminants. Groundwater Resources Association. Sacramento, California.

Perriello, F., Abrams, P.G., and Abrams, A.P. 2003. 1,4-Dioxane Degradation Using Butane Biostimulation. In: 1,4-Dioxane and Other Solvent Stabilizer Compounds in the Environment. The Ninth Symposium in GRA's Series on Groundwater Contaminants. Groundwater Resources Association. Sacramento, California.

Platz, J., Sehested, J., Mgelberg, T., Nielsen O. J., and Wallington, T.J. 1997. Atmospheric chemistry of 1,4-dioxane Laboratory studies. *Journal of the Chemical Society. Faraday Transactions Online*. **93**(16): 2855-2863.

Poss, M., Couch, T., Odufu, A., McCann, J., Mellon, J., Melnick, B., and Jenke, D. 2003. Determination of 1,4-Dioxane Impurity Levels in Triton X-100 Raw Material by Gas Chromatography with Mass Spectrometric Detection. *Journal of Chromatographic Science*. **41**(8): 410-417.

Prescott, G. W. 1970. How to Know The Freshwater Algae. Wm. C. Brown Publishers, Debuque, Iowa.

Pundlik, M.D., Sitharaman, B., and Kaur, I. 2001. Gas Chromatographic Determination of 1,4-Dioxane at Low Parts-Per-Million Levels in Glycols. *Journal of Chromatographic Science*. **39**(2): 73-76.

Quinonez-Diaz, M., Karpiscak, M., Ellman, E., and Gerba, C. 2001. Removal of Pathogenic and Indicator Microorganisms by a Constructed Wetland Receiving Untreated Domestic Wastewater. *Journal of Environmental Science & Health, Part A -- Toxic/Hazardous Substances & Environmental Engineering*. **A 36**(7): 1311-1320.

Ray, A.K. 1998. A new photocatalytic reactor for destruction of toxic water pollutants by advanced oxidation process. *Catalysis Today*. **44**(1-4): 357-368.

Roudebush, E.M. 2006. The Apache Nitrogen Wetland - Groundwater Denitrification Using Constructed Wetland. *Southwest Hydrology*. **5**(1): 22-23.

Roy, S.K., Thilagar, A.K., and Eastmond, D.A. 2005. Chromosome breakage is primarily responsible for the micronuclei induced by 1,4-dioxane in the bone marrow and liver of young CD-1 mice. *Mutation Research/Genetic Toxicology and Environmental Mutagenesis*. **586**(1): 28-37.

- Rundle, C.C. 2000. A Beginners Guide to Ion-Selective Electrode Measurements. www.nico2000.net. Nico 2000. Nico 2000 Ltd. London, UK.
- Ryer, A.D. 1998. Light Measurement Handbook. International Light Incorporated. Newburyport, Ma.
- Sabba, D. and Witebsky, S. 2003. The Nature and Extent of 1,4-Dioxane at Three Solvents Plumes Site. In: 1,4-Dioxane and Other Solvent Stabilizer Compounds in the Environment. The Ninth Symposium in GRA's Series on Groundwater Contaminants. Groundwater Resources Association. Sacramento, California.
- Schnoor, J.L. 2002. Phytoremediation of Soil and Groundwater. Technical Evaluation Report TE-02-01. Department of Civil and Environmental Engineering, University of Iowa. Ground-Water Remediation Technologies Analysis Center (GWRTAC) . Johnstown, Pa.
- Schnoor, J.L. 1997. Phytoremediation. Technical Evaluation Report TE-98-01. Department of Civil and Environmental Engineering, University of Iowa. Ground-Water Remediation Technologies Analysis Center (GWRTAC) . Johnstown, Pa.
- Schwarzenbach, R. P., Gschwend, P. M. and Imboden, D. M. 1993. Environmental Organic Chemistry. John Wiley & Sons, Inc., New York, NY.
- Shangraw, T., Plaehn, W., Richtel, S., and Bollmann, D. 2003. Biological Treatment Option for 1,4-Dioxane in Landfill Leachate. In: 1,4-Dioxane and Other Solvent Stabilizer Compounds in the Environment. The Ninth Symposium in GRA's Series on Groundwater Contaminants. Groundwater Resources Association. Sacramento, California.
- Sharp, J., Mahendra, S., and Alvarez-Cohen, L. 2005. Oxygenase - Catalyzed Biodegradation of Emerging Water Contaminants: 1,4-Dioxane and N-Nitrosodimethylamine. In: 2005 Partners in Environmental Technology Symposium & Workshop. SERDP and ESTCP Program Office. Herndon, Virginia .
- Simazaki, D., Amasi, M., Nishimura, T., Kunikane, S. and Magara, Y. 2006. Occurance of 1,4-Dioxane and MTBE in drinking water source in Japan. *Water Science and Technology*. **6**(2): 47-53.
- Singh, S.K. and Beck, M.B. 2003. Dispersion Coefficient of Streams from Tracer Experiment Data. *Journal of Environmental Engineering*. **129** (6): 539-546.
- Siver, P.A. 2007. ALGAL-ED. Connecticut College. New London, CT.

- Son, H.-S., Choi, S.-B., Khan, E., and Zoh, K.-D. 2006. Removal of 1,4-dioxane from water using sonication: Effect of adding oxidants on the degradation kinetics. *Water Research*. **40**(4): 692-698.
- Song, D. and Zhang, S. 1997. Rapid determination of 1,4-dioxane in water by solid-phase extraction and gas chromatography-mass spectrometry. *Journal of Chromatography A*. **787**(1-2): 283-287.
- Stefan, M.I. and Bolton, J.R. 1998. Mechanism of the Degradation of 1,4-Dioxane in Dilute Aqueous Solution Using the UV/Hydrogen Peroxide Process. *Environmental Science & Technology*. **32**(11): 1588-1595.
- Stickney, J.A., Sager, S.L., Clarkson, J.R., Smith, L.A., Locey, B.J., Bock, M.J., Hartung, R., and Olp, S.F. 2003. An updated evaluation of the carcinogenic potential of 1,4-dioxane. *Regulatory Toxicology and Pharmacology*. **38**(2): 183-195.
- Suh, J.H.J.H. and Mohseni, M. 2004. A study on the relationship between biodegradability enhancement and oxidation of 1,4-dioxane using ozone and hydrogen peroxide. *Water Research*. **38**(10): 2596-2604.
- Taylor, G. 1954. The Dispersion of Matter in Turbulent Flow through a Pipe. *Proceedings of the Royal Society of London. Series A, Mathematical and Physical Sciences (1934-1990)*. **223**(1155): 446-468.
- Thurston, J.A., Gerba, C.P., Foster, K.E., and Karpiscak, M.M. 2001. Fate of indicator microorganisms, giardia and cryptosporidium in subsurface flow constructed wetlands. *Water Research*. **35**(6): 1547-1551.
- Topp, G.C., Davis, J.L. and Annan, A.P. 1980. Electromagnetic determination of soil water content: Measurements in coaxial transmission lines. *Water Resources Research*. **16**(3): 574-582.
- Tossell, R., Newman, L., and Rose, K. 1997. Evaluation of Phytoremediation for Management of Chlorinated Solvents in Soil and Groundwater. EPA 542-R-05-001. Phytoremediation of Organics Action Team. U. S. Environmental Protection Agency. Washington, D.C.
- U.S. Army Corps of Engineers 1997. Environmental Quality - Design, Installation and Utilization of Fixed-Fenceline Sample Collection and Monitoring Systems. EM 200-1-5. Environmental Quality - Engineering. Department of the Army-National Technical Information Service. Springfield, VA.

U.S. EPA 2006. Volatile Organic Compounds by Vacuum Distillation in Combination with Gas Chromatography/Mass Spectrometry (VD/GC/MS). 8261A. EPA Test Methods. U. S. Environmental Protection Agency. Washington, D.C.

U.S. EPA 2005. Analytical Method for AROCLORS. OREAP- 01.0. EPA Contract Laboratory Program. U.S. Environmental Protection Agency. Washington, D.C.

U.S. EPA 2002. Drinking Water Standards and Health Advisories (2002 Edition). EPA 822R02038. EPA Office of Groundwater and Drinking Water. United States Environmental Protection Agency. Washington, DC.

U.S. EPA 1996. Solvents Study - 4.4 1,4-Dioxane. Annual Solvents Study. EPA - Office of Solid Waste Management. U. S. Environmental Protection Agency . Washington, D.C.

U.S. EPA 1994. Air Emissions Models for Waste and Wastewater. EPA-453/R-94-080A. Office of Air Quality Planning and Standards - Research Triangle Park. U.S. Environmental Protection Agency. North Carolina.

Ucisik, A. 2007. Uptake of chemicals and metabolism kinetics related to toxic effects and consideration of phytoremediation as a remediation option. Technical University of Denmark. Kongens Lyngby, Denmark.

Vallombroso, T. M. 2001. Organic Chemistry Pearls of Wisdom. Boston Medical Publishing Corporation, Boston, MA.

Valsaraj, K. T. 1995. Elements of Environmental Engineering - Thermodynamics and Kinetics. CRC Press, Boca Raton, Florida.

Vidales Contreras, J.A. 2001. Removal of viruses and pollution indicators in constructed wetlands. Doctor of Philosophy Dissertation. Department of Soil, Water and Environmental Science. University of Arizona. Tucson, Arizona.

Walsom, G.D. and Tunnicliffe, B. 2002. 1,4-Dioxane -- a little known compound. *Environmental Science & Engineering*.

Wass, R.D. 2006. The Tres Rios Wetlands: From Demonstration Project to Full-Scale Facilities. *Southwest Hydrology*. **5**(1): 18-19.

Whitmer, S., Baker, L., and Wass, R. 2000. Loss of Bromide in a Wetland Tracer Experiment. *Journal Environmental Quality*. **29**: 2043-2045.

- Williams, J.B. 2002. Phytoremediation in Wetland Ecosystems: Progress, Problems, and Potential. *Critical Reviews in Plant Sciences*. **21**(6): 607-635.
- Woodbury, A., Sudicky, E., Urych, T.J., and Ludwig, R. 1998. Three-dimensional plume source reconstruction using minimum relative entropy inversion. *Journal of Contaminant Hydrology*. **32**(1-2): 131-158.
- Xu, S., Leri, A.C., Myneni, S.C.B., and Jaffe, P.R. 2004. Uptake of Bromide by Two Wetland Plants (*Typha latifolia* L. and *Phragmites australis* (Cav.) Trin. ex Steud). *Environmental Science & Technology*. **38**(21): 5642-5648.
- Yeh, T.-C.J. 1999. Characterization, Monitoring, and Modeling of the Vadose Zone: Flow and Transport. In: *Characterization, Monitoring, and Modeling of the Vadose Zone: Flow and Transport*. University of Arizona.
- Yeh, T.-C.J. and Guzman-Guzman, A. 1995. Tensiometry. In: Handbook of Vadose Zone Characterization & Monitoring. Eds. Gray, W.L., Everett Lorne G. and Cullen, S.J. Lewis Publishers, Ann Arbor, Michigan.
- Zenker, M.J., Borden, R.C., and Barlaz, M.A. 2004. Biodegradation of 1,4-Dioxane Using Trickling Filter. *Journal of Environmental Engineering*. **130**(9): 926-931.
- Zenker, M.J., Borden, R.C. and Barlaz, M.A. 2003. Occurrence and Treatment of 1,4-Dioxane in Aqueous Environments. *Environmental Engineering Science*. **5**: 423-432.
- Zenker, M.J., Borden, R.C., and Barlaz, M.A. 2002. Modeling Cometabolism of Cyclic Ethers. *Environmental Engineering Science*. **19**(4): 215-228.
- Zimmo, O.R., van der Steen, N.P., and Gijzen, H.J. 2003. Comparison of ammonia volatilisation rates in algae and duckweed-based waste stabilisation ponds treating domestic wastewater. *Water Research*. **37**(19): 4587-4594.